Interactions of Bunyamwera Virus Nucleocapsid Protein and Encapsidation of Viral RNA

by

JANE C. OSBORNE

A THESIS PRESENTED FOR THE DEGREE OF DOCTOR OF PHILOSOPHY IN THE FACULTY OF BIOMEDICAL AND LIFE SCIENCES AT THE UNIVERSITY OF GLASGOW

IBLS Division of Virology
Church Street
Glasgow
G11 5JR

Summary

This project concerns the identification and characterisation of some of the molecular interactions of the Bunyamwera virus (BUN) nucleocapsid (N) protein, and attempts to construct a model for encapsidation of viral RNA by N.

BUN is the prototype virus of the *Bunyaviridae*, a family of negative-strand viruses with tripartite genomes. All BUN genome and antigenome RNAs are encapsidated by N. This interaction was investigated *in vitro* by expressing His-tagged BUN N in bacteria, purifying it in its native form and developing binding assays to analyse its association with a short radiolabelled riboprobe consisting of the termini of the BUNS segment. N was demonstrated to bind the riboprobe by Northwestern, gel electrophoretic mobility shift (GEMSA) and filter-binding assays. The complexes were found to possess a similar level of resistance to digestion with ribonuclease as authentic nucleocapsids. Analysis by GEMSA was interpreted to indicate complete encapsidation of the riboprobe by N, with a number of discrete complexes presumed to be intermediates in the sequential encapsidation process apparent. Filter-binding assays were utilised to determine the binding kinetics. The resultant dissociation constant was similar to dissociation constants obtained for other negative-strand virus N-RNA interactions and implied that binding was strong. Supporting the latter observation was the ability of complexes to form over a wide range of ionic conditions. The binding kinetics also indicated that the binding of N to the riboprobe was co-operative, reinforced by the demonstration that the capacity of N to bind RNA was dependent on its concentration.

The 5' terminus of each segment RNA had been implicated in encapsidation initiation, but no direct evidence had been produced. To investigate the presence of an encapsidation signal, competitive binding assays were set up with various RNA species. The 5' 32 terminal nucleotides of the BUN S segment were bound selectively, implicating this region in encapsidation initiation. In addition, N was capable of binding any RNA non-selectively and to a low degree, indicating the presence of two modes of binding. Predictions of the secondary structure of 5' terminal sequences revealed potential stem-loops containing a consensus sequence in the loop region that had previously been found to be essential for transcription of a recombinant BUN S segment in a minireplicon system. The stem-loop was suggested to constitute an encapsidation signal, supported by the inability of an RNA containing the same sequence but not predicted to form the stem-loop to be bound selectively.

BUN mRNA is not normally encapsidated and possesses a capped, heterogeneous primer sequence on its 5' end. The predictions of secondary structure were extended to propose a mechanism of inhibition of encapsidation by the primer sequence, which, under certain circumstances, was suggested to be reversible when required. The information obtained on N-RNA interactions was used to propose a model for encapsidation in BUN.

The co-operative nature of N-RNA binding suggested that multimerisation of N took place. This was investigated by expressing N as fusion proteins in the mammalian two-hybrid system, and a potential self-association was identified. This was supported by the co-immunoprecipitation of native N with His-tagged N in mammalian cells. However, neither the amino nor the carboxy half of N was found to be capable of interacting with His-tagged N exclusively.

No evidence of an interaction between the viral polymerase, L, and N or between L and the non-structural viral protein NSs was obtained using the mammalian two-hybrid system, and NSs was not found to multimerise. However, a weak interaction between N and NSs was identified. The potential role of this interaction in the mechanisms of transcription inhibition or interferon antagonism ascribed to NSs is discussed.

Acknowledgements

I am indebted to Professor Richard Elliott for his outstanding supervision, patience and enthusiasm, as well as the use of his critical reading skills and laboratory facilities.

I would like to express my gratitude to my industrial supervisor, Dr. Charles Craig, and my assessor, Dr. Arvind Patel. My thanks also go to my colleagues at the Institute for their exceptional assistance and advice, and to the support staff for their excellent help.

The project was partly funded by Roche Products Ltd., and I would like to thank everyone at Roche for their help and financial support.

The friends I made in Glasgow are very dear to me. I am grateful for their considerable friendship and support, and for spending many long and happy hours with me in Bar Zoo.

My warmest thanks go to my parents, whose phenomenal love and support have always been inspiring, and I am indebted to them. They appear to possess an unrivalled ability to retrieve me from sticky situations. I would also like to thank the rest of my family for their support. Finally, I must acknowledge my parents' cat Barney, who, when awake, has provided a great deal of warmth and entertainment during the time I have spent writing my thesis.

Unless otherwise stated, all results were obtained by the author's own efforts.

This thesis is dedicated to the memory of my grandfather Thomas Beech ('Poppy'), whose relentless determination and extraordinary strength of character were a great inspiration to all who knew him.

Contents

List of figures

Abbreviations

^{14}C	carbon-14
^{32}P	phosphorous-32
^{35}S	sulphur-35
A	adenine
A_{280}	absorbency at 280nm
AD	activation domain
BD	binding domain
BSA	bovine serum albumin
BUNL	Bunyamwera virus L segment
BUNM	Bunyamwera virus M segment
BUNS	Bunyamwera virus S segment
C	cytosine or carboxy
$CaCl_2$	calcium chlroide
CAT	chloramphenicol acetyltransferase
cDNA	complementary DNA
Ci	Curie
cm	centimetre
CoA	co-enzyme A
cpm	counts per minute
cRNA	complementary RNA
CsCl	caesium chloride
CTP	cytidine triphosphate
dATP	deoxyadenosine triphosphate
dCTP	deoxycytidine triphospate
DDAB	dimethyldioctadecyl ammonium bromide
dGTP	deoxyguanosine triphosphate
DMEM	Dulbecco's modified Eagle medium
dNTP	deoxynucleotide
DOPE	dioloeoyl L-α-phosphatidyl ethanolamine
dTTP	deoxythymidine triphosphate
DEAE	
dH_2O	de-ionised water
DI	defective-interfering
DMSO	dimethylsulphoxide
DNA	deoxyribonucleic acid
ds	double-stranded
DTT	dithiothreitol
ECL	enhanced chemiluminescence
E. coli	*Escherichia coli*
EDTA	ethylenediaminetetra-acetic acid
ER	endoplasmic reticulum
G	guanine
g	gram or gravity
GEMSA	gel electrophoretic mobility shift assay
h	hour
HCl	hydrogen chloride
HFRS	haemorrhagic fever with renal syndrome
hnRNP	heterogeneous nuclear ribonucleoprotein
HPS	hantavirus pulmonary syndrome
Hsp	heat-shock protein
IGR	intergenic region
IP	immunoprecipitation
IPTG	isopropyl β-D-thiogalactoside
IRES	internal ribosome entry site
IRF	interferon response factor

kb	kilobase
KCl	potassium chloride
kD	kilo Dalton
k_d	dissociation constant
KOAc	potassium acetate
LiCl	lithium chloride
M	molar
M2H	mammalian two-hybrid
mA	milli Amp
µCi	micro Curie
min	minute
mg	milligram
µg	microgram
$MgCl_2$	magnesium chloride
$MgSO_4$	magnesium sulphate
ml	millilitre
µl	microlitre
mm	millimetre
µm	micron
mmol	millimole
moi	multiplicity of infection
mRNA	messenger RNA
N	nucleocapsid protein or amino
Na	sodium
NaCl	sodium chloride
NaOH	sodium hydroxide
ng	nannogram
$(NH_4)_2SO_4$	ammonium sulphate
Ni^{2+}	nickel
nm	nannometre
NP	nucleoprotein
NP40	Nonidet P40
NS	non-structural
NSV	negative-strand virus
nt	nucleotide
NTA	nitrilotriacetic acid
NTP	nucleoside triphosphate
OAS	origin of assembly sequence
oligo	oligonucleotide
ORF	open reading frame
PAGE	polyacrylamide gel electrophoresis
PBS	phosphate-buffered saline
PCR	polymerase chain reaction
PEG	polyethylene glycol
PEI	polyethylene imine
pg	picogram
pmol	picomole
RNA	ribonucleic acid
RNase	ribonuclease
rpm	revolutions per minute
s	second
SDS	sodium dodecyl sulphate
SL	stem-loop
ss	single-stranded
T	thymine
TAE	Tris-acetate EDTA
TBE	Tris-borate EDTA
TCA	trichloroacetic acid
TE	Tris-EDTA
TEMED	NNN'N' tetramethyl-ethylenediamine
TEN	Tris-EDTA-NaCl
TLC	thin-layer chromatography
TnT	transcription and translation
tRNA	transfer RNA
TSB	transformation and storage buffer

U	uracil or unit
UTR	untranslated region
V	Volts
vRNA	viral RNA
w/v	weight by volume

Abbreviated virus names

BAT	Batai virus
BUN	Bunyamwera virus
BUNdelNSs	BUN lacking the NSs ORF
CCHF	Crimean-Congo haemorrhagic fever virus
CE	California encephalitis virus
CV	Cache Valley virus
DOB	Dobrava virus
DUG	Dugbe virus
GER	Germiston virus
GRO	Guaroa virus
HIV	human immunodeficiency virus
HTN	Hantaan virus
JC	Jamestown Canyon virus
JS	Jerry Slough virus
KEY	Keystone virus
KRI	Kairi virus
LAC	La Crosse virus
LUM	Lumbo virus
MAG	Maguari virus
MD	Main Drain virus
MEL	Melao virus
NOR	Northway virus
PUU	Puumala virus
RSV	respiratory syncytial virus
RVF	Rift Valley fever virus
SEO	Seoul virus
SeV	Sendai virus
SNV	Sin Nombre virus
SSH	Snowshoe hare virus
SV40	simian virus 40
TMV	tobacco mosaic virus
TSWV	tomato spotted wilt virus
TVT	Trivittatus virus
VSV	vesicular stomatitis virus

Amino acids

A	Ala	alanine
B	Asx	asparagine /aspartic acid
C	Cys	cysteine
D	Asp	aspartic acid
E	Glu	glutamic acid
F	Phe	phenylalanine
G	Gly	glycine
H	His	histidine
I	Ile	isoleucine
K	Lys	lysine
L	Leu	leucine
M	Met	methionine
N	Asn	asparagine
P	Pro	proline

Q	Gln	glutamine
R	Arg	arginine
S	Ser	serine
T	Thr	threonine
V	Val	valine
W	Trp	tryptophan
Y	Tyr	tyrosine
Z	Glx	glutamine or glutamic acid

Chapter 1: Introduction

1.1. The *Bunyaviridae*

1.1.1. Classification and taxonomy

The family *Bunyaviridae* consists of over 300 members, isolated on every continent except Antarctica (Karabatsos, 1985). Criteria for inclusion in the family are based on morphology, serological relationships, biochemical properties and coding and replication strategies (Bishop, 1980). Members of the *Bunyaviridae* are arthropod or rodent-borne. The viruses are capable of infecting birds, mammals or plants, sometimes causing severe disease.

Members of the *Bunyaviridae* are divided into the five genera *Bunyavirus*, *Hantavirus*, *Nairovirus*, *Phlebovirus* and *Tospovirus* according to their morphological, morphogenetic and serological relationships and replication and coding strategies (Murphy *et al.*, 1973; Martin *et al.*, 1985). They are also referred to by the vernacular terms bunyaviruses, hantaviruses, nairoviruses, phleboviruses and tospoviruses, respectively. In addition there are a number of viruses meeting the criteria for inclusion in the *Bunyaviridae* but that are currently unassigned to a serogroup or genus (Karabatsos, 1985; Elliott *et al.*, 2000).

1.1.2. Structure and morphology

Bunyaviridae virions have been reported to be spherical or pleomorphic on cryo-electron microscopy. The particles are between 75 and 115nm in diameter with a 4nm thick membrane. The surface is punctuated by glycoprotein projections approximately 10nm long (Talmon *et al.*, 1987). Differences in the appearance of virion surface structure between genera were found to be attributable to the glycoproteins (Martin *et al.*, 1985; Schmaljohn, 1996b).

Within the virion the tripartite negative-sense RNA genome exists associated with the nucleocapsid protein N and the viral polymerase L in loosely helical ribonucleoprotein structures termed nucleocapsids (Fig.1.1; reviewed by Elliott, 1990). These are usually the only RNA species found in the virion; mRNA is not assembled into viral particles. The three segments are named according to their size: L (large), M (medium) and S (small). Nucleocapsids were found to possess a buoyant density of 1.31g/ml, similar to that of Sendai virus (SeV) and vesicular stomatitis virus (VSV), which suggests that

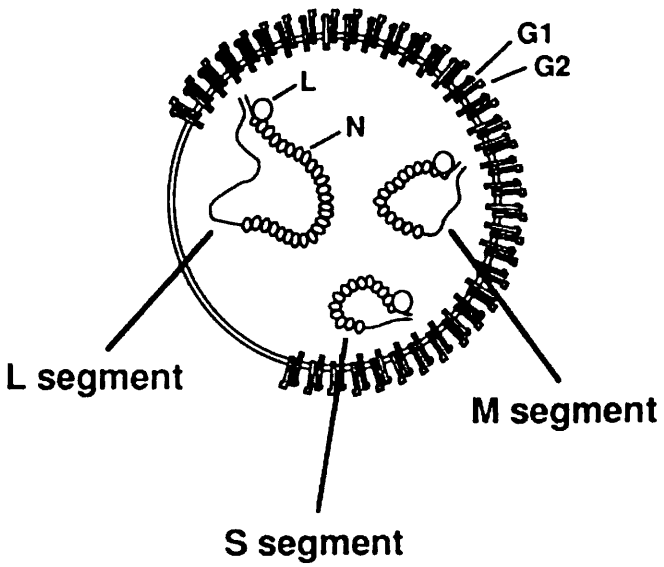

Fig.1.1. Schematic of the structure of members of the *Bunyaviridae*. The three RNA segments S, M and L are present encapsidated by the nucleocapsid protein N and associated with the viral polymerase L within nucleocapsid structures. Surrounding the nucleocapsids is a lipid envelope in which the two viral glycoproteins G1 and G2 are anchored. Figure courtesy of R Pettersson.

they are composed of 96% protein and 4% RNA by weight (Obijeski & Murphy, 1977). N is present at approximately 2100 molecules per virion, L at approximately 25 molecules (Obijeski *et al.*, 1976). The terminal sequences of each segment of RNA are highly conserved and complementary (Fig.1.2). They are believed to hydrogen-bond in infected cells and in virions to form panhandle structures, conferring a circular appearance to nucleocapsids when viewed by electron microscopy (Bouloy *et al.*, 1973/74; Pettersson & von Bonsdorff, 1975; Samso *et al.*, 1975; Hewlett *et al.*, 1977; Pardigon *et al.*, 1982; Raju & Kolakofsky 1989). Pardigon *et al.* (1982) isolated the termini of Germiston virus (GER) as a short duplex molecule after self-annealing and RNase digestion, and Patterson *et al.* (1983) isolated an approximately 30bp double-stranded panhandle structure from deproteinised La Crosse virus (LAC) nucleocaspids with RNase treatment. In addition, Raju and Kolakofsky (1989) were able to chemically cross-link the termini of LAC.

Members of the *Bunyaviridae* contain two glycoproteins designated G1 and G2 according to their relative electrophoretic mobilities, with G1 being the slower migrating and therefore the larger protein. However, they lack a matrix protein-equivalent and thus assembly of the particle may be driven by association of the nucleocapsid with the glycoproteins or Golgi membrane (Pettersson & von Bonsdorff, 1987; Talmon *et al.*, 1987).

1.1.3. Transmission and disease

Members of the *Bunyaviridae* that are important pathogens are listed in Table 1.1, and are reviewed in Elliott (1997).

1.1.3.1. Genus *Bunyavirus*

The prototype of both the *Bunyavirus* genus and the family *Bunyaviridae* is Bunyamwera virus (Bunyamwera serogroup), which was isolated in 1943 from *Aedes* species mosquitoes in the Semliki Forest in Uganda (Smithburn *et al.*, 1946). Bunyaviruses comprise the largest genus in the family, with 177 viruses divided into 19 groups (Elliott *et al.*, 2000). Bunyaviruses are arboviruses, the majority transmitted by mosquitoes, with isolation from culicoid flies, ticks, phlebotomines and tabanids (horse and deerflies) also reported (Wright *et al.*, 1970; Karabatsos, 1985). Transovarial transmission has been established in some cases. Vertebrate hosts have been described for a small number of viruses. A number of bunyaviruses have been

Bunyavirus	3'-UCAUCACAUGA.....UCGUGUGAUGA-5'
Hantavirus	3'-AUCAUCAUCUG.....AUGAUGAU-5'
Nairovirus	3'-AGAGUUUCU.....AGAAACUCU-5'
Phlebovirus	3'-UGUGUUUC.....GAAACACA-5'
Tospovirus	3'-UCUCGUUAG.....CUAACGAGA-5'

Fig.1.2. Consensus terminal sequences of Bunyaviridae genome RNA segments. The terminal sequences are complementary and conserved within each genus.

Genus	Pathogen	Disease
Bunyavirus	Bunyamwera virus	human; fever, rash
	Germiston virus	human; fever
	Oropouche virus	human; fever
	Snowshoe hare virus	human; encephalitis
	La Crosse virus	human; La Crosse encphalitis
	California encephalitis virus	human; California encephalitis
	Cache Valley virus	sheep; foetal abnormalities
	Akabane virus	ruminants; foetal abnormalities
	Inkoo virus	human; fever
	Jamestown Canyon virus	human; encephalitis
	Tahyna virus	human; influenza-like
Hantavirus	Black Creek Canal virus	human; hantavirus pulmonary syndrome
	Convict Creek virus	human; hantavirus pulmonary syndrome
	Dobrava-Belgrade virus	human; HFRS*
	Hantaan virus	human; HFRS
	Puumala virus	human; HFRS
	Seoul virus	human; HFRS
	Sin Nombre virus	human; hantavirus pulmonary syndrome
Nairovirus	Crimean-Congo haemorrhagic fever virus	human, ruminants; haemorrhagic fever
	Dugbe virus	human; ruminants
	Nairobi sheep disease	sheep
Phlebovirus	Rift Valley fever virus	human, ruminants; Rift Valley fever
	Sandfly fever virus	human; fever
	Toscana virus	human; meningitis
	Punta Toro virus	human; fever
Tospovirus	Tomato spotted wilt virus	plants
	Impatiens necrotic spot virus	plants

*HFRS: haemorrhagic fever with renal syndrome

Table.1.1. Members of the *Bunyaviridae* that are important pathogens. Adapted from Calisher (1996) and Gonzalez-Scarano *et al.* (1996).

associated with diseases. Members of the California serogroup cause the most relevant human diseases, which include encephalitis caused by La Crosse virus (LAC), California encephalitis virus (CE), and Jamestown Canyon virus (Gonzalez-Scarano *et al.*, 1996). Other medically important members of the serogroup include Inkoo virus, which causes a febrile illness in humans, and Tahyna virus which is responsible for an influenza-like illness in Europe. Bunyamwera and Germiston viruses, both members of the Bunyamwera serogroup, and Oropouche virus, which is a member of the Simbu serogroup, cause a febrile illness in humans. Cache Valley (Bunyamwera serogroup) and Akabane (Simbu serogroup) viruses have been shown to cause foetal abnormalities and abortions in ruminants.

1.1.3.2. Genus *Hantavirus*

The hantaviruses consist of twenty-two viruses in a single serogroup with the prototype virus Hantaan (HTN; Elliott *et al.*, 2000). There is no evidence that hantaviruses are arboviruses; instead, they are transmitted by rodents, which are their natural hosts. Some are associated with disease in humans, transmission occurring via inhalation of virus present in dried urine and faeces. The new-world disease hantavirus pulmonary syndrome (HPS) is the most severe illness, with a case fatality rate of approximately 43%, and is usually attributed to Sin Nombre virus (Nichol *et al.*, 1996; Leslie *et al.*, 1999). Symptoms resemble those of acute respiratory distress syndrome, with rapid progression of respiratory failure and shock. Other hantaviruses such as HTN, Dobrava (DOB), Seoul (SEO) and Puumala (PUU) cause haemorrhagic fever with renal syndrome (HFRS) with case fatality rates ranging from 0.1 to 15% throughout Europe and Asia (McKee *et al.*, 1991; Lee, 1996).

1.1.3.3. Genus *Nairovirus*

The *Nairovirus* genus includes seven serogroups with a total of 34 viruses transmitted by ticks and, less commonly, culicoid flies and mosquitoes (Calisher, 1996: Elliott *et al.*, 2000). The prototype Dugbe (DUG) and Nairobi sheep disease cause disease in humans and cattle, and Crimean–Congo haemorrhagic fever (CCHF) virus is the causative agent of a severe disease of the same name. CCHF occurs throughout Africa, Asia and Eastern Europe and possesses a mortality rate of up to 20% (Gonzalez-Scarano *et al.*, 1991).

1.1.3.4. Genus *Phlebovirus*

Phleboviruses are divided into three serogroups incorporating 44 viruses (Elliott *et al.*, 2000). Most are transmitted by phlebotomine flies (hence their name), with mosquitoes and ticks also identified as vectors (Calisher, 1996). The most serious pathogen is Rift Valley fever virus (RVF), which causes a haemorrhagic fever of the same name in humans and also causes serious disease in cattle across sub-Saharan Africa (Morrill & McClain, 1996). Mortality rates among cattle vary between 10 and 30%, with very young animals demonstrating rates of up to 100%. In humans only a low proportion (less than 1%) normally develops an acute haemorrhagic syndrome, although this figure is often higher during outbreaks. Nevertheless, among those that do develop acute illness the case fatality rate is approximately 50% and can include severe complications during convalescence, including encephalitis (Morrill & McClain, 1996).

1.1.3.5. Genus *Tospovirus*

The eight members of the *Tospovirus* genus are unique among the *Bunyaviridae* in that they infect plants and are transmitted by thrips (Elliott *et al.*, 2000). They occur worldwide, infecting an extensive range of plant species (more than 800 species from 82 families) and causing crop losses exceeding $1 billion per annum (Goldbach & Peters, 1994 & 1996; Prins & Goldbach, 1998).

1.1.4. Stages of the infectious cycle

The stages of infection and replication in animal cells and possibly also insect cells are summarised in fig.1.3 as follows (Bishop, 1996):

1. Adsorption, entry and uncoating. Virion glycoproteins attach to cellular receptors that have only been defined thus far for hantaviruses, which utilise the β3 integrin receptor (Gavrilovskaya *et al.*, 1998). The virion enters the cell by a process of endocytosis. The virion envelope fuses with the membrane of the endosome and thereby releases the nucleocapsids into the cytoplasm.

2. Transcription to make mRNA. This takes place in the cytoplasm and involves cleavage of capped sequences from host cellular mRNAs by the viral polymerase (L protein). These are then used to prime transcription of the S, M and L mRNAs by L.

3. Translation. Translation yields N, L, the glycoproteins and any nonstructural proteins. Cellular ribosomes are utilised for translation of the viral proteins. In the case

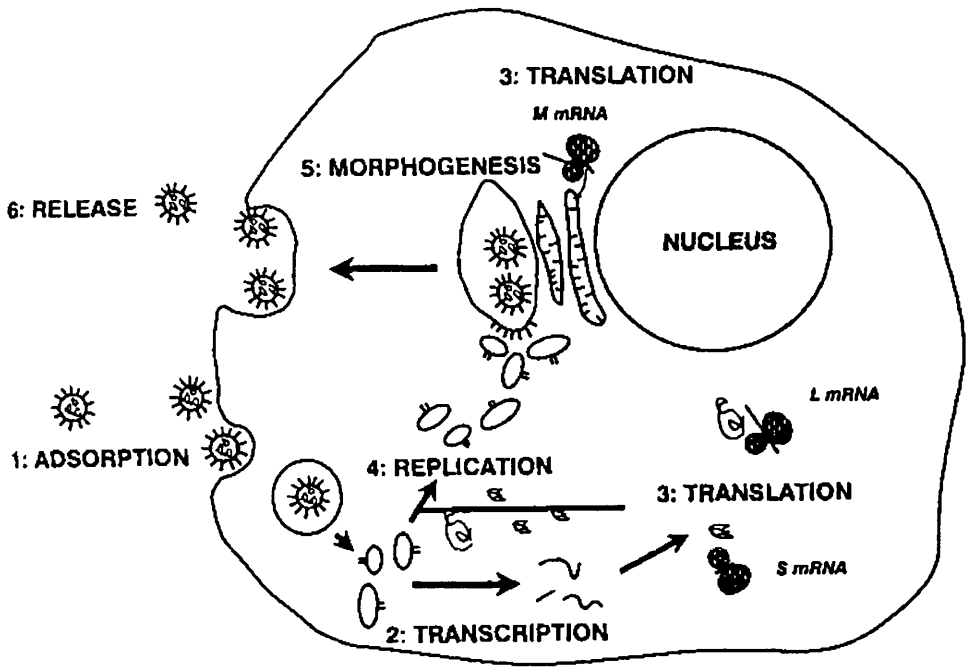

Fig.1.3. General schematic of the infection course of members of the *Bunyaviridae*. Portrayed are the infection stages of animal cells; infection of insect cells may differ in detail. Hantaviruses and phleboviruses assemble at the plasma membrane. Tospovirus infection of plant cells involves NSm-mediated intercellular transport through plasmodesmata. From Bishop (1996).

of the glycoproteins the ribosomes are bound to the membrane of the endoplasmic reticulum and the glycoproteins are processed in the Golgi apparatus.

4. Replication of the viral genome and secondary transcription. Replication occurs via copying of each segment by L into a full-length positive-sense intermediate antigenome which is subsequently copied back into the negative-sense genome, also by L. The switch from transcription to replication is unknown. A second round of transcription to generate the viral mRNAs can then take place and more viral proteins are synthesised. Replication is ongoing.

5. Morphogenesis. Viral proteins of bunyaviruses accumulate in the Golgi apparatus and viral assembly takes place. However, some hantaviruses and phleboviruses have been observed to assemble at the plasma membrane (Anderson & Smith, 1987; Goldsmith *et al.*, 1995; Ravkov *et al.*, 1997); hantavirus components reach their assembly point by association with actin filaments (Ravkov *et al.*, 1998). Tospoviruses assemble in the endoplasmic reticulum (Goldbach & Peters, 1996). Nucleocapsids are probably packaged into virions by an undefined association with the glycoproteins.

6. Release. The virions are transported to the plasma membrane in vesicles which fuse with the membrane and release the virions. Virions that assemble at the plasma membrane bud directly into the extracellular space. In tospovirus infection of plant cells the nucleocapsids are transported to a neighbouring cell through plasmodesmata, or bud into the endoplasmic reticulum.

1.1.5. Coding strategies

The coding strategies for the L, M and S segments of the different genera of the *Bunyaviridae* are shown in Fig.1.4. The size of segments varies considerably between genera; the L segment ranges between 6.4kb for BUN to 12.2kb for DUG, whereas the M segment ranges from 3.2kb (for UUK) to 4.9kb (for DUG), and the S segment shows a difference in size from 0.9kb (for BUN) to 2.9kb (for TSWV).

In general, the L segment encodes the L protein, the M segment encodes the glycoproteins G1 and G2 and the S segment codes for the N protein. In the case of bunyaviruses, tospoviruses and some phleboviruses, a nonstructural protein NSm is also encoded by the M segment. In addition, bunyavirus, tospovirus and phlebovirus S segments encode another nonstructural protein termed NSs.

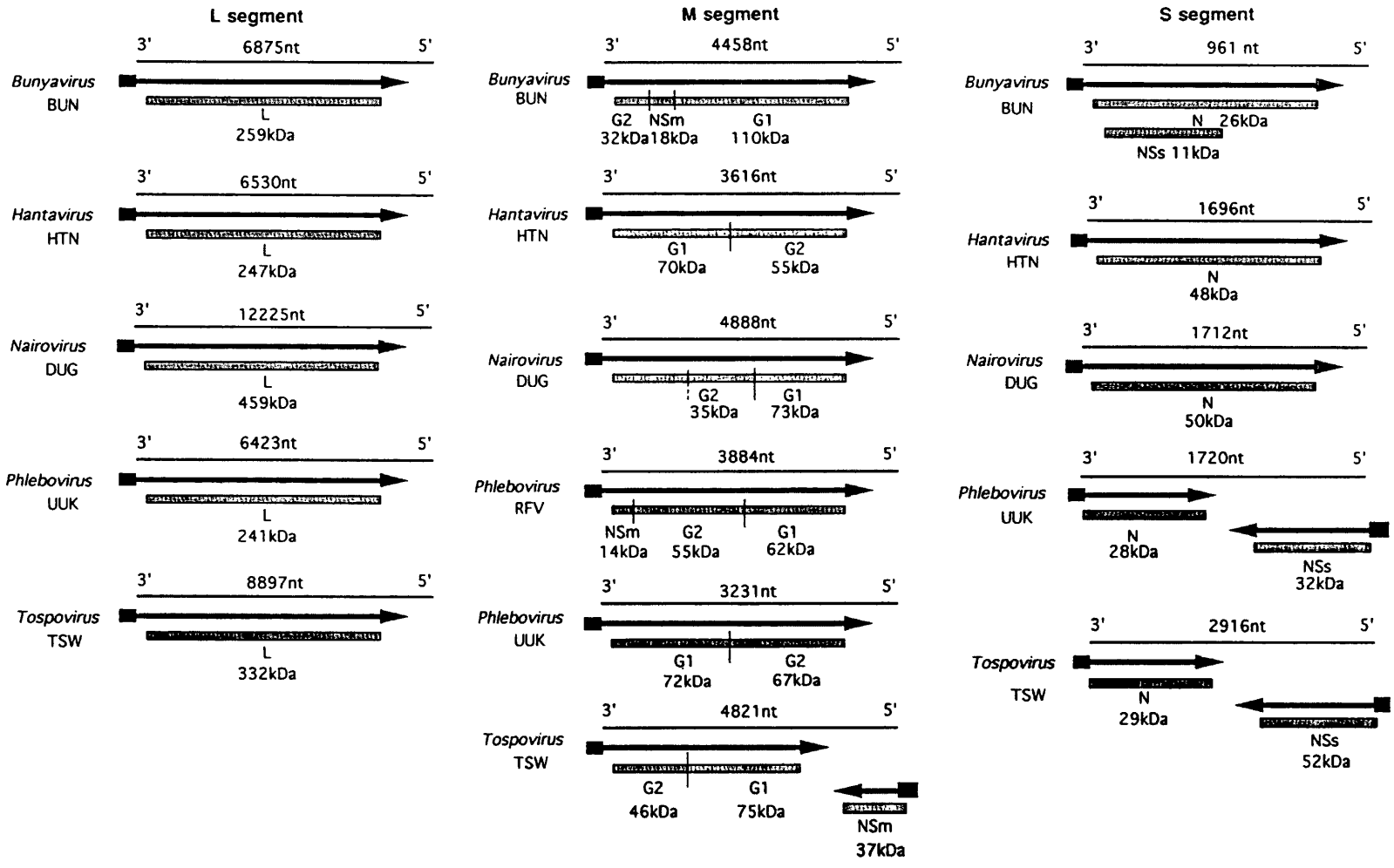

Fig.1.4. Coding strategies of members of the *Bunyaviridae*. Shown are the various strategies employed by the L, M and S segments of different genera of the *Bunyaviridae*. Thin lines represent the viral genome RNA, arrows mRNA, and grey rectangles polypeptides. The caps on mRNAs are depicted as black rectangles. Two different phlebovirus M segment strategies are shown. From Elliott (1996).

The S segment of phleboviruses and M and S segments of tosposviruses possess an ambisense coding strategy, in which one of the ORFs is present in the opposite (positive-sense) orientation (Fig.1.4; Ihara *et al.*, 1984; de Haan *et al.*, 1990; Simons *et al.*, 1990; Law *et al.*, 1992). The genes present in the positive-sense orientation encode the NSs proteins of phleboviruses and tospoviruses, and the NSm protein of tospoviruses. The mRNAs for these genes are transcribed from the -antigenome RNA, not the negative-sense genome. The two ORFs of opposite orientation are separated by an intergenic region thought to harbour transcriptional termination elements (Emery & Bishop, 1987).

Bunyavirus S segments encode the NSs protein ORF as a separate reading frame within the N gene, but in the same orientation (Bishop *et al.*, 1982; Bouloy *et al.*, 1984; Eliott *et al.*, 1989).

1.1.6. Gene products

1.1.6.1. N

The nucleocapsid proteins of the *Bunyaviridae* are the most abundant proteins in virions and infected cells and range in size from 26 to 50 kD. It is interesting that in hantaviruses and nairoviruses, neither of which encode an NSs protein, the N protein is almost twice the size of that of the other members of the *Bunyaviridae*. This has led to speculation that the function of NSs is contained within the N proteins of these viruses. N proteins of other negative-strand viruses (NSVs) appear to have diverse functions generally involved in encapsidation of the viral genome and regulation of replication (discussed in section 1.2.3.). N proteins of the *Bunyaviridae* are positively charged as expected for proteins thought to bind RNA. However, N proteins of different genera of the *Bunyaviridae* share little or no sequence homology and although hantavirus N proteins have been shown to bind RNA, they do not contain an RNA-binding consensus sequence (Gött *et al.*, 1993). The RNA-binding properties of hantavirus N will be discussed in section 1.2.4.2. However, there is some homology between N proteins of viruses within a genus, and regions of homology tend to be clustered which might indicate conservation of functional domains. Within the Bunyamwera serogroup there exists approximately 62% identity between N proteins, with approximately 40% identity with those of the California serogroup (Dunn *et al.*, 1994; Elliott, 1995). Furthermore, the C-terminus of hantavirus and nairovirus N proteins indicate a high degree of

conservation within each genus. The C-termini of hantavirus N proteins have been reported to have identities of 85% (Schmaljohn, 1996b), and some nairovirus N proteins demonstrate 80% identity in the C-terminus (Marriott & Nuttall, 1992). However, the N protein of phleboviruses do not possess highly conserved C-termini (Giorgi *et al.*, 1991). An analysis of conservation of residues in the N proteins of 17 bunyaviruses from three serogroups was provided by Elliott (1996), has been adapted graphically in Fig.1.11, and is discussed in section 1.2.4.3. Much or most of the immune response has been found to be directed towards the N protein of hantaviruses, nairoviruses and tospoviruses during infection (de Avila *et al.*, 1990; El-Ghorr *et al.*, 1990; Schmaljohn, 1996b).

1.1.6.2. NSs

NSs proteins are generated by bunyaviruses, phleboviruses and tospoviruses and range in size from 11 to 52kD. The function of phlebovirus and tospovirus NSs, both of which are generated by ambisense transcription from the S segment, is unknown, and there is no evidence that they share common functions. The positive polarity of their genes suggests that they are not required early on in infection as the genome RNA must first be copied into the antigenome RNA before NSs can be expressed. Indeed, phlebovirus NSs is not detected until 2h after the N protein is detected (Ulmanen *et al.*, 1981). Analysis of cells infected with various phleboviruses has suggested that it localises in the nucleus, cytoplasm or Golgi, and that it can be associated with virions and nucleocapsids, or with the 40S ribosomal subunit (reviewed by Giorgi, 1996).

Until recently the function of bunyavirus NSs protein was unknown, although its involvement in termination of viral transcription had been speculated (Vialat & Bouloy, 1992). Advances have now shown that it appears to possess a number of functions, namely as an antagonist of β-interferon and a virulence factor (Bridgen *et al.*, 2001), and an inhibitor of viral transcription (Weber *et al.*, 2000).

Bridgen *et al.* (2001) generated a mutant BUN virus in which the NSs ORF was destroyed by five point mutations (all silent in the N ORF), using the rescue system previously established (Bridgen & Elliott, 1996). The resultant virus, designated BUNdelNSs, did not express NSs. The mutant virus exhibited a plaque size of 1-2mm in diameter, as opposed to the 3-5mm plaques generated by wt BUN, and viral titres an order of magnitude lower. The amount of N in the infected cell was approximately 10-

fold higher. Host protein synthesis was impaired but not shut-off, in contrast to wild-type BUN, implicating NSs in the shut-off mechanism. Intracranial inoculation of mice with BUNdelNSs still resulted in infection of neurones and death in every case but the mice generally survived longer than those inoculated with wt BUN and the virus was less able to spread. Hence NSs was determined to be important in pathogenesis and not to be essential for growth of the virus in cell culture or mice.

One of the mechanisms by which NSs might work as a virulence factor is its ability to antagonise interferon production by the host cell by inhibiting the interferon-β promoter (Bridgen *et al.*, 2001). This effect was found not to be attributable to host protein shut-off although the mechanism has not been elucidated.

NSs was observed to inhibit mRNA synthesis and replication by L in the BUN minireplicon system (Weber *et al.*, 2001). The purpose of this effect is uncertain but might serve to prevent an excess of viral RNA in the infected cell. If the rate of RNA synthesis were to exceed that of N protein expression, the result would be an accumulation of unencapsidated RNA of both polarities, which could then base-pair to form double-stranded RNA, triggering the cell's interferon-β response. The function of NSs in transcription regulation might therefore be related to its role as an interferon antagonist. Another possibility is the prevention of superinfection of the cell by a closely related virus. This was supported by the observation that NSs proteins of other bunyaviruses were also found to inhibit transcription by BUN L in minireplicon system. In addition, superinfection typically occurs later in infection, which is when levels of NSs are highest.

1.1.6.3. M segment proteins

The M segment encodes the two viral glycoproteins G1 and G2, as well as the nonstructural protein NSm in bunyaviruses, tospoviruses and some phleboviruses. It should be noted that the designation of the glycoproteins corresponds only to their respective electrophoretic mobility and not to their functions or gene order.

The M segment proteins are expressed as a single polyprotein that is co-translationally cleaved (Fazakerly *et al.*, 1988). Cleavage is thought to be due to a host cell signal peptidase located within the ER lumen. However, a proportion of RVF (phlebovirus) G1 protein in the infected cell appears to result from translation initiation at a different start codon, and is therefore not produced by cleavage of the polyprotein (Suzich *et al.*, 1990).

The function of the NSm proteins of bunyaviruses and phleboviruses is presently unknown. They possess similar sizes (14kD for bunyaviruses, 18kD for phleboviruses) but the positions of their genes relative to those of the glycoproteins are different; in bunyaviruses the NSm gene is found between the glycoprotein genes, whereas in phleboviruses it is located upstream of the glycoprotein genes. Bunyavirus NSm may be an integral membrane protein as it possesses a number of hydrophobic domains and was reported to localise to the Golgi apparatus of infected cells (Nakitare & Elliott, 1993).

1.1.6.3.1. Glycoproteins

The size of the viral glycoproteins ranges from 32kD (BUN G2) to 110kD (BUN G1). They are type I membrane-spanning glycoproteins thought to span the membrane once, with the C-terminus of each facing towards the cytoplasm and the N-terminus external to the cell (reviewed by Pettersson & Melin, 1996). Both glycoproteins are predicted to be preceded by a hydrophobic signal sequence in the precursor polyprotein for translocation across the ER membrane (Eshita & Bishop, 1984; Lees *et al.*, 1986; Grady *et al.*, 1987; Schmaljohn *et al.*, 1987; Pardigon *et al.*, 1988; Arikawa *et al.*, 1990; Kormelink 1992c; Pettersson & Melin, 1996). In addition, sequences yielded a predicted C-terminal anchor. The NSm proteins of bunyaviruses and phleboviruses also appear to possess both an N-terminal signal sequence and a C-terminal anchor, suggesting that they are also integral membrane proteins.

G1 and G2 generally have a high cysteine content (approximately 5-7%), with the positions of cysteine residues highly conserved, implying relatively extensive disulphide bridge formation (Eshita & Bishop, 1984; Grady *et al.*, 1987; Elliott, 1990). N (Asn)-linked glycosylation sites have been found on both glycoproteins, but not on NSm (Eshita & Bishop, 1984; Schmaljohn *et al.*, 1986; Grady *et al.*, 1987; Pardigon *et al.*, 1988; El-Ghorr *et al.*, 1990; Ruusala *et al.*, 1992). In LAC and Inkoo viruses it was determined that G2 possesses mostly high-mannose glycans, whereas G1 has both complex and intermediate-type, although the type is thought to be dependent on the cell line (Madoff & Lenard, 1982). In hantaviruses both glycoproteins were found to possess high-mannose glycans (Schmaljohn *et al.*, 1986; Antic *et al.*, 1992; Ruusala *et al.*, 1992). The mature bunyavirus glycoproteins were determined to be sensitive to the enzyme endo-H which cleaves high-mannose sugars. As endo-H sensitivity is usually

removed in the smooth ER and Golgi, the viral glycoproteins were thought to be incompletely processed.

1.1.6.3.2. TSWV NSm

The 37kD NSm protein of TSWV was found to demonstrate some characteristics typical of viral movement proteins, which transport nucleocapsids intercellularly via the plasmodesmata of plant cells. TSWV NSm was found to co-localise with nucleocapsids and plasmodesmata and to trigger tubule formation in infected cells, the tubules penetrating the plasmodesmata (Kormelink *et al.*, 1994; Storms *et al.*, 1995). Subsequently NSm was shown to possess the ability to bind N and bind nonspecifically to ssRNA, apparently permitting a transient association with nucleocapsids during transport (Soellick *et al.*, 2000). NSm was also found to bind the cellular protein DnaJ, a key regulator of the Hsp-70 chaperone which is involved in microtubule formation and probably intercellular transport (Soellick *et al.*, 2000). Hence, it has been characterised as a viral movement protein.

1.1.6.4. L

Bunyaviridae L proteins are encoded by the L segment and vary in size from 240 to 460kD (Fig.1.4). Detergent-disrupted preparations of members of the *Bunyaviridae* were found to demonstrate weak transcriptase activity which was attributable to the L protein, identifying it as the viral RNA-dependent RNA polymerase (Bouloy & Hannoun, 1976; Patterson *et al.*, 1984). Jin and Elliott (1991) demonstrated activity of a recombinant BUN L in amplifying S segment RNA from nucleocapsids transfected into mammalian cells. Subsequently, the BUN L and N proteins were found to be sufficient for efficient transcription of a recombinant RNA in a reverse genetic system (Dunn *et al.*, 1995). L is also believed to possess an endonuclease activity utilised to generate transcription primers by cleaving the 5' ends from host mRNAs (Patterson *et al.*, 1984; see section 1.1.8.3.). *Bunyaviridae* L proteins lack extensive sequence homology with the polymerases of other NSVs. However, they contain the four polymerase motifs A-D identified in all RNA-dependent RNA polymerases (Poch *et al.*, 1989; Jin & Elliott, 1992; Ishihama & Barbier, 1994) and also the additional motifs pre-motif A and E (Muller *et al.*, 1994). In particular, all *Bunyaviridae* L proteins contain the amino acid sequence SDD within the C motif, which is the catalytic domain. The SDD sequence is

a common feature of segmented NSVs and ambisense viruses, as opposed to GDD or GDN in the C motif of other viral polymerases (Elliott, 1996).

1.1.7. Attachment and entry

LAC virions that were subjected to proteolytic treatment to remove their surface spikes (i.e. protruding glycoproteins) demonstrated an extensive drop in infectivity (Obijeski *et al.*, 1976), implying that the glycoproteins are necessary for recognition of, attachment to and entry into the host cell. Subsequently, LAC G1 has been proposed as the attachment protein for vertebrate cells. When only G1 was subjected to proteolytic treatment, G2 alone could not mediate infection of vertebrate cells (Kingsford & Hill, 1983). However, Ludwig *et al.* (1989) observed an increased degree of infectivity of invertebrate cells by virions possessing proteolytically-treated G1, leading them to propose that G2 is important in attachment to receptors present on mosquito cells.

The only receptor identified for recognition by a member of the *Bunyaviridae* thus far is the β3-integrin receptor, found to be important in infection by Sin Nombre and New York hantaviruses that cause hantavirus pulmonary syndrome (Gavrilovskaya *et al.*, 1998). Blocking of attachment with the use of ligands or antibodies against the receptor reduced infectivity, whereas transfection of a non-permissive cell line with β3-integrin receptors increased infectivity substantially.

Bunyaviruses have been demonstrated to undergo pH-dependent fusion, presumably related to a change in the structure of the glycoproteins and fusion of the viral envelope with the membrane of the endosome (Gonzalez-Scarano *et al.*, 1984 & 1985; Gonzalez-Scarano, 1985).

1.1.8. Transcription

1.1.8.1. General principles

On infection of the cell, RNA synthesis by members of the *Bunyaviridae* begins with primary transcription, i.e. synthesis of mRNA, which is translated to generate the viral proteins required for subsequent transcription. The genome is then replicated via an antigenome intermediate prior to secondary transcription taking place, which generates the majority of viral mRNA in the cell (Cunningham & Szilagy, 1987). The minimal template for both transcription to generate mRNA and replication is the encapsidated RNA. In the case of the phlebovirus and tospovirus ambisense segments, the genome

RNA is used as a template to generate mRNA for one gene, and the antigenome as a template to generate mRNA for the other gene. Hence, the gene present as a positive-sense copy in the genome requires copying of the genome into the antigenome before its mRNA can be generated.

Negative-sense genome RNA is therefore both transcribed to positive-sense mRNA, which in non-ambisense segments is truncated at the 3' end by approximately 50-110nt relative to the antigenome RNA and possesses a non-templated capped sequence at the 5' end (Bishop *et al.*, 1983; Jin & Elliott; 1993a; Patterson & Kolakofsky, 1984), and copied to full-length positive-sense antigenome RNA (Fig.1.5). The antigenome is then copied back to full-length genome RNA, which is approximately 6-fold more abundant in the cell (Raju & Kolakofsky, 1987b). The genome and antigenome RNA species are both encapsidated by N but mRNA is not (Bouloy *et al.*, 1984). The process of mRNA synthesis by members of the *Bunyaviridae* therefore possesses similarities with that of influenza virus, although mRNA of members of the *Bunyaviridae* is thought not to be polyadenylated and influenza virus mRNA synthesis occurs in the nucleus.

1.1.8.2. Untranslated regions

The coding regions of each segment of every member of the *Bunyaviridae* do not extend to either terminus of the segment. Instead, an untranslated region (UTR) flanks the coding region and is therefore situated at either terminus. The lengths of the UTRs of members of the *Bunyaviridae* range from fewer than 20nt to almost 340nt, with the 5' UTR always being significantly longer than the corresponding 3' UTR (discussed in Dunn, 2000). The termini of the segments of all members of the *Bunyaviridae* possess inverted complementarity which might cause them to hydrogen-bond to form a panhandle structure (Bouloy *et al.*, 1973/74; Samso *et al.*, 1976; Raju & Kolakofsky, 1989). The first eleven nucleotides of the 5' and 3' termini are conserved among all bunyavirus segments. In addition, the subsequent four nucleotides of the 5' and 3' termini of the BUN S and L segments, and three nucleotides of the M segment termini are conserved for each segment in viruses within a serogroup (Elliott, 1990; Elliott *et al.*, 1991).

By analogy with other NSVs, the UTRs of members of the *Bunyaviridae* were thought to contain the *cis*-acting signals necessary for transcription of the genome. Raju & Kolakofsky (1987b) suggested that the encapsidation of the LAC S segment initiates within the 5' UTR (discussed in section 1.2.4.1.). Dunn *et al.* (1995) developed a

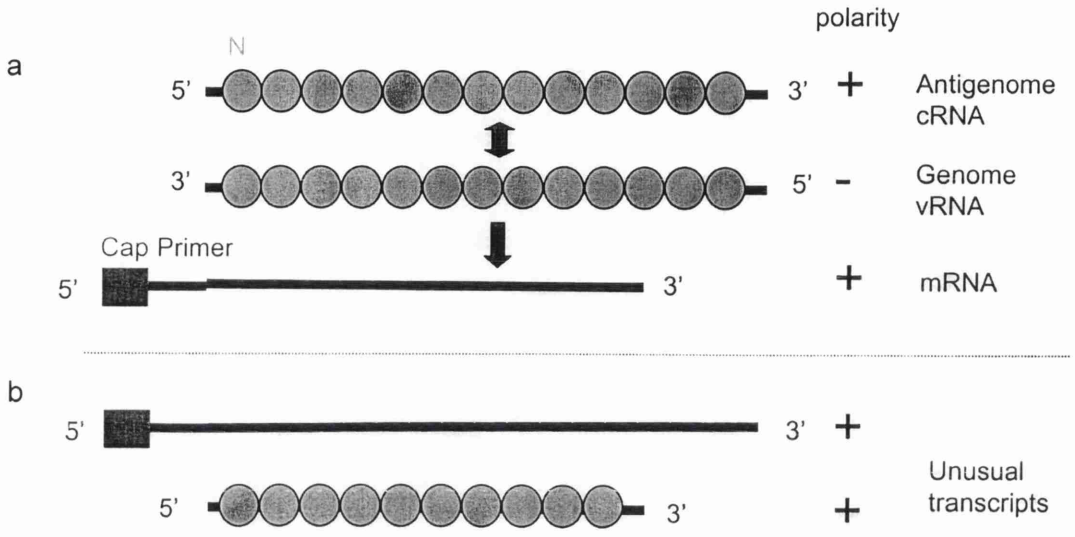

Fig.1.5. Transcription and replication strategies. (a) mRNA synthesis occurs first. During mRNA synthesis, L cleaves a capped sequence from cellular mRNAs and uses this to prime transcription using the negative-sense, encapsidated genome RNA as a template. The positive-sense viral mRNAs therefore possess a capped, heterogeneous sequence at the 5' end. They are also truncated at the 3' end relative to the template RNA and are not encapsidated. On subsequent replication, the encapsidated negative-sense genome of members of the *Bunyaviridae* is copied to a full-length positive-sense antigenome intermediate that is also encapsidated. This is then copied back into full-length negative-sense genome RNA which is encapsidated. (b) Late in LAC infection, a minor population of RNA species were discovered that consisted of full-length, positive-sense RNA that possessed the capped heterogeneous sequence and was unencapsidated, and truncated, positive-sense RNA that lacked the capped sequence but was encapsidated (Raju & Kolakofsky, 1987b). This led to the proposal that encapsidation is initiated at the 5' terminus and is inhibited by the capped heterogeneous sequence.

reverse genetic system for analysis of the *cis*-acting signals involved in BUN transcription by using a negative-sense chloramphenicol acetyltransferase (CAT) RNA flanked by the negative-sense BUN termini (discussed in section 1.1.14.). It was determined that the 5' and 3' UTRs were sufficient for transcription and replication of the recombinant RNA template to take place *in vivo*. Hence, the BUN UTRs were thought to contain the viral promoter and any encapsidation initiation signals necessary for encapsidation and transcription of the RNA. Further work using the reverse genetic system involved the use of termini truncated to the first 20nt of each terminus, or 32nt of the 5' terminus and 33nt of the 3' terminus (Dunn, 2000). The recombinant RNA containing only the first 20nt of each terminus was minimally active as a template, but the RNA containing 32nt of the 5' terminus and 33nt of the 3' terminus was active. Hence, it was determined that the signals essential for transcription are present within the region of RNA from each end of the segment to a point within the first 20-32nt of the 5' terminus, and 20-33nt of the 3' terminus, and that this region must therefore include the viral promoter. Replacement of one of the termini with that from a different segment resulted in an inactive template, suggesting that the 5' and 3' UTRs of different segments are incompatible and that the region beyond the first conserved eleven nucleotides is essential for transcription (Dunn, 2000). When the complementarity of the termini was increased beyond the first eleven nucleotides to include the first 18nt, activity in the assay was restored. Hence, complementarity would appear to be an important feature in the UTRs for providing transcriptional regulatory signals.

The structure of the UTRs is unknown. The high degree of complementarity between the 5' and 3' termini suggests that a strict panhandle structure might exist, involving base-pairing between one terminus and the other. However, intra-strand base-pairing that has been suggested for influenza virus (see section 1.2.3.4.3.) might exist, and a hairpin structure was proposed for Germiston virus RNA (Pardigon *et al.*, 1982). However, mutations in the termini of the BUN S segment used in the reverse genetic system (Dunn, 2000) did not support the corkscrew model proposed for influenza virus panhandles (Flick *et al.*, 1996).

1.1.8.3. Transcription intiation

Transcription of mRNA begins at the 3' end of each segment (Clerx van Haaster *et al.*, 1980; Cash *et al.*, 1979). L is thought to possess endonuclease activity which it uses to cleave the 5' ends of host cytoplasmic mRNAs in a process termed 'cap-snatching'

(Patterson *et al.*, 1984). The resulting 5'-capped fragments are then thought to be utilised to prime transcription in a mechanism analogous to that of influenza virus (detailed in section 1.2.3.4.4.; Krug, 1981; Plotch *et al.*, 1981; Patterson & Kolakofsky, 1984; Kolakofsky & Hacker, 1991). Supporting this theory is the observation that mRNAs of members of the *Bunyaviridae* possess 5' terminal, capped, non-templated extensions of approximately 10-18nt (Bishop *et al.*, 1983; Patterson & Kolakofsky, 1984; Eshita *et al.*, 1985; Ihara *et al.*, 1985; Collett, 1986; Bouloy *et al.*, 1990; Hacker *et al.*,1990; Simons & Pettersson, 1991; Kormelink *et al.*, 1992b; Vialat & Bouloy, 1992; Jin & Elliott, 1993b). Moreover, LAC L was found to cleave foreign RNA at the position expected for the length of the 5' capped extensions (Patterson *et al.*, 1984). However, unlike influenza virus mRNAs, those of the *Bunyaviridae* are thought not to be extensively polyadenylated as they were reported not to bind oligo(dT) cellulose (Cash *et al.*, 1979; Pattnaik & Abraham, 1983; Pattersson *et al.*, 1985).

Jin & Elliott (1993a) characterised the sequences of nontemplated primers present on the 5' termini of BUN S mRNAs generated in infected cells. Of interest was the discovery of a preference for the triplet 'AGU' or 'GGU' at the extreme 3' end of the primer, with a greater preference for the third position than the second, and for the second position than the first. Hence, the sequence from position –3 relative to the template RNA read:

'5'-...AGU AGU AGU...3'

with the 3' three nucleotides of the primer underlined. The authors proposed that the triplet was added by L as it was absent on the corresponding host donor mRNAs. Interestingly both AGU and GGU are able to base-pair with the UCA triplet at the 3' terminus of genome RNA during priming for mRNA synthesis initiation.

Similar preferences exist for other viruses. For instance, influenza mRNAs, which start with the sequence AGCA, prefer primers ending in CA or GCA (Lamb *et al.*, 1981; Shaw & Lamb, 1994). Phlebovirus transcripts starting with ACAC prefer primers ending in AC (Simons & Pettersson, 1991); Nairovirus mRNAs starting with UCUC prefer UC (Jin & Elliott, 1993b). The incorporation of bases mirroring those at the 5' terminus of transcripts was therefore found to be common among the *Bunyaviridae* and was similar to mechanisms utilised by influenza virus for transcript initiation.

1.1.8.4. The 'prime-and-realign' hypothesis

An explanation for the presence of the repeated motif discussed above is a mechanism in which L slips backward on the template shortly after initiation, and the first two or three bases are repeated (Jin & Elliott, 1993b). This 'prime-and-realign' model for primed transcription was also suggested for hantaviruses (Garcin *et al.*, 1995). In hantavirus genomic segments the 3' terminal sequence is AUC AUC AUC, but transcription primers were found with a strong preference only for G at the 3' end. Hence, transcription was proposed to be primed by annealing the priming G to the C at +3 on the template, elongating a few bases and then realigning the chain back four bases such that the priming G was relocated to position –1 relative to the template (Fig.1.6a). The newly-synthesised UAG sequence then anneals to the terminal AUC sequence on the template and transcription elongation commences. Support for a prime-and-realign model for transcription initiation in BUN was provided by Dunn (2000) using the BUN reverse genetic system, in which the deletion of the 3' terminal nucleotide of the BUN S segment was tolerated by L. It was proposed that, if L primed the transcript and then realigned the primer, the deletion would not interfere with transcription initiation as observed.

1.1.8.5. Transcription termination

Treatment of LAC-infected cells with the protein synthesis inhibitors cycloheximide or puromycin resulted in a greatly reduced production of mRNA transcripts. When studied *in vitro*, the S mRNA transcripts synthesised by L under these conditions were found to have terminated prematurely, resulting only in aberrantly short transcripts (Raju & Kolakofsky, 1986). This effect could be reversed by addition of reticulocyte lysate. The authors therefore proposed that transcription was dependent on translation of LAC S mRNA. As a recombinant BUN virus lacking the NSs protein has been successfully generated recently (Bridgen *et al.*, 2001), it would appear that ongoing synthesis of the NSs protein of bunyaviruses is not essential for transcription, thereby implicating the N protein. However, no translation dependency was observed for either GER bunyavirus or Punta Toro phlebovirus transcription (Ihara *et al.*, 1985; Gerbaud *et al.*, 1987). The dependency may therefore actually be for host cellular factors. Aberrant transcripts detected both *in vitro* and *in vivo* were found to terminate at nucleotide 175 (Raju & Kolakofsky, 1986 & 1987a). This region displays homology to a region in proximity to the authentic termination sequence at nucleotide 886 (Bellocq *et al.*, 1987). Disruption

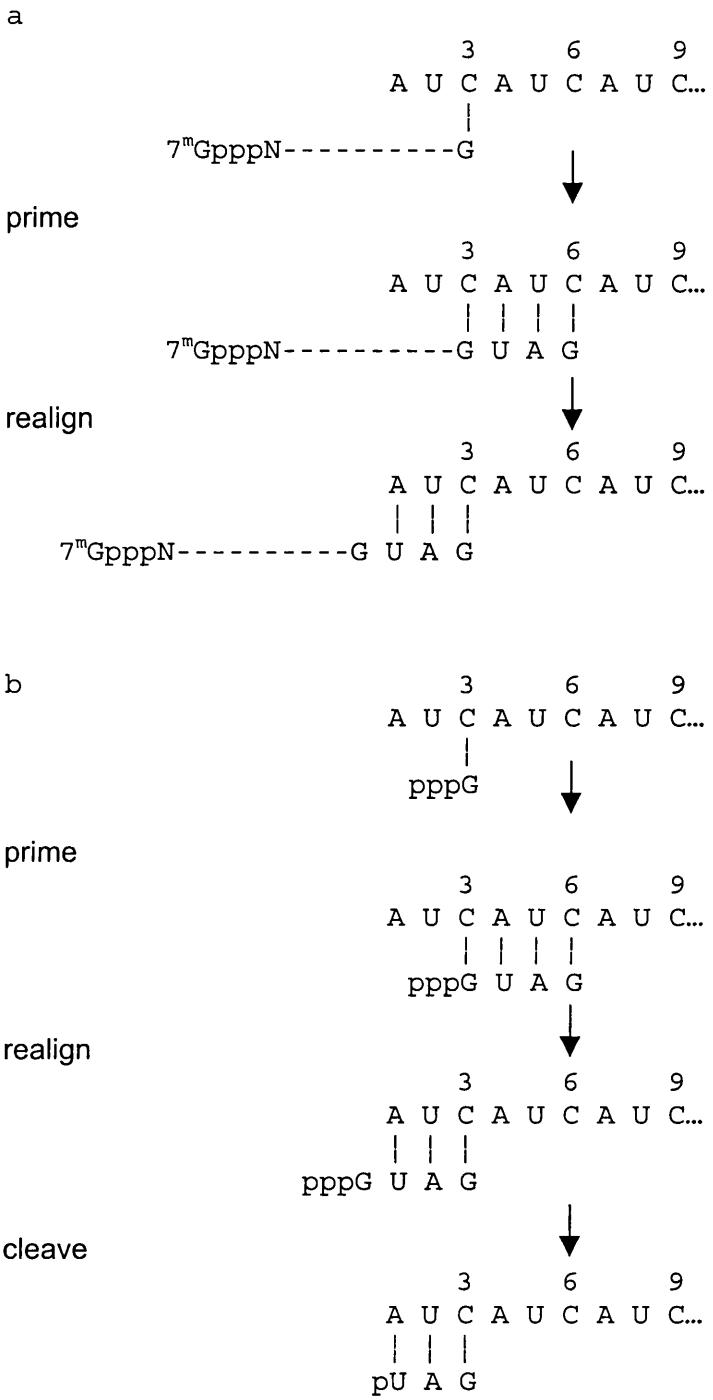

Fig.1.6. Prime-and-realign model for initiation of mRNA synthesis and replication in HTN. Synthesis of mRNA begins with the annealing of a transcription primer on the 3' terminus of genome RNA (a). After synthesis of a few nucleotides the terminal G of the primer is then realigned to position –1 and elongation proceeds. On initiation of replication, a single G is used to prime transcription and is subsequently realigned to position –1 before being cleaved to yield a monophosphorylated U at the 5' terminus of the nascent chain (b). Adapted from Garcin *et al.* (1995).

of putative secondary structure at the aberrant termination site resulted in read-through, whereas the formation of stronger hydrogen bonds increased aberrant transcription termination. In the light of these results the authors propose that secondary structure forms in the nascent RNA chain in the absence of translation and results in premature termination (Bellocq & Kolakofsky, 1987).

Supporting the theory that secondary structure is important in transcription termination is the proposal that the termination of mRNA species from ambisense segments in phleboviruses and topsoviruses involves the formation of a hairpin structure in the intercistronic region (Emery & Bishop, 1987; de Haan *et al.*, 1990), similar to the intergenic region (IGR) that is thought to provide regulatory signals in the similarly ambisense arenaviruses (reviewed in Bishop & Auperin, 1987). Transcription termination signals in bunyavirus S segments have been predicted to be U-rich or GU-rich sequences such as 3'-(G/C)UUUUU-5' (LAC and SSH), 3'-UUGGGUGUUUU-5' (BUN) and 3'-GUUUGU-5' (GER; Patterson & Kolakofsky, 1984; Eshita *et al.*, 1985; Bouloy *et al.*, 1990; Jin & Elliott, 1992). Some members of he *Bunyaviridae* may therefore possess a transcription termination mechanism analogous to that of influenza, in which uridines are thought to disrupt the stability of the polymerase complex on the template RNA (Seong & Brownlee, 1992). In addition, secondary structure in the nascent transcript in BUN transcription may further destabilise L (Kolakofsky & Hacker, 1991). Alternatively, there is evidence that a conserved 3'-CCCACCC-5' sequence signals transcription termination by inducing endonuclease activity in L. This sequence was identified as the termination signal of hantavirus S mRNA and is present to the 3' end of the GU-rich sequences identified in bunyaviruses (Hutchinson *et al.*, 1996; Kolakofsky & Hacker, 1991).

1.1.9. Replication

Replication involves transcription of full-length genome and antigenome RNA which is primer-independent; hence, it requires a switch in the mode of operation of L. This also results in suppression of the transcription termination signals. The switch from mRNA transcription to replicative transcription is unknown but may involve the N protein binding L and changing its replicative mode. Similar to mRNA synthesis, replication of the SSH genome was found to be inhibited by translational inhibitors, demonstrating a requirement for ongoing protein synthesis (Vezza *et al.*, 1979; Eshita *et al.*, 1985). In

some other NSVs replication requires a pool of soluble nucleoprotein (detailed in section 1.2.3.). A similar mechanism, in which N encapsidates transcription primers or interacts directly with L and/or the promoter sequence to inhibit mRNA synthesis and promote replication, may exist for the *Bunyaviridae* (Bishop, 1996). This might also constitute the anti-termination mechanism.

In hantaviruses and possibly also nairoviruses the 'prime-and-realign' model constructed for the initiation of mRNA synthesis has also been proposed to be applicable to genome replication (Garcin *et al.*, 1995). It has not been proposed for the other genera. The difference in the model for replication initiation in hantaviruses is that priming is performed by a single, uncapped pppG (Fig.1.6b). This is annealed at position +3 and subsequently realigned at –1 before being cleaved to yield the pU at position +1 that is observed on the 5' end of authentic antigenome sequences. As initiation with a U has not previously been documented for any viral polymerase and would result in a triphosphorylated U at +1, the presence of the terminal monophosphorylated U implies that priming, realigning and a cleavage event may occur.

1.1.10. Transport, assembly and packaging

As mentioned previously, some hantaviruses and phleboviruses are thought to bud from the plasma membrane, and tospoviruses from the ER (section 1.1.4.), whereas generally the *Bunyaviridae* bud through the Golgi membranes. When analysed by immunofluorescence, glycoproteins and nucleocapsids of UUK were observed to accumulate within the Golgi, with the nucleocapsids localising below the Golgi membrane (Kuismanen *et al.*, 1984). The glycoproteins are thought to heterodimerise in the ER, so are present in the Golgi as dimers (Pettersson & Melin, 1996). The mechanism of Golgi localisation of the glycoproteins is apparently due to a Golgi retention signal present on at least one of the glycoproteins, the other being retained in the Golgi complex by their association. The property of Golgi retention is presumably due to an interaction of the cytoplasmic tail with the Golgi cytoskeleton, the formation of a lattice by the C-terminal tails in the Golgi lumen, or the recycling process in which the viral glycoproteins are transported to and from the plasma membrane (Pettersson & Melin, 1996). The mechanism of transport of the nucleocapsids to the Golgi is unknown. The absence of a matrix protein to provide an association between the glycoproteins and the nucleocapsids in the *Bunyaviridae* means that packaging of nucleocapsids

must occur through another method. One possibility is that nucleocapsids bind the cytoplasmic tail of one of the glycoproteins (Pettersson & Melin, 1996). However, preliminary experiments to attempt to identify an association between the cytoplasmic tail of G2 and the N protein of BUN using a mammalian two-hybrid system did not demonstrate an interaction (S Jacobs, personal communication). The mechanism of packaging the three segments into the virion is also unknown. However, there is evidence that it might be a random event as the three segments are rarely purified from virions in equimolar ratios. The S segment often predominates, perhaps relating to the fact that the S segment is the most abundant segment in the infected cell (Bouloy *et al.*, 1973/74; Obijeski *et al.*, 1976; Gentsch *et al.*, 1977; Bishop & Shope, 1979). In fact, it is thought that bunyaviruses are actually diploid for the S segment (Iroegbu & Pringle, 1981; Rozhon *et al.*, 1981; Urquidi & Bishop, 1992). LAC, UUK and TSWV viruses were all found to contain cRNA segments (antigenome; Raju & Kolakofsky, 1989; Simons *et al.*, 1990; Kormelink *et al.*, 1992a;). Interestingly, the cRNA segments that were found to be packaged in UUK and TSWV were exclusively ambisense segments, i.e. UUK S cRNA and TSWV M and S cRNAs. Hence, the signal for packaging of the segments into the virion has been proposed to be linked to the promoter region of each segment, which in ambisense segments is present in both vRNA and cRNA. The mechanism responsible for the presence of LAC cRNA in virions is unknown but the phenomenon has been reported only for virions produced by insect cells (Raju & Kolakofsky, 1989).

1.1.11. Defective-interfering (DI) RNAs

DI RNAs are generated when deletion or rearrangement takes place during replication of a viral genome (Perrault, 1981). The resulting particles have a replicative advantage over the wild-type genomes due to their reduced size. DI RNAs have been detected in cells infected with bunyaviruses and tospoviruses, and in every case they were found to originate from the L segment (Kascask & Lyons, 1978; Resende *et al.*, 1991; Patel & Elliott, 1992; Scallan & Elliott, 1992; Inoue-Nagata *et al.*, 1998). In bunyaviruses the DI particles have been found to be associated with persistent infection (Patel & Elliott, 1992; Scallan & Elliott, 1992) and in tospoviruses they are thought to be responsible for symptom attenuation (Inoue-Nagata *et al.*, 1992; Resende *et al.*, 1991 & 1992). All bunyavirus and tospovirus DI RNAs characterised have intact 5' and 3' terminal sequences which was to be expected as these harbour the *cis*-acting sequences required for replication. Tospovirus DI RNAs showed a preference for the maintenance

of the reading frame and truncated L proteins could be detected in virions (Inoue-Nagata *et al.*, 1998), whereas in the case of BUN they could not (Patel & Elliott, 1992). Inoue-Nagata (1998) suggested that in tospoviruses the majority of DI RNAs were generated by nonhomologous recombination events and that local secondary structure is important for junction sites, acting by stalling the polymerase and causing it to switch templates. Resende *et al.* (1992) reported that the deleted regions of the L segment were flanked by short sequence repeats, presumably having a similar effect on the polymerase or causing it to jump on the template.

1.1.12. Effects on the host cell

Bunyavirus infection results in morphological changes in the host cell, with proliferation of the Golgi vesicles and similar, less marked effects on the endoplasmic reticulum (Murphy *et al.*, 1973). Despite extensive vacuolisation thought to be due to the viral glycoproteins, the Golgi complex retains its functional integrity. In addition to causing cytopathic infection, bunyaviruses and phleboviruses also produce a persistent, self-limiting infection in mosquitoes and hantaviruses cause a similar persistent infection in rodents, i.e., the reservoir host in each case, although replication can still take place (Calisher, 1991).

1.1.12.1. Persistent infection

Initial non-cytopathic infection of the cell involves an acute phase during which viral RNAs accumulate rapidly in the infected cell. The persistent phase is reached when the viral RNA levels subsequently decline. DI RNAs have been reported to be associated with persistence in BUN-infected mosquito cells (Patel & Elliott, 1992; Scallen & Elliott, 1992). In LAC-infected cells, however, no DI RNAs could be detected and the process was suggested to be due to a gradual structural change in the ends of nucleocapsids which resulted in a decrease in the rate of mRNA synthesis (Rossier *et al.*, 1988; Raju & Kolakofsky, 1989), as well as translational control mediated by N encapsidating its mRNA (Hacker *et al.*, 1989). In another theory, Meyer & Schmaljohn (2000) suggested that replication-incompetent, 3'-truncated segments found to accumulate on persistent infection by Seoul hantavirus are responsible for the self-limiting nature of infection. They proposed that the truncations are attributable to the endonuclease activity of L, and that some cleaved terminal fragments are used to prime transcription, thus

repairing the damaged RNAs and causing the variations in viral RNA synthesis observed in persistently-infected rodent cells.

1.1.12.2. Host cell shut-off

Cytopathic infection by bunyaviruses and phleboviruses results in shut-off of host protein synthesis, although production of virus is ongoing. For instance, BUN infection of BSC-1 cells resulted in almost total shut-off of host protein synthesis within 7h post-infection, whereas viral protein synthesis was detected up to 22h post-infection (Pennington *et al.*, 1977). Raju & Kolakofsky (1988) reported that infection of rodent cells with LAC resulted in the loss of cellular mRNAs due to the induction of mRNA instability. They proposed that the instability was the result of L cleaving the cap from cellular mRNAs. Bridgen *et al.* (2001) determined that BUN NSs contributes extensively to the process of host cell shut-off as a virus lacking NSs (BUNdelNSs) caused only a relatively small reduction in host cell synthesis. The role of NSs in shut-off is currently unknown but is unlikely to be related to its role as an interferon antagonist as Raju & Kolakofsky (1988) found no evidence of the involvement of an interferon-induced pathway.

1.1.13. Evolution

Members of the *Bunyaviridae* undergo a high rate of evolution. This can be explained by the following mechanisms:

- Genetic shift caused by segment reassortment, requiring superinfection of a cell by two different viruses. Reassortment is considered to extensively enhance the potential for evolution in the *Bunyaviridae* by allowing a rapid alteration in adaptation, host range and virulence. It can be demonstrated in the laboratory, in which it has been used to elucidate coding assignments and biological roles of viral gene products, and detected in nature. As an example of the latter, separate assays for M and S segment gene products in six bunyaviruses yielded segregation of the viruses into two separate sets of three different groups, depending on the segment assayed (Casals & Whitman, 1961; Shope & Causey, 1962). This was considered evidence of reassortment between viruses. The generation of reassortants in the laboratory by superinfection with different viruses led to the determination that reassortment is facilitated when viruses are more closely related (reviewed in Pringle, 1996). In addition, heterologous reassortment (between viruses in different serogroups) could not be demonstrated despite extensive

crosses between viruses. This has also been observed in other NSVs (Pringle, 1996). In addition to generating reassortant viruses using superinfection, reassortant virus containing the L and M segments of BUN and the S segment of MAG was rescued entirely from cDNAs by Bridgen and Elliott (1996).

- Genetic drift. This is caused by insertions, deletions, and inversions, as well as a high spontaneous point mutation rate due to the lack of a proof-reading function in the viral polymerase. Recombination is also thought to play a role and may be a mechanism for some types of drift. Similarly to reassortment, recombination requires superinfection of a cell with two related viruses. In RNA viruses recombination is attributable to template switching by the viral polymerase (also called 'copy-choice') and is hence fundamentally different to the breakage and rejoining mechanism performed by enzymes in DNA recombination (Worobey & Holmes, 1999). Recombination is thought to be a tool for repairing damaged viral genomes and increasing pathogenicity. However, the rate of recombination in NSVs is hampered by the tight association of the RNA with the nucleoprotein, restricting the ability of the polymerase to switch templates (Worobey & Holmes, 1999). It has been described in the hantavirus Tula, in which virus homologous recombination was observed in the S segment (Sibold *et al.*, 1999), and has been suggested to be responsible for the generation of tospovirus DI RNAs (Resende *et al.*, 1992; Inoue-Nagata *et al.*, 1998; see section 1.1.11.).

1.1.14. Reverse genetics

Reverse genetic systems are useful tools for elucidating the roles of viral proteins in transcription and replication, and identifying the *cis*-acting signals that regulate these processes (Garcia-Sastre & Palese, 1993). The system involves the reconstitution of an active nucleocapsid *in vivo* from its recombinant constituents. Dunn *et al.* (1995) developed a reverse genetic system for BUN, involving the encapsidation of a recombinant, negative-sense RNA template containing a negative-sense chloramphenical acetyltransferase (CAT) gene by recombinant N protein in cells, and transcription of the template by the viral polymerase. The RNA template is transcribed from the plasmid pBUNSCAT. The negative-sense CAT gene is flanked by the 5' and 3' UTRs of the negative-sense BUN S segment, thought at the time of the development of the system to include all *cis*-acting signals necessary for transcription. The viral proteins are encoded by plasmids transfected into the cells along with the BUNSCAT RNA. They are under the control of a T7 promoter, and T7 polymerase provided by infection with a

recombinant vaccinia virus (Fuerst *et al.*, 1986) or establishment of a cell-line carrying a Sindbis virus-derived replicon (Agapov *et al.*, 1998), both expressing T7 polymerase. Once the RNA is encapsidated by N it serves as a transcription template for L, which has been shown both to transcribe the RNA to generate mRNA and to replicate the template using a positive-sense intermediate. Transcription results in a functional mRNA containing a positive-sense CAT transcript, which is then translated to yield the CAT protein, detected by its ability to acetylate chloramphenicol in the presence of acetyl Co-A. The BUN reverse genetic system has been utilised to investigate protein function and signals within the 5' and 3' UTRs necessary for transcription.

1.1.15. Virus rescue

An infectious clone of BUN was rescued from cloned cDNAs by Bridgen and Elliott (1996). This was the first time that a segmented NSV had been rescued entirely from cDNAs and BUN remains the only member of the *Bunyaviridae* that has been rescued. Virus rescue involves the assembly of an active, infectious virion from recombinant components *in vivo* and, as such, is an extension of the reverse genetic system in that it allows the functions of viral components to be studied by reconstituting a functional system. Rescue of BUN entirely from cDNAs initially involved the expression of all viral proteins under the control of modified T7 promoters and transcription of all three viral segment RNAs with ribozyme sequences, also under the control of modified T7 promoters. T7 polymerase was provided by recombinant vaccinia virus. Hence, the procedure involved the transfection of six plasmids into a single cell and the subsequent correct expression, processing and assembly of viral components into an infectious virion. Bridgen *et al.* (2001) have subsequently rescued BUN lacking the NSs protein. The phenotype of this virus is described in section 1.1.6.2.

1.2. The role of the nucleoprotein in encapsidation and replication in RNA viruses

Encapsidation or coating of the viral genome is thought to have many roles including protection of the genome, preventing secondary structure and forming a transcriptionally active complex with genomes belonging to NSVs. It is increasingly apparent that the nucleoproteins of NSVs play a central role in the infectious cycle, including their implication in the switch from mRNA synthesis to replication.

1.2.1. Encapsidation in HIV-1 (*Retroviridae*)

The retrovirus HIV-1 possesses a genome comprising two positive-sense RNA molecules. On infection these are reverse-transcribed into double-stranded DNA that is then integrated into the host genome. The 55-amino acid, multi-functional nucleocapsid protein NCp7 is a proteolytic product of the polyprotein Gag. Its various functions include participation in the annealing of tRNA to the genome to prime reverse transcription, dimerisation of genomic RNA, encapsidation of the viral genome (all reviewed in Darlix *et al.*, 1995) and regulation of the reverse transcriptase (Berat *et al.*, 1993). Encapsidation involves both modestly specific binding to an encapsidation signal and nonspecific binding to the rest of the genome. NCp7 contains two CCHC-type zinc finger motifs with the general structure:

$$Cys\text{-}X_2\text{-}Cys\text{-}X_4\text{-}His\text{-}X_4\text{-}Cys$$

where X is any amino acid (Henderson *et al.*, 1990; Fig.1.7a). These were found to participate in binding to the encapsidation signal, which consists of four stem-loops, SL1-4, and is designated the psi-sequence (Fig.1.7b). Whilst all stem-loops have been implicated in binding, SL3 is sufficient to direct the packaging of heterogeneous sequences into virus-like particles (Hayashi *et al.*, 1992). Binding of NCp7 to SL3 has been investigated using nuclear magnetic resonance spectroscopy (de Guzman *et al.*, 1998). A sequence to the amino-terminal side of the zinc fingers forms a helix which lies along the major groove of the A-helix formed by the stem of SL3 (Fig.1.7). Contacts are made non-specifically with the phosphate backbone of the stem in the positions shown in boxes. In addition, three of the four bases that form the loop of SL3 are bound specifically by hydrophobic pockets formed by residues in both zinc fingers, and a basic

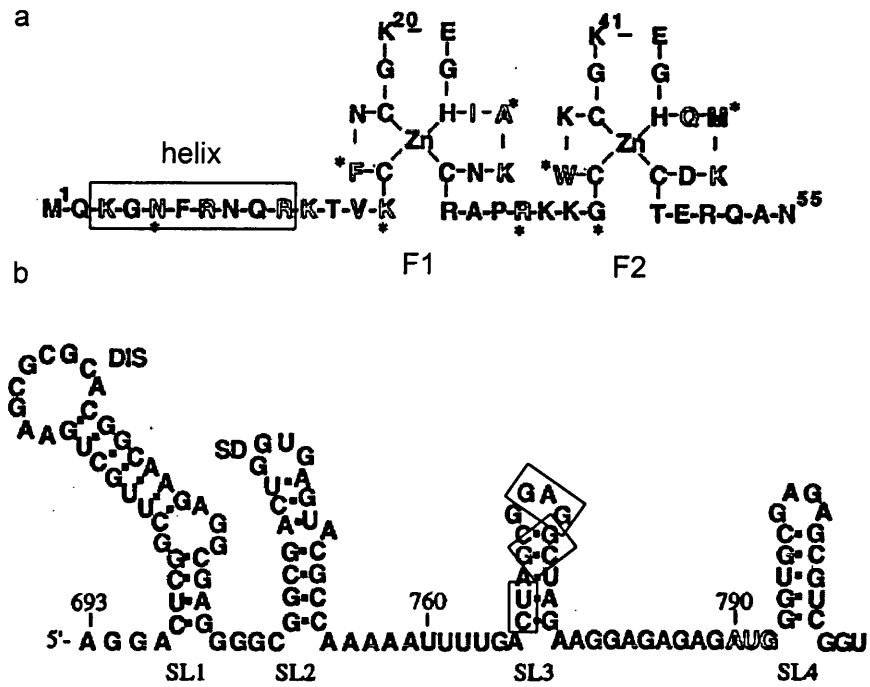

Fig.1.7. Encapsidation by HIV-1 NCp7. NCp7 sequences involved in binding the SL3 RNA domain consist of two zinc finger motifs, F1 and F2, and an amino-terminal tail that forms a helix (a). The psi sequence recognised by NCp7 consists of four stem-loops (b). Binding of SL3 by NCp7 has been elucidated and involves the amino-terminal tail binding the major groove of the helix formed by the stem of SL3. Important residues are shown as hollow letters. Interactions are made with the phosphate groups of the bases that are boxed. The A and second and third Gs (boxed) in the loop are bound by both zinc fingers and residue R32. Adapted from de Guzman *et al.* (1998).

residue in the sequence between them. Interestingly, the Asn residue in the amino-terminal helix is also capable of specific interaction with bases in the stem-loop.

1.2.2. Encapsidation in positive-strand viruses

1.2.2.1. Introduction and general features

The major difference between positive and negative-strand viruses is that negative-strand viruses must transcribe mRNA using their genome as a template for synthesis, whereas in the case of most positive-strand viruses the genome itself is utilised as the mRNA on infection. This has the result that most positive-strand virus genomes are themselves infectious. Genomes are tightly encapsidated by a coat or core protein. The encapsidation initiation signals for some positive-strand viruses are generally more extensively studied and the encapsidation mechanism better understood than for any NSV.

In positive-strand viruses a common feature of the coat or core protein is a high proportion of lysine and arginine residues, resulting in a high positive charge (Khromykh & Westaway, 1996). Both sequence specific and non-specific binding have been reported for a number of proteins, for instance in turnip crinkle virus, in which specific and non-specific binding have been suggested to occur at separate, distinct sites on the coat protein (Wei & Morris, 1991).

Sequence-specific or preferential binding can involve the 3' UTR, for instance in the plant viruses brome mosaic virus (Duggal & Hall, 1993), alfalfa mosaic virus (Reusken *et al.*, 1994) and turnip crinkle virus (Wei & Morris, 1991), and the coronavirus infectious bronchitis virus (Zhou *et al.*, 1996). In the flavivirus Kunjin the terminal sequences were bound specifically (Khromykh & Westaway, 1996). Binding to leader RNA located at the 5' terminus of genomic and subgenomic RNA has been reported for another coronavirus, mouse hepatitis virus (Stohlman *et al.*, 1988), and selective binding to an internal site was reported for southern bean mosaic virus (Hacker, 1995). It is notable that in tobacco mosaic virus, alfalfa mosaic virus, mouse hepatitis virus, infectious bronchitis virus, turnip crinkle virus and southern bean mosaic virus, the binding was proposed to be attributed to secondary structure in the RNA, particularly stem loops (Stohlman *et al.*, 1988; Wei & Morris, 1991; Reusken *et al.*, 1994; Hacker *et al.*, 1995; Zhou *et al.*, 1996; Butler, 1999; Wang & Simon, 2000). In infectious bronchitis virus stem-loop structures were found to increase binding specificity (Zhou *et al.*, 1996).

1.2.2.2. Tobacco mosaic virus

One of the best-understood encapsidation mechanisms in positive-strand RNA viruses is that of the rod-shaped tobacco mosaic virus (TMV; reviewed in Butler, 1999). The encapsidation signal is called the origin of assembly sequence (OAS) and consists of a stem-loop structure with a guanine in every third position for 18nt, located 0.9kb from the 3' terminus. It interacts with coat protein present in a disc structure, with approximately 17 monomers per disc (Fig.1.8). The OAS is inserted into the central hole of the disk where it is bound specifically. The stem of the OAS then melts to allow the interaction of the rest of the genome with the coat protein. The interaction causes the coat protein to dislocate into a 'locked washer', proto-helical conformation. During this event the two rings that make up each disc condense and seize the genomic RNA between them. As more proteins are recruited to the helix the coat protein assembles around the RNA, which becomes trapped within the growing helix. Assembly is then bi-directional. Elongation of nucleation in the 5' direction involves the RNA being encapsidated as a 'travelling loop' structure and the addition of complete disc structures onto the helix. The 3' end of the genome is packaged more slowly as the the RNA must be drawn through the hole in the centre of the helix, and does not involve the addition of discs. Bacteriophage R17 packaging takes place in essentially the same way (reviewed in Witherell *et al.*, 1991).

1.2.3. Replication and encapsidation in negative-strand viruses

1.2.3.1. Introduction

Similarly to members of the *Bunyaviridae*, all other NSVs also perform transcription by synthesising unencapsidated mRNA from the encapsidated negative-sense genome RNA, and replicate their genome using an encapsidated positive-sense antigenome as a replicative intermediate. NSVs possess conserved, complementary terminal sequences within which the *cis*-regulatory signals for transcription reside.

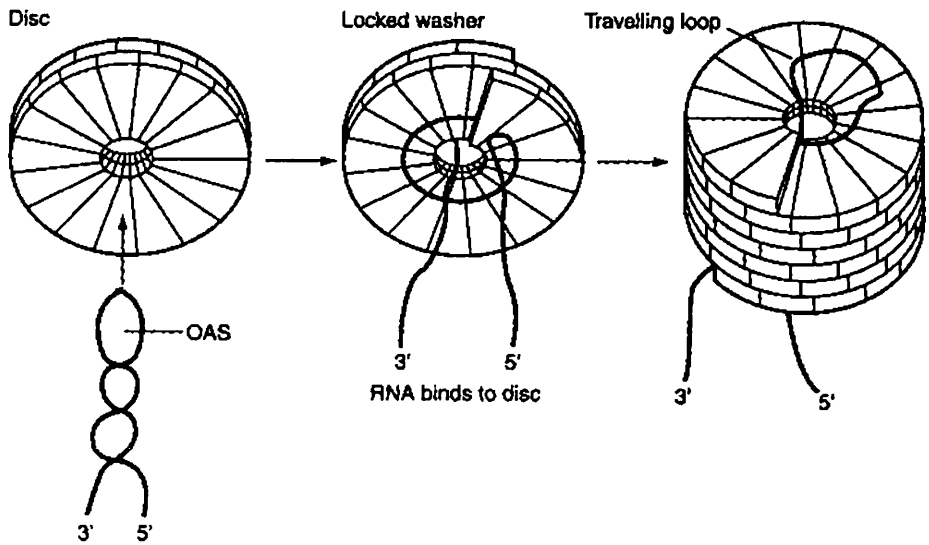

Fig.1.8. Assembly of tobacco mosaic virus particles. From Cann (1997). The origin of assembly sequence (OAS) consists of a stem-loop that is inserted into the hole in the centre of a coat protein disc. Binding of the RNA in the groove between protein rings results in a conformational change in the disc, which takes on a locked washer structure and traps the RNA. Coat protein i then added to the structure bidirectionally, with discs being added on elongation in the 5' direction and monomers added in the 3' direction.

1.2.3.2. Nonsegmented NSVs: *Rhabdoviridae*

1.2.3.2.1. VSV transcription

Viruses in the *Rhabdoviridae* family possess two species of leader RNA, complementary to the 3' end of the genomic or antigenomic RNAs. During transcription to make mRNA, vesicular stomatitis virus (VSV) polymerase transcribes the 47nt leader RNA from the 3' end of the genome. The separate mRNAs are then transcribed in the order that they appear in the genome by the polymerase (L) terminating and re-initiating transcription. The polymerase complex possesses methyltransferase activity (Horikami & Moyer, 1982; Horikami *et al.*, 1984; Hercyk *et al.*, 1988) and is thought to mediate the capping of viral mRNA, which can only occur in *cis* (Rose, 1975; Moyer & Banerjee, 1976; Hercyk *et al.*, 1988;). In fact, the process might be attributable to the GTP/GDP binding ability of the polymerase-associated cellular translation elongation factor, EF-1 (Das *et al.*, 1998). Theories involving the process of capping in VSV suggest that capping occurs following de novo transcript initiation (Chanda & Banerjee, 1981), or that a polymerase-mediated cleavage event occurs prior to capping and initiation of transcription (Shuman, 1997). The capping/methylation events were found to be separable from initiation and it was proposed that L undergoes abortive transcription if a transcript is not modified properly (Stillman & Whitt, 1999).

1.2.3.2.2. VSV replication

VSV replication requires a pool of soluble N protein, leading to the proposal that N is involved in the switch from transcription to replication and which might be attributable to the binding of N to the nascent RNA chain (Wertz *et al.*, 1987). Replication was found to require an association of L with an N-P complex, whereas transcription does not require the N protein but is dependent on the L protein complexing with two or three monomers of P (Das *et al.*, 1997).

1.2.3.2.3. VSV encapsidation

The helical VSV nucleocapsid is fully resistant to digestion with ribonuclease. The 49kD VSV N protein is capable of assembling into nucleocapsid-like structures when expressed alone (Sprague *et al.*, 1983). N possesses a 10-fold higher affinity for positive-sense leader RNA, which is thought to contain the encapsidation signal, than for a non-specific sequence (Blumberg *et al.*, 1983). N was originally thought to initiate

encapsidation within the first 14-17nt of the nascent positive-sense leader RNA (Blumberg *et al.*, 1983; Giorgi *et al.*, 1983; Moyer *et al.*, 1991; Smallwood & Moyer, 1993). This region of the leader RNA possesses an adenine at every third position, which may be important in the binding of N to the encapsidation initiation signal (Nichol & Holland, 1987), thus:

5'-ACGAANACNANNAAA-3'

where N differs between VSV isolates. This region is predicted to be unstructured which is proposed to aid recognition by N. However, Moyer *et al.* (1991) suggested that encapsidation is initiated at nucleotides 14-16 of VSV leader RNA and that encapsidation then progresses bidirectionally. Both encapsidation and replication were found to require the C-terminal 5 amino acids of VSV N (Das *et al.*, 1999). In VSV-infected cells it was proposed that P provides N with sequence-specific RNA binding properties (as opposed to sequence-selective binding) and keeps it in a replication-competent state (Masters & Banerjee, 1988; Howard & Wertz, 1989; La Ferla *et al.*, 1989; Takacs *et al.*, 1993). VSV P protein was also suggested to act as a transient binding site for N by mimicking the RNA template, thereby allowing N to be transiently removed from the template during transcription to allow the viral polymerase access to the bases (Hudson *et al.*, 1986).

1.2.3.2.4. Rabies virus encapsidation

Rabies virus N protein was found to bind specifically to an encapsidation signal within nucleotides 20 to 30 of the leader RNA sequence (Yang *et al.*, 1998). Similarly to VSV, affinity for the leader RNA was found to be five to ten-fold higher than that for non-specific RNA, and it was suggested that adenine-rich sequences are important for encapsidation, the proposed encapsidation sequence being:

5'-AAGAAAAAACA-3'

This is also predicted to be unstructured. Rabies virus P protein was found to increase the specificity of N for the leader sequence by preventing the interaction of N with non-leader RNA (Yang *et al.*, 1998).

Again, rabies virus N was implicated in the switch from transcription to replication, preventing its use in initiating transcription (Wunner, 1991). This was proposed to be through its encapsidation of leader RNA. Indeed, following synthetic dephosphorylation of rabies virus N or expression of unphosphorylated N its affinity for the leader RNA was found to increase, and a decrease in the rates of transcription and, to a lesser extent, replication was observed (Yang *et al.*, 1999). Hence, N appears to regulate transcription and replication by modulation of leader RNA encapsidation. The reason for the decrease in replication was not immediately apparent but has been suggested to be due to unphosphorylated N affecting the interacting the interaction of L with the template RNA.

Recently, a low-resolution 3D reconstruction of recombinant rabies virus N-RNA complexes was generated by averaging electron micrographs of the complexes (Schoehn *et al.*, 2001). Similarly to images of reconstituted influenza virus complexes, rabies N could be seen to assemble into ring structures on short RNAs, with 9 to 11 monomers present in each ring (Fig.1.9, a-d). N was found to assemble into helical structures on binding longer RNAs, resembling those visualised in infected cells. Importantly, the 3D reconstruction of complexes led to an understanding of the structure of N and how it multimerises. N appears to be present as a bi-lobed structure similar in shape to a kidney. As expected, each monomer has at least two sites of contact with each neighbouring monomer, situated either side of the top and bottom of each lobe. There is no contact between adjacent central regions of monomers. The location of the RNA on the structure could not be distinguished but when the positions of P proteins on the structure and the size of the perimeter of the ring structures was taken into consideration, the authors proposed that the RNA is present at the top of the rings. A significant difference was observed between the structure of N-RNA complexes in infected cells and virions, also observed in VSV (Nakai & Howatson, 1968; Newcomb *et al.*, 1982). This is explained by the ring structure, with approximately ten monomers per turn, converting in the presence of longer RNA into a loose helical structure with 15 monomers per turn observed in infected cells (Fig.1.9, e & f). On packaging into virions the helix is condensed into a tighter structure with approximately 54 monomers per turn. This requires an 18 degree difference in the angle of N which then places the RNA on the inside of the intra-virion nucleocapsid. The model is consistent with a model for VSV packaging (Nakai & Howatson, 1968). In VSV the process of condensation is thought to be attributable to the matrix protein (Newcomb & Brown, 1981).

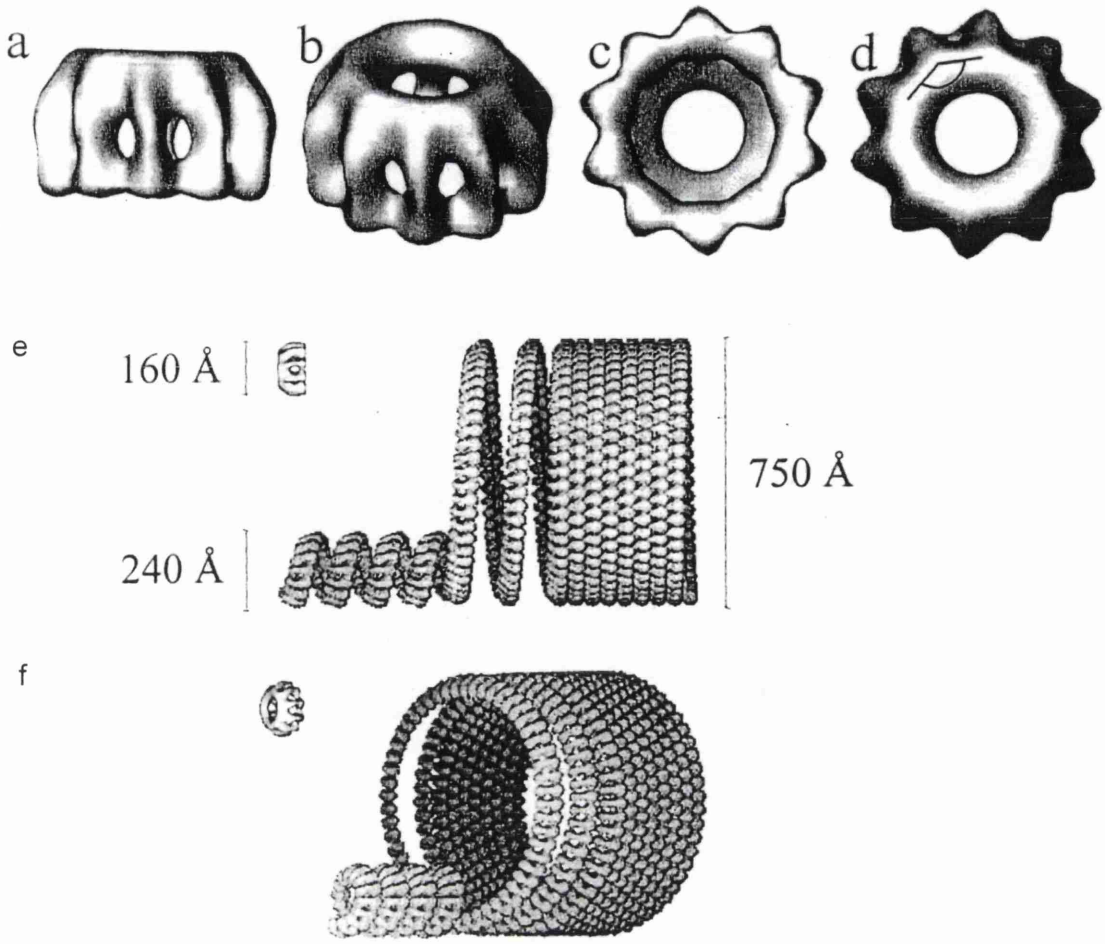

Fig.1.9. Models of rabies virus N-RNA complexes. 3D reconstructions of N-RNA rings are shown from the side (a), tilted (b), from underneath (c), and from above (d). The bi-lobed structure of N is visible, with each N monomer having two binding sites for each neighbouring monomer. The model for the structure of the nucleocapsid is shown in (d), and at an angle in (e). The 240A-diameter structure of free nucleocapsids is depicted adjacent to the 160A-diameter N-RNA ring structure and the 750A-diameter structure of nucleocapsids as they are thought to exist in virions. From Schoehn *et al.* (2001).

1.2.3.3. Nonsegmented NSVs: *Paramyxoviridae*

1.2.3.3.1. Transcription in *Paramyxoviridae*

NP has been implicated in the switch from transcription to replication in both Sendai virus (SeV) and measles virus; in the latter case, measles virus N protein was demonstrated to bind the viral polymerase and thereby regulate replication and nucleocapsid assembly (Bankamp *et al.*, 1996). SeV replication requires a pool of NP bound to P but not to RNA (Horikami *et al.*, 1992). P is thereby thought to act as a chaperone to prevent NP multimerising until it is bound to RNA, at which point P dissociates from NP (Curran *et al.*, 1995). It has been proposed that P mimics the RNA template in order to transiently remove NP from it, reflecting the function proposed for VSV P (Myers & Moyer, 1997).

1.2.3.3.2. Encapsidation in *Paramyxoviridae*

Similarly to VSV nucleocapsids, those of SeV are resistant to digestion by ribonuclease. The 58kD SeV NP protein can assemble into nucleocapsid-like structures when expressed alone (Buchholz *et al.*, 1993 & 1994). The same property was observed in measles virus N protein in both insect and mammalian cells (Spehner *et al.*, 1991; Fooks *et al.*, 1993). The model of encapsidation in SeV concerns sequence-specific binding of NP to the 54nt leader RNA followed by co-operative assembly of NP on the growing RNA chain via non-specific interactions with the RNA (Lamb & Kolakofsky, 1996).

1.2.3.4. Segmented NSVs: Influenza virus

1.2.3.4.1. Influenza virus NP-RNA interactions

Influenza virus contains eight segments of negative-sense RNA. The nucleoprotein (NP) is expressed as both a 56kD and a lower-molecular weight form in infected cells (Becht & Weiss, 1991; Zhirnov & Bukrinskaya, 1984). NP is associated with infected cell membranes, exposed at the cell surface and secreted (Yewdell *et al.*, 1981; Cook *et al.*, 1988; Stitz *et al.*, 1990; Prokudina & Semenova, 1991). It has also been found to associate with actin to retain influenza virus nucleocapsids in the cytoplasm (Digard *et al.*, 1999).

Influenza virus NP demonstrates a single-stranded RNA-binding property that appears to have no sequence-specificity (Scholtissek & Becht, 1971; Kingsbury *et al.*, 1987; Yamanaka *et al.*, 1990; Baudin *et al.*, 1994); increased affinity observed for the 5' end of segment RNA was considered 'hardly significant' (Baudin *et al.*, 1994). Influenza virus nucleocapsids are totally susceptible to digestion by ribonucleases, in contrast to VSV nucleocapsids, suggesting that the RNA is located on the outside of the NP (Duesberg, 1969; Pons *et al.*, 1969; Baudin *et al.*, 1994). NP was reported to bind viral RNA co-operatively with a dissociation constant of $2x10^{-8}$M (Yamanaka *et al.*, 1990; Baudin *et al.*, 1994; Digard *et al.*, 1999) and was originally found to bind to a limited degree through a site in its N-terminus (Kobayashi *et al.*, 1994; Albo *et al.*, 1995). Subsequently RNA-binding sites were discovered throughout the protein, leading to the suggestion that high-affinity binding requires the interaction of multiple regions of the protein (Elton *et al.*, 1999b). The multiple contacts made between NP and RNA were proposed to drive the conformational change that NP was observed to undergo on binding RNA. Influenza virus NP possesses a large number of basic residues divided over the primary structure without clustering. The positive charges of lysine and arginine are thought to make electrostatic contacts with the phosphate-sugar backbone of the RNA molecule, with the phosphate groups protected in a general manner without definite footprints (Baudin *et al.*, 1994). Elton *et al.* (1999b) suggested that planar interactions between aromatic side chains and the bases also occurs. It is interesting to note that the degree of binding of NP to viral RNA increased with the length of the template; an RNA of length 12nt was not bound at all, whereas 100% of a 17nt RNA was bound (Yamanaka *et al.*, 1990).

1.2.3.4.2. Influenza virus NP-NP interactions

NP was found to form oligomers *in vitro* (Ruigrok & Baudin, 1995) and dimeric and trimeric forms have been detected in infected cells (Prokudina-Kantorovich & Semenova, 1996). The oligomers observed in infected cells were determined to be sensitive to boiling and took approximately 10min to form (Prokudina-Kantorovich & Semenova, 1996). *In-vitro* translated NP was demonstrated to interact with immobilised NP-fusion proteins in an assay that allowed the removal of contaminating nucleic acids (Elton *et al.*, 1999a). NP could self-associate in the absence of RNA implying that RNA is not required for the interaction. The dissociation constant was calculated as approximately $2x10^{-7}$M, characterising the interaction as approximately 10-fold weaker

than the interaction between NP and RNA, and leading the authors to suggest that NP binds RNA prior to oligomerising. The interaction took place in the centre and C-terminal regions of the protein, although interestingly the C-terminal 23 residues inhibited oligomerisation. Removal of this region resulted in an increase in self-association but a decrease in transcription *in vivo*, and removal of the C-terminus increased binding to the viral polymerase protein PB2. Hence it would appear to act as a general regulatory element (Biswas *et al.*, 1998; Elton *et al.*, 1999a). Theories to explain the function of the C-terminal domain include its involvement in obscuring interacting regions, changing the protein's conformation or sequestering cellular factors (Biswas *et al.*, 1998). Oligomerisation of NP was found to have the effect of increasing its hydrophobicity, which was proposed to be responsible for its ability to associate with cell membranes (Prokudina-Kantorovich & Semenova, 1996).

1.2.3.4.3. Influenza virus nucleocapsid structure

The nucleocapsid adopts a double helical structure that persists when RNA is removed and is thus thought to be attributable to NP, as NP self-assembles into coiled structures analogous to nucleocapsid structures (Pons *et al.*, 1969; Ruigrok & Baudin, 1995). Ortega *et al.* (2000) studied reconstituted influenza virus nucleocapsids by electron microscopy and image processing. They obtained an image of circular or elliptic toroidal structures believed to be NP-RNA complexes, and resolved the polymerase complex on the outside of the structure (Fig.1.10). The structures apparently appeared as circles only because relatively short RNAs were used; longer RNAs would presumably have yielded helical structures. Typically ten to twelve NP monomers could be observed in each ring. However, the highest replication efficiency was obtained with even numbers of NP monomers, leading them to propose that NP is incorporated as a dimer. Supporting the theory was the detection of NP dimers in influenza virus-infected cells (Prokudina-Kantorovich & Semenova, 1996). This is in contrast to the observation that NP has a higher affinity for RNA than for itself (Elton *et al.*, 1999a).

The termini of each RNA segment are inversely complementary which might be important in recognition of segments on packaging into virions (Desselberger *et al.*, 1980; Hsu *et al.*, 1987). Although the terminal sequences were found to be base-paired in free RNA, thereby forming a panhandle structure, binding of NP was reported to melt the secondary structure, separating the strands and exposing the bases to the solvent (Baudin *et al.*, 1994). A fork-like structure with separation of the extreme terminal

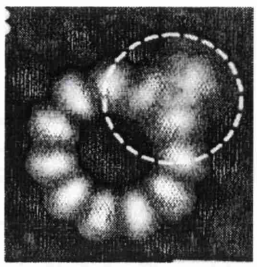

Fig.1.10. Averaged electron micrograph of influenza virus NP binding RNA. Twelve NP monomers can be visualised in a ring. The polymerase complex is resolved on the outside of the ring structure, depicted within a broken circle. From Ortega *et al.* (2000)

sequences was proposed by Fodor *et al.* (1995). Subsequently the terminal sequences were suggested to form a corkscrew conformation (or 'binary hook') on recognition by the polymerase complex (Flick *et al.*, 1996; Flick & Hobom, 1999). A similar hook structure has also been proposed for the Thogoto orthomyxovirus vRNA terminal sequences; however, a panhandle structure was demonstrated in the cRNA and no evidence for a hook structure was found (Leahy *et al.*, 1997 & 1998; Weber *et al.*, 1997). The structure of influenza virus termini would therefore appear to be dynamic, with NP playing a major role in the transition between structures.

1.2.3.4.4. Influenza virus transcription and replication

Influenza virus transcription and replication occur in the cell nucleus (Herz *et al.*, 1981; Jackson *et al.*, 1982). Transcription to make mRNA utilises the cap-snatching activity assigned to the polymerase complex, a relatively well-defined process in influenza virus. Binding of the polymerase complex to the 5' vRNA template activates the recognition of cellular cap structures by the PB2 subunit of the polymerase complex (Tiley *et al.*, 1994; Cianci *et al.*, 1995). Interaction with the 3' terminal sequences through the panhandle structure and binding of the PB1 subunit to RNA then result in the activation of endonuclease activity and the cap structure plus a short 5' sequence is cleaved from the cellular RNA (Hsu *et al.*, 1987; Hagen *et al.*, 1994). The cRNA template was found to be incapable of stimulating cap-snatching (Leahy *et al.*, 1998). The resulting capped sequence is then utilised to prime transcription (Braam *et al.*, 1983).

The initiation of replicative transcription requires a switch from mRNA transcription. Soluble NP (not associated with RNA) is required for replication, but not mRNA transcription, to take place, leading to the proposal that NP regulates the polymerase complex (Beaton & Krug, 1986; Shapiro & Krug, 1988). In addition, the RNA-binding property of N was found to be essential for replicative transcription (Medcalf *et al.*, 1999). The nature of the switch is not yet understood but some theories exist. NP might alter the function of the polymerase complex through direct contact with it (Biswas *et al.*, 1998; Mena *et al.*, 1999), or interact with the promoter and modify the transcription signals (Fodor *et al.*, 1994; Hsu *et al.*, 1987; Klumpp *et al.*, 1997). Alternatively NP might only act by cotranscriptionally encapsidating segments (Shapiro & Krug, 1988).

Influenza virus mRNA is truncated and polyadenylated relative to full-length segments. Polyadenylation is thought to take place because the polymerase complex stays bound

to a sequence upstream of the polyuridine sequence, preventing processive transcription through it (Tiley *et al.*, 1994; Poon *et al.*, 1998; Pritlove *et al.*, 1998). NP has also been implicated in this process (Honda *et al.*, 1988).

1.2.4. Encapsidation in the *Bunyaviridae*

1.2.4.1. Location of a proposed encapsidation initiation signal

In bunyavirus-infected cells unencapsidated mRNA and full-length, encapsidated genome and antigenome RNAs are detected. The fact that mRNA is truncated by approximately 100nt at the 3' end relative to antigenome RNA implicates the 3' end of positive-sense RNA in the encapsidation process. However, in LAC-infected cells the detection of a low proportion of interesting 'unusual' transcripts was reported late in infection (Fig.1.5; Raju & Kolakofsky, 1987b). Normal LAC genome and antigenome-sense S segments are 983nt long, whereas S-mRNA runs from approximately nt –15 (due to the non-templated primer) to nt 886. The unusual transcripts consisted of encapsidated mRNAs (nt -15 to 886), encapsidated positive-sense RNA from nt 1 to 886, and unencapsidated positive-sense RNA from nt –15 to 983. The detection of the latter two RNA species led the authors to speculate that the origin of nucleocapsid assembly is located at the 5' end of positive-sense LAC transcripts. They suggested that the presence of the non-templated primer on the 5' end hindered encapsidation by placing the recognition sequence out of context, or by recruiting a cytoplasmic cap-binding factor and masking the site.

Raju & Kolakofsky (1989) addressed the question of how the ends of segments can be base-paired when they are encapsidated by N in the nucleocapsid. They suggested that N is either displaced from the RNA or remains attached to the ribose-phosphate backbone, the latter implying sequence-nonspecific binding in the fashion observed for influenza virus NP (Baudin *et al.*, 1994). However, they stressed that N would be unlikely to dissociate from the complex because of putative interactions with other N proteins.

The proposed existence of an encapsidation initiation signal within the UTRs was supported by the reverse genetic system developed for BUN by Dunn *et al.* (1995; section 1.1.14.). Using this system it was determined that the 5' and 3' UTRs are sufficient to provide the signals required for transcription and replication of a recombinant segment RNA template. In addition, the signals were mapped to the

stretch of RNA from each end of the RNA to the terminal 20-33nt of each UTR (Dunn, 2000).

1.2.4.2. Hantavirus N-RNA interactions

Expression of HTN M and S segment RNA in cells by recombinant baculovirus or vaccinia virus resulted in the assembly of nucleocapsid-like and virus-like particles (Betenbaugh *et al.*, 1995). This suggested that N was able to assemble into authentic structures on its own, similar to the properties observed by nucleoproteins of other NSVs. Agarose GEMSA of Puumala virus (PUU) bacterially-expressed, His-tagged N-ssRNA complexes indicated the formation of complexes that shifted further up the gel with increasing protein concentration, indicating an increase in size of the complexes (Gött *et al.*, 1993). No sequence-specific binding was reported with hantavirus N *in vitro* on preincubation with the competitor RNA species tRNA and polyU RNA and with the first 520nt of the 5' negative-sense PUU S segment as the radiolabelled RNA. However, a preference was found for double-stranded nucleic acids as polyA/U RNA and salmon sperm DNA competed fully. In addition, a partially double-stranded RNA template consisting of 520nt of the 5' negative-sense PUU S segment annealed to 308nt of the 3' terminus formed large complexes with PUU N that were shifted to the top of an agarose gel on GEMSA ('well-shift'). This was proposed to imply co-operative binding (Gött *et al.*, 1993). The 'well-shift' could not be mediated by the 5' terminal sequences alone and the profile of binding to the 5' terminal sequences was not distinguishable from that to RNA lacking the terminal sequences.

1.2.4.3. Implications for encapsidation and regulation of replication in BUN

By analogy to other nucleocapsid proteins, BUN N probably encapsidates RNA by interactions with both the RNA and other N monomers. It is also likely to play a role in the regulation of replicative transcription. However, as mentioned previously, BUN N contains no consensus RNA-binding domain and little homology with other N proteins outside the *Bunyavirus* genus. Amino acid sequence alignment of 19 bunyaviruses from three serogroups indicates that the C-terminal half of the protein is more highly conserved (Fig.1.11), which is surprising as the N-terminal half shares its part of the gene with the NSs ORF. However, hantaviruses and nairoviruses, none of which encode an NSs protein, have also been reported to have high degrees of conservation in the C-termini of N proteins (section 1.1.6.1). A region of low homology is present in

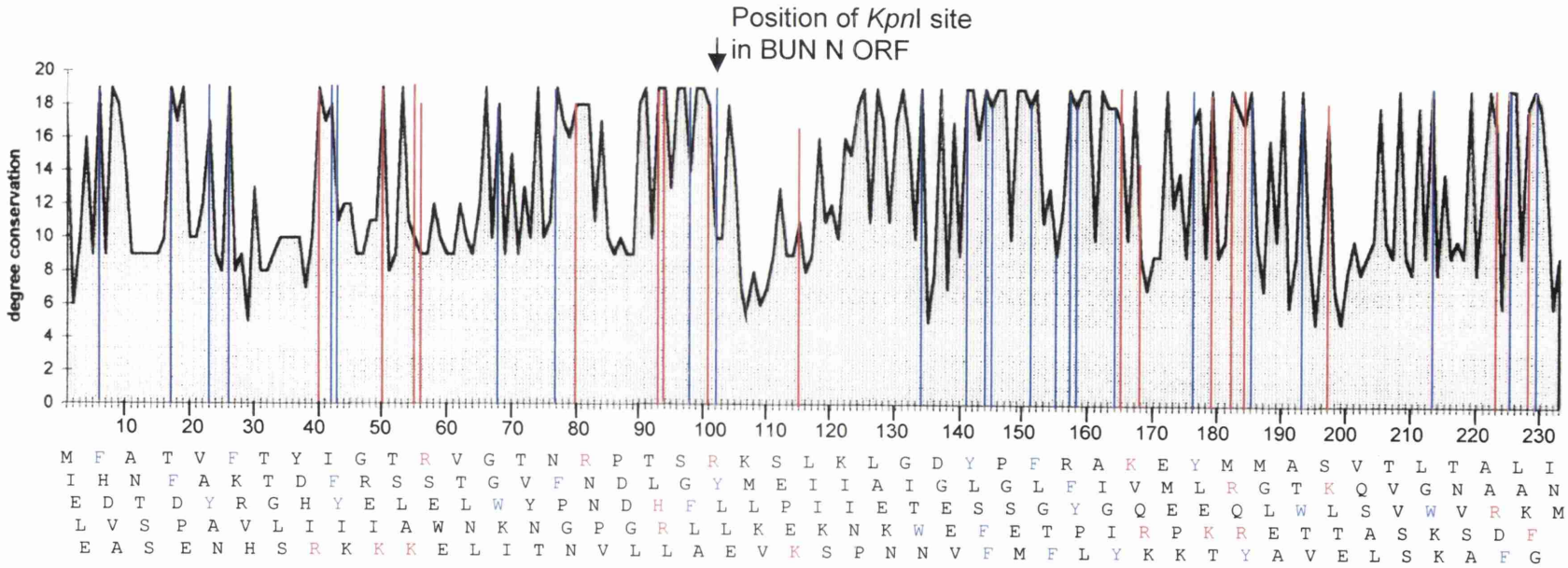

Fig.1.11. Map of conserved residues in bunyavirus N proteins. Amino acid sequence alignments of N proteins from bunyaviruses LAC, SSH, CE, LUM, JC, JS, KEY, MEL, TVT, CV, NOR, MAG, BAT, BUN, MD, GER, GRO, KRI and AINO (19) were analysed for conserved residues (shown as the graph; residue numbering according to BUN). The sequence of BUN N is shown below the graph. Conserved basic residues are shown in red; aromatic in blue. A red or blue line exceeding the level shown in the graph is indicative of conservation of that specific type of amino acid. Unexpectedly the N-terminal half of the protein is less conserved although this region of the N gene also contains the NSs ORF. A region of low conservation extends from approximately residues 105-125. The location of the *Kpn*I site in the BUN N ORF is indicated and can be seen to be close to the region of low conservation. The region from residues 142-165 is particularly highly conserved and contains a high concentration of aromatic residues. This is followed by approximately 20 residues with a high concentration of basic residues. Sequence alignment data and conserved residues taken from Elliott (1996).

approximately the centre of BUN N which might suggest a two-domain structure. Fortuitously a *Kpn*I site is situated upstream of this region in the BUN N ORF, facilitating construction of vectors capable of expressing either half of the protein with minimal disruption. Of particular interest is a highly-conserved region containing a high concentration of conserved aromatic amino acids (residues 142-165), followed to the C-terminal side by a cluster of conserved basic residues. General, sequence non-specific RNA-binding may involve such conserved basic residues and it is interesting that they are absent from the N-terminus and the centre of the primary sequence, possibly excluding these regions of the molecule from this function.

A BUN N mutant truncated by 23 amino acids at the C-terminus (terminating at residue 211) was found to be inactive in the BUN minireplicon system. However, the system presumably requires N to bind itself, RNA and L so it is to be expected that even a small truncation would have a large effect on the activity of the system (Elliott, personal communication). Nevertheless, the result could implicate the C-terminus as an important region of the protein.

Bunyavirus nucleocapsids are relatively resistant to digestion by RNase (Hacker *et al.*, 1989; Kolakofsky & Hacker, 1991). Hence, their structures would appear to be different to those of influenza virus nucleocapsids, which are fully sensitive to digestion, and those of nonsegmented NSVs, which are fully resistant. Bunyavirus nucleocapsids are also stable in CsCl gradients, suggesting that strong and stable interactions exist within the nucleocapsid (Obijeski & Murphy, 1977).

The mechanism of encapsidation has yet to be elucidated. Despite the inference that an encapsidation initiation signal is present within the UTRs, the initiation event could in fact be mediated by another viral component which would serve to deliver N to the RNA. The high positive charge attributed to N and lack of specific binding observed with hantavirus N suggests that N-RNA binding might occur through non-specific interactions with the viral RNA.

As yet, no interaction between N and L has been demonstrated in any member of the *Bunyaviridae*, although an interaction is to be expected. Nucleoprotein-polymerase interactions have been characterised in segmented and nonsegmented NSVs and may appear as fundamental contributors to proper encapsidation *in vivo*, as well as taking part in the regulation of replication. However, by analogy to other NSVs the switch from mRNA synthesis to replication may be based on interactions of N with the viral promoter or by encapsidation of non-templated transcription primers.

The role of NSs in bunyavirus infections has only recently started to be understood and the mechanisms of its functions are currently elusive. It is quite possible that NSs interacts with a component of the nucleocapsid such as N when exerting its inhibitory effect on transcription.

Aims of the project

The main aim of the project was to investigate the interactions of the BUN nucleocapsid protein and to elucidate the mechanism of encapsidation of viral RNA. A minor aim was to identify interactions between other viral proteins that could be useful in describing further viral mechanisms. At the start of the project, interactions of the hantavirus N protein with its RNA had been reported (Gött et al., 1993). No interactions of N with RNA or any other molecule had been reported for any other member of the family, and the function of BUN NSs was unknown.

A major goal was to identify and characterise any interaction of N with viral RNA using biochemical methods. In addition, this would be used to provide information on the process of encapsidation of viral RNA, and to address the question of why non-viral RNA and mRNA are normally not encapsidated. A second objective was to identify whether N is capable of self-association, and if so, to determine the domains responsible. A third aim was to investigate any interaction between N and L, which was considered to be likely to take place. The final objective was to detect any interactions between NSs and itself, N or L, with the intent to provide information on the function of NSs.

Chapter 2: Materials and Methods

2.1. Materials

2.1.1. Enzymes

Restriction endonucleases *Bbs*I, *Bsa*I, *Bsm*BI, *Bst*YI, *Fau*I, *Mnl*I and *Tsp*509I, T4 DNA polymerase and T4 RNA ligase were purchased from New England Biolabs. *Pfu* Turbo polymerase was purchased from Stratagene. T7 RNA polymerase, RQ1 RNase-free DNase and recombinant ribonuclease inhibitor rRNasin® were purchased from Promega. RNase A was purchased from Sigma. *Taq* DNA polymerase was purchased from Qiagen. T4 DNA ligase was purchased from Gibco BRL. All other enzymes were purchased from Roche Diagnostics.

All enzymic reactions took place under the conditions specified by the manufacturer unless stated otherwise.

2.1.2. Radiochemicals

Radiochemicals possessed the following specific activities and were purchased from the following sources:

Compound	activity	source
α-[^{32}P] CTP	3000Ci/mmol	DuPont NEN®
[^{35}S] L-methionine	800Ci/mmol	Amersham
[^{14}C] chloramphenicol	58.5mCi/mmol, 0.1μCi/μl	Amersham

2.1.3. Synthetic oligonucleotides

Oligonucleotides were purchased from MWG Biotech or synthesised on a Cruachem PS250 automated synthesiser.

The sequences of novel oligonucleotides are as follows.

T7 PCR: 5'-CTAATACGACTCACTATA

5SL1T7: 5'-CTAAATCAACATTATATTGTTAATGGTATTTTAATATA GTGAGTCGTATTAG (T7 promoter)

EVYL1: 5'-CTAATACGACTCACTATAGATGGAGAGAGGAAG (T7promoter)

EVYL2: 5'-CTAATACGACTCACTATAGATCCCGATTGCTAAGGG (T7promoter)

M2HN1:	5'-CTGCGAATTCATGATTGAGTTGGAATTTCACG	(*Eco*RI)
M2HN2:	5'-CTGCGGATCCTTACATGTTGATTCCGAATTTAGC	(*Bam*HI)
M2HN3:	5'-CTGCAAGCTTTTACATGTTGATTCCGAATTTAGC	(*Hind*III)
M2HN4:	5'-ATGATTGAGTTGGAATTTC	
M2HN5:	5'-CATGTTGATTCCGAATTTAGC	
M2HL1:	5'-CGTGGGATCCATTCGCTTGCCATTTCAAGCCACG	(*Bam*HI)
M2HL2:	5'-CGTGTCTAGAATCTTTAGCTGTCTTTTGGCCC	(*Xba*I)
M2HL3:	5'-CTGCGAATTCATGGAGCACCAAGCTTATCAATACC	(*Eco*RI)
M2HS1:	5'-CTGCGAATTCATGATGTCGCTGCTAACACC	(*Eco*RI)
M2HS2:	5'-CTGCGGATCCTCAGCATCTTCTCAAGTAGG	(*Bam*HI)
5N390:	5'-CAGCAGGGTCTCCCATGCTACTTGAGAAGATGCTGAA	(*Bsa*I)
3N390:	5'-CAGCAGCTCGAGTTAGTACCTGGCAAGGAATCCA	(*Xho*I)
NHISN1:	5'-CAGCAGCTCGAGTTAGTGATGGTGATGGTGATG	
	CCCGGGCATGTTGATTCCGAATTT	(*Xho*I)
NHISN2:	5'-CAGCAGGGTCTCCCATGCATCACCATCACCATCA	
	CCCCGGGATGATTGAGTTGGAATTTC	(*Bsa*I)

Oligonucleotides 5 and 6 were provided by F Weber (unpublished results). Oligonucleotide S4 was provided by E Dunn (Dunn, 2000).

2.1.4. Expression vectors and plasmids

The construction of some plasmids used in the project is described in the following:

Plasmid	reference
pBUNSCAT	Dunn *et al.*, 1995
pT7BUNS5'(32)/3'(33)	Dunn, 2000
pBUNS32CAT	Dunn, 2000
pT7riboBUNM	Bridgen & Elliott, 1996
pT7riboBUNS	Bridgen & Elliott, 1996
pT7riboBUNN	Bridgen *et al.*, 2001
pUCL	Jin & Elliott, 1991
Mammalian two-hybrid plasmids:	
pSG424	Sadowski & Ptashne, 1989
pVP16AASV19N	Aso *et al.*, 1992
pG5BCAT	Martin *et al.*, 1990

The plasmids pTM1 (Moss et al., 1990) and pTZ18 (Pharmacia) were supplied by RM Elliott. Plasmids for the mammalian two-hybrid system were supplied by A Easton (Mammalian Matchmaker Two-Hybrid Assay kit plasmids; Clontech) R Banerjee (original plasmids) and F Weber (pVPMxA and pGalMxA). The plasmid pQE30 was supplied by Qiagen, and pQEBunN by RM Elliott.

2.1.5. Bacterial strains

The bacterial strain used for maintenance and propagation of plasmids was *Escherichia coli* DH5α™: Φ80d *lac*ZΔM15, *rec*A1, *end*A1, *gyr*A96, *thi*-1, *hsd*R17(r_{K-}, m_{K+}), *sup*E44, *rel*A1, *deo*R, Δ(*lac*ZYA-*arg*F) U169.

Expression of proteins for purification utilised the *Escherichia coli* strain M15[pREP4]: *Nal*^{s}, *Str*^{s}, *rif*^{s}, *lac*$^{-}$, *ara*$^{-}$, *gal*$^{-}$, *mtl*, F^{-}, *rec*A^{+}, *uvr*$^{+}$. Supplied by Qiagen.

2.1.6. Virus

The recombinant, T7 polymerase-expressing vaccinia virus vTF7-3 (Fuerst *et al.*, 1986) was originally supplied by B Moss.

2.1.7. Tissue culture

All reagents used in tissue culture were purchased from Gibco BRL. Cells were grown at 37°C in 5% CO_2 in a humidified incubator.

BHK-21 clone 13 is a baby hamster kidney cell line. Cells were grown in Glasgow modified Eagle's medium supplemented with 10% new born calf serum and 5mM L-glutamine, 10% tryptose phosphate broth and 14ml/400ml of 7.5% sodium bicarbonate.

The cell lines 293 and HeLa are of human origin and were grown in Dulbecco's modified Eagles medium supplemented with 10% foetal calf serum and 5mM L-glutamine.

The primate cell line COS7 was maintained under the same conditions as the human cell lines.

2.1.8. Reagents, chemicals and solutions

All reagents and chemicals were purchased from BDH Chemicals Ltd or Sigma Chemicals Co except as noted.

2YT broth: 5g NaCl, 16g Bactopeptone and 10g yeast extract per litre.

Acid phenol, pH 4.5: Purchased from Ambion.

Acrylamide/bis-acrylamide stock solution: 30% (w/v) acrylamide, 0.8% (w/v) bis-acrylamide, final ratio 37.5:1. Purchased from Roche Diagnostics and Scotlab. Source was discovered to affect GEMSA outcome.

Agarose gel loading buffer: 20% Ficoll 400; 0.1M Na_2EDTA, pH8; 1% SDS; 0.25% bromophenol blue; 0.25% xylene cyanol.

Ammonium persulphate: from Biorad.

Blocking buffer (Northwestern blotting): 5% non-fat milk in PBS with 1mM DTT.

Blocking buffer (Western blotting): 0.1% Tween-20 in PBS(A) with 10% (w/v) non-fat milk

Coomassie blue stain: 10% methanol, 10% acetic acid, 0.1% Coomassie blue.

DEAE-dextran: 10mg/ml DEAE-dextran in Tris-buffered saline, filtered.

Dialysis buffer: 10mM NaCl; 10mM Tris, pH 8.

En^{3}Hance: from DuPont.

Factor Xa buffer 1: 25mM Tris-HCl pH8.0, 0.5mM $CaCl_2$, 50mM NaCl.

Factor Xa buffer 2: 15mM Tris-HCl pH8.0, 0.3mM $CaCl_2$, 30mM NaCl.

Factor Xa buffer 3: 35mM Tris-HCl pH8.0, 0.7mM $CaCl_2$, 70mM NaCl.

GB 002 gelblot paper (Scleicher & Schuell)

Gel fix: 50% (v/v) methanol, 10% (v/v) acetic acid, 40% dH_2O.

GEMSA 6% non-denaturing polyacrylamide gel: 10ml 30% acrylamide/bisacrylamide (37.5:1); 32ml dH_2O (autoclaved); 5ml 50% glycerol (autoclaved); 2.5ml 10x TBE (autoclaved); 0.45ml ammomium persulphate; 50µl TEMED.

GEMSA loading dye (autoclaved): 30% glycerol; 0.25% bromophenol blue; 0.25% xylene cyanol.

HBB (1x): 25mM Hepes, pH 7.5; 25mM NaCl; 5mM $MgCl_2$; 10mM DTT.

Hybridisation buffer (1x): RNA-protein binding buffer + 0.5% NP40.

IP buffer: 150mM NaCl; 10mM Tris, pH 7.4; 1% sodium deoxycholate; 1% Triton X-100; 0.1% SDS; 1mM PSF.

LB agar: L-broth plus 1.5% (w/v) agar.

L-broth: 10g NaCl, 10g Bactopeptone and 5g yeast extract per litre.

LiCl wash buffer: 0.5M LiCl in 0.1M Tris-Cl, pH 7.5.

Lysis solution: 0.2M NaOH; 1% SDS.

Neutralisation solution: 1.32M KOAc, pH4.8.

Nickel-agarose: from Qiagen.

PEI (polyethylene imine): PEI (Fluka), 50% in water. Working stock: 450µg/ml in dH_2O, neutralised with HCl and filtered.

Pfu PCR buffer (10x): 200mM Tris-HCl (pH8.8), 20mM $MgSO_4$, 100mM KCl, 100mM $(NH_4)_2SO_4$, 1% Triton X-100, 1mg/ml nuclease-free BSA. From Stratagene.

Phenol:chloroform:isoamyl alcohol (25:24:1): 1 part TE-buffer saturated phenol mixed with 1 part choloform:isoamyl alcohol.

Protein dissociation mix: 100mM Tris-HCl (pH6.8), 4% (w/v) SDS, 200mM β-mercaptoethanol, 20% (v/v) glycerol, 0.2% (w/v) bromophenol blue.

Protein sample buffer: 15% w/v SDS; 1.5% w/v bromophenol blue; 50% v/v glycerol.

RNA-protein binding buffer (1x): 10mM Hepes, pH 7.3; 150mM NaCl; 20mM KCl; 5mM $MgCl_2$; 1mM EDTA. Autoclaved. DTT added separately to binding reaction.

RNase A stock solution (10mg/ml): pancreatic RNase A in 10mM Tris-HCl (pH7.5), 15mM NaCl, heated at 100°C for 15min to inactivate DNase, cooled and stored at -20 °C.

SDS-PAGE running buffer: 25mM Tris-base, 192mM glycine, 0.1% SDS

Sequencing gel mix: 6% (w/v) acrylamide/bisacrylamide (57:3), 8M urea, 1xTBE. From Scotlab.

Sonication buffer: 50mM sodium phosphate, pH 7.5; 300mM NaCl

STET lysis solution: 8% w/v sucrose; 5% Triton X-100; 50mM EDTA; 50mM Tris-Cl, pH8. Stored at 4°C.

Substrate buffer for ECL: 50mM Tris-Cl, pH 7.5

T7 RNA polymerase optimised transcription buffer (10x): 200mM Tris-HCl (pH 7.5), 30mM $MgCl_2$, 10mM spermidine, 50mM NaCl. From Promega.

TAE: 40mM Tris-acetate (pH 8.0), 1mM EDTA. From Roche Diagnostics.

TBE: 90mM Tris-HCl (pH 8.0), 90mM boric acid, 1mM EDTA (pH 8.0). From Roche Diagnostics.

TEMED: from Bio-Rad.

TEN: 150mM NaCl, 40mM Tris-HCl (pH 7.5), 1mM EDTA (pH 8.0).

Transfer buffer: 15mM Tris; 120mM glycine; 20% methanol.

Trypsin solution: 0.25% (w/v) Difco trypsin dissolved in Tris-saline solution plus 0.005% (w/v) phenol red.

TSB: 10% PEG; 5% DMSO; 10mM $MgCl_2$; 10mM $MgSO_4$ in 2YT or LB broth.

TSB/glucose: TSB + 3.6mg/ml glucose.

Versene solution: PBS supplemented with 0.6mM EDTA and 0.0015% (w/v) phenol red.

Visualisation solution for ECL: from Amersham Life Sciences.

Wash buffer for protein purfication: 50mM sodium phosphate, pH 7.5; 300mM NaCl; 10% glycerol; pH 6.0.

2.1.9. Equipment and miscellaneous materials

3MM blotting paper (Whatman)

400H powerpack (Gibco BRL)

anti-pentaHis antibody (Qiagen)

BA85 nitrocellulose membrane (Schleicher & Schuell)

Branson sonifier 450 (Branson electronics)

Cosmid miniprep kit (Hybaid)

Econosystem chromatography machine (Bio-Rad)

GB 002 gel-blot paper (Schleicher & Schuell)

Gradient Master gradient former (Biocomp)

horizontal gel electrophoresis apparatus Horizon 58 (5.7 x 8.3 x 0.3cm) and H5 (14x11x0.5cm; Gibco BRL)

Hybond C nylon blotting membrane (Amersham)

in vitro transcription kit (Promega)

Lipofectamine transfection reagent (Gibco BRL)

liquid scintillation counter (Beckmann)

MEGAshortscript *in vitro* transcription kit (Ambion)

mini-quick spin RNA columns (Roche Diagnostics)

Nescofilm (Nipon, Bando Chemical Ind.)

Opti-MEM media (Gibco BRL)

Pansorbin cells (Calbiochem-Novabiochem)

Plasmid miniprep kit (Qiagen)

Polygram SIL G (0.25mm) TLC plates (Camlab)

Progene Thermal cycler (Techne)

protein A-sepharose beads (Sigma P3391)

Qiafilter maxiprep kit (Qiagen)

quick-spin columns (Ambion)

Quick TnT® Coupled Transcription/Translation system (Promega)

SDS-PAGE standards broad range (Bio-Rad)

semi-dry electrophoresis apparatus (LKB Bromma)

sterile Acrodisc filter, 0.2μm (Gelman Sciences)

tissue culture materials (Nunc)

ultrasonic bath (Grant)

Vivaspin concentrating columns with 10kD molecular weight cut-off (Vivascience)

Wizard maxiprep kit (Promega)

X-Omat S x-ray film (Kodak)

2.2. Methods

2.2.1. DNA manipulation and cloning procedures

2.2.1.1. Plasmid preparation

2.2.1.1.1. Small-scale plasmid preparation: cosmid miniprep kit (Hybaid)

Used to make sequencing-quality DNA

One and a half ml of a culture of *E. coli* strains DH5α or M15[pREP4] containing the desired plasmid was centrifuged at 13000rpm in a benchtop centrifuge for 30s and the resultant pellet resuspended in 50μl pre-lysis buffer. One hundred μl alkaline lysis solution was added and the cell suspension mixed by inversion until the solution was clear. Seventy-five μl neutralisation solution was added and the solution mixed by inversion and centrifuged for 2min to pellet cell debris. The supernatant was transferred to a spin filter and 250μl binding buffer added and mixed by inversion. The buffer was removed by centrifugation for 1min and the filter washed with 350μl wash solution and centrifugation for 1min. The filter was dried by centrifugation for 1min and the binding beads resuspended in 30μl dH_2O. The DNA was collected by centrifugation for 30s and frozen.

2.2.1.1.2. Small-scale plasmid preparation: Qiagen plasmid miniprep kit

Used to make transfection-quality DNA

Performed according to manufacturer's protocol.

2.2.1.1.3. Small-scale plasmid preparation: boil-lysis method

Used for diagnostic restriction digestion

One and a half ml of a culture of *E. coli* strains DH5α or M15[pREP4] containing the desired plasmid was centrifuged at 13000rpm in a benchtop centrifuge for 30s, the resultant pellet broken up by agitation and incubated in 450μl STET lysis solution containing 200μg lysozyme on ice for 5min. The solution was boiled for 40s, centrifuged at 13000rpm for 20min and the pelleted debris removed with a sterile tooth-pick. Four hundred and fifty μl isopropanol was added to the supernatant, incubated at -20°C for 30min and centrifuged at 13000rpm for 10min. The pellet was washed with 70% ethanol, air-dried and resuspended in dH_2O.

2.2.1.1.4. Small-scale plasmid preparation: alkaline lysis method

Used for diagnostic restriction digestion

1.5ml of a culture of *E. coli* strains DH5α or M15[pREP4] containing the desired plasmid was centrifuged at 13000rpm in a benchtop centrifuge for 30s and the resultant pellet resuspended in 100μl cell resuspension solution (Promega). Two hundred μl fresh lysis solution was added to the bacteria and mixed by inversion, then incubated on ice for 3min. One hundred and fifty μl cold neutralisation solution was added, mixed by inversion and incubated on ice for 5min. The debris was pelleted at 13000rpm for 5min and DNA precipitated from the supernatant by ethanol precipitation. The pellet was washed with 70% ethanol, air-dried and resuspended in dH_2O.

2.2.1.1.5. Large-scale plasmid preparation: Promega 'Wizard'

Used for bulk preps of DNA

A 300ml culture of *E. coli* strains DH5α or M15[pREP4] containing the desired plasmid was centrifuged at 3000rpm for 10min in a swing-bucket rotor and the bacteria resuspended in 15ml resuspension solution. Fifteen ml cell lysis solution was added and mixed by inversion until the solution was clear. Fifteen ml neutralisation solution was added and mixed by inversion. The cell debris was pelleted by centrifugation at 3000rpm for 10min. The DNA was precipitated from the supernatant by incubation with an equal volume of isopropanol at -20°C for 10min, pelleted by centrifugation at 2500rpm in a swing-bucket rotor for 10min and resuspended in 2ml dH_2O. Ten ml DNA purification resin was added and mixed and the solution passed through a column under vacuum. The column was washed with 25ml column wash solution and 5ml 80% ethanol and dried by centrifugation at 2500rpm in a swing-bucket rotor for 5min and by application of vacuum for 5min. The column was incubated with 1.5ml dH_2O at 65°C for 1min and the DNA eluted by centrifugation at 2500rpm in a swing-bucket rotor for 5min. The eluate was filtered through a 0.2μm syringe filter and stored at -20°C.

2.2.1.1.6. Large-scale plasmid preparation: Qiagen 'Qiafilter'

Used for bulk preps of transfection-quality DNA

A 100ml (high-copy) or 250ml (low-copy) culture of *E. coli* strains DH5α or M15[pREP4] containing the desired plasmid was centrifuged at 3000rpm for 10min in a swing-bucket rotor and the bacteria resuspended in10ml buffer P1. Ten ml

buffer P2 was added, the solution was inverted and incubated for 5min. Ten ml buffer P3 was added, the solution was inverted and incubated for 10min in a cartridge barrel. A tip was equilibrated by applying 10ml buffer QBT and the column emptied by gravity flow. The bacterial lysate was cleared by being passed through the filter of the syringe into the tip and entered the resin by gravity flow. The tip was washed with 2x 30ml buffer QC and the DNA eluted with 15ml buffer QF, then precipitated with 10.5ml isopropanol and pelleted by centrifugation at 2500rpm for 3h in a swing-bucket rotor at 4°C. The pellet was washed with 70% ethanol, air-dried, resuspended in 1ml dH_2O and stored at -20°C.

2.2.1.2. Phenol:chloroform extraction and ethanol precipitation

The volume of the solution was increased to 100 or 150µl with dH_2O and an equal volume of 50% phenol (pH 7.9 for DNA, pH 4.5 for RNA); 49% chloroform; 1% isoamyl alcohol was added, mixed extensively by vortexing and centrifuged at 13000rpm in a benchtop centrifuge for 5min. The upper phase was retained, mixed with an equal volume of chloroform and centrifuged as before. The upper phase was retained and 1/10 of the volume of 3M sodium acetate, pH 5.2 (for DNA) or 7.5M ammonium acetate (for RNA) and 3 volumes (for DNA) or 2.5 volumes (for RNA) of 100% ethanol were added. The solution was incubated at -20°C for 1h or on dry ice for 20min and the nucleic acid pelleted by centrifugation at 13000rpm for 20min. The pellet was washed with 50µl 70% ethanol, air-dried and resuspended in dH_2O.

2.2.1.3. Restriction endonuclease digestion of DNA

For the analysis of plasmid DNA from small-scale preparations, restriction enzyme digestions were set up in 10µl volumes containing 5µl DNA (8µl in the case of low-copy plasmids), 1µl 10x specific reaction buffer, and 2U restriction endonuclease. 50ng/µl bovine serum albumen was added if specified. The reaction volume was increased to 10µl with dH_2O and the reaction incubated at the specified temperature for 2h. The DNA fragments were then separated on an agarose gel.

For the preparation of DNA to be used in subcloning, 5 to 10µg DNA were digested in a 20 to 50µl reaction volume as above, with 2U restriction endonuclease per µg DNA, and incubated overnight.

2.2.1.4. End-repair of DNA with the Klenow fragment of *E. coli* polymerase I

Cohesive ends of plasmid DNA were blunt-ended using the Klenow fragment of *E. coli* polymerase I, which lacks the 3' to 5' exonuclease activity of *E. coli* polymerase

I. To a 20µl restriction digestion reaction were added 1µl each of 0.5M dATP, dGTP, dCTP and dTTP and 1-5U Klenow fragment. The reaction was incubated at 30°C for 15min and the DNA purified by phenol:chloroform extraction.

2.2.1.5. Polymerase chain reaction (PCR) amplification of DNA

PCR was performed using both *Taq* DNA polymerase (for diagnostic purposes) and *Pfu* Turbo DNA polymerase. In each case the reaction was carried out in the buffer supplied and under the conditions recommended by the manufacturer. Reactions were performed in a thin-walled 0.5ml reaction tube, and using a Techne thermal cycler that does not require the reaction to be overlaid with oil.

A typical diagnostic reaction with *Taq* DNA polymerase follows. A master mix was used to set up several reactions at once.

dH_2O	22.86µl
10x *Pfu* or *Taq* buffer	3µl
25mM $MgCl_2$	1.2µl
25mM dNTPs	0.24µl
bacterial culture	1µl
primer 1, 16pmol/µl	0.75µl
primer 2, 16pmol/µl	0.75µl
Taq DNA polymerase, 5 U/µl	0.2µl
	30µl

A typical reaction with *Pfu* Turbo polymerase:

dH_2O	81.2µl
10x *Pfu* buffer	10µl
25mM dNTPs	0.8µl
template DNA, 100ng/µl	1µl
primer 1, 16pmol/µl	2.5µl
primer 2, 16pmol/µl	2.5µl
Pfu Turbo DNA polymerase, 2.5 U/µl	1µl
	100µl

Thermal cycler parameters:

segment 1 (strand separation)	94°C	1min
segment 2 (annealing)	50-60°C	1min
segment 3 (extension)	72°C	2.5min/kb

Typically 30 cycles were utilised, including a final extension step of 72°C for 10min. PCR products were purified from an agarose gel.

2.2.1.6. DNA ligation

Ligation reactions were set up at three molar ratios (1:1, 1:3 and 1:5) of linearised vector to insert DNA in a 10μl reaction volume. The reaction included 100ng vector DNA, insert DNA, 2μl 5x ligation buffer and 1U T4 DNA ligase and the volume was increased to 10μl with dH_2O. The reaction was incubated at 16°C overnight.

2.2.1.7. Agarose gel electrophoresis of DNA

DNA species were separated in a horizontal slab gel (5.7x8.3x0.3cm) containing 1% (w/v) agarose in 1xTBE or 1xTAE. DNA containing 0.1 volumes of loading dye was loaded into the wells and the gel was run in 1xTBE or 1xTAE containing 0.5μg/ml ethidium bromide. Electrophoresis was performed at 100V (for TAE gels) or 150V (for TBE gels).

2.2.1.8. Purification of DNA from agarose gel

DNA in an agarose gel was purified using a Quick Spin column (Ambion), which contains a filter that retains the gel and allows the DNA to pass through it. The gel slab was frozen at –20°C for 1h, then placed in a Quick Spin column and centrifuged at 13000rpm in a benchtop centrifuge for 5min and the filter discarded. The DNA present in the eluate was purified by phenol:chloroform extraction and ethanol precipitation.

2.2.2. Expression, purification and analysis of non-radiolabelled proteins

2.2.2.1. N Protein purification

A 350ml culture of *E. coli* strain M15[pREP4] containing a pQE-based plasmid was incubated for 3h at 37°C with vigorous shaking in 2YT or LB broth containing 100μg/ml ampicillin and 25μg/ml kanamycin. Expression of the N gene was induced

by addition of IPTG to 1mM and the culture incubated for a further 3h at 37°C. The bacteria were pelleted by centrifugation at 5000rpm in a GS3 rotor at 4°C for 20min, resuspended in 10ml sonication buffer and pelleted again at 2500rpm in a swing-bucket rotor. The pellet was frozen at -20°C or resuspended in 5ml sonication buffer and the bacteria lysed by freeze-thawing three times on dry ice and at 37°C. The lysate was subjected to sonication for 2 min at an output of 2.5 and duty cycle 40 and debris pelleted by centrifugation at 10000rpm in an SS34 rotor at 4°C for 20 min.

A nickel-agarose column was washed with 5ml sonication buffer at a flow rate of 2ml/min and the protein loaded onto the column by passing the bacterial lysate through it at a flow rate of 0.5ml/min with the use of an Econosystem chromatography machine. The column was washed with sonication buffer until the A_{280} of the flow-through was less than 0.01, and then with 5ml of wash buffer at 0.5ml/min. The protein was eluted with a linear gradient of 0 to 0.5M imidazole in wash buffer in a total volume of 30ml at 0.5ml/min. One ml fractions were collected between 34 and 66min (of a total of 80min) and 5μl of each subjected to analysis by SDS-PAGE. Fractions containing large amounts of N protein were pooled, dialysed against a 1l solution of dialysis buffer for 16h and stored at 4°C. Protein was concentrated in a Vivaspin concentrating column by centrifugation at 2500rpm in a swing-bucket rotor for 30min at 4°C.

2.2.2.2. Determination of protein concentration.

The concentration of protein purified from bacterial cells was initially determined using the method described by Bradford (1976). The Bradford assay was performed according to the instructions of the Bradford reagent manufacturer (Bio-Rad).

The absorbency of the protein at 280nm was also measured, and the absorbence co-efficient calculated as:

$$\text{Concentration (}\mu\text{g/ml) protein / } A_{280} \text{ (1:10 dilution)}$$

For N the absorbence coefficient was calculated as approximately 800, so that an A_{280} reading of 0.3 would give a concentration of 240μg/ml.

2.2.2.3. SDS-PAGE

Fractionation of proteins was performed by electrophoresis through a miniature or medium-sized polyacrylamide gel with SDS, using a discontinuous buffer system

(Laemmli, 1970). The gel apparatus and glass plates were assembled according to the manufacturer's instructions. TEMED was added to the resolving gel mix just prior to its use and mixed well. The resolving gel was then poured between the glass plates leaving sufficient space for the stacking gel (1cm). One ml isopropanol was added to the top of the resolving gel to ensure a smooth interface with the stacking gel. After polymerisation of the resolving gel, the isopropanol was poured off and any remaining isopropanol removed by blotting with 3MM paper. TEMED was added to the stacking gel solution as before, and the solution was poured between the glass plates, on top of the resolving gel. All bubbles were removed and a comb placed into the top of the stacking gel mix to form the wells. After polymerisation of the stacking gel the comb and lower gel dam were removed and the wells washed with SDS-PAGE running buffer. The gel was placed in the electrophoresis apparatus and the reservoirs filled with SDS-PAGE running buffer (2x SDS-PAGE running buffer for peptide separation gels). Samples in protein sample buffer or protein dissociation mix were boiled for 5min unless otherwise stated, then loaded into the wells along with broad-range protein molecular markers. The gel was run at 40mA until the bromophenol blue reached the bottom of the resolving gel. The gel was then removed from between the plates and either immersed in Coomassie blue stain for 30min and then in gel fix solution for at least 30min, or was immersed in gel fix solution for 30min, En^{3}Hance for 30min and washed with water four times for 15min each. It was then dried under vacuum for 2h and, if required, exposed to X-Omat film overnight at –70°C.

SDS-acrylamide solution, medium gel (makes 80ml):

	15% peptide separation gel	stacking gel
30% acrylamide/bisacrylamide stock:	25ml	3.9ml
1M Tris pH 8.8	9.4ml	
1M Tris pH 6.8		3.6ml
10% SDS (w/v)	375ml	300µl
dH_2O	1ml	18ml
10% ammonium persulphate	125µl	150µl
TEMED	25µl	30µl

SDS-acrylamide solution, miniature gel:

	15%	20%	stacking gel
30% acrylamide/bisacrylamide stock:	4ml	5.3ml	1ml
1M Tris pH 8.8	3.75ml	3.75ml	
1M Tris pH 6.8			0.63ml
10% SDS (w/v)	100µl	100µl	100µl
dH_2O	2.05ml	0.75ml	8ml
10% ammonium persulphate	100µl	100µl	100µl
TEMED	10µl	10µl	5µl

2.2.2.4. Western blotting

Proteins to be analysed by Western blotting were subjected to SDS-PAGE. The gel, 6 sheets of 3MM paper and Hybond C nitrocellulose membrane were then equilibrated in transfer buffer. A gel stack was assembled containing, (from the bottom), 3 sheets of 3MM paper, the nitrocellulose membrane, the gel and 3 more sheets of 3MM paper. The gel stack was subjected to a current of $2mA/cm^2$ for 1h in a semi-dry electrophoresis apparatus and the nitrocellulose membrane incubated in blocking buffer for 16h. The membrane was incubated with primary antibody in blocking buffer for 1h with agitation and washed four times with PBS(A)/0.1% Tween-20. The membrane was then incubated with secondary antibody and washed as before, then subjected to enhanced chemiluminescence.

2.2.2.5. Enhanced chemiluminescence

Nitrocellulose membrane containing immunoprobed protein was incubated twice in substrate buffer for 15min each and transferred to freshly-mixed visualisation solution in which it was incubated for 1min. The membrane was wrapped in mellotex film and exposed to an autoradiograph film for 0.5s to 10min.

2.2.2.6. Factor Xa protease digestion

Purified N protein contained a factor Xa proteolytic cleavage site to the C-terminal side of the His-tag. Hence, the His-tag could theoretically be cleaved from the protein using factor Xa. Reactions were assembled containing 3.5µg N protein and 0.1U factor Xa in factor Xa buffer A, B or C. Reactions were incubated at room

temperature for 3, 6 or 24h and the size of the resultant polypeptides analysed by Western blotting using rabbit polyclonal antiserum raised against BUN.

2.2.3. Manipulation of RNA

2.2.3.1. *In vitro* transcription to make radiolabelled RNA

2.2.3.1.1. Generation of radiolabelled transcripts longer than 200nt

An *in vitro* transcription kit (Promega) was used to generate radiolabelled transcripts in excess of 200nt. Reactions were assembled in the following order at room temperature:

water to a final volume of 25μl	
5 x transcription-optimised buffer	5μl
100mM DTT	2μl
rRNasin	1.5μl
2.5mM ATP, GTP, UTP	4μl
100μM CTP	2.4μl
linearised DNA template, 5μg	xμl
α ^{32}P-CTP, 3000Ci/mmol	5μl
T7 RNA polymerase	1μl
	25μl

The reaction was incubated at 37°C for 2h and with 1μl RQ1 RNase-free DNase at 37°C for 15min prior to acid phenol:chloroform extraction and ethanol precipitation. One μl of the reaction was retained for calculation of specific activity after treatment with DNase.

2.2.3.1.2. Generation of radiolabelled transcripts shorter than 200nt

The MEGAshortscript T7 kit (Ambion) was used to generate transcripts shorter than 200nt. Reactions were assembled in the following order at room temperature:

RNase-free dH_2O	3μl
10x reaction buffer	2μl
75mM ATP	1μl
75mM GTP	1μl
75mM UTP	1μl
75μM CTP	1μl
linearised template DNA	5μl
α ^{32}P-CTP, 3000Ci/mmol	5μl
enzyme mix	1μl
	20μl

The reaction was incubated at 37°C for 4-6h and with 1μl DNase at 37°C for 15min. One μl of the reaction was retained for calculation of specific activity. Free NTPs were removed by passing the reaction through an RNA quick spin column (Roche Diagnostics) and the reaction acid phenol:chloroform extracted and ethanol precipitated.

2.2.3.2. *In vitro* transcription to generate non-radiolabelled RNA

All non-radiolabelled transcripts generated were shorter than 200nt in length and were generated using the MEGAshortscript T7 kit (Ambion). Transcripts shorter than 32nt were produced using the standard reaction conditions recommended by the manufacturer. Transcripts between 32 and 200nt were produced in a reaction assembled in the following order at room temperature:

RNase-free dH_2O	8μl
10x reaction buffer	2μl
75mM ATP	1μl
75mM GTP	1μl
75mM UTP	1μl
75mM CTP	1μl
linearised template DNA	5μl
enzyme mix	1μl
	20μl

The reaction was incubated at 37°C for 2h and with 1µl DNase at 37°C for 15min. Free NTPs were removed by passing the reaction through an RNA quick spin column (Roche Diagnostics) and the reaction acid phenol:chloroform extracted and ethanol precipitated. The concentration was determined by UV spectrophotometry at 260nm. Prior to the use of unlabelled RNA in an experiment, it was passed through an RNA quick spin column and its concentration was determined by UV spectrophotometry again. This constituted a control for degradation of the RNA.

2.2.3.3. Removal of unincorporated NTPs

Unincorporated NTPs present in *in vitro* transcription reactions were removed by passing the reaction through an RNA mini quick spin column (Roche Diagnostics). The sephadex matrix in the column was resuspended by inverting and flicking. The cap was removed, the tip broken off and the column centrifuged in 1.5ml tube at 1000xg for 1min with the arrow pointing towards the middle of the rotor. The column was placed in a fresh tube and 20-75µl dH_2O added to the centre of the matrix. The tube was centrifuged at 1000xg for 4min with the arrow pointing towards the centre of the rotor and the eluate retained.

2.2.3.4. Calculation of specific activity

2.2.3.4.1. TCA precipitation

The radiolabelled nucleic acid was diluted 1:10 in dH_2O and 1µl spotted onto a glass fibre filter (Whatman GF/C). 5ml dH_2O was added and the sample counted by Cerenkov counting in a liquid scintillation counter (Beckman).

One µl of the dilution was mixed with 100µg yeast RNA and 0.5ml ice-cold 5% TCA and incubated on ice for more than 5min. The sample was applied under vacuum to a filter pre-wet with 5% TCA and washed twice with 5ml 5% TCA. The filter was counted as before.

2.2.3.4.2. Calculation of specific activity from TCA precipitation data

Percent incorporation

= incorporated cpm / total cpm x 100

Total cpm incorporated

= incorporated cpm x dilution factor x reaction volume / volume counted

nmol labelled rNTP

= µCi rNTP in reaction / isotope concentration, µCi/nmol

Total nmol limiting rNTP

= nmol labelled rNTP + nmol limiting unlabelled rNTP

Maximum theoretical yield

= total nmol limiting rNTP x 4 [number of rNTPs] x 330 [molecular mass]

Total μg RNA synthesised

=(% incorporation /100) x maximum theoretical yield

Specific activity

=total incorporated cpm / total μg synthesised RNA

2.2.4. RNA-protein binding analysis

2.2.4.1. RNA-protein binding reactions

N protein was associated with RNA in binding reactions adapted from Gött *et al.* (1993). Binding reactions were assembled on ice in the following order:

Dialysis buffer (autoclaved):	to 10μl
10x binding buffer	1μl
40mM DTT	0.5μl
rRNasin	0.5μl
RNA	1μl
N protein	xμl
	10μl

In the case of negative control reactions, the N protein was replaced with an equal volume of autoclaved dialysis buffer. Reactions were mixed by vortexing and incubated for 20min at 30°C.

2.2.4.2. North-Western blotting

The analysis of RNA-protein interactions by North-Western blotting was first described by Boyle and Holmes (1986).

N protein was subjected to SDS-PAGE and blotted onto a Hybond C extra nitrocellulose membrane (see Western blotting). The membrane was washed twice in PBS, incubated in blocking buffer for 16h, washed four times with HBB, washed once with hybridisation buffer and probed with a ^{32}P-labelled riboprobe for 2h. The membrane was then washed three times with hybridisation buffer, wrapped in mellotex film and exposed to X-Omat film overnight.

2.2.4.3. Polyacrylamide gel electrophoretic mobility shift assay (GEMSA)

RNA-protein binding reactions were run on a medium-sized 6% non-denaturing polyacrylamide gel containing 5% glycerol. The gel apparatus was washed, treated with 100% ethanol and prepared according to the manufacturer's instructions. Immediately after addition of TEMED and mixing, the acrylamide gel mix was poured between the glass plates to 0.5cm below the top of the plate. Bubbles were removed and a comb inserted into the top of the gel mix to form the loading wells. When the gel had polymerised fully (best results were obtained when left overnight) the comb and the bottom gel dam were removed and the gel secured in the electrophoresis apparatus. The reservoirs were filled with GEMSA running buffer at 4°C. The wells were washed with GEMSA running buffer prior to each sample in 12.5% glycerol (autoclaved) being loaded into the wells. GEMSA loading buffer was run in separate wells to mark the progress of electrophoresis, and the gel run at 200V for 2h at 4°C. The gel was then immediately dried for 2h at 80°C under vacuum and exposed to X-Omat film with intensifying screen at –70°C overnight.

6% GEMSA gel:

30% acrylamide:bisacrylamide stock:	10ml
dH_2O	32ml
10x TBE	2.5ml
50% glycerol	5ml
ammonium persulphate	450µl
TEMED	50µl

TEMED was added shortly before use.

2.2.4.4. Agarose gel electrophoretic mobility shift assay (GEMSA)

RNA-protein binding reactions were run on a horizontal 1% agarose gel (14x11x0.5cm), containing 0.5xTBE and run in 0.5xTBE (autoclaved). Bubbles were removed from the loading wells and the binding reactions in 12.5% glycerol were loaded into the wells. GEMSA loading buffer was run in separate wells to mark the progress of electrophoresis. The gel was run at 200V for 1h at 4°C, then immediately dried without heat and under vacuum, between eight sheets of 3MM paper at the bottom (as large as possible, to absorb the large amount of radioactive buffer) and mellotex film at the top. When dry, the gel stuck to the sheet of mellotex

film. Another sheet of film was placed on the naked side of the gel and it was exposed to X-Omat film with an intensifying screen overnight at –70°C.

2.2.4.5. Filter-binding

An RNA-protein binding reaction was placed on ice and the volume increased to 100µl with 1x binding buffer. A BA85 nitrocellulose filter was soaked in dH_2O for 1h and in 1x binding buffer for 30min, then placed in a dot-blot apparatus above a sheet of GB 002 gel-blot paper that had been soaked in 1x binding buffer briefly. Unused wells were sealed with tape. The binding reaction was applied to the apparatus, vacuum applied and the wells washed with 0.5ml 1x binding buffer. The region of the membrane to which the reaction had been applied was excised and counted in a liquid scintillation counter using Cerenkov counting. All filter-binding assays were performed in triplicate.

2.2.4.6. CsCl density ultracentrifugation

Formation of CsCl gradients was performed using a Gradient Master gradient former (Biocomp). Five ml 40% CsCl in TEN (autoclaved) was layered below 5ml 20% CsCl in TEN (autoclaved) in a TST41 tube. Twenty percent CsCl was then added to the top of the tube to increase the volume to that specified in the Gradient Master manual. The cap supplied with the Gradient Master was fitted to the tube and bubbles removed by suction. The tube was then attached to the Gradient Master and a the two CsCl solutions mixed using the specified parameters. When the program had finished, the cap was removed and 0.5ml of the solution was removed from the top of the gradient and replaced with 5% sucrose in TEN (autoclaved). An RNA-protein binding reaction (containing radiolabelled RNA) or control reaction lacking protein was added to the top of the sucrose and the gradients subjected to ultracentrifugation on a TST41 rotor at 32000rpm for 16h at 12°C. The gradients were fractionated from below using a capillary tube inserted to the bottom of the TST41 tube, connected to the fraction collector unit of an Econosystem chromatography machine, and suction provided by a peristaltic pump. The gradients were automatically fractionated into fractions of 12 drops each, corresponding to approximately 1ml. 200µl of each fraction was then subjected to TCA precipitation in the presence of 10µg yeast RNA to remove degraded RNA, and the remaining counts determined by Cerenkov counting.

2.2.5. Tissue culture

2.2.5.1. Maintenance of cell lines

Cell monolayers were harvested by washing the monolayer once with versene solution, then with a 5:1 mix of versene and trypsin solutions. Cells were incubated at 37°C for 15min before resuspension in 5ml of media. Cells were routinely split 1:6 into flasks (80cm^2 or 175cm^2; 1x10^6 cells added to a 175cm^2 flask) or seeded into 35mm dishes at the stated concentrations.

2.2.5.2. Tissue culture stocks

To make a stock of a cell-line, a monolayer from a 175cm^2 flask was harvested, centrifuged for 30s at 2000rpm in a swing-bucket rotor and resuspended in 2ml media containing 10% dimethyl sulphoxide (DMSO). The cells were then placed in a screw-cap cryotube and stored overnight at –70°C. The following day they were transferred to liquid nitrogen. To revive the cells, they were thawed on ice and used to seed an 80cm^2 flask.

2.2.5.3. Transfection of mammalian cells

2.2.5.3.1. DEAE-dextran transfection

The plasmid DNA to be transfected was ethanol precipitated and resuspended in Tris-buffered saline (TBS), then added to 10mg/ml DEAE-dextran at 37°C in a volume determined by the final concentration of DEAE-dextran required:

Concentration in media	total volume	DNA in TBS	DEAE-dextran, 10mg/ml
μg/ml	μl	μl	μl
400	90	30	60
200	45	15	30
100	22.4	7.4	15
50	11.1	3.7	7.4

The DNA-DEAE dextran mix was added to 1.5ml Opti-MEM per dish and added to 35mm dishes of subconfluent cells at 400, 200, 100 or 50 μg/ml. The cells were incubated at 37°C for 3-4h, the media removed and the cells incubated with 1.9ml 10% DMSO (in PBS) for 1min. The cells were washed with 1ml PBS and incubated with media.

2.2.5.3.2. Polyethyleneimine (PEI) transfection

This is based on the method described by Boussif *et al.* (1995).

DNA to be transfected was mixed with a total volume of 50μl 150mM NaCl and incubated for 10min. PEI was mixed with a total volume of 50μl 150mM NaCl at 3μl PEI /μg DNA and incubated for 10min. The two solutions were mixed and incubated another 10min, then added to 500μl optimem. Cells were washed with optimem, the DNA / PEI / Opti-MEM mix added and the cells incubated at 37°C for 3-4h, then incubated in media.

2.2.5.3.3. Preparation of cationic liposomes

This method is based on that described by Rose *et al.* (1991).

Dimethyldioctadecyl ammonium bromide (DDAB) was diluted to 4mg/ml in clhoroform and 1ml was mixed with 1ml dioleoyl L-α-phosphatidyl ethanolamine (DOPE, 10mg/ml in chloroform) and the chloroform evaporated with a stream of nitrogen. The remaining mixture was lyophilised for 16h in a freeze drier and resuspended in 10ml sterile distilled water by sonication in an ultrasonic bath followed by a sonication probe on ice (constant duty cycle; power 5; 2-3min intervals) until almost clear. The final suspension had a 1:2.5 ratio by weight of DDAB to DOPE and could be stored at 4°C for up to one month.

2.2.5.3.4. Lipofection with in-house liposomes

The DNA to be transfected was mixed with 250μl optimem. 165μl liposomes were mixed thoroughly and added to 2.75ml optimem. 250μl of the liposome / Opti-MEM mix was added to DNA / Opti-MEM mix in a drop-wise fashion, the solutions mixed thoroughly and incubated for 15min. A subconfluent monolayer of cells in a 35mm dish was washed with 1ml PBS and the DNA / liposome mix added in a drop-wise fashion, swirled to mix and incubated at 37°C for 3h. The cells were washed twice with PBS and 1ml medium added.

2.2.5.3.5. Lipofection with Lipofectamine (Gibco BRL)

The DNA to be transfected was diluted in 100μl Opti-MEM. Five μl Lipofectamine per reaction was added to Opti-MEM. The lipofectamine-Opti-MEM solution was then added to the DNA-Opti-MEM solution and they were incubated at room temperature for 45min. A monolayer of cells in a 35mm dish was washed with 1ml Opti-MEM, then 800μl Opti-MEM was added to the DNA-Lipofectamine mix and this

was applied to the cells in a drop-wise fashion. The cells were incubated for 3 to 5h, the Lipofectamine mix was removed and 2ml media added to each dish.

2.2.5.4. Infection with vaccinia virus vTF7-3

Recombinant vaccinia virus vTF7-3 (Fuerst *et al.*, 1986) was used to express T7 polymerase in cells.

A confluent monolayer of cells was washed with Opti-MEM and vaccinia virus added as $4.2x10^6$pfu/35mm dish in 500µl optimem. The cells were incubated at 37°C for 1h, after which time they were ready for transfection.

2.2.6. Chloramphenicol acetyltransferase (CAT) assay and thin-layer chromatography (TLC)

The CAT enzyme assay system is an adaptation of that described by Gorman *et al.* (1982) and Cullen (1987).

Cells were scraped using a rubber policeman and pelleted by centrifugation at 13000rpm for 30s in a benchtop centrifuge. The pellet was washed in 400µl TEN and centrifuged as before. The pellet was resuspended in 75µl 0.25M Tris, pH 7.5 and cells lysed by freeze-thawing three times on dry ice and at 37°C. Cell debris was pelleted by centrifugation at 13000rpm for 5min and the cell extract incubated with 1µl acetyl CoA, 1µl ^{14}C-radiolabelled chloramphenicol and 13µl 0.25M Tris, pH 7.5 at 37°C for 2h. Two hundred and fifty µl ethyl acetate was added to the reaction, mixed by vortexing for 30s and centrifuged at 13000rpm for 5min. The upper phase was lyophilised and then resuspended in 25µl ethyl acetate before being applied to a TLC plate (polygram SIL G; Machery-Nagel) which was placed in a tank containing 95ml chloroform / 5ml methanol in a fume hood. When the chloroform / methanol mix had reached the top of the TLC plate it was air-dried and subjected to autoradiography for 16h.

2.2.7. Expression and analysis of radiolabelled proteins

2.2.7.1. Coupled *in vitro* transcription/translation reactions.

Cell-free protein synthesis was performed using the Quick TnT® Coupled Transcription/Translation system (Promega).

Expression plasmids were added to reactions containing 10µl Quick TNT reaction mix (consisting of a master mix of reaction components) and 0.5µCi ^{35}S-methionine. The reaction volume was increased to 25µl with dH_2O. The mix was incubated at

30°C for 1h and then boiled in 10μl protein dissociation mix for 5min or used in an IP assay.

2.2.7.2. *In vivo* protein labelling

A confluent monolayer of cells in a 35mm dish was washed with PBS, 1ml methionine-deficient (met$^-$) Eagles A + B medium added, and the cells incubated at 37°C for 30min. The medium was removed and replaced with 1ml met$^-$ Eagles A + B medium containing ^{35}S-methionine (100μCi/ml). The cells were incubated for another 3h at 37°C, washed twice with PBS and subjected to IP or scraped into 200μl protein dissociation mix and subjected to SDS-PAGE.

2.2.7.3. Immunoprecipitation (IP) assay

One hundred mg protein A-sepharose beads (Sigma P3391) were added to 5ml IP buffer and incubated for 16h at 4°C. The beads were pelleted by centrifugation at 2500rpm for 1min in a swing-bucket rotor and resuspended in 800μl IP buffer. Radiolabelled cells in a monolayer in a 35mm dish were washed with PBS. The cells were then scraped into 0.5ml PBS using a rubber policeman and pelleted at 13000rpm for 2min. The cells were incubated with 0.5ml IP buffer on ice for 30min and the nuclei pelleted by centrifugation at 13000rpm for 5min. If the IP was performed on a TnT reaction, the reaction was then supplemented with 0.5ml IP buffer. Fifty μl of the supernatant was retained and added to 50μl protein dissociation buffer to be used as an expression control; the rest was incubated with 50μl Pansorbin cells (Calbiochem-Novabiochem) at 4°C for 1-2h with rotation. The Pansorbin was pelleted at 13000rpm for 30s and the supernatant incubated with antibody (1μl commercial stock) at 4°C for 16h with rotation. Sixty μl pre-swollen protein A-sepharose beads were added and the samples incubated a further 1h at 4°C with rotation. The beads were pelleted at 13000rpm for 30, washed with 300μl LiCl wash buffer three times and boiled in protein dissociation buffer for 5min before being subjected to SDS-PAGE.

2.2.8. Miscellaneous techniques

2.2.8.1. Purification of synthetic oligonucleotides

Oligonucleotides synthesised on an automated synthesiser were supplied immobilised on a matrix. They were purified from the matrix by slowly moving 1.5ml ammonia though the matrix between two 2ml syringes over 1h. The solution was

treated for 5-16h at 55°C to remove the base-protecting groups and then the ammonia was removed by lyophylisation. The dried oligonucleotide pellet was dissolved in 100µl of dH_2O, mixed with 1ml of butanol and centrifuged for 10min in a benchtop centrifuge. The butanol was then removed by evaporation and the pellet resuspended in dH_2O.

2.2.8.2. Production and transformation of competent bacterial cells

Transformation of competent bacterial cells was always performed within 24h of the synthesis of the competent cells. Two hundred µl of *E. coli* strain DH5α or M15 [pREP4] were incubated in 50ml 2YT broth without antibiotics at 37°C with agitation until the A_{600} of the solution had reached 0.2. The bacteria were pelleted by centrifugation at 3000rpm in a swing-bucket rotor for 10min and the pellet resuspended in 2ml TSB, incubated on ice for 10min and divided into 200µl aliquots. Plasmid DNA was added to an aliquot, mixed by flicking and incubated on ice between 5 and 30min. Eight hundred µl TSB + glucose was added, mixed by flicking and the bacteria incubated at 37°C for 1h. The bacteria were pelleted by centrifugation at 13000rpm in a benchtop centrifuge for 30s and 800µl supernatant removed. The pellet was resuspended in the remaining 200µl and spread on an LB-agar plate containing the appropriate antibiotic. The plate was incubated at 37°C for 16h.

2.2.8.3. Bacterial glycerol stocks

Duplicate glycerol stocks were made by mixing 200µl of a fresh overnight culture with 200µl 80% (w/v) glycerol in sterile vials which were then stored at –70°C.

Results and Discussion

Chapter 3: Development of RNA-N protein binding assays

3.1. Introduction

By analogy to the nucleocapsid proteins of other negative-strand viruses, the BUN N protein is believed to encapsidate the BUN viral RNA. This chapter describes the development of assays to detect and analyse any encapsidation processes. From experiments using the BUN minireplicon system the N protein was known to be essential for transcription and replication of a synthetic viral mini-genome, and the BUN S segment terminal sequences were determined to be sufficient to provide the viral promoter and any encapsidation signals. These signals were mapped to the 32b at the 5' terminus and 33b at the 3' terminus. It was therefore decided that an analysis of any encapsidation mechanism should utilise these sequences.

An *in-vivo* approach was considered to be too restrictive to allow a detailed analysis as it would not allow a precise dissection of the encapsidation events. For instance, a mammalian three-hybrid system to investigate RNA-protein interactions *in vivo* would allow the analysis of the binding of a single protein molecule to an RNA molecule, but would not provide any information on the subsequent binding of proteins. In addition, it could not easily be used to determine binding kinetics or to analyse the binding event by biochemical methods.

An *in vitro* approach required the production of a relatively pure and soluble recombinant N protein, the production of a relevant RNA and the development of binding reactions and assays. It was decided to express the N protein as a 6xHis-tagged protein in bacteria in order to purify it, and to generate the RNA as a radiolabelled transcript in an *in vitro* transcription reaction.

3.2. Expression and purification of N

3.2.1. Introduction to the expression and purification of 6xHis-tagged proteins

The Qia-Express system (Qiagen) consists of a series of vectors for the inducible expression of recombinant proteins containing a tag of six histidine residues, termed a 6xHis tag. In the Qia-Express pQE system the gene for the protein of interest is cloned downstream of a bacteriophage T5 promoter,which is regulated by two *lac* operator sequences, a synthetic ribosome binding site and a sequence for an N-terminal 6xHis tag (Fig.3.1). Proteins are expressed in the *E. coli* K12-based strain M15[pREP4] which contains the pREP4 plasmid encoding the *lac* repressor protein expressed from the lac I gene. *lac* represses the T5 promoter by binding to the *lac* operator sequences. The plasmid pREP4 also provides resistance to kanamycin. The *lac* repressor is inactivated by the addition of isopropyl-β-D-thiogalactoside (IPTG), resulting in the activation of the T5 promoter and expression of the protein.

The purification of 6xHis tagged proteins is based on the affinity of histidine for nickel ions, which it binds through its imidazole ring. The nickel is supplied bound to nitrilotriacetic acid (NTA), coupled to Sepharose; His binds four of the Ni^{2+} ions' six ligand binding sites, leaving the other two free to bind His (Fig.3.2). Thus, the protein of interest can be anchored to a Ni^{2+}-NTA matrix through the binding of its His tag by nickel. Elution of the protein from the matrix involves the addition of imidazole, which competes with the imidazole ring present in the histidine residues for binding to the Ni^{2+} ions (Fig.3.3).

3.2.2. Purification of N

The N ORF had previously been amplified by PCR and subcloned into the vector pQE30 from the Qia-Express system (Fig.3.4). The resultant plasmid was designated pQEBunN and allowed for expression of N with an N-terminal 6xHis tag. A factor Xa protease recognition sequence had been engineered downstream of the tag sequence to provide the opportunity for removal of the tag after purification. A pQE plasmid encoding the N-terminal half of N with an N-terminal His-tag was constructed by cleaving pQEBunN with restriction endonucleases *Kpn*I and *Hin*dIII, blunting the ends and re-ligating the plasmid (Fig.3.5). The resulting plasmid was designated pQENN.

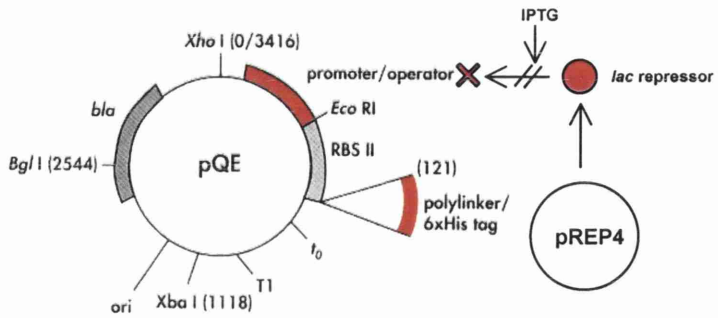

Fig.3.1. Schematic of a pQE expression plasmid. The protein of interest is expressed with a 6xHis tag under the control of a T5 promoter. The promoter is repressed by the *lac* repressor, expressed from the plasmid pREP4. On induction, the *lac* repressor is inactivated by IPTG, thus causing the promoter to become active. Adapted from Qiagen (1997).

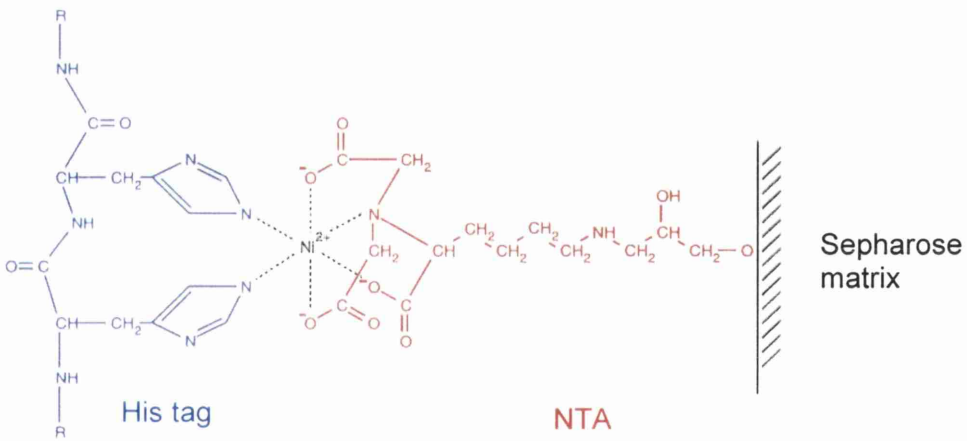

Fig.3.2. Binding of His by a nickel ion anchored to NTA. Four of the nickel ion's six ligand binding sites are taken up in binding NTA, leaving two to bind His residues in the 6xHis tag. Adapted from Qiagen (1997).

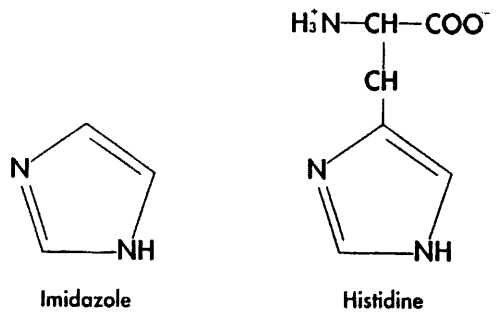

Fig.3.3. Comparison of the molecular structures of imidazole and His. Nickel ions bind His through its imidazole ring. Hence, imidazole can be used to compete for binding to nickel ions and is used to elute the His-tagged protein from the matrix. Adapted from Qiagen (1997).

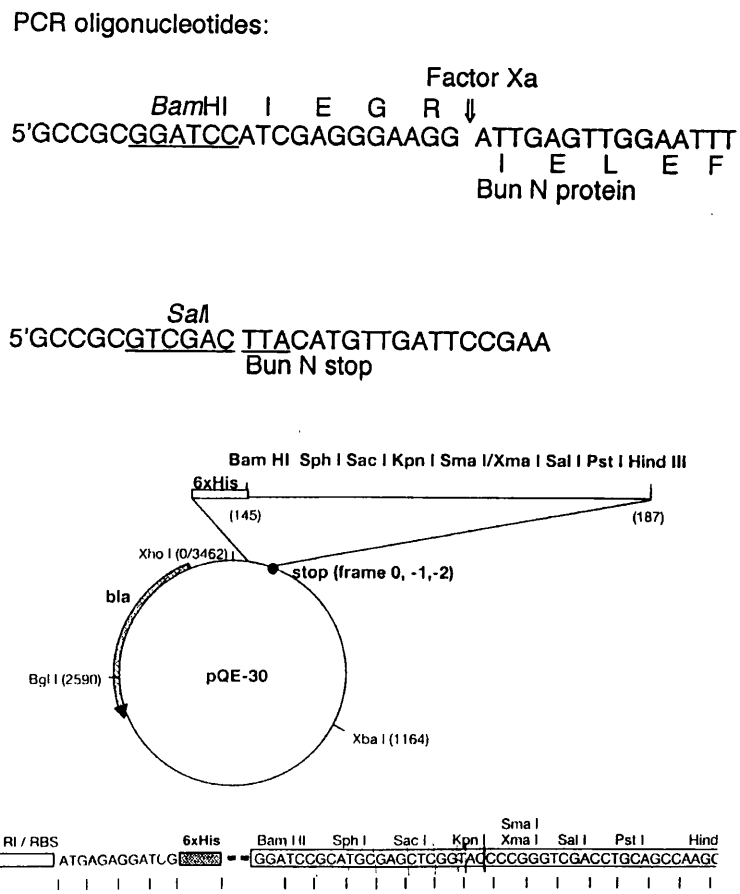

Fig.3.4. Previous construction of pQEBunN. The plasmid had been generated by amplifying the N ORF by PCR and ligating into the *Bam*HI and *Sal*I sites of pQE30. A factor Xa site had been engineered into the 5' primer to facilitate removal of the 6xHis tag. Figure courtesy of RM Elliott.

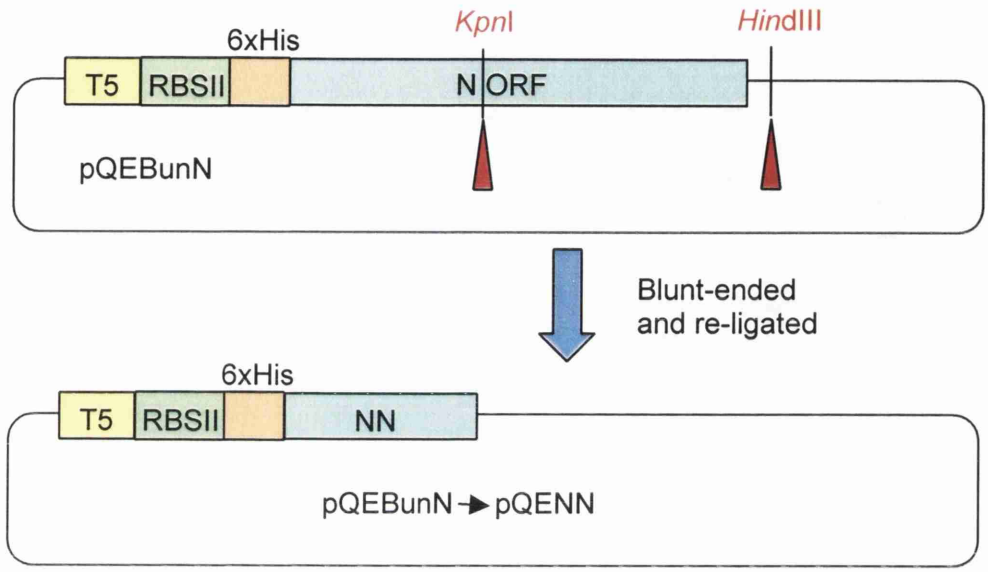

Fig.3.5. Construction of the plasmid pQENN. The plasmid pQEBunN was cleaved with *Kpn*I and *Hin*dIII, blunt-ended and re-ligated to remove the C-terminal half of the N ORF from the *Kpn*I site. Thus, the resultant construct would express only the N-terminal half of N up to the *Kpn*I site in the cDNA.

The pQEBunN plasmid was transformed into *E. coli* M15[pREP4] and the bacteria grown for three hours, induced with 10mM IPTG for a further three hours and lysed. The N protein was purified from the lysate in its native form by liquid chromatography using an Econosystem chromatography machine (Bio-Rad). To this end, the bacterial lysate was loaded onto a Ni^{2+}-NTA/agarose column, the column washed and bound N protein eluted with a linear gradient of 0-500mM imidazole. The optical density at 280nm of material eluted from the column was monitored with an ultra-violet spectrophotometer which showed a peak of optical density (Fig.3.6). 1ml fractions of the eluate were collected throughout the peak and checked for N protein content by SDS-PAGE analysis and staining with Coomassie blue (Fig.3.7). The observed protein was estimated to be the correct size for His-tagged N as it possessed slightly decreased electrophoretic mobility to that previously observed for the 26.7kD non-tagged N protein (probably mainly attributable to the positive charge of the His tag), and was relatively free of contaminating bands. Fractions containing a large amount of N were dialysed to remove the imidazole and stored at 4°C.

N was found to be highly soluble and stable both in bacteria and when stored at 4°C for approximately three weeks after purification. The yield was high and the eluted protein pure. Elution took place at imidazole concentrations above approximately 250mM, suggesting that the His tag is not freely accessible for binding to the Ni^{2+}-NTA but rather may be buried within the protein.

The plasmid pQENN was also transformed into *E. coli* M15[pREP4] and expression of the product (termed NN) was induced using the same procedure as for the N protein. NN was not purified as the expression levels were found to be too low to allow a useful yield.

3.2.3. Characterisation of purified N

3.2.3.1. Western blot analysis of N and NN

Purified N protein or bacterial lysate from bacteria expressing N from pQEBunN or the NN polypeptide from pQENN were subjected to analysis by Western blotting in order to verify their identification. The proteins were not heated prior to SDS-PAGE unless otherwise indicated. The monoclonal anti-pentaHis antibody (Qiagen), which recognises a stretch of five consecutive His residues and should therefore detect the His tag, and anti-BUN polyclonal antiserum raised against BUN virus in rabbits was previously

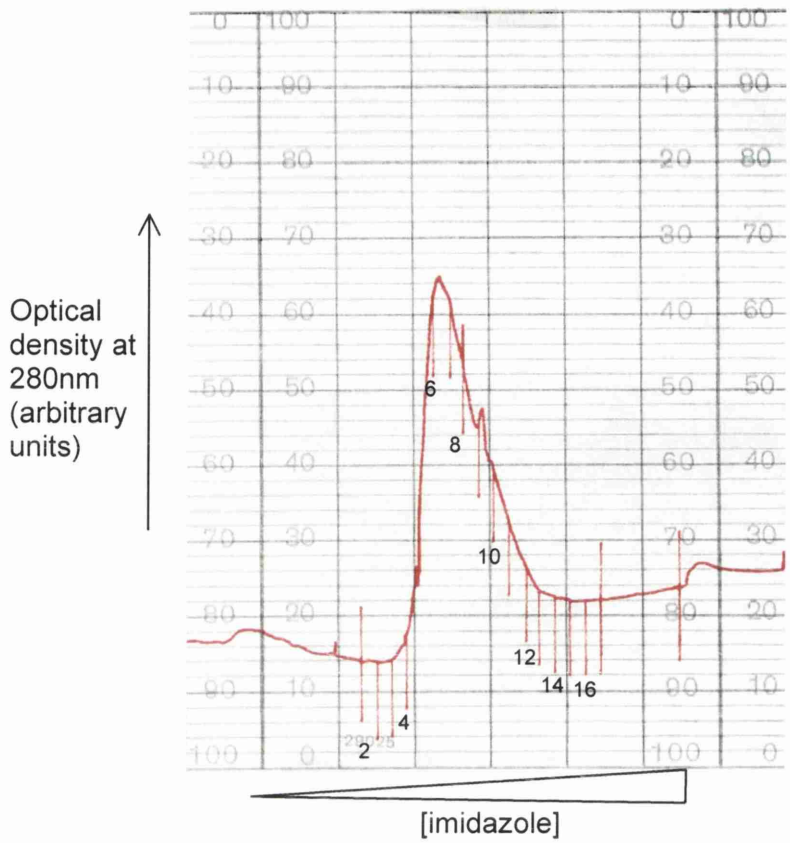

Fig.3.6. Optical density of material eluted from the Ni-NTA sepharose matrix. Eluate from a column loaded with lysate from bacteria expressing His-tagged N was observed to reach a peak in optical density at 280nm at a point in the elution gradient corresponding to an imidazole concentration of approximately 250mM. Fractions of the eluate were collected throughout the peak period. Fraction numbers are indicated.

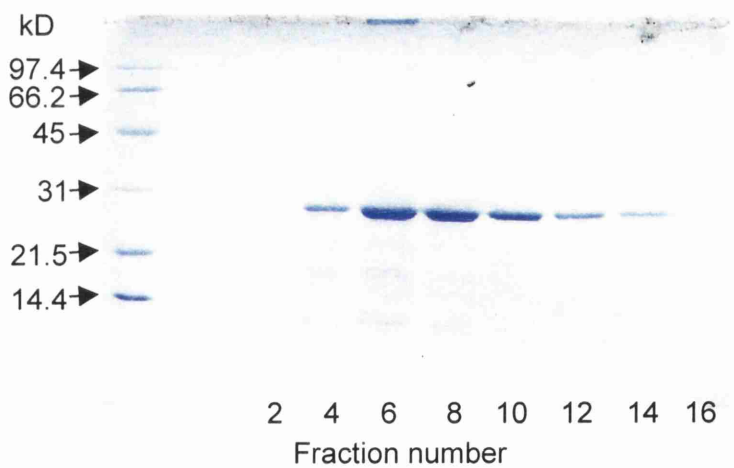

Fig.3.7. Coomassie-blue stained 15% SDS-PAGE of fractions taken from the eluate. The fraction numbers correspond to those in Fig.3.6. A band corresponding in size to His-tagged N was resolved. Most of the protein appeared to be in fractions 6-10.

shown to detect N (Watret *et al.*, 1985). Both exclusively detected the same band when low concentrations of eluate or lysate were analysed (Fig.3.8, lanes 1 and 6). The bands were determined to be the same size as the band observed on Coomassie blue-stained SDS-PAGE gels of eluate fractions (Fig.3.7). The eluted protein was hence believed to be N. A significant amount of N was detected by anti-pentaHis in lysate from uninduced bacteria expressing N, so it would appear that the T5 promoter was leaky. Lower bands in lane 3 were interpreted to be degradation products of the protein. This was the only incidence of apparent degradation observed.

Western blotting of lysate from bacteria expressing NN with anti-pentaHis detected a weak band of the expected size (Fig.3.8, lane 4). The level of expression of the protein was found to be too low to allow purification of useful amounts.

On analysis of a ten-fold greater amount of N by Western blot using the anti-pentaHis antibody, anti-BUN polyclonal antiserum or rabbit polyclonal antiserum raised against purified N (anti-N) up to two additional bands of higher molecular weight became apparent (Fig.3.8 lanes 3, 7 and 10, hollow arrows). All bands were absent in the control lysate from bacteria transformed with empty pQE30 vector DNA (lanes 2 and 5). The additional bands were thought to correspond to dimers and trimers of N, suggesting that the recombinant protein was capable of multimerisation. However, another explanation was that two or three N monomers were binding to the same piece of RNA, which was acting as a bridge between them and thus responsible for the bands of apparent dimers and trimers. This theory was tested by incubating the purified protein with 5mg/ml RNase A, approximately 5000-fold more than necessary to digest RNA in nucleocapsids (section 4.3.2), before subjecting it to analysis by Western blotting with anti-BUN antiserum. The intensity of the bands of higher molecular weight was unaffected by the RNase treatment (lane 8, compare with lane 7). In addition, the intensity of the band of higher molecular weight detected by anti-N was reduced on boiling of the sample for 2min (lane 9). It is possible that it was a heat-sensitive protein, but taken with the fact that it was detected by all antibodies implies that the higher bands were multimers of N.

3.2.3.2. Attempts to cleave the 6xHis tag

The introduction of a factor Xa protease recognition sequence between the His tag codons and the N ORF in pQEBunN allowed the possibility of cleaving the 6xHis tag from the purified N protein (Fig.3.4). Purified N was incubated with factor Xa for 3, 6 or

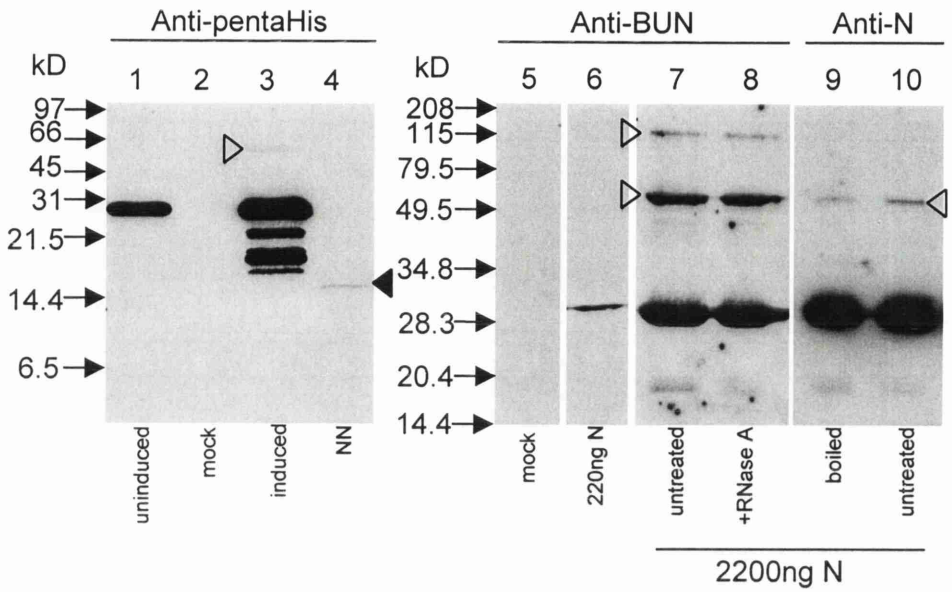

Fig.3.8. Western blots of N and NN. 220 or 2200ng N, lysate from bacteria containing pQE plasmids containing N, NN, or the empty parent plasmid (mock, lanes 2 and 5) were subjected to SDS-PAGE on a 20% (lanes 1 to 4) or 15% (lanes 5-12) gel. A Western blot was performed with monoclonal anti-pentaHis antibody (1:1000), which detects five consecutive His residues (lanes 1 to 4), rabbit polyclonal antiserum raised against BUN (1:500) (lanes 5 to 8), and rabbit polyclonal antiserum raised against purified N (1:200) (lanes 9 & 10). A band corresponding to His-tagged N was detected by all antibodies when N was present but not in the mock samples. In the lanes containing a large amount of N bands of higher molecular weight were detected by all antibodies (lanes 3, 7 and 10, indicated with a hollow arrow). These bands were found to be unaffected by treatment with 5mg/ml RNase A (lane 8) but were partially sensitive to boiling (lane 9), suggesting that they are multimers of N. The multiple bands present below the major band in lane 3 are presumed to be degradation products of N. Lane 4 is a Western blot of lysate from bacteria expressing the NN polypeptide using anti-pentaHis antibody. A band of the expected size was resolved (indicated by a solid arrow) but is significantly less intense than that observed for N, suggesting that the polypeptide was expressed at a lower level.

24h under different conditions and then analysed by Western blotting using polyclonal antiserum raised against BUN (Fig.3.9). The size and charge of the His tag had previously been shown to alter the electrophoretic mobility of N sufficiently to allow the forms of the protein with and without the His tag to be distinguished on SDS-PAGE (RM Elliott, personal communication). However, even after a 24h treatment with factor Xa no change in electrophoretic mobility was observed, leading to the assumption that the tag was not cleaved. This could be explained by the cleavage site being buried within the molecule, similarly to the His-tag (section 3.1.2).

It might have been possible to remove the tag by denaturing the protein to make the cleavage site accessible to the protease. However, all previous attempts to renature N once it was denatured had failed (RM Elliott, personal communication). The presence of the His-tag was not considered to be important. The tag is uncharged at physiological pH and does not generally affect the structure or function of purified proteins (Qiagen, 1997).

3.3. Generation of radiolabelled transcripts

3.3.1. Introduction

In order to investigate the binding of N to the termini of the BUN S segment it was necessary to generate an RNA transcript containing the appropriate sequences. The ideal transcript would be small so as to aid resolution of structures in gel mobility shift assays and would contain the precise segment terminal sequences. From experiments using the BUN reverse-genetic minireplicon system it had previously been determined that the initial 5' 32 and 3' 33 bases of the BUN S segment were sufficient to direct encapsidation and transcription of the reporter gene that they flanked. The DNA template chosen to generate radiolabelled transcripts for analysis of N-RNA binding was a construct based on the vector pUC118 and had been used as an intermediate step in making the reporter construct for the reverse genetic system, termed pT7BUNS5'(32)/3'(33) (Fig.3.10; Dunn, 2000). On linearisation with the restriction endonuclease *Bbs*I the plasmid could be used in run-off transcription reactions to generate a 69nt RNA transcript consisting of the precise 32 bases of the 5' and 33 bases of the 3' terminal sequences of BUNS with a 4-base linker region, termed BUNS5'(32)/3'(33). The precise 5' terminus was generated by means of a truncated T7 promoter lacking the final GGG motif. The T7 polymerase was thereby forced to initiate

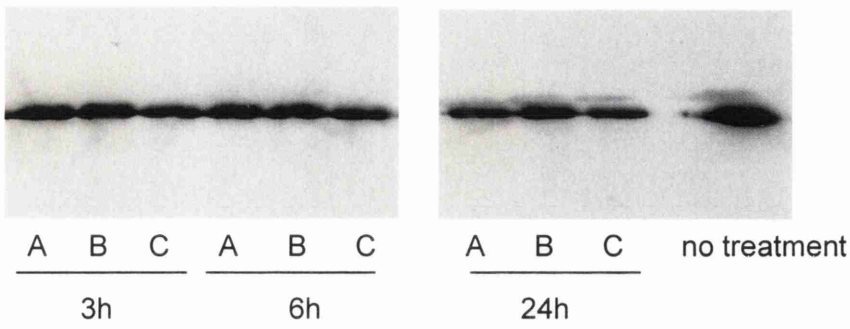

Fig.3.9. Attempts to cleave the His tag from purified N. N was treated with factor Xa under different conditions (A, B, C) for 3, 6 or 24 hours and subjected to SDS-PAGE on a 15% gel. A Western blot was performed with anti-BUN polyclonal antiserum. No change in the electrophoretic mobility of the protein was observed after treatment with the protease, indicating that the tag had not been removed.

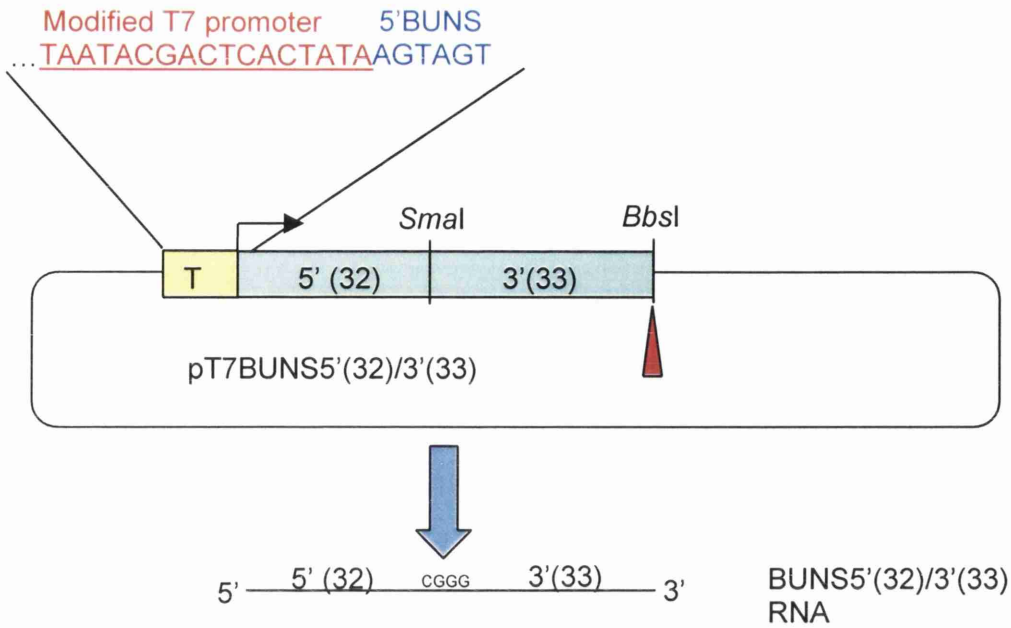

Fig.3.10. Generation of BUNS5'(32)/3'(33) RNA. The plasmid pT7BUNS5'(32)/3'(33) was linearised with *Bbs*I. Run-off *in vitro* transcription initiated from the plasmid's modified T7 promoter and terminated at the *Bbs*I cleaved site. The resulting transcript consisted of the precise first 32 bases and 33 bases of the 5' and 3' terminal sequences of BUNS, respectively, linked by a 4-base sequence.

Fig.3.11. Sequence of the 5' end of BUNS5'(32)/3'(33) RNA. The first C is located at position 10, whereas the other bases are all incorporated in the first three positions. It is beneficial to use C as the limiting NTP to avoid abortive transcription initiation.

transcription with the first base of the template sequence and not with one of the final Gs. The precise 3' terminus was formed by digesting the plasmid with *Bbs*I. The recognition site of *Bbs*I is remote from its cleavage site. Note also that in the template DNA the hinge region between the two terminal sequences comprises part of an intact *Sma*I site that could be used for linearisation of the plasmid at this point to allow run-off transcription to generate only the 5' 32 bases of BUNS.

3.3.2. Optimisation of transcription conditions

Generation of short radiolabelled transcripts by *in vitro* transcription is technically challenging due to the large number of transcription initiation events that must take place to make a relatively low mass of RNA, as initiation is the limiting factor in transcription. The sequence of the RNA was analysed in order to determine the best radiolabelled NTP to use (Fig.3.11). CTP was chosen as the best NTP because it is the last of the four NTPs to be incorporated, the first C appearing at base 10. The radiolabelled NTP would be the limiting NTP, particularly when generating short transcripts which benefit from an otherwise high concentration of NTPs, and attempts to incorporate a limiting NTP too soon after transcription initiation were thought to possibly result in misincorporation or abortive initiation of the transcription at that position. The optimal specific activity of the radiolabelled NTP is that which will allow a high specific activity of transcript whilst allowing a useful mass of transcript to be produced. Thus, an NTP with a specific activity of 400Ci/mmol will allow for a greater mass of transcript of lower specific activity than will an NTP with 800Ci/mmol. However, others generating radiolabelled transcripts of similar sizes had found that using NTPs with specific activities up to 3000Ci/mmol was possible (P Yeo, personal communication). 3000Ci/mmol was found to be sufficient in this case and therefore chosen as the appropriate specific activity of the ^{32}P-CTP.

Initial attempts to generate the BUNS5'(32)/3'(33) radiolabelled transcript utilised the *in vitro* transcription kit from Promega, using the standard protocol. In order to visualise the reaction product the RNA was extracted from the reaction using acid phenol:chloroform, ethanol precipitated in the presence of ammonium acetate, denatured and subjected to analysis by denaturing PAGE (Fig.3.12). The result was a small amount of transcript and a large pool of unincorporated radiolabelled NTPs that ran towards the bottom of the gel. After numerous attempts were made over a range of

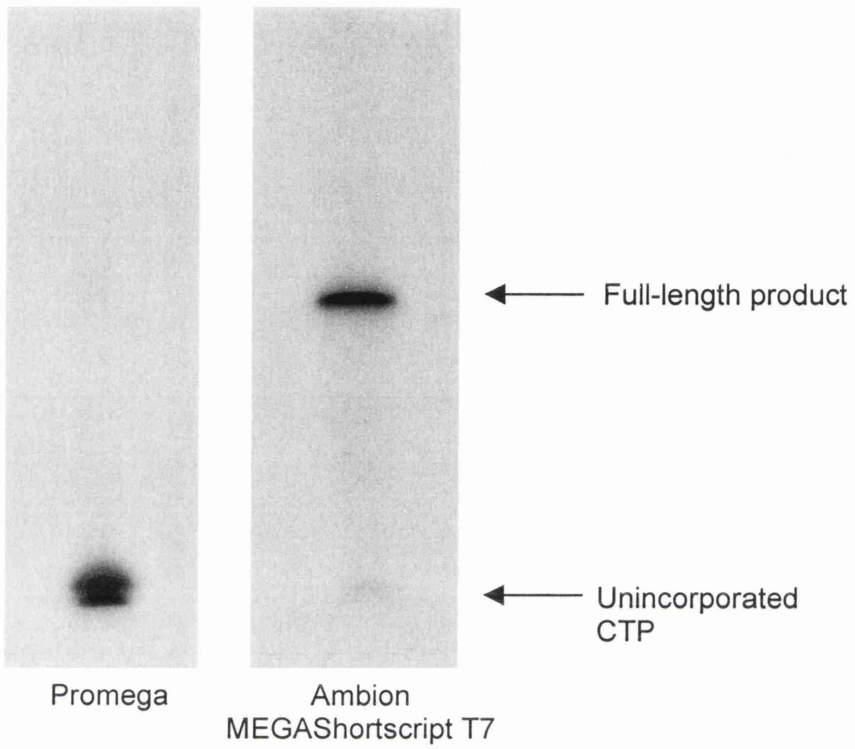

Fig.3.12. Comparison of the products of *in vitro* transcription. The products of reactions using the Promega *in vitro* transcription kit or Ambion MEGAshortscript T7 kit were phenol:chloroform extracted, subjected to denaturing PAGE on a 6% gel and analysed by autoradiography. When the MEGAshortscript kit was used the majority of CTP was incorporated into full length product, whereas very little was incorporated when the Promega kit was used.

conditions it became apparent that the kit was unable to support transcription of a 69-base radiolabelled transcript. To attempt to increase the yield of transcript the MEGAshortscript T7 kit (Ambion) was utilised. The kit is specifically designed for high-yield transcription of RNA between 20 and 200 bases in length and achieves this by supplying the NTPs and the T7 polymerase at high concentrations, thereby allowing more transcription initiation and fewer premature transcription termination events per mass unit of DNA template. The transcription plasmid is also added at a high concentration to increase the concentration of template in the reaction, and reaction times are typically longer to increase yield. Due to its reliance on high concentrations of reaction components the kit is not designed for the production of radiolabelled transcripts, in which the limiting NTP must be at a lower concentration than the other NTPs; however, the kit had previously been used successfully for this purpose by others (P Yeo, personal communication). Use of the MEGAshortscript T7 kit to generate radiolabelled BUNS5'(32)/3'(33) immediately resulted in much higher yields than the Promega kit (Fig.3.12). Incomplete linearisation of the transcription template prior to transcription results in the generation of unwanted longer transcripts not produced by run-off transcription. Analysis of the reaction products by denaturing PAGE indicated that such transcripts were absent due to complete restriction digestion by *Bbs*I.

The final optimisation step concerned the concentration of unlabelled limiting NTP, in this case CTP. This NTP must be at a relatively low concentration to allow for incorporation of the radiolabelled NTP, otherwise it would affect the specific activity of the final product. However, if its concentration were too low, the result would be a low yield due to insufficient quantities of CTP present in the reaction mix. A concentration of unlabelled CTP 1000-fold lower than that of the non-limiting NTPs was found to yield a sufficient mass of high specific-activity transcript (see Materials and Methods). Typically each reaction produced approximately 10ng of BUNS5'(32)/3'(33) transcript with a specific activity of at least $1x10^8$cpm/μg.

3.4. Development of RNA-N protein binding assays

3.4.1. Northwestern blot analysis

In order to establish whether purified N was capable of binding the BUNS terminal sequences it was necessary to set up *in vitro* RNA-protein binding assays. The binding buffer chosen for use with N was modified from the buffer used by Gött *et al* (1993) to

investigate binding of RNA by hantavirus N protein (the NaCl concentration was increased to 150mM to strengthen any interaction that were to take place). Northwestern blot analysis is a useful tool for determining whether a protein binds RNA because it is simple, rapid, and can be used to check the conditions necessary for binding as well as the identification of the molecule binding the RNA. N was subjected to SDS-PAGE and immobilised on a nitrocellulose membrane as during a Western blot. The membrane was incubated with BUNS5'(32)/3'(33) riboprobe in binding buffer, washed and exposed to film (Fig.3.13, lane 1). A single band was observed at the same size as the band detected on Coomassie blue-stained SDS-PAGE (Fig.3.7) and Western analysis of purified N (Fig.3.8). It was interpreted as the riboprobe binding to the N protein on the membrane. The band was not present in lysate from bacteria containing the empty pQE30 vector (Fig.3.13, lane 2).

3.4.2. Gel electrophoretic mobility shift assay (GEMSA)

GEMSA is a tool for analysing RNA-protein interactions, allowing interactions between multiple molecules to be visualised. The principle behind GEMSA is that a nucleic acid will run with decreased electrophoretic mobility ('shift') on a non-denaturing gel when complexed with a protein. Naked RNA can therefore be distinguished from complexed RNA by this technique. Binding assays between N and BUNS5'(32)/3'(33) riboprobe were set up using the binding buffer from Gött *et al.* (1993) that had been shown to work in Northwestern analysis. Reactions were run on a 6% non-denaturing polyacrylamide gel strengthened with 5% glycerol and subsequently analysed by autoradiography (Fig.3.14). The riboprobe was found to run towards the bottom of the gel after electrophoresis for 3h at 150V. Subsequently these gels were run for 2h at 200V at 4°C. Initial results yielded a shift of the riboprobe into two bands with decreased electrophoretic mobility on addition of N. The protein was shown to saturate the riboprobe, i.e. was able to shift it completely at high concentrations of N in the reaction. When lysate from control bacteria containing only the parent plasmid pQE30 and subjected to the same purification regime as N was used in binding reactions in the place of N, no mobility shift resulted, implying that the observed shift was attributable to N (Fig.3.14).

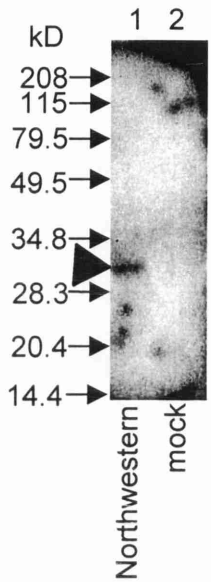

Fig.3.13. Northwestern blot analysis of N-RNA binding. N was subjected to SDS-PAGE on a 15% gel, blotted and probed with BUNS5'(32)/3'(33) riboprobe (lane 1). A band corresponding to N was observed (arrow). No band was detected in lysate from bacteria containing empty pQE30 (lane 2).

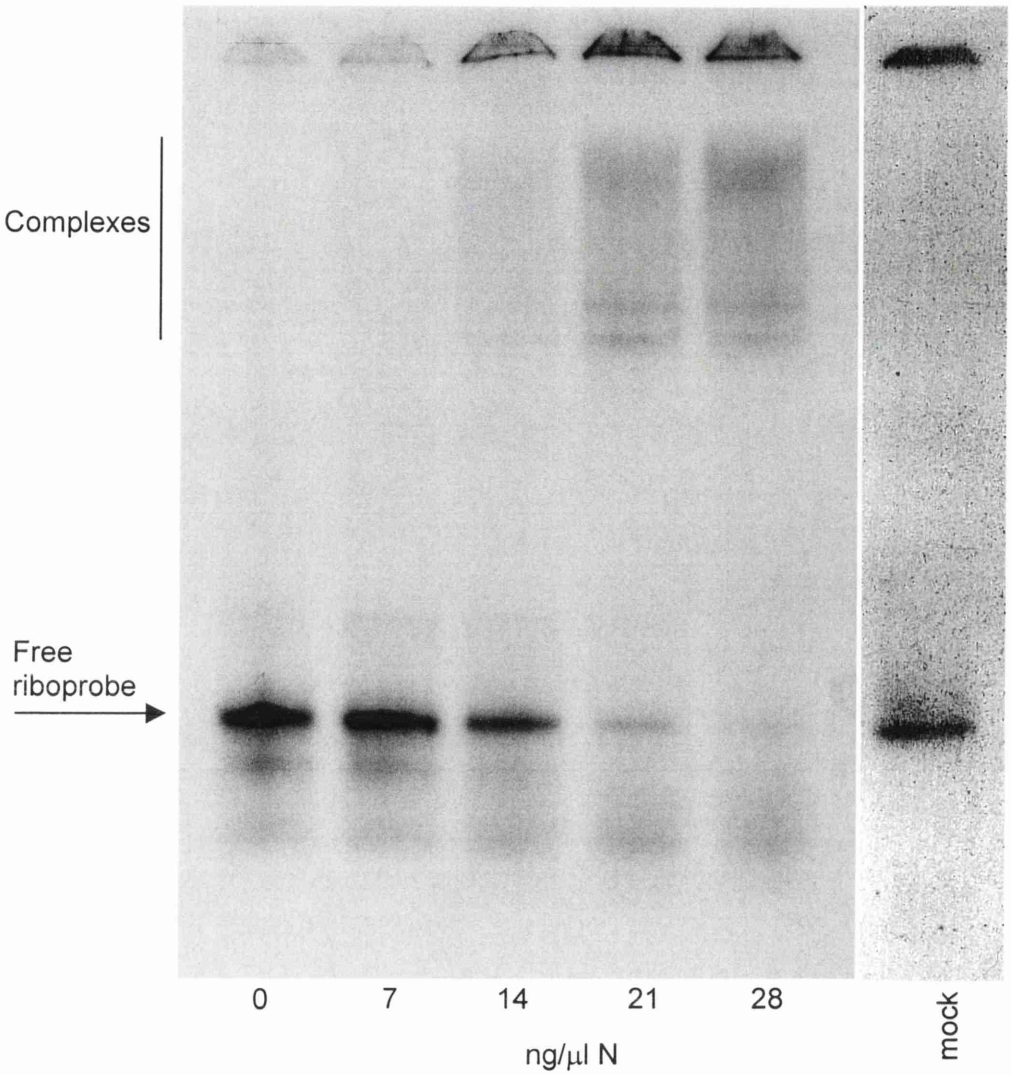

Fig.3.14. Preliminary GEMSA. The gel shows that N is able to shift the riboprobe into higher bands. Binding reactions containing 100pg riboprobe and different concentrations of N were subjected to non-denaturing PAGE on a 6% gel and analysed by autoradiography. N was found to saturate the riboprobe, which was shifted into two bands and a smear towards the top of the gel. Lysate from bacteria containing empty pQE30 plasmid and subjected to the same purification regime as N was unable to cause a shift in the mobility of the riboprobe ('mock').

3.4.3. Optimisation of binding conditions

3.4.3.1. Effect of pH on binding by N

The optimal pH for RNA binding by N was investigated. Binding reactions were performed over a range of different pH conditions and run on a non-denaturing gel as before (Fig.3.15). Mobility shifts appeared to occur at and above pH 6.9. Below pH 6.9 no shifts were observed but the riboprobe appeared to be degraded. It is possible that the rRNasin ribonuclease inhibitor, which works by binding RNases in a 1:1 ratio, was affected by low pH and inactivated, causing the riboprobe to be digested by any RNases present in the protein stock. pH 7.3 was chosen for further work as it is far enough removed from pH 6.9 to allow for slight changes in pH to occur without affecting binding.

3.4.3.2. Effect of ionic strength on binding by N

To investigate the effect of salt concentration on binding, reactions containing 100pg riboprobe and 54ng/μl N were incubated in binding reactions containing 150mM-2M NaCl and 0-20mM $MgCl_2$. The reactions were analysed by GEMSA on a 1% agarose gel (Fig.3.16) to allow comparison with recent studies on the binding of turnip crinkle virus coat protein and, more recently, TSWV N protein to RNA under various ionic conditions (Wei & Morris, 1991; Richmond *et al.*, 1998). It was apparent that binding took place in all ionic conditions tested, as shown by the absence of the band corresponding to free riboprobe in each case. In the case of NaCl, concentrations of 500mM and above resulted in a smearing of the riboprobe up the gel. This was believed to be an effect of the high salt conditions on the mobility of the complex through the gel, and was also observed by Wei & Morris (1991). As higher salt concentrations did not appear to affect RNA binding by N, the ionic conditions in subsequent binding reactions were unaltered from those originally used (150mM NaCl; 5mM $MgCl_2$).

3.4.3.3. Use of frozen protein preparation

It would be useful to be able to freeze the purified N protein preparation to increase the time that it is active and thus avoid repeated purification procedures and discrepancies between different preparations. To this end, aliquots of purified N were frozen in 25% glycerol in aliquots at –70°C and subsequently thawed slowly on ice and used in binding

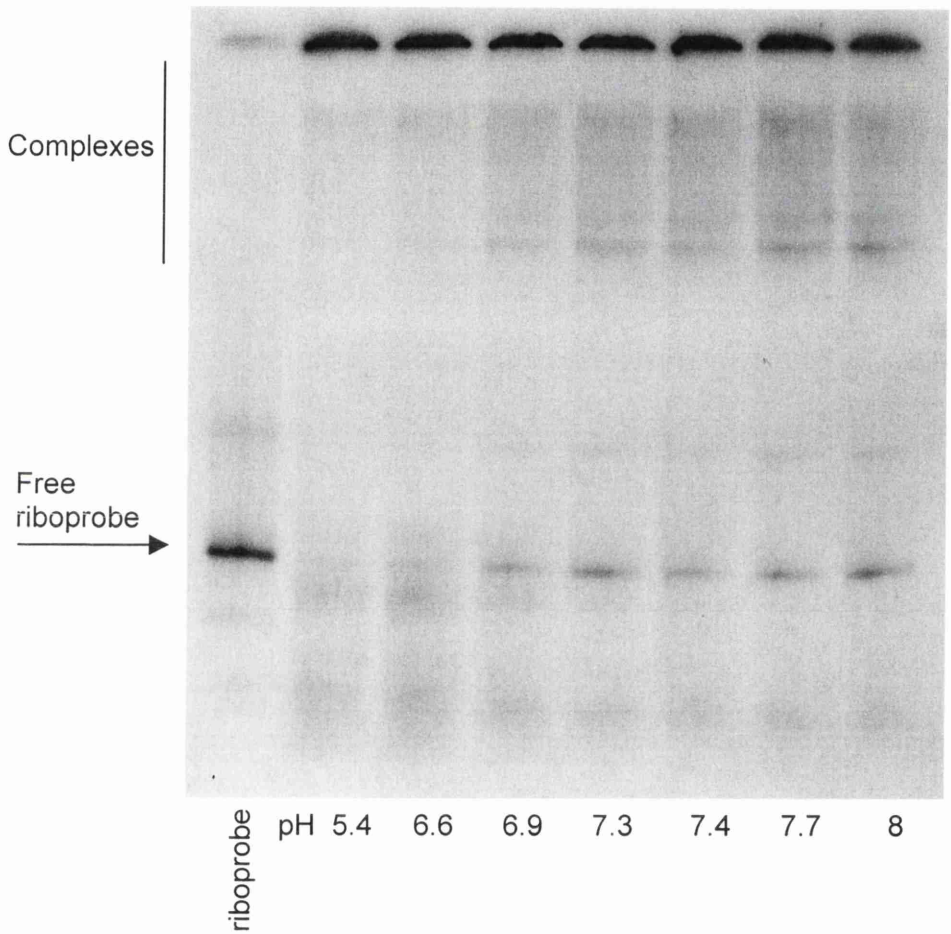

Fig.3.15. Effect of pH on binding reactions. Binding reactions containing 100pg riboprobe, 28ng/μl N and with a range of pH conditions were analysed by GEMSA on a 6% gel as before. Significant mobility shift was not observed below pH6.9 but the free riboprobe was heavily degraded under these conditions, suggesting that the RNase inhibitor was inactive in these reactions. Binding was observed from pH 6.9 to pH8, apparent as a mobility shift of the riboprobe.

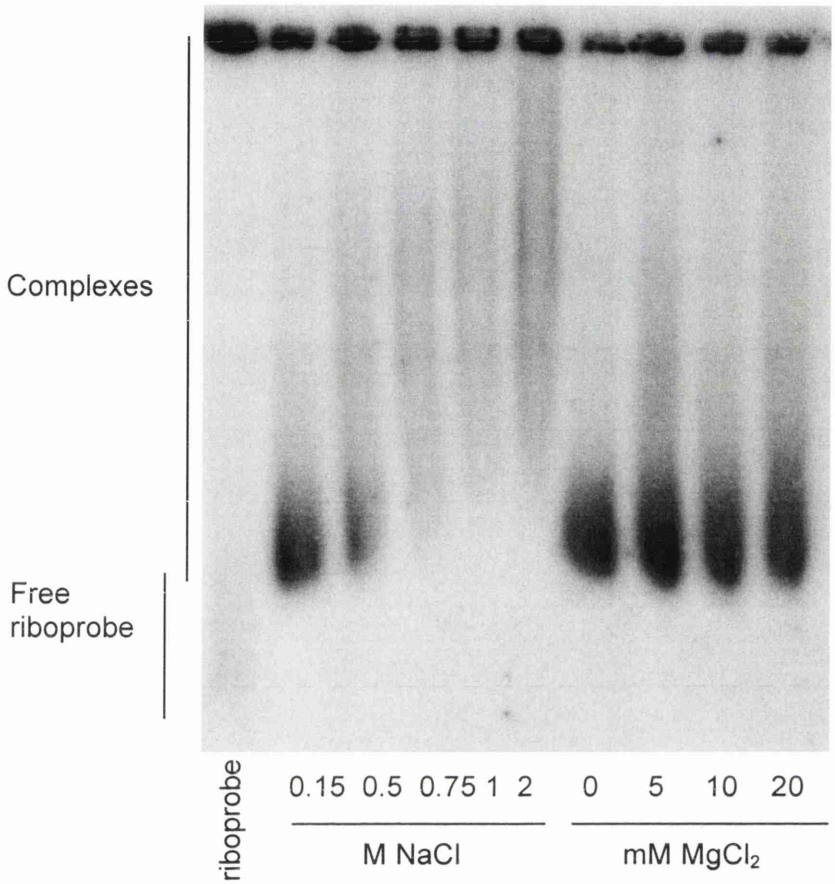

Fig.3.16. Effect of ionic strength on complex formation. Binding reactions containing 100pg riboprobe and N at 54ng/μl were incubated with different concentrations of NaCl or $MgCl_2$ and run on a 1% agarose gel. No free riboprobe was present under any conditions, implying that binding can take place in a wide range of concentrations. The smear observed at high concentrations of NaCl is presumed to be due to the effect of high salt concentrations on the mobility of the complex through the gel.

reactions. On analysis of the reactions by GEMSA it was found that the protein was still capable of causing a mobility shift of the riboprobe but no saturation of the riboprobe could be achieved, even at much higher concentrations of N than previously used (Fig.3.17). The different banding pattern to that seen previously was subsequently discovered to be dependent on the individual protein stock and different gel-running conditions and was not a result of the protein having been frozen. The fact that N was still able to cause a shift but unable to saturate the riboprobe suggested that the concentration of active molecules in the preparation had decreased, presumably through being damaged during the freezing and thawing processes. As the frozen N stock was clearly not behaving identically to the fresh preparation it was not used subsequently.

3.5. Summary

This chapter can be summarised as follows:

- 6xHis-tagged BUN N protein was expressed in bacteria and purified in its native form by nickel affinity chromatography in large-scale preparations.
- Analysis of N by SDS-PAGE and Western blotting indicated that purified N was pure and ran with the expected electrophoretic mobility. N could be detected by an antibody to the His-tag and by rabbit polyclonal antiserum raised against BUN.
- The approximate N-terminal half of N was also expressed in bacteria and was detected by an antibody to the His-tag in bacterial lysate, but expression levels were too low for purification of significant amounts.
- Analysis of large amounts of unheated, purified N by Western blotting using an antibody to the His-tag and polyclonal antisera raised against BUN or N indicated the presence of higher molecular-weight bands that were not affected by RNase treatment but were partially sensitive to boiling, leading to their identification as putative multimers of N.
- The His-tag could not be cleaved by treatment with factor Xa despite the presence of an appropriate site between the tag and the protein. Hence, this region of the polypeptide was suggested to be inaccessible to the protease.
- A 69nt, ^{32}P CTP-labelled riboprobe designated BUNS5'(32)/3'(33) and consisting of the terminal 32nt of the 5' and 33nt of the 3' termini of the BUN S segment joined by a short linker region was generated by *in vitro* transcription, and the transcription conditions optimised.

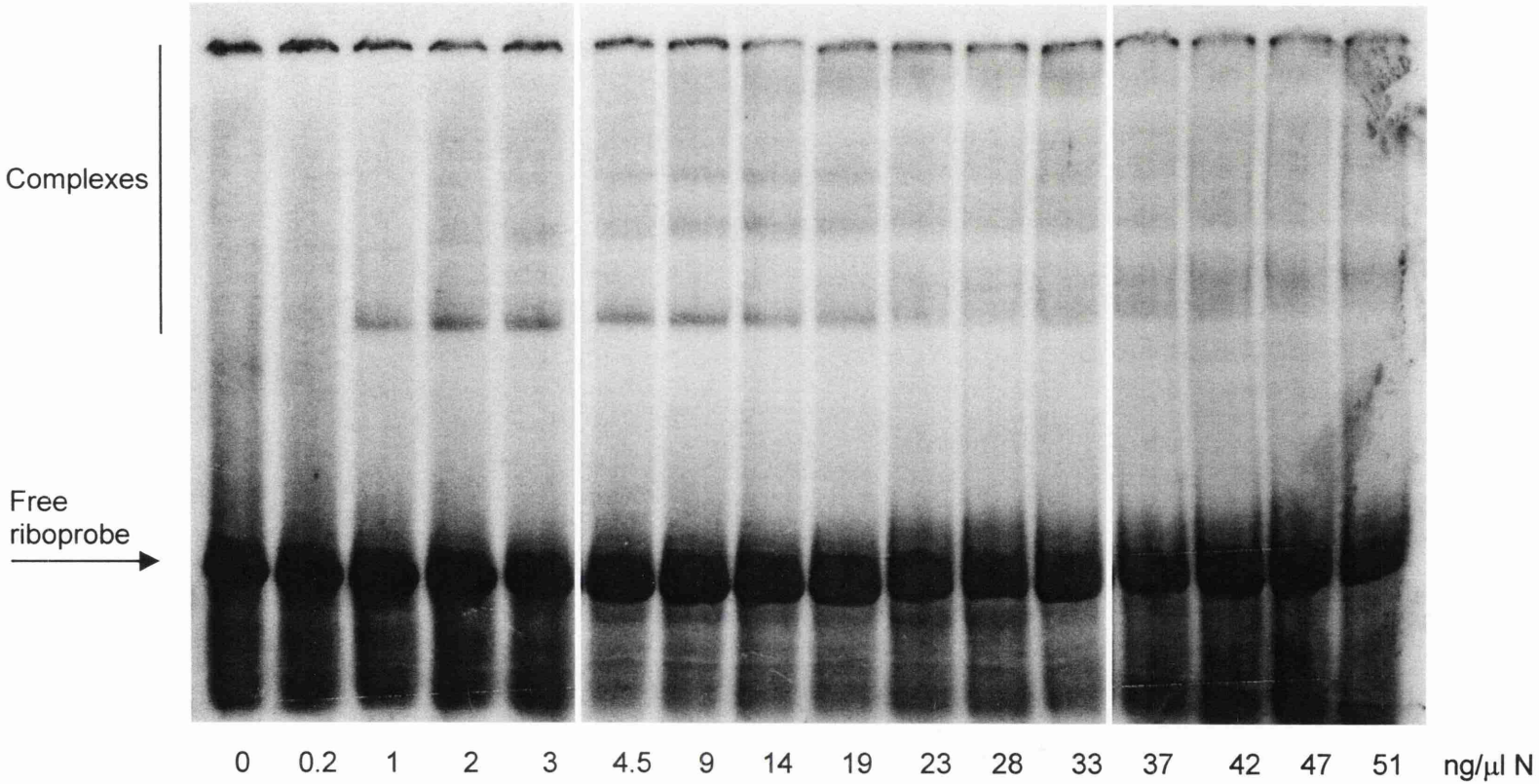

Fig.3.17. GEMSA using N stored at –70°C in 25% glycerol. Binding reactions containing 100pg riboprobe and different concentrations of N were incubated and analysed on a 6% polyacrylmide gel as before. N was found to shift the riboprobe into higher complexes but was unable to saturate it, even at high concentrations (cf. Fig.3.14), implying that N had been damaged during the freeze-thawing process. The difference in the banding pattern on comparison with Fig.3.14 is due to differences in the protein stocks. This figure also represents a longer exposure than Fig.3.14.

- Binding reactions were performed containing BUNS5'(32)/3'(33) and N. BUNS5'(32)/3'(33) was found to bind exclusively to N on analysis by Northwestern blotting.
- Gel electrophoretic mobility shift assays (GEMSA) were developed to investigate N binding to BUNS5'(32)/3'(33), and saturation of the riboprobe by N in binding reactions was demonstrated.
- Binding could be detected at pH6.9 and above, and was found to take place over a wide range of ionic conditions.
- N stored at –70°C was found to be incapable of saturating the riboprobe and its use was therefore discontinued.

Chapter 4: Analysis of N-RNA binding

In the previous chapter it was shown that purified recombinant N protein could bind a synthetic RNA containing the BUNS termini, and the binding event could be visualised as a shift in the electrophoretic mobility of the RNA on a non-denaturing gel. In this chapter the techniques developed above are applied to analyse the encapsidation process.

4.1. Analysis by GEMSA

4.1.1. Analysis of binding by polyacrylamide GEMSA

A polyacrylamide GEMSA of binding reactions using a different N protein stock than that used in Fig.3.14, run at 200V for 2h at 4°C, resulted in the production of multiple mobility shift bands (Fig.4.1). At low concentrations of N a proportion of the riboprobe was shifted into a single band of decreased electrophoretic mobility. When the concentration of N was increased a ladder of multiple distinct bands was resolved. On saturation, the riboprobe was shifted diffusely towards the top of the gel. A ladder of bands in GEMSA has been reported to be indicative of sequential filling of multiple binding sites on RNA (Black *et al.*, 1998). The ladder-like profile would therefore appear to be composed of distinct N-RNA complexes, presumably due to different numbers of N molecules binding the riboprobe. It might therefore be representative of an intermediate step in the sequential binding of N along the RNA.

This particular gel was limited by its inability to resolve saturated complexes. Nucleoprotein-RNA complexes from other viruses have previously been observed to be unable to enter the gel due to their increased size and extensive charge or insolubility, a phenomenon known as 'well-shift', and has been observed for instance with hantavirus N-RNA complexes (Gött *et al.*, 1993). This occurrence is also indicative of aggregation of the protein at high concentrations. During optimisation of gel-running conditions a GEMSA had been produced showing resolution of saturated N-RNA complexes within the gel (Fig.4.2). The majority of saturated complexes was observed to have run into the gel and form discrete bands just below the wells. It would therefore appear that N protein at concentrations high enough to saturate the RNA does not aggregate and

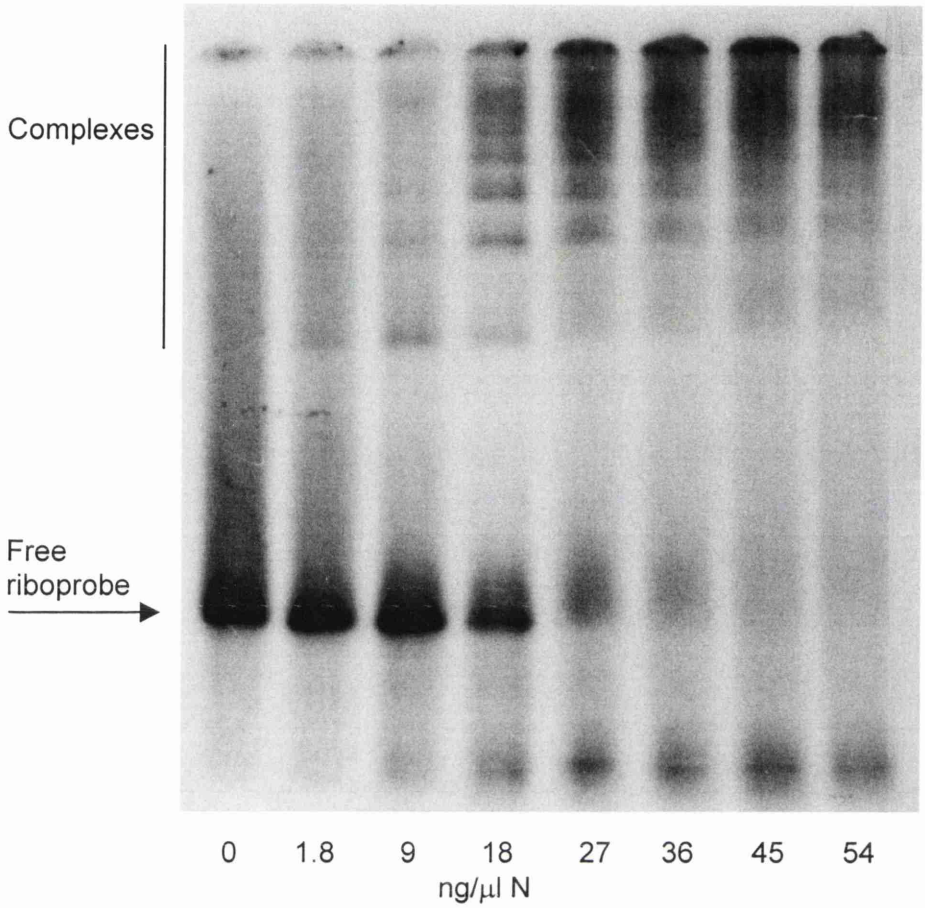

Fig.4.1. GEMSA showing shifting of the riboprobe into a ladder of higher bands. Reactions containing 100pg riboprobe were subjected to analysis on a 6% gel. The riboprobe was shifted into a single band of decreased mobility by a low concentration of N. At higher concentrations the riboprobe was shifted into multiple complexes in a ladder-like profile typical of sequential binding. On saturation the riboprobe was shifted towards the top of the gel.

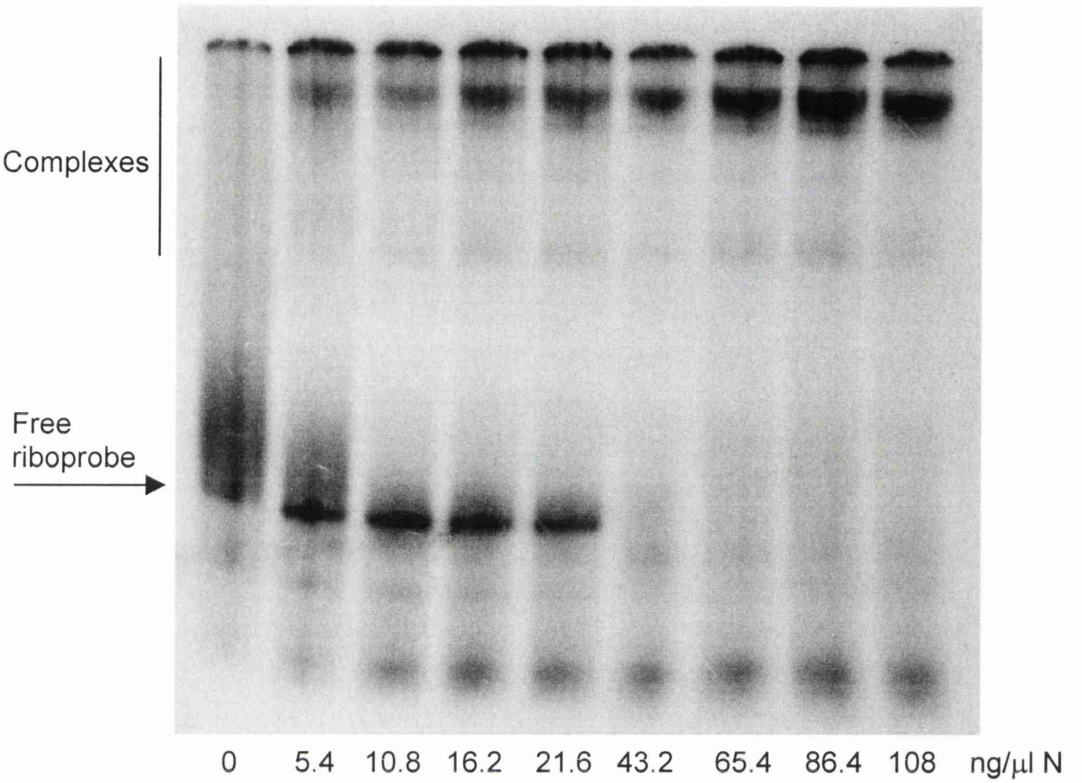

Fig.4.2. GEMSA showing localisation of riboprobe saturated with N below the wells. Binding reactions containing 100pg riboprobe were subjected to analysis on a 6% polyacrylamide gel. The presence of saturated riboprobe below the wells indicates that saturated complexes are soluble and small enough to enter the gel matrix.

complexes are small enough to run into the gel matrix. Despite multiple attempts the exact gel conditions to produce this particular shift could not be repeated.

4.1.2. Analysis by agarose GEMSA

Groups that had experienced well-shift of large or insoluble complexes had resorted to using agarose gels to resolve them (e.g. Gött *et al.*, 1993). To attempt to gain a more detailed view of saturated N-RNA complexes, binding reactions using the same protein preparation and identical to those used in the polyacrylamide GEMSA in Fig.4.1 were run on a 1% agarose gel and detected by autoradiography (Fig.4.3). As with the polyacrylamide GEMSA the riboprobe was found to run towards the bottom of the gel. In the presence of N the riboprobe was shifted into at least one complex, resolvable as one diffuse band. Even at N protein concentrations well above the saturation point the complex was observed to run a long way into the gel. Of particular interest is the fact that on saturation of the riboprobe, the complexes reached a finite maximum size which was unaffected by an increase in N protein concentration. When N was replaced with bovine serum albumin (BSA) in binding reactions, no mobility shift resulted. This implies that the shift is specific for N.

4.1.3. Concentration-dependency of binding

The saturation point in the binding of N to RNA has thus far been defined as the lowest concentration of N at which all of the RNA shifted into complexes in a GEMSA. However, at this point N is not necessarily saturated by the RNA, i.e., N may possess a capacity for binding more RNA than that available to it at the saturation point. Binding reactions were set up containing 100pg riboprobe and N at a concentration 3-fold above that necessary to achieve the saturation point previously determined (to allow for experimental discrepancies) plus different amounts of unlabelled BUNS5'(32)/3'(33), i.e. homologous unlabelled RNA. Reactions were subjected to agarose GEMSA (Fig.4.4). On the resulting gel reactions with increasing mass of RNA are shown from left to right. The point at which the protein was no longer able to saturate the RNA was indicated by the appearance of discernible free riboprobe at the bottom of the gel. This was observed first in a reaction containing 50ng of unlabelled homologous RNA, corresponding to a 500-fold mass excess over the riboprobe. Hence, with a three-fold increase in concentration of N above that at which it is only just capable of saturating 100pg of RNA, its capacity for binding RNA increased almost 500-fold. This was

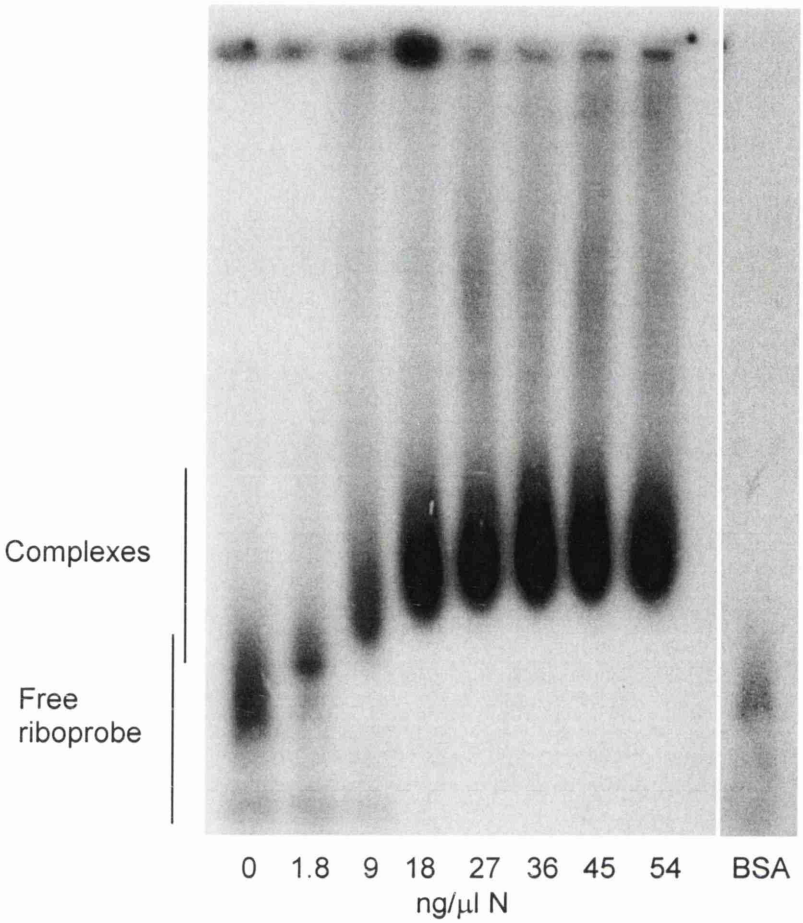

Fig.4.3. Agarose GEMSA. Binding reactions identical those used in Fig.4.1 were run on a 1% agarose gel and analysed by autoradiography. The riboprobe was shifted into a single band that ran well into the gel. The band reached a finite maximum size on saturation of the riboprobe with N. Replacement of N with 500ng BSA in the binding mix did not result in a mobility shift (BSA lane).

Fig. 4.4. Agarose GEMSA showing the point of saturation of N with RNA. Binding reactions containing 100pg riboprobe, different amounts of unlabelled, homologous RNA and 54ng/μl N were analysed on a 1% agarose gel. At this concentration N was able to saturate 40ng but not 50ng of RNA, observable as free riboprobe in reactions containing at least 50ng RNA but not in those containing 40ng or less. To clarify the point of saturation on the gel it was exposed to a phosphorimager screen and scanned using a phosphorimager. The relative density of the bands in the digital picture was then analysed by image analysis software (lower images). Densities were plotted along horizontal and vertical axes depicted on the image. The plot for the horizontal axis is shown at the top, the plot for the vertical axis at the side. The horizontal axis was positioned at the same height as the lower band of free riboprobe; its plot indicates the amount of free riboprobe in each lane of the gel. A peak in density can be seen at 50ng RNA and not below. The vertical axis was placed along the lanes corresponding to reactions containing 30 or 90ng homologous RNA. Its plot demonstrates an increase in density at the position in which free riboprobe is expected to run at 90ng RNA but not at 30ng RNA, indicating that the increased density observed in the horizontal plot is due to free riboprobe.

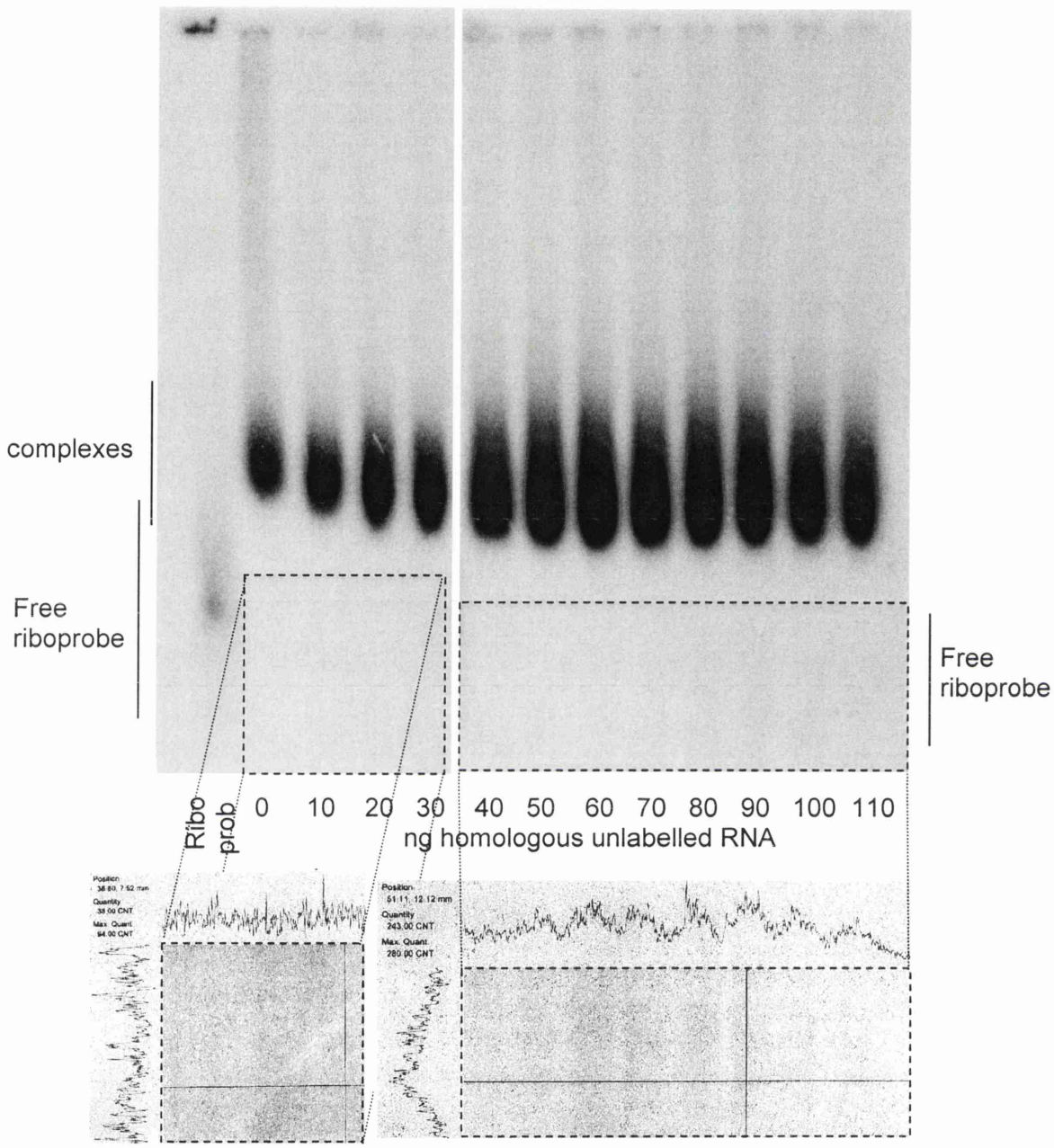
complexes
Free riboprobe
Free riboprobe
Ribo prob
0 10 20 30 40 50 60 70 80 90 100 110
ng homologous unlabelled RNA

interpreted as indicating that the ability of N to bind RNA is dependent on its concentration, which suggests there is co-operativity in the binding event.

4.2. Analysis by filter-binding

4.2.1. Binding kinetics

Whilst effective at providing an image of N binding to the RNA, GEMSA does not allow easy quantification of the degree of binding, particularly when multiple binding sites are present. Quantification would be possible by excising gel fragments containing bands and analysing these by scintillation counting but the diffuse nature of bands, their tendency to overlap, the loss of some complexes from the gel due to well-shift and quenching by the gel matrix make quantification technically difficult and inaccurate. However, filter-binding provides a highly quantifiable measurement of the extent of binding. The data obtained can be analysed by mathematical techniques.

Filter-binding operates on the premise that protein is immobilised on a nitrocellulose filter of appropriate charge, whereas nucleic acids pass through it. Thus, in an assay concerning the binding of a protein to a radiolabelled nucleic acid, the amount of nucleic acid bound is detectable as the amount of radiolabel immobilised on the filter by the association of the nucleic acid with the protein. N-RNA binding reactions were passed under vacuum through a nitrocellulose filter that had been pre-soaked in binding buffer. The filter was washed with binding buffer and the amount of RNA retained on it determined by Cerenkov counting. The data were plotted as concentration of N against percentage binding, with the highest number of counts obtained taken as 100% (Fig.4.5). The resulting curve reflected the kinetics of N binding to RNA, with an increase in N protein concentration corresponding to an increase in binding as expected. The saturation point was determined as the point at which no further binding could take place, namely $7x10^{-7}$M, or 18ng/μl. This differs from the saturation point determined from GEMSA analysis and may be due to complexes dissociating more easily on GEMSA analysis. The dissociation constant, k_d, is a measurement of the strength of binding. It was calculated as $½V_{max}$, or half the protein concentration necessary to yield half-maximal binding, which is approximately $7x10^{-8}$M. This indicates a relatively strong interaction.

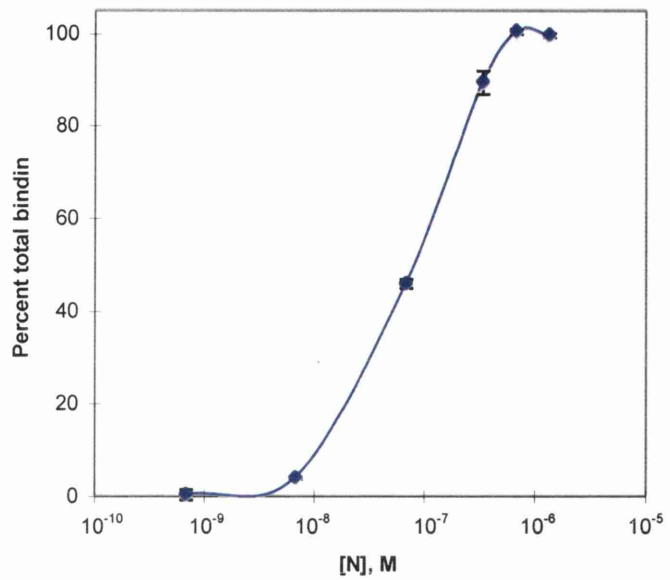

Fig.4.5. Kinetics of N binding BUNS5'(32)/3'(33) RNA. Reactions containing 100pg were subjected to filter-binding and background counts subtracted. The dissociation constant k_d was calculated as $1/2V_{max}$, which is approximately $7x10^{-8}$M. Error bars indicate the standard deviation.

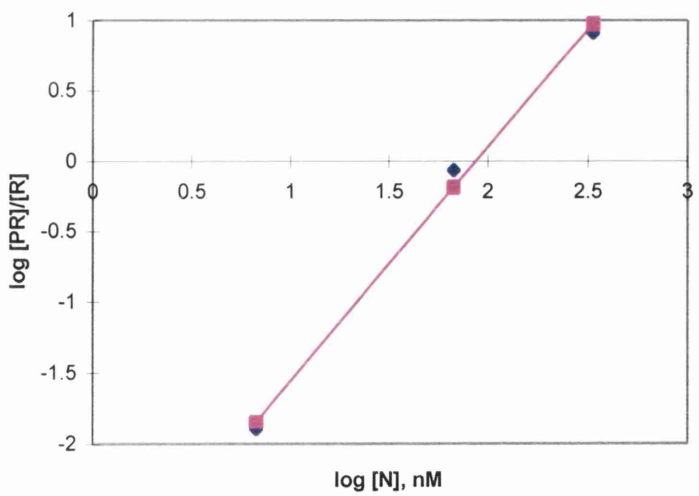

Fig.4.6. Hill plot analysis of N binding BUNS5'(32)/3'(33) RNA. The data obtained from filter-binding in Fig.4.5 were plotted as log [N] in nM against log [PR]/[R], where PR is bound riboprobe and R is free riboprobe. Data points from the extremes of the binding curve were excluded because they correspond to the first and final binding events. Linear regression analysis was performed, and the gradient of the resultant line calculated as approximately 1.66, indicating a low degree of co-operativity.

4.2.2. Co-operativity of the binding event

Co-operativity is the influence of the binding of a protein to a binding site on the binding of subsequent proteins to separate sites. It can be positive, thereby facilitating the binding of subsequent proteins, or negative, in which case there is an inhibitory effect (Black *et al.*, 1998). The degree of co-operativity can be measured by performing a mathematical analysis of binding data and plotting the results as a Hill plot, in which log [protein] is plotted against log ([bound riboprobe] / [free riboprobe]). Performing linear regression on the data yields a best-fit line through the data points. The gradient of the line is termed the Hill coefficient and is a measure of the degree of co-operation between sites. The coefficient is a measurement of the theoretical number of sites that can be bound co-operatively. Thus, a value above 1 indicates a positive co-operation, whereas a value below 1 means that there is negative co-operativity. A value of exactly 1 implies a lack of co-operativity, i.e. that only one protein is binding or that all sites are filled independently of one another.

The binding data obtained from filter-binding were subjected to Hill plot analysis as described above (Fig.4.6). Data points taken from the extremes of the binding curve were excluded from the analysis as they represent binding of the first and final proteins, which cannot be co-operative (Creighton, 1993). The only binding events that can be co-operative are those represented by the middle of the binding curve. The resultant Hill coefficient, calculated as the gradient of the best-fit line by Excel, was approximately 1.7 which indicates a low degree of positive co-operativity.

4.3. The authenticity of *in vitro* assembled complexes

4.3.1. Determination of the buoyant densities of N-RNA complexes

Authentic nucleocapsids purified from infected cells have been reported to band at 1.31g/ml in a 20-40% CsCl gradient (Obijeski & Murphy, 1977). This property could be used to judge whether the synthetic N-RNA complexes formed in *in vitro* binding reactions share some properties with authentic nucleocapsids. Instead of using the time-consuming conventional method of creating CsCl gradients which involves mixing changing concentrations of 20% and 40% solutions together as the gradient is made, a Gradient Master machine (Biocomp) was used. To make the gradient 20% CsCl was layered below an equal volume of 40% CsCl, the tube was sealed and air bubbles

removed. The solutions were then mixed by rotation of the tube by the machine at a pre-determined speed, angle and time. As the method will not necessarily yield a linear gradient, the first gradient was fractionated and the density of representative fractions determined. The first gradient was found to be significantly non-linear (Fig.4.7a). When the time and angle of rotation were increased an almost linear gradient was produced, which was thought to provide greater accuracy in measuring the density of complexes run on the gradient (Fig.4.7b). After centrifugation the gradient was found to span densities of approximately 1.21 to 1.42g/ml (Fig.4.7c).

To make the result as representative as possible, the entire BUN S segment RNA was used in binding reactions instead of BUNS5'(32)/3'(33). A ^{32}P-labelled riboprobe, consisting of the precise BUN S segment RNA, was transcribed by run-off transcription from a PCR product consisting of the entire S segment cDNA downstream of a modified T7 promoter. The PCR product was generated by amplifying the S segment cDNA and T7 promoter of the plasmid pT7riboBUNS using primers to the T7 promoter and 3' end of the cDNA (Fig.4.8). The riboprobe was incubated with N in a binding reaction, which was then layered onto a sucrose cushion on top of the gradient and subjected to ultracentrifugation for 16h. A duplicate gradient to which a control binding reaction lacking N had been added was also run. The gradients were fractionated from the bottom and fractions subjected to TCA precipitation to remove degraded RNA and screened for RNA content by Cerenkov counting. The resultant graphs show that the naked RNA was located towards the bottom of the gradient (Fig.4.9b), whereas the RNA present in binding reactions with N was localised at the top of the gradient (Fig.4.9a). Apparently, most of the complexes banded with a density of 1.25g/ml or lower.

4.3.2. Resistance to digestion with ribonuclease

Another property of viral nucleocapsids purified from infected cells is a limited resistance to digestion of the RNA with ribonuclease (Hacker *et al.*, 1989; Kolakofsky & Hacker, 1991; Obijeski *et al.*, 1976b). It was considered possible that the authenticity of N-RNA complexes formed in binding reactions could also be tested by analysing the effect of ribonuclease treatment on them. Binding reactions with 100pg BUNS5'(32)/3'(33) riboprobe and containing or lacking 54ng/μl N were incubated with a range of RNase A concentrations, then the riboprobe RNA extracted and subjected to denaturing PAGE (Fig.4.10). All reactions contained 20U of rRNasin RNase inhibitor

a

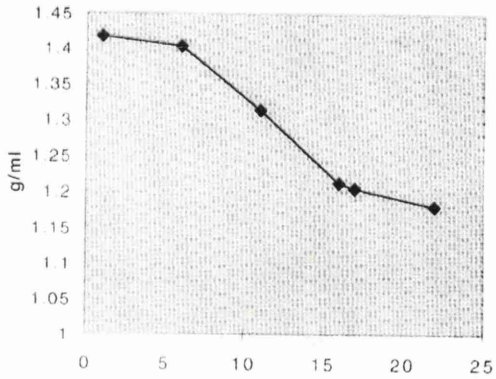

b

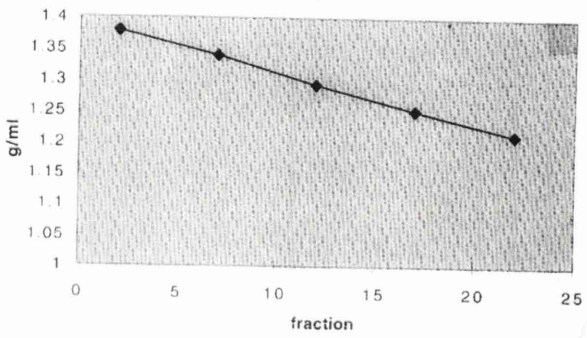

c

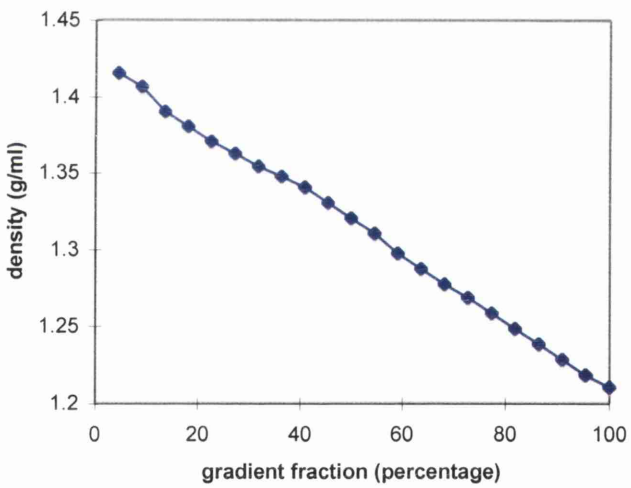

Fig.4.7. Optimisation of CsCl gradient formation. Gradients were made using a Gradient Master (Biocomp) and the densities of representative fractions determined. An initial attempt using an angle of rotation of 65° for 2min 19s at 25rpm yielded a highly non-linear gradient (a). Mixing of the two CsCl solutions was increased by changing the conditions to an angle of 70° for 4min at 25rpm. The resulting gradient was almost totally linear (b), allowing increased accuracy in determining the buoyant density of complexes analysed on the gradient. After a gradient had been subjected to centrifugation the densities of fractions indicated that it remained relatively linear and spanned approximately 1.21 to 1.42 g/ml (c).

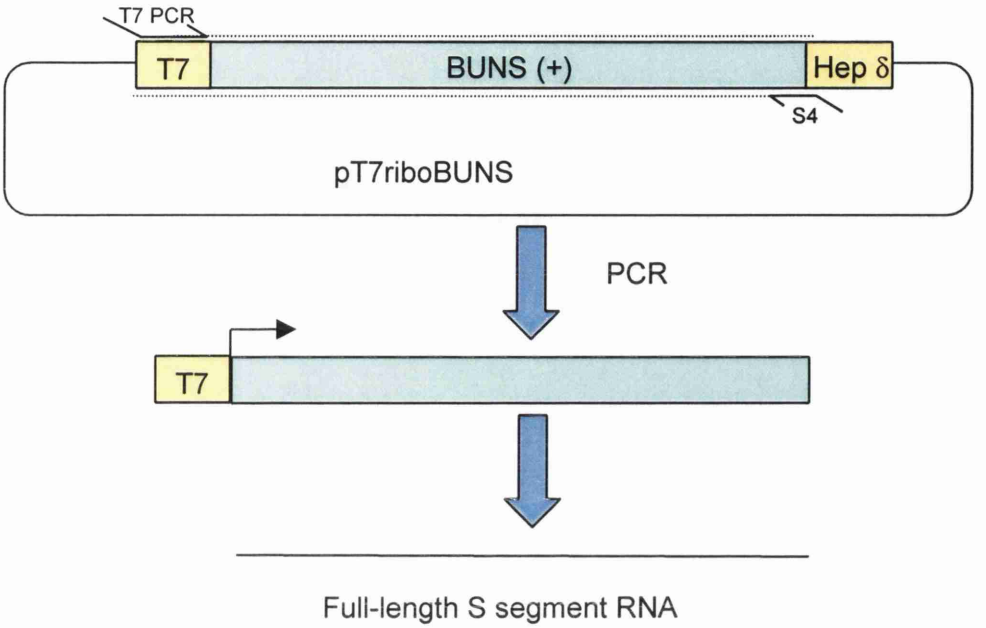

Fig.4.8. Generation of full-length S segment RNA. The entire S segment cDNA in pT7riboBUNS plus the T7 promoter upstream of the cDNA were amplified by PCR. The precise S segment transcript was then generated by run-off transcription of the PCR product.

a

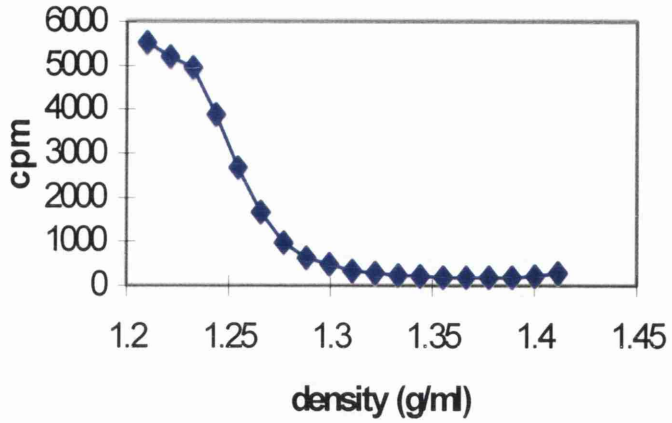

b

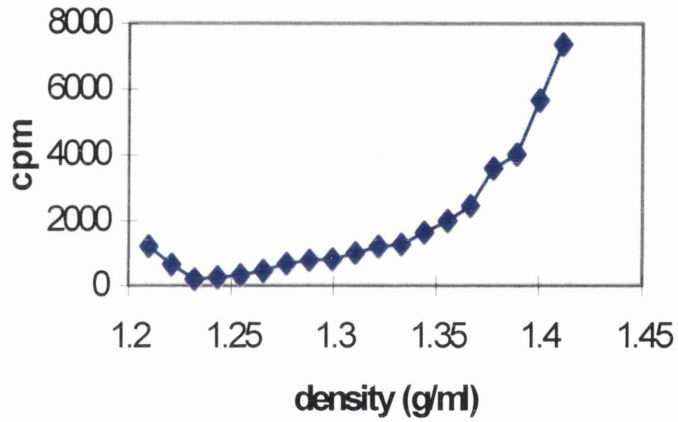

Fig.4.9. Determination of the buoyant density of N-RNA complexes. *In vitro* assembled complexes consisting of 54ng/μl N and full-length S segment riboprobe (a) or free riboprobe (b) were run on 20-40% CsCl gradients. The gradients were fractionated, degraded RNA removed by TCA precipitation and the amount of RNA in each fraction determined by Cerenkov counting. The free riboprobe accumulated at the bottom of the gradient (b), whereas complexed RNA accumulated at a density lower than 1.25g/ml (a).

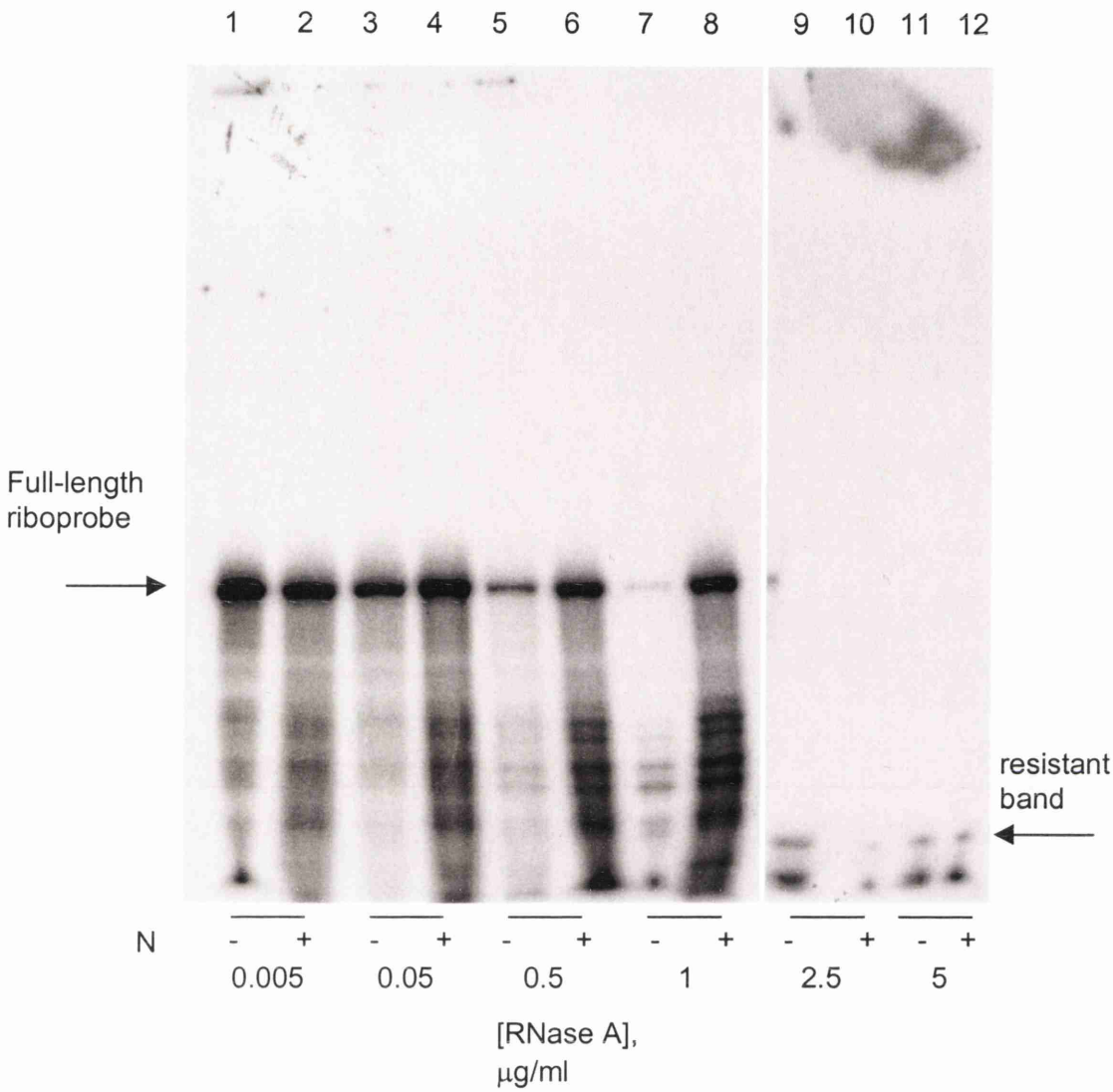

Fig.4.10. Resistance of N-RNA complexes to digestion with RNase A. Naked riboprobe (odd-numbered lanes) or riboprobe complexed with N (even-numbered lanes) was treated with RNase A at the concentrations indicated, phenol:chloroform extracted and analysed by denaturing PAGE on a 6% gel. At 1μg/ml the naked RNA was almost completely digested (lane 7) whereas the complexed RNA appeared almost fully resistant (lane 8). At concentrations above this all full-length RNA was digested (lanes 9-12). However, a band of low molecular weight was observed in these lanes implying that there is a highly-resistant motif in both naked and complexed RNA.

(Promega), which is required to inhibit any RNases present in the protein stock; this amount of rRNasin was considered to exert a nominal effect on the amount of RNase A added (1U of rRNasin inhibits 5ng of RNase A by 50%; Promega). The N-RNA complexes were observed to be fully resistant to digestion by up to 1μg/ml RNase A, despite the naked RNA being almost completely degraded at this concentration. Incubation of the complex with concentrations of RNase A greater than 1μg/ml resulted in digestion of the RNA. Although the full-length RNA was completely digested, a small band was still visible at the bottom of the gel at RNase A concentrations up to 5μg/ml. This band appeared to be resistant to high concentrations of RNase A and is thus likely to be double-stranded as RNase A can only digest single-stranded RNA. It might constitute a stem-loop or panhandle structure in the RNA.

4.4. Discussion

This chapter described a biochemical analysis of the binding of BUN N to a synthetic RNA containing the BUNS termini. Binding was investigated by polyacrylamide and agarose GEMSA and filter-binding assays. Multiple N proteins binding in a sequential fashion were visualised as a ladder on a polyacrylamide GEMSA (Fig.4.1; Black *et al.*, 1998).

Binding was found to be strong on analysis of both binding kinetics (Fig.4.5). The dissociation constant was determined to be $7x10^{-8}$M, which is similar to that obtained for influenza virus and hantavirus N-RNA interactions (Baudin *et al.*, 1994; Digard *et al.*, 1999; Severson *et al.*, 1999). The molar ratio of RNA to protein at the saturation point was approximately 1:1500. Such high ratios are not unusual for coat or nucleoproteins binding RNA, and suggest a low proportion of active protein molecules (Wei & Morris, 1991). However, it is also possible that, as the protein binds along the RNA, a higher molar ratio of protein to RNA is required.

The apparent lack of salt dependency observed in Fig.3.16 on optimisation of the binding conditions also suggests that the binding is strong and stable (3.4.3.2). In addition, salt dependency indicates the type of binding that takes place between the RNA and protein. Cations screen the electrostatic field of the RNA molecule, thus preventing electrostatic interactions mediated by basic residues in the protein to take place. The fact that binding occurred at a high concentration of salt implies that electrostatic interactions are not the sole basis for the binding event. Hantavirus and tospovirus N proteins were also found to bind over a range of ionic conditions, although

TSWV N-RNA binding was disrupted at 300mM NaCl and eliminated at 600mM NaCl (Richmond *et al.*, 1998; Severson *et al.*, 1999).

According to previous studies one bunyavirus N protein molecule is believed to bind 6 nucleotides of viral RNA (Bishop & Shope, 1979). The 69nt riboprobe used in the binding assays would therefore presumably have sufficient binding sites for approximately 11 protein monomers to bind, if indeed BUN N binds in its monomeric form. Each 'rung' of the ladder observed on polyacrylamide GEMSA is thought to be indicative of a distinct N-RNA complex, with higher shifts corresponding to greater numbers of N proteins binding (Fig.4.1). Although the exact number of bands cannot be resolved, an approximate figure can be extrapolated from the pattern of well-resolved bands on the gel and this would appear to approximate the figure of 11 calculated above. This and other evidence point to the N protein binding along the full length of the RNA molecule. On treatment of the N-RNA complex with RNase A the intensity of the band corresponding to full-length riboprobe was unaffected up to reasonably high concentrations of the ribonuclease (Fig.4.10). If the RNA was only partially bound by N a decrease in the intensity of the band plus the appearance of a lower band would be expected, corresponding to the digestion of the unbound region of the riboprobe. This was not observed. In addition, the complexes were found to reach a finite maximum size independent of a further increase in protein concentration, on both polyacrylamide and agarose GEMSA (Figs.4.2 & 4.3). If the riboprobe were not fully bound at the concentration of N required for saturation of the RNA, an increase in the size of the complex proportional to the corresponding increase in protein concentration would be expected as remaining sites were filled. Again, this was not observed.

The latter observation was also interpreted to indicate that only the exact number of protein molecules required to saturate the RNA bind it. If N multimerises to an unrestricted extent prior to or after binding RNA the degree of multimerisation would presumably increase with protein concentration, resulting in the size of the complexes increasing in proportion to N protein concentration. However, the complexes reach a finite maximum size indicating that there is no further association of N with saturated RNA.

The apparent multimers of N visualised in Western blots in chapter 3 can then be explained in a number of ways (Fig.3.8). Firstly, N might have assembled along bacterial RNA present in the protein stock. Secondly, N proteins may multimerise in

solution at high concentrations but be unable to bind RNA in this form. Thirdly, N may actually bind in a multimerised state.

Structures of nucleoprotein multimers from negative-strand viruses exist for influenza and rabies viruses (Ortega *et al.*, 2000; Schoehn *et al.*, 2001), which are discussed in section1.2.3, and respiratory syncytial virus (RSV; P. Yeo, personal communication). In each case the multimer was seen to possess a toroidal structure on electron microscopy, each circle containing 9-12 monomers of nucleoprotein. Rabies virus N protein was found to progress from a ring to a helical structure in the presence of long pieces of RNA (Schoehn *et al.*, 2001). Electron micrographs of BUN N-RNA complexes yielded ring structures extensively smaller than those of the viruses mentioned above (data not shown), which were therefore considered unlikely to be N multimers. However, it is quite possible that BUN N multimerises in a similar fashion. If this is the case, it is possible that BUN N can bind RNA as a monomer or multimer and monomers can add to the multimer until a complete toroid results. The presence of a single toroid as a discrete unit would then explain the absence of complexes larger than the saturated complex. This would be particularly true if, similar to RSV, a discrete unit consists of 11 monomers as this is the exact number believed to bind the 69nt riboprobe used in the assays. However, it is interesting that a low proportion of the riboprobe shifted into a single band of decreased electrophoretic mobility on polyacrylamide GEMSA at a low concentration of N (Fig.4.1). This phenomenon was also seen recently with TSWV N protein (Richmond *et al.*, 1998). It suggests either that the initial binding event is undertaken by a monomer or that it takes place at a protein concentration too low to allow multimers to form. Analysis of the binding of influenza virus nucleoprotein NP to both itself and RNA yielded dissociation constants of $2x10^{-7}$M (Elton *et al.*, 1999) and $2x10^{-8}$M (Baudin *et al.*, 1994; Digard *et al.*, 1999) respectively, suggesting that the NP-RNA interaction takes place before multimerisation (Elton *et al.*, 1999). However, Ortega *et al.* (2000) reported that influenza NP was expected to bind RNA as a dimer when the length dependence of the RNA and the number of nucleotides bound by each NP were compared.

A small increase in protein concentration was found to result in a large and disproportionate increase in its capacity for binding RNA (Fig.4.4). In addition, binding of N was determined to be slightly positively co-operative on Hill plot analysis of filter-binding data (Fig.4.6). Positive co-operativity is defined as the facilitation of binding of subsequent proteins to a binding site. This is presumably attributable to interactions

between N proteins, and does not exclude the possibility that proteins bind as multimers of definite size.

Binding of N to RNA appears to take place along the length of the molecule in a co-operative fashion. It was shown to be strong, both by the dissociation constant and its ability to take place over a range of ionic conditions. N provided the RNA with limited resistance to digestion by RNase A similar to that observed in authentic nucleocapsids (Hacker *et al.*, 1989; Kolakofsky & Hacker, 1991). Taken together these data indicate that N encapsidates the RNA in *in vitro* binding reactions.

The resistance of RNA in N-RNA complexes and nucleocapsids to digestion by RNase A (Fig.4.10) suggests that the RNA is not exposed on the surface of the nucleocapsid as is the case for influenza virus nucleocapsids, which do not impart any resistance on the RNA (Baudin *et al.*, 1994).

The buoyant density of the range of N-RNA complexes tested appeared to be less than 1.25g/ml, different to that reported for authentic nucleocapsids (Fig.4.9; 1.31g/ml; Obijeski & Murphy, 1977), although the fact that the complexes remained intact suggests that the RNA was encapsidated. For comparison, TSWV and PUU *in-vitro* assembled N-RNA complexes were determined to possess buoyant densities of 1.32g/ml and 1.36g/ml, respectively (Gött *et al.*, 1993; Richmond *et al.*, 1998). The apparent low density of BUN complexes could be attributed to the lack of L in the complex, or possibly the presence of the complex in a relaxed conformation, as opposed to the supercoiled state of authentic nucleocapsids. A more accurate analysis of the relative buoyant densities of nucleocapsids and synthetic N-RNA complexes could be provided by running authentic nucleocapsids on the same gradient as the synthetic complexes.

Chapter 5: Competitive binding assays

5.1. Introduction

There have been reports implicating the terminal sequences, in particular the 5' terminus, of RNA segments of members of the *Bunyaviridae* in the encapsidation event (Raju & Kolakofsky, 1987b; Dunn 2000). Such an involvement might be borne out by a preference of N for one or both termini. This was investigated in the negative-sense S segment of BUN using competitive binding assays, in which any preference by N for an unlabelled competitor RNA over that for BUNS5'(32)/3'(33) riboprobe was determined. Competitor RNAs consisted of 5' or 3' BUN terminal sequences, BUN single and double-stranded internal sequences and non-viral RNA. Filter-binding was chosen to measure the preference of binding due to its speed, reproducibility and ease of quantification.

5.2. Generation of competitor RNAs

The competitor RNAs consisting of BUNS sequences are summarised in Fig.5.1.

BUNS5'(32)/3'(33)

Unlabelled BUNS5'(32)/3'(33) RNA was generated in the same fashion as radiolabelled BUNS5'(32)/3'(33) riboprobe but necessitated different reaction conditions (see materials and methods; Fig.3.10).

BUNS5'(32)

The BUNS5'(32) transcript consists of the first 32nt of the 5' terminus of BUNS. It was made by run-off transcription of pBUNS5'(32)/3'(33) that had been linearised with *Sma*I, which separates the two termini cDNAs in this construct (Fig.5.2a). It was produced to ascertain whether N requires both terminal sequences to bind S segment RNA, or if the 3' terminal sequences are dispensable.

BUNS5'(65)

BUNS5'(65) comprises the first 65nt of the 5' BUNS terminus. It was generated by run-off transcription from the plasmid pBUNSCAT that had been linearised with *Fau*I (Fig.5.2b).

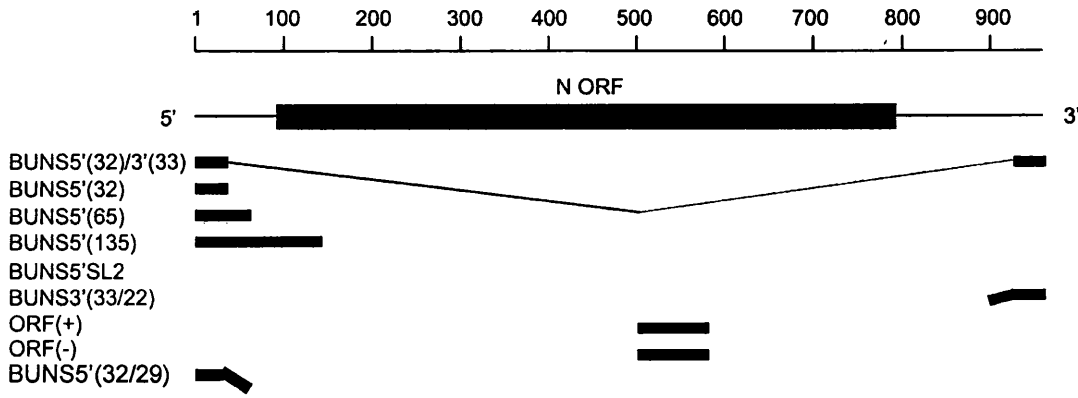

Fig.5.1. Competitor RNAs consisting of BUNS sequences. The RNAs are shown in relation to the BUNS segment, with the N ORF indicated.

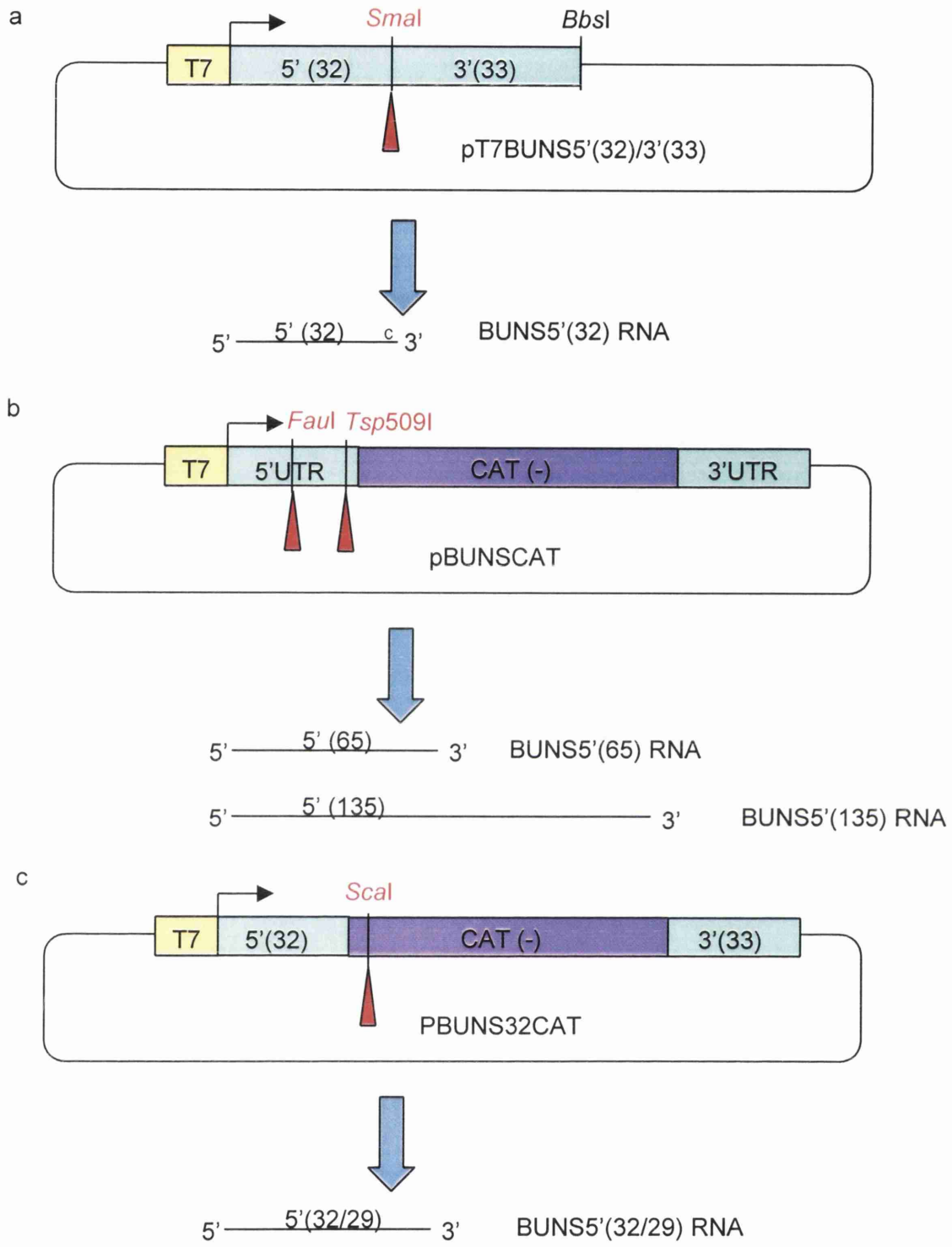

Fig.5.2a,b,c. Generation of BUNS5'(32) (a), BUNS5'(65), BUNS(135) (b) and BUNS5'(32/29) (c) RNA species by *in vitro* transcription. BUNS5'(32) RNA was transcribed from pT7BUNS5'(32)/3'(33) linearised with *Sma*I (a). BUNS5'(65) and BUNS5'(135) were transcribed from pBUNSCAT linearised with *Fau*I and *Tsp*509I, respectively (b), and BUNS5'(32/29) from pBUNS32CAT linearised with *Sca*I (c).

BUNS5'(135)

This RNA consists of the first 135nt of the BUNS 5' terminus and was made by run-off transcription of pBUNSCAT that had been linearised with *Tsp*509I (Fig.5.2b).

BUNS5'(32/29)

The plasmid pBUNS32CAT contains a negative-sense CAT gene flanked by the first 32 and 33nt of the 5' and 3' termini of negative-sense BUNS, respectively (Dunn, 2000). The transcript was generated by run-off transcription from pBUNS32CAT linearised with *Sca*I, which cut 29nt along the negative-sense CAT gene. The resulting RNA therefore consisted of the first 32nt of the 5' terminus of BUNS plus 29nt of non-viral RNA situated downstream (Fig.5.2c). It was generated to determine the effects of a region of non-viral RNA on binding of N to the 5' terminal sequence.

BUNS5'SL2

This is an 18nt transcript representing bases 23 to 56 of BUNS. It was made by run-off transcription of a partially double-stranded template made by annealing an oligo consisting of a truncated T7 promoter with an oligo containing the antisense T7 promoter and the template sequence (Fig.5.2d). It was predicted to form a stem-loop (designated stem-loop 2) present in BUNS5'(65), discussed later.

BUNS3'(33/22)

BUNS3'(33/22) RNA was transcribed from plasmid pTZBUNS3'(33/22). The construct was generated by ligating the *Sma*I/*Xba*I fragment, containing the cDNA of the 33 bases of the 3' BUNS terminus plus the *Bbs*I site, into pTZ18. After linearisation with *Bbs*I, run-off transcription was initiated from the full-length T7 promoter of pTZ18 and resulted in a transcript containing 22nt of vector multiple cloning site sequence at the 5' end, followed by the exact 33nt of the 3' terminus (Fig.5.2e). This RNA was used to determine whether N is capable of binding the 3' terminal sequence in the absence of the 5' terminal sequence.

BUNM+5'(65)

This transcript is the first 65nt of the positive-sense BUN M segment and was generated by run-off transcription of pT7riboM linearised with *Eco*RI (Fig.5.2f). It was expected that use of this RNA species in competitive binding assays would indicate

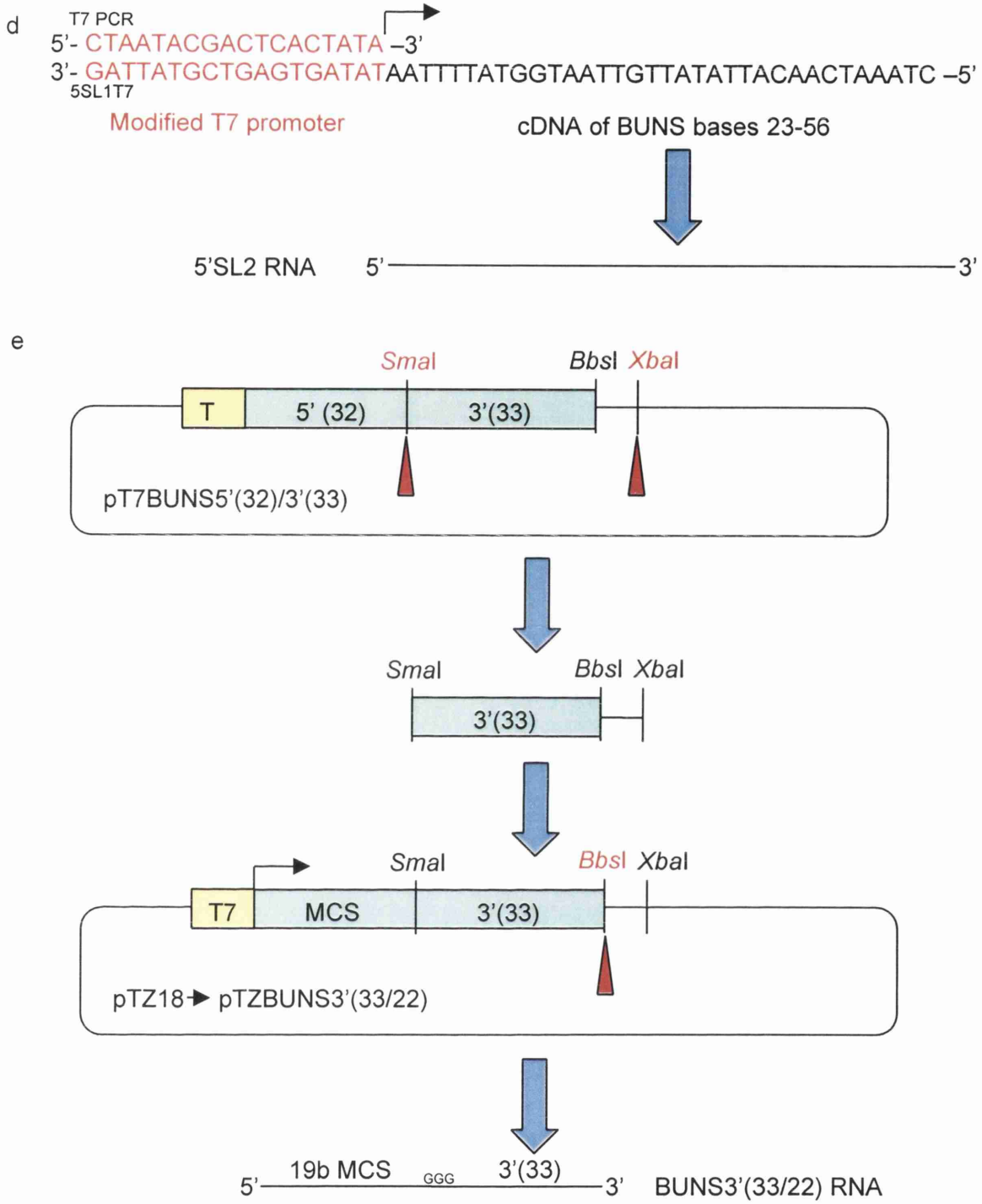

Fig.5.2d,e. Generation of 5'SL2 (d) and BUNS3'(33/22) (e) RNA. 5'SL2 was transcribed from two annealed oligonucleotides constituting a double-stranded T7 promoter and single-stranded transcription template (d). The plasmid for transcription of BUNS3'(33/22) was made by ligating the *Sma*I/*Xba*I fragment of pBUNS5'(32)/3'(33) into pTZ18 (e). The plasmid was linearised with *Bbs*I prior to transcription.

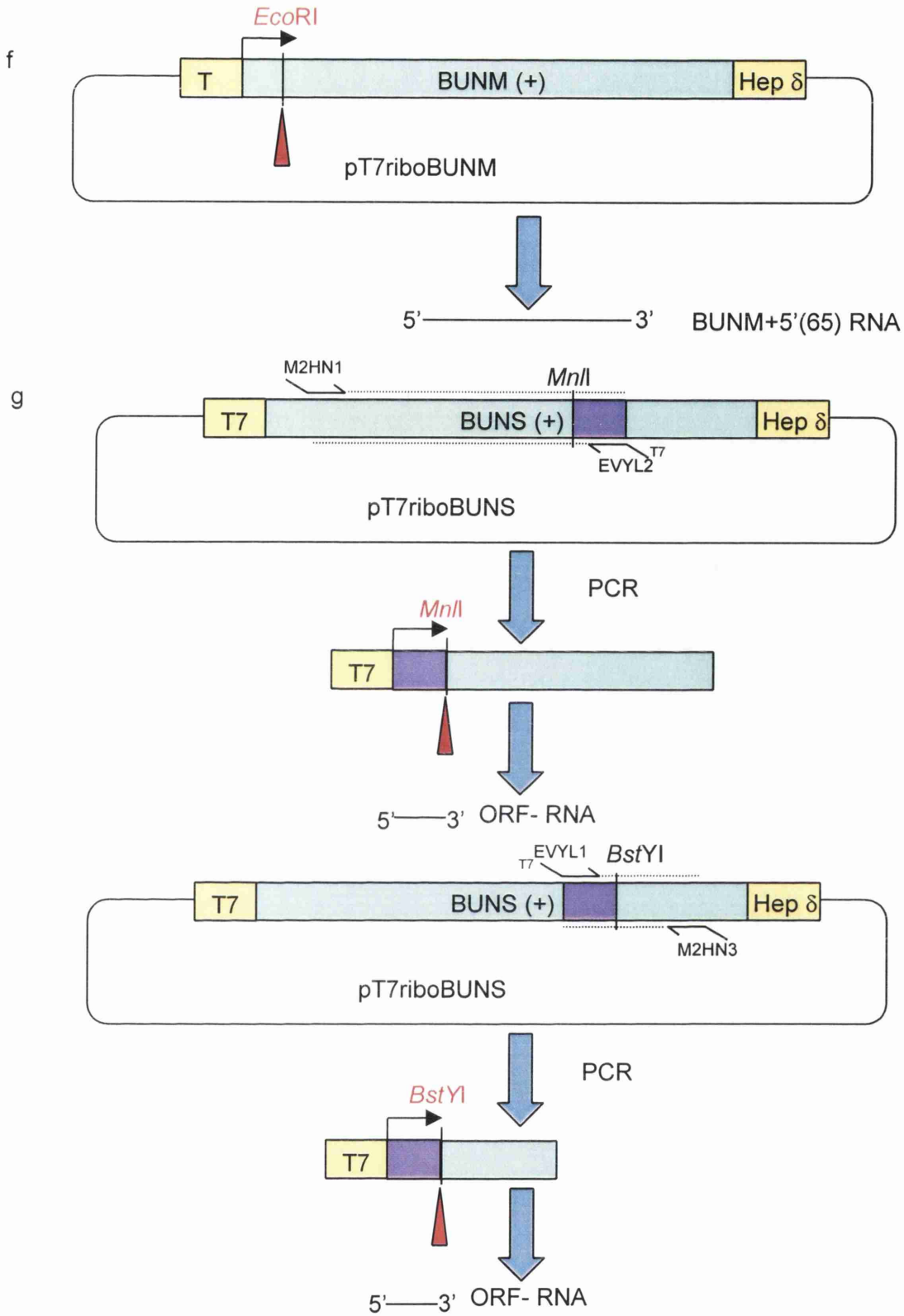

Fig.5.2f,g. Generation of BUNM+5'(65) (f), ORF- and ORF+ RNA (g). BUNM+5'(65) was transcribed from pT7riboBUNM linearised with *Eco*RI (f). ORF- and ORF+ were transcribed from products of PCR amplification of part of the S segment cDNA in pT7riboS (g). A modified T7 promoter was added at the 5' end of each product which was cleaved by *Mnl*I or *Bst*YI, respectively, to result in an 87nt transcript.

whether N is capable of binding a 5' terminal sequence from a different segment in positive polarity.

ORF+, ORF- and dsORF

The templates for generating ORF+ and ORF- RNA were produced by PCR amplification of part of the N ORF. A truncated T7 promoter was added as a tag upstream of the 5' primer (for ORF+) or downstream of the 3' primer (for ORF-). The PCR products were linearised with *Bst*YI or *Mnl*I in the case of ORF+ and ORF-, respectively, to allow run-off transcription to occur. The resulting transcripts consisted of the same stretch of N ORF in positive (ORF+) or negative (ORF-) polarity, each 87nt in length (Fig.5.2g). They were annealed to produce the double-stranded RNA, dsORF. These RNA species were generated to ascertain whether N can bind sequences internal to the N ORF, and whether there is a difference between binding to single-stranded and double-stranded RNA.

5.3. Competitive binding assays

The unlabelled competitor RNA was mixed with 100pg riboprobe in triplicate binding reaction lacking protein, with the competitor present at a 1000-fold mass excess over the riboprobe. Mass excess was chosen over molar excess despite the probable presence of only one preferred binding site per RNA molecule. This was because if RNA species much larger than BUNS5'(32)/3'(33) were added at a molar excess the increase in mass might skew the results as N may be capable of binding any RNA indiscriminately. N was added to the binding reaction at 9ng/μl, which was close to the saturation point determined by filter-binding. The reaction was incubated and filter-binding performed. Thus, the amount of BUNS5'(32)/3'(33) riboprobe detected on the filter was a measurement of the preference of N for the riboprobe over the competitor (Fig.5.3). Backgrounds counts, measured as the amount of riboprobe binding the filter in the absence of N, were subtracted.

All RNA species containing the first 32 5' BUNS bases competed to a high degree, and no other species competed to this level. BUNS5'(65) competed to the highest degree, exhibiting an average of 97% competition. BUNS5'SL2, consisting of a region of BUNS5'(65), showed 20% competition (discussed further in the next chapter). Interestingly, BUNS5'(32/29), consisting of BUNS5'(32) with a 29nt stretch of non-viral RNA downstream, failed to compete to a high level (less than 20%). BUNS3'(33/22),

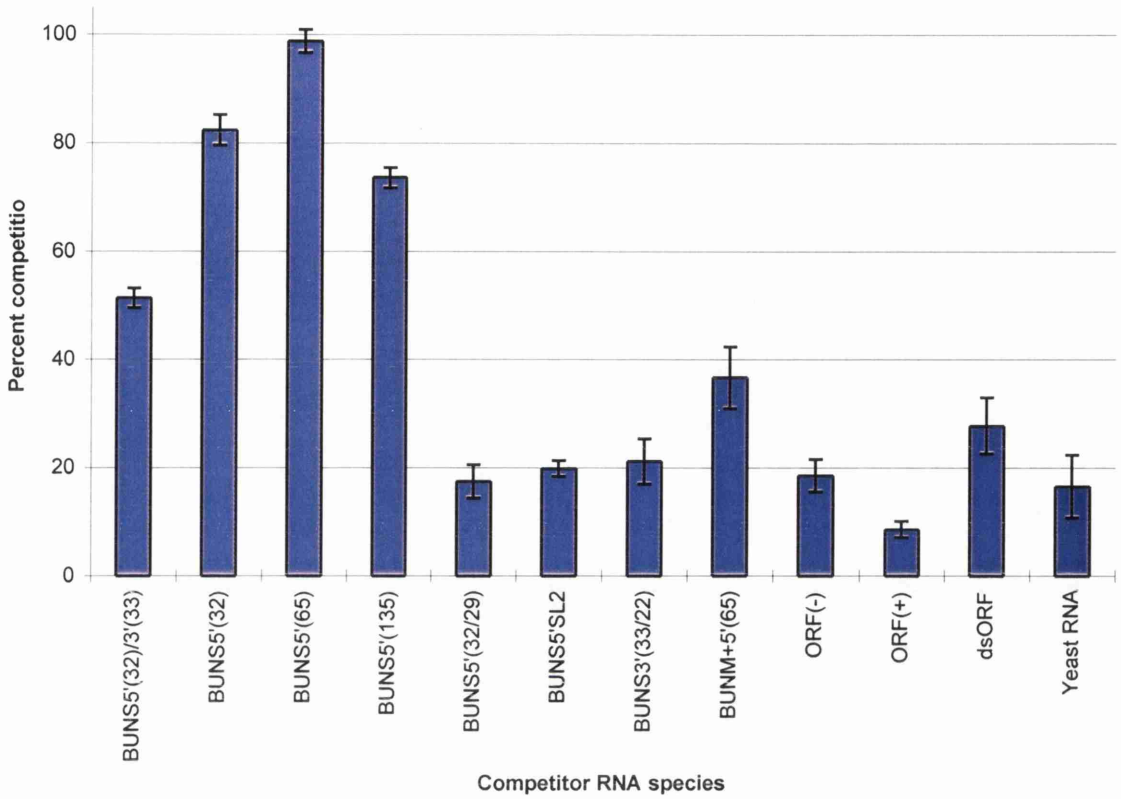

Fig.5.3. Competition of RNA species for binding by N. 100pg BUNS5'(32)3'(33) riboprobe was mixed with a 1000-fold excess of each unlabelled competitor RNA species in triplicate binding reactions. N was added at 9ng/μl and the reactions incubated and subjected to filter-binding. The results were calculated as a percentage of the total counts retained on the filter by a reaction containing no competitor, after background counts due to naked riboprobe binding the filter had been subtracted. They are plotted as the degree of competition. Hence, a high value would indicate that most of N was binding the competitor, and a low value that N was binding the riboprobe. A high degree of competition for binding was observed with BUNS5'(32), BUNS5'(65) and BUNS5'(135), all of which contained the first 32nt of BUNS. This sequence with 29b heterologous RNA downstream failed to compete to a high level (BUNS5'(32/29)). BUNS5'(65) was the best competitor, competing to 97%. Homologous RNA competed to approximately 50%, and BUNM+5'(65), consisting of the first 65b of the positive-sense M segment, to almost 40%. Double-stranded RNA (dsORF) competed to a higher degree than the remaining competitors, which competed up to approximately 20%.

consisting of the 3' terminus with 22 non-viral bases placed upstream, competed to a similar level. BUNS5'(32)/3'(33), BUNM+5'(65) and the double-stranded species dsORF gave intermediate values of competition. The species consisting of single-stranded internal sequences ORF(-) and ORF(+) and yeast RNA showed a low level of competition, again up to 20%.

As the assay involves the detection of riboprobe, results showing an apparently high degree of competition could theoretically reflect ribonuclease digestion of the riboprobe. In order to test this the RNA species that showed an apparently high degree of competition were incubated in binding reactions with the riboprobe. The riboprobe was then acid phenol:chloroform extracted and analysed by denaturing PAGE (Fig.5.4). The riboprobe was intact in each case, suggesting that the small amount of riboprobe detected on the filter was not due to nuclease digestion.

The apparent preference of N for the 5' terminus of BUNS was tested using GEMSA in order to confirm the result obtained with filter-binding. Binding reactions containing 100pg riboprobe, a 1000-fold mass excess of BUNS5'(32)/3'(33) or BUNS5'(65) competitor RNA and N at 54ng/μl were analysed by polyacrylamide GEMSA (Fig.5.5). The BUNS5'(65) competitor showed a high level of competition, observed as the complete failure of the riboprobe to be shifted into higher bands by N. In contrast, reactions containing unlabelled BUNS5'(32)/3'(33) RNA showed partial competition, indicated by a proportion of the riboprobe being shifted into a ladder of bands of decreased electrophoretic mobility. This reflects the results obtained with filter-binding.

5.4. Kinetics of N binding competitor RNAs

5.4.1. Kinetics of N binding BUNS5'(65) RNA

The RNA species showing the highest degree of competition was BUNS5'(65). As the degree of competition seen with this RNA was much higher than that observed with BUNS5'(32)/3'(33) its binding kinetics were analysed to see if binding to the 5' terminus was distinguishable from binding to both termini together. BUNS5'(65) was produced as a ^{32}P-CTP radiolabelled riboprobe using the same protocol as used for BUNS5'(32)/3'(33) and used in binding reactions with N. The binding kinetics were established using filter-binding assays (Fig.5.6). The K_d was calculated as for BUNS5'(32)/3'(33) and was determined to be approximately $7x10^{-8}$M, thus similar to that calculated for BUNS5'(32)/3'(33). The Hill coefficient for binding of N to BUNS5'(65)

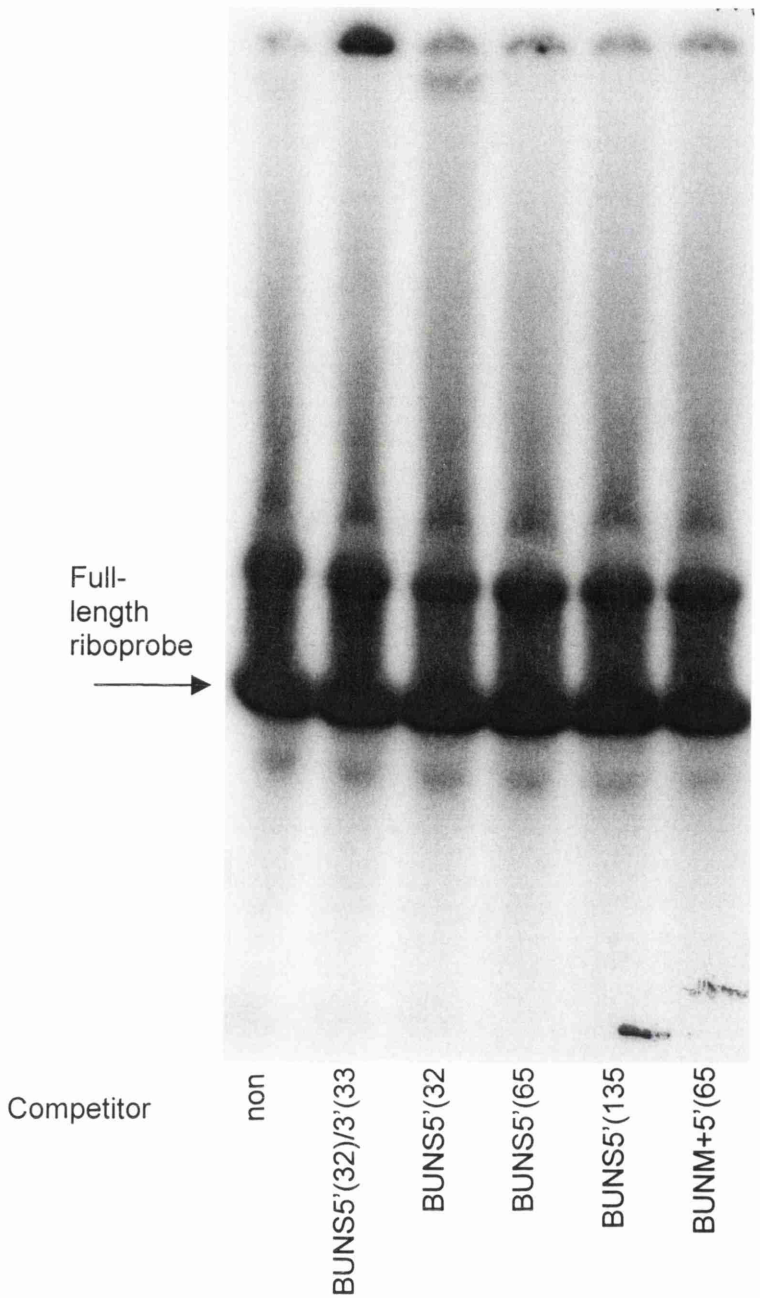

Fig.5.4. Assay for degradation of the riboprobe by RNases. Riboprobe was incubated with the competitor RNA in binding reactions and analysed by 6% denaturing PAGE. No degradation of the riboprobe was observed in those lanes with reactions containing competitor RNA. The band above the full-length riboprobe band is presumed to be due to secondary structure in the RNA as a result of it not being fully denatured. The band indicated as full length riboprobe was identified by its position in the gel relative to the bromophenol blue and xylene cyanol dye fronts.

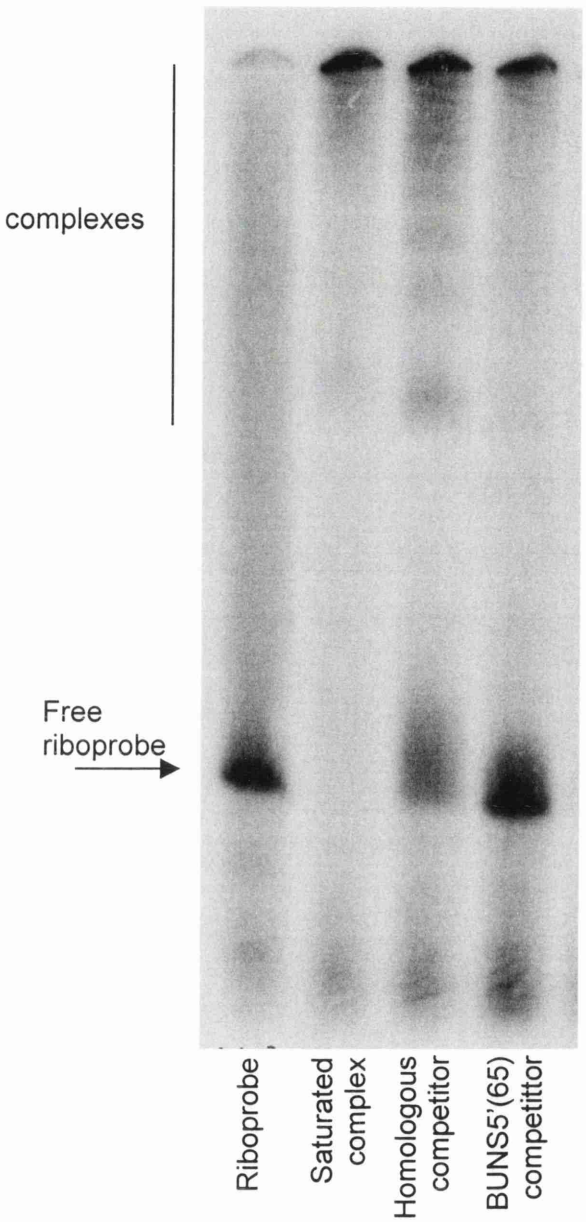

Fig.5.5. GEMSA showing selective binding of N to BUNS5'(65) competitor RNA. Competitive binding reactions identical to those used in filter-binding assays were analysed by 6% polyacrylamide GEMSA. The presence of BUNS5'(32)/3'(33) (homologous) competitor resulted in a low level of competition shown by the presence of some free riboprobe and the ladder profile observed previously at low concentrations of N. In contrast BUNS5'(65) competitor resulted in a high level of competition indicated by the large amount of free riboprobe.

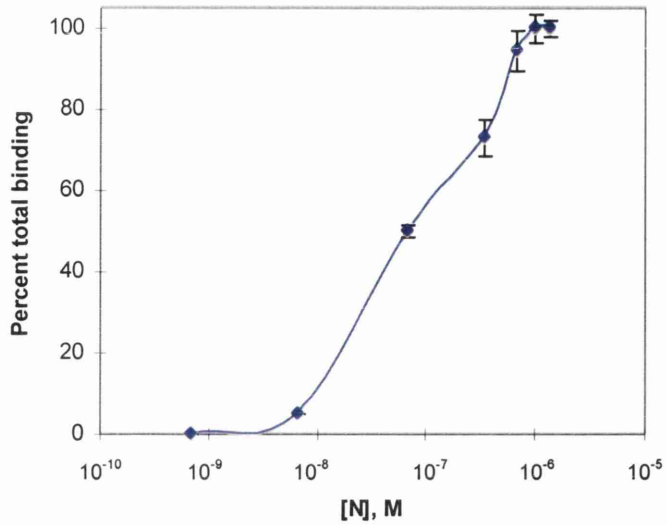

Fig.5.6. Kinetics of N binding BUNS5'(65) RNA. Reactions containing 100pg were subjected to filter-binding and background counts subtracted. The dissociation constant k_d was calculated as $1/2V_{max}$, which is approximately $7x10^{-8}$M and is similar to that obtained for binding to BUNS5'(32)/3'(33). Error bars indicate the standard deviation.

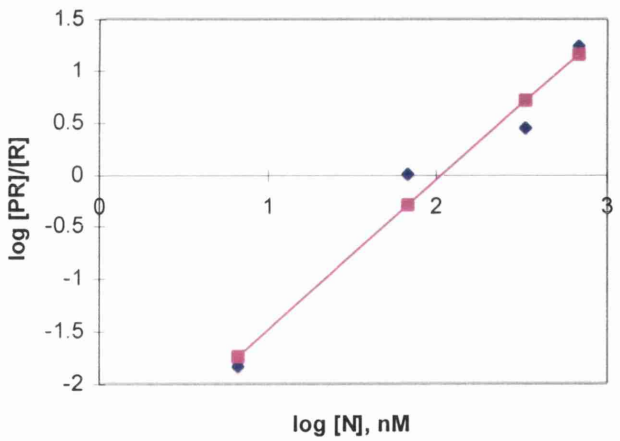

Fig.5.7. Hill plot analysis of N binding BUNS5'(65) RNA. The data obtained from filter-binding in Fig.30 were plotted as log [N] in nM against log [PR]/[R], where PR is bound riboprobe and R is free riboprobe. Points taken from the extremes of the binding curve were excluded as these correspond to the first and final binding events. Linear regression analysis was performed, and the gradient of the resultant line calculated as 1.44, indicating a low degree of co-operativity similar to that obtained for binding to BUNS5'(32)/3'(33).

was calculated using the same method as for BUNS5'(32)/3'(33) and was determined as approximately 1.4 (fig.5.7). Again, this is similar to the value obtained for binding BUNS5'(32)/3'(33). Hence there does not appear to be a significant difference in the kinetics of N binding BUNS5'(32)/3'(33) and BUNS5'(65).

5.4.2. Kinetics of N binding non-selected RNA

N showed a high degree of selection for competitor RNA species containing the 5' terminus of BUNS. However, this does not exclude the possibility that N is capable of binding any RNA, albeit possibly with different kinetics. The fact that a 1000-fold mass excess of non-selected competitor RNA could apparently compete consistently to approximately 20% suggests that some binding of these species still occurs. This was tested by generating non-viral radiolabelled RNA and using it in binding reactions with N. The plasmid pTZ18 was linearised with *Xba*I and a 32nt ^{32}P-CTP labelled RNA was generated by run-off transcription in a reaction identical to that used to generate BUNS5'(32)/3'(33) and BUNS5'(65) riboprobes, using the T7 promoter in pTZ18. Binding reactions containing N at those concentrations used to investigate the kinetics of N binding to BUNS5'(32)/3'(33) and BUNS5'(65) were incubated and analysed by filter-binding assays (Fig.5.8). Binding reactions containing BUNS5'(32)/3'(33) were also processed as a control. In Fig.5.8 the curve of N binding BUNS5'(32)/3'(33) has been extended from that in Fig.4.5. The decrease in binding observed at N protein concentrations above approximately $7x10^{-7}$M is presumably due to digestion of the riboprobe by ribonuclease present in the protein stock. There was a high degree of variation in data points with the non-viral riboprobe at high concentrations of N, which resulted in the determination of the saturation point and hence the dissociation constant for N binding non-viral RNA being unsuccessful. However, at a concentration of N of $2x10^{-6}$M, only 25% of the binding observed with BUNS5'(32)/3'(33) was obtained with the non-viral riboprobe once the data had been adjusted for the relative specific activities. Hence, N was found to be capable of binding non-viral RNA, but to a lower degree.

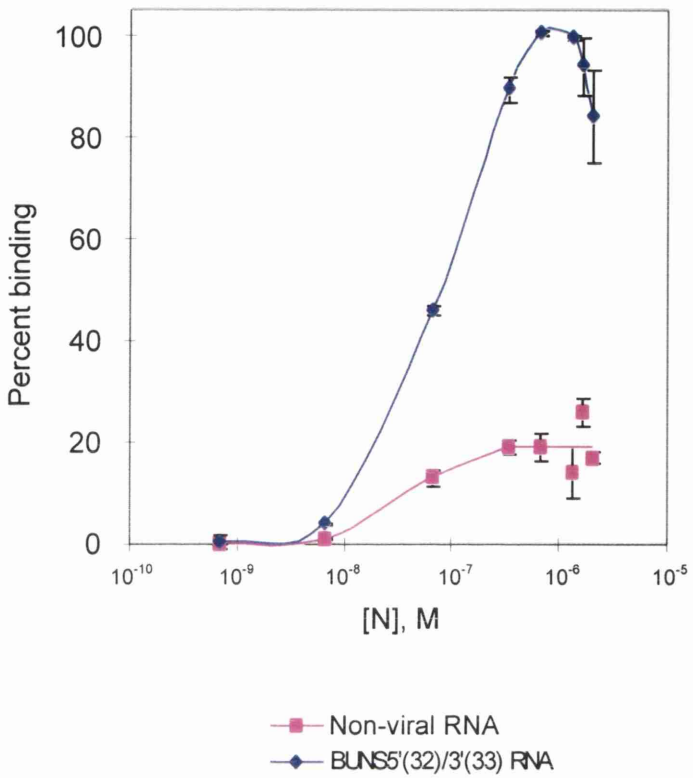

Fig.5.8. Kinetics of N binding non-selected RNA. Binding reactions containing 100pg non-viral RNA were subjected to filter-binding. The resulting data are presented as the percent maximum binding by N to BUNS5'(32)/3'(33) RNA after different specific activities were taken into account. The curve representing N binding BUNS5'(32)/3'(33) RNA is shown for comparison (two additional data points for this curve compared to that in Fig.4.5 are shown to facilitate comparison). The region of the curve for non-viral RNA connecting the last five data points was calculated as a trendline using Excel.

5.5. Discussion

In this chapter the ability of N to bind a variety of RNA species in the presence of the riboprobe, consisting of the ends of both negative-sense BUNS termini, was investigated. The only species exhibiting a high level of competition all contained the first 32nt of negative-sense BUNS (Fig.5.3). However, not all species containing these sequences competed to a high level, and this will be discussed in the next chapter. The reason for the competition for binding by N is due to N binding the competing RNA species selectively, that is, preferentially binding them among a population of other RNA species. This would make sense when N is required to selectively encapsidate a viral segment in the presence of other RNA species. It would appear that there is a signal for selective binding at the 5' terminus, which might be responsible for the 5' terminus being implicated in encapsidation (Raju & Kolakofsky, 1987b; Dunn, 2000). Hantavirus N was found to possess an increased preference for full-length S segment RNA over the N ORF (Severson *et al.*, 1999). Recently this has been reported to be attributable to the first 39nt of the 5' terminus of the negative-sense S segment (Severson *et al.*, 2001), supporting the hypothesis presented here that selective binding occurs within the first 32nt of the negative-sense BUNS segment.

Sequences not bound selectively by BUN N were still bound by N to a reasonable degree (20% competition at 1000-fold mass excess over the riboprobe; Fig.5.3)). Firstly, this phenomenon could be due to N 'scanning' RNA for a selective binding signal but this is unlikely as the location of the signal at the extreme of the terminus would abolish the requirement for scanning. Secondly, the low level of binding to RNA lacking the signal might be representative of binding to viral RNA once encapsidation has been initiated, which might progress in a strictly non sequence-specific fashion but would be driven and strengthened in the case of encapsidation by co-operativity between the binding and bound N proteins.

The apparent presence of two modes of binding by N, namely selective and non-specific, has been observed in other proteins. Rabies virus, Sendai virus, VSV and HIV nucleoproteins have been found to bind an encapsidation signal selectively (Blumberg *et al.*, 1983; Moyer *et al.*, 1991; Berkowitz *et al.*, 1993; Smallwood & Moyer, 1993; Allen *et al.*, 1996; Lamb & Kolakofsky, 1996; Berglund *et al.*, 1997; Yang *et al.*, 1998;). Many positive-sense RNA virus core or coat proteins also bind specific sequences selectively, often binding stem-loop structures, as well as binding RNA nonspecifically (Wei &

Morris, 1991; Wei *et al.*, 1992; Duggal & Hall, 1993; Reusken *et al.*, 1994; Hacker 1995; Zhou *et al.*, 1996; Banerjee *et al.*, 1997; Stohlman *et al.*, 1988; Wang & Simon, 2000). Heterogeneous nuclear ribonucleoproteins (hnRNPs) can bind certain sequences preferentially but are also capable of less sequence-specific binding when there is an abundance of the protein over high-affinity sites, mediated by co-operative protein-protein interactions (Varani & Nagai, 1998). This probably serves to accelerate binding to high-affinity sites and hinder the formation of secondary structure in RNA. The latter is also thought to be one of the roles of N within the nucleocapsid.

Selective binding is unlikely to be due only to any double-stranded RNA that might exist in the competitor RNA as competition by the competitor BUNS5'SL2, predicted to form a stem-loop structure (discussed next chapter) and double-stranded dsORF RNA failed to compete to a high level. However, the degree of competition of dsORF slightly above that of the other non-selected RNAs suggests that binding of N to extensively double-stranded RNA is different. Gött *et al.* (1993) observed that N proteins of hantaviruses shifted double-stranded terminal sequences into the wells of an agarose gel, suggesting a preference for dsRNA. However, TSWV N protein was discovered to be incapable of binding double-stranded RNA (Richmond *et al.*, 1998). It is interesting that TSWV N did not demonstrate preferential binding to viral sequences, although binding to terminal sequences was not investigated (Richmond *et al.*, 1998).

The relatively low level of competition by the homologous competitor, i.e. BUNS5'(32)/3'(33), is surprising. However, the best competitor, BUNS5'(65), was bound with similar kinetics to BUNS5'(32)/3'(33) whereas non-viral RNA was bound poorly. This shows that the reason for the mediocre level of competition by BUNS5'(32)/3'(33) RNA is not due to a difference in the affinity of N for the RNA. Instead, it is possibly a result of the high concentration of homologous competitor in the solution. As each molecule of BUNS5'(32)/3'(33) RNA contains partially complementary sequences, at sufficiently high concentrations the sequences are likely to base-pair with one another and form concatamers of the RNA. Thus, binding of N to one unlabelled (competitor) molecule of BUNS5'(32)/3'(33) RNA which is linked directly or indirectly through a chain of concatamers to a labelled molecule will result in the labelled molecule apparently being bound. This would reduce the level of apparent competition by the homologous species. Initially it was believed that this problem could be overcome by supplying the 5' and 3' terminal sequences as separate molecules annealed to one another to form the same RNA but lacking the hinge region between

them. However, on further analysis this system could be confounded by the unknown method of binding of N. For instance, it is possible that as N binds the terminal sequences in BUNS5'(32)/3'(33) it melts them from each other, as observed when influenza virus NP binds panhandle RNA (Baudin *et al.*, 1994). If the termini were supplied as two annealed RNAs the separation of the two unlinked halves would have the effect of removing the 3' terminal sequence altogether.

The necessity for a 1000-fold excess of competitor RNA to achieve the degree of competitive binding observed was baffling. The N protein concentration in competitive binding reactions of 9ng/μl had been chosen as it was slightly below the saturation point on the binding curve and thus the concentration-dependent ability of N to bind large amounts of RNA at high concentrations should not have been an issue. It is possible that, at high concentrations of RNA, the effective co-operativity of binding by the protein drops due to the abundance of binding sites available. This would result in more RNA molecules being bound but fewer being fully encapsidated, and could explain the ladder-like profile of bands observed in the polyacrylamide GEMSA of competitive binding by homologous RNA (Fig.5.5). This was similar to the profile obtained in standard binding conditions when N was present at one-third of the concentration (Fig.4.1).

Chapter 6: A putative encapsidation signal in the 5' terminus

In the last chapter it was determined that competitor RNA species containing the first 32nt of the 5'BUNS segment were bound selectively by N. This chapter describes an analysis of possible mediators of the preferential binding observed, their application to other segments and how they might be disrupted when encapsidation is not required.

6.1. Sequences and putative secondary structure at the 5' terminus

The high preference of N for the BUNS 5' terminus suggests that there is an element within this region responsible for selective binding, and that may constitute an encapsidation signal. The sequences of the competitor RNAs containing the 5' terminus were analysed by the Mfold RNA-folding program (Matthews *et al.*, 1999; Zuker *et al.*, 1999) to investigate secondary structure in this region (Fig.6.1). All further predictions of secondary structure were also made using the Mfold program.

In rhabdoviruses, adenine motifs have been implicated as the chief component of the encapsidation signal on leader RNAs (Blumberg *et al.*, 1983; Yang *et al.*, 1998). The encapsidation signal was proposed to be a polyA sequence or a stretch of regularly-spaced As. There is a high percentage of As throughout the BUN genome and the termini are no exception. The 32nt of negative-sense 5'BUNS and 33nt of positive-sense 5'BUNL have the motif AAAANNNAAAA (from positions 19 and 21, respectively). However, the 32nt of the negative-sense M and L segment possess four consecutive As (from positions 21 and 22), and the analogous positive-sense 5' BUNS and M regions have only a stretch of three consecutive As (from positions 21 and 25, respectively). The next AAA sequence in positive-sense 5'BUNM is located at nt 151. The remaining adenines are not equally spaced in the first 32nt except for a single sequence in the positive-sense L terminus (positions 14-23). The polyA stretches in the 32nt of 5' BUNS are predicted to be unstructured in RNA species competing to a high degree, making them available for binding N (Fig.6.1, green boxes). However, the competitor BUNS5'(32/29) was also predicted to contain the two unstructured polyA sequences but competed to a low degree (Fig.6.1f). In addition, the competitor RNA

Fig.6.1. Secondary structure predicted in the 5' termini of competitor RNA species. Predictions were made using the Mfold RNA-folding program (Matthews *et al*., 1999; Zuker *et al*., 1999). For BUNS sequences, the stem-loop SL1 (blue box) and/or CUC from the CU(A)CC motif usually found in the loop (red box) is indicated, as are polyA sequences (green boxes). The most highly energetically-favourable Mfold predictions for all species showing a high degree of competition indicated the presence of SL1 at the extreme 5' terminus (b-e). BUNS5'(32/29) did not compete to a high degree and lacked SL1, but possessed two unstructured polyA stretches (f). The homologous competitor was predicted to form a strict panhandle structure (a). BUNM+5'(65) was also predicted to form a similar stem-loop at the 5' terminus (g).

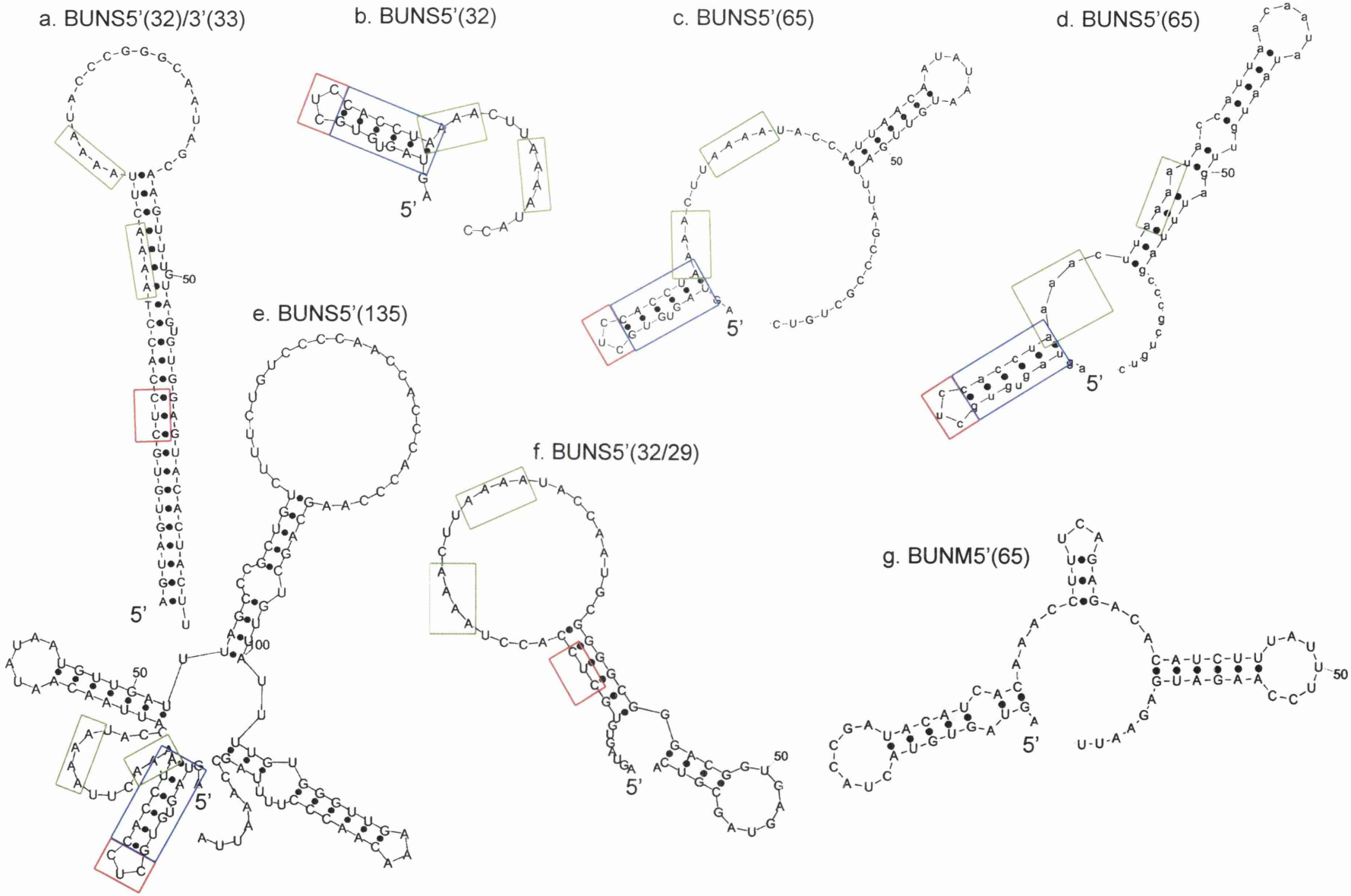
a. BUNS5'(32)/3'(33)
b. BUNS5'(32)
c. BUNS5'(65)
d. BUNS5'(65)
e. BUNS5'(135)
f. BUNS5'(32/29)
g. BUNM5'(65)
5'
50
100

ORF- possesses three stretches of three consecutive As, also predicted to be unstructured, but is not bound selectively (Fig.6.2a).

Encapsidation signals are often present as structural motifs, particularly stem-loops (discussed in the Introduction). The most highly energetically-favourable structures calculated included a stem-loop, designated SL1, at the 5' terminus which was present in all RNAs that competed to a high level (depicted in a red and blue box in Fig.6.1). A similar stem-loop was predicted in BUNM+5'(65), which competed to an intermediate level (Fig.6.1g). A second stem-loop, SL2, was predicted downstream of SL1 in BUNS5'(65), the RNA that competed to the highest extent. It was predicted in two forms, either a stem-loop (Fig.6.1c) or a longer stem-loop with two bulges (Fig.6.1d). SL2 was not predicted in the other competitors and was found not to be able to direct selective binding by itself (Fig.5.3, BUNS5'SL2. This competitor RNA consists of the region of BUNS5'(65) predicted to form SL2, and was anticipated to fold into the stem-loop shown in Fig.6.1c). Hence, it was thought not to be essential for selective binding and may act to stabilise SL1 in BUNS5'(65), thereby increasing the degree of competition by this RNA species. SL1 was the only secondary structure predicted in BUNS5'(32), which competed to a high level. It was anticipated in the RNA at both 30 and 37°C, corresponding to the cellular environment and reaction conditions. The two competitor RNAs containing the first 32nt of BUNS but exhibiting a relatively low level of competition, BUNS5'(32)/3'(33) (~50%) and BUNS5'(32/29) (~20%), were predicted to lack SL1 (Fig.6.1a and f, respectively). Hence, if encapsidation initiation is mediated by secondary structure in the BUN S segment, SL1 may serve as the encapsidation signal. The logical progression of this hypothesis was to investigate the presence of a similar structure in other BUN segments. To this end the sequences of other 5' BUN segments were analysed by the Mfold program (Fig.6.3). Predicted structures were found to differ but stem-loops similar in size and position to SL1 were observed in all other segments. Despite the stem-loops being relatively heterogeneous in structure, a CUC or CUCC sequence was predicted in the loops of BUNS and L in both polarities. In negative-sense BUNS the sequence CUCC is present although only CUC is predicted in the loop, as it is predicted to consist of only three nucleotides. In the case of M segment predictions in either polarity the corresponding sequence would be CUACC. Hence, this sequence will be referred to as CU(A)CC. The possible relevance of this sequence will be discussed later.

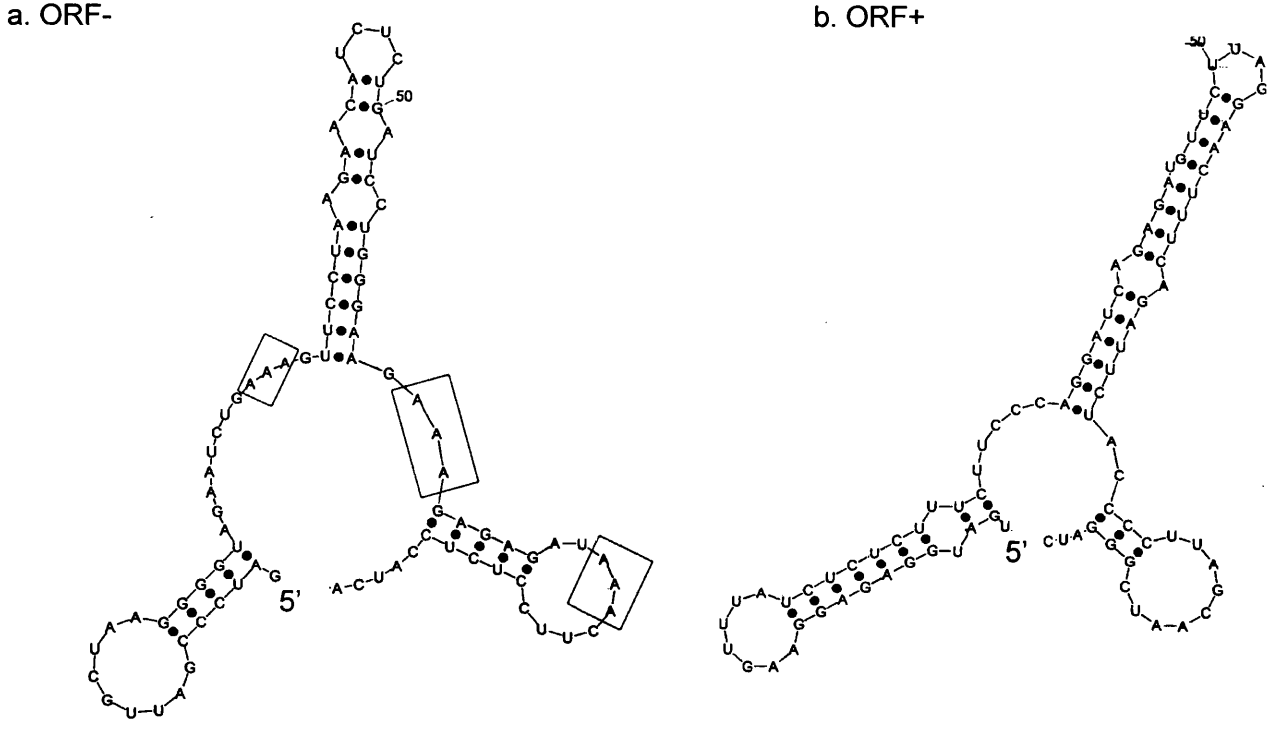

Fig.6.2. Secondary structure predicted in ORF RNA species. Predictions were made using the Mfold RNA-folding program (Matthews *et al.*, 1999; Zuker *et al.*, 1999). PolyA sequences are shown in a green box. The species ORF- and ORF+ were expected to form a high degree of secondary structure (only the most energetically-favourable form of ORF+ is shown; b). ORF- contains three polyA sequences which were predicted to be unstructured (a).

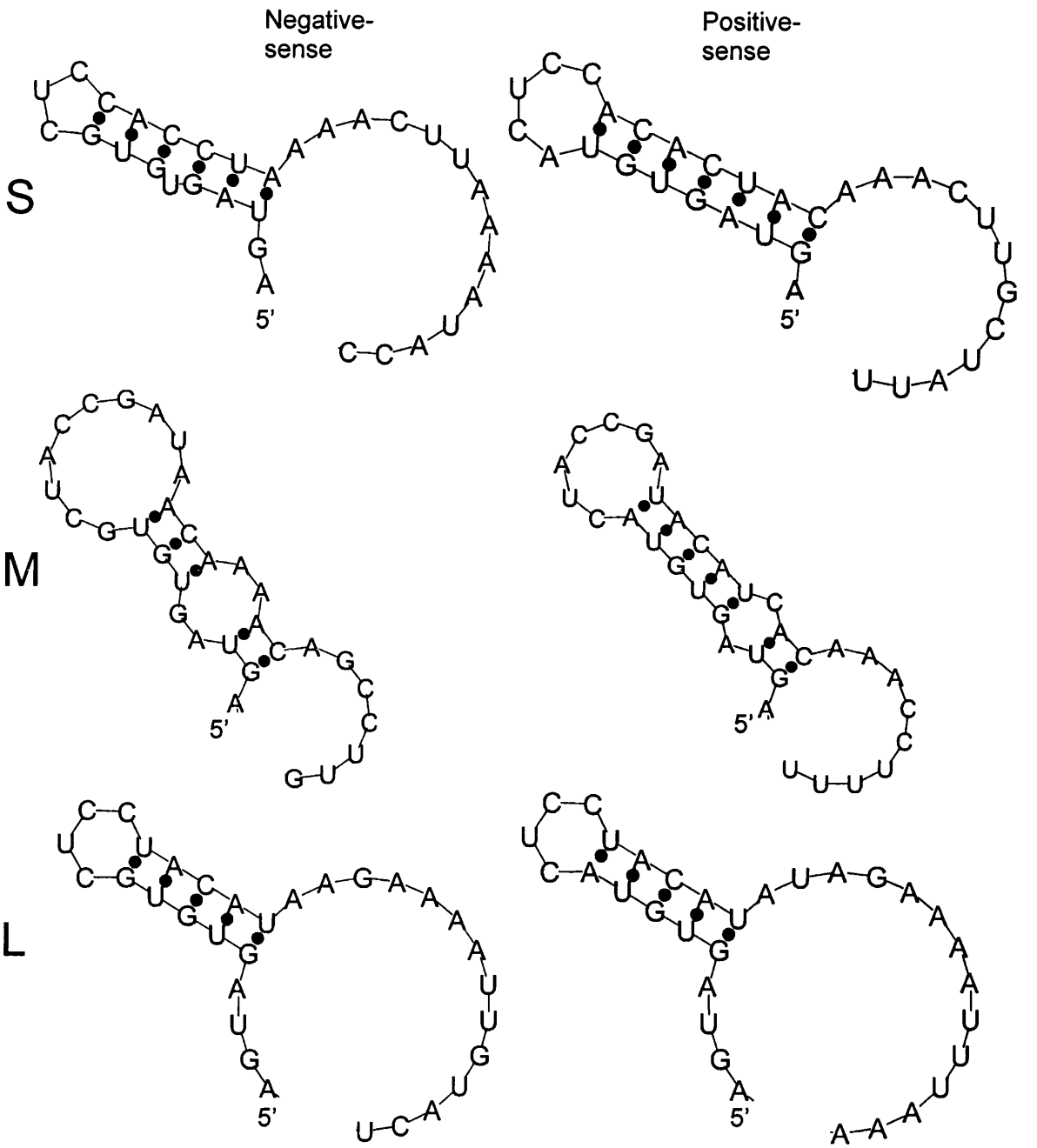

Fig.6.3. Secondary structure predicted in the 5' termini of BUN segment RNAs. Predictions were made using the Mfold RNA-folding program (Matthews *et al.*, 1999; Zuker *et al.*, 1999). Shown are RNA species consisting of the first 32b of the 5' termini of BUN segments. Stem-loops were predicted in each case, with the sequence CUC or CUCC (S and L), or CUACC (M) within the loop.

6.2. The possible effect of the non-templated primer

It had been reported that mRNA is generally not encapsidated in the infected cell (Bouloy *et al.*, 1984). This effect might be attributable to the cap present on the mRNA transcripts recruiting factors to the RNA, thereby blocking the binding of N (Raju & Kolakofsky, 1987b). However, it is possible that the non-templated primer present exclusively on mRNA transcripts affects the structure of the RNA, possibly interfering with an encapsidation signal. The sequences of some non-templated primers on BUN mRNAs had previously been determined and published (Jin & Elliott, 1993a). One of these, designated S1, was placed upstream of the BUN segment positive-sense 5' termini and analysed by the Mfold program to determine whether they would exert an effect on the putative secondary structure present in this region (Fig.6.4). Most of the primer sequences published contain an AGU or GGU motif at their immediate 3' end which probably plays a role in transcription initiation (Jin & Elliott, 1993a). However, this sequence was also predicted to base-pair with the ACU at bases 23-25 of the positive-sense S transcript, thereby not destroying the putative encapsidation signal but elongating it and adding two bulges in the stem. In the case of the M and L segments the original stem-loop was destroyed and another stem-loop predicted in its place.

The possible effect of the other published primers on the positive-sense S segment was then analysed in an attempt to establish if they all exerted a similar effect (Fig.6.5). The predicted structures almost exclusively fell into two groups, those elongating the stem-loop by binding the ACU sequence at bases 23-25 (top row) and/or those that did not interfere with the stem-loop but generally formed another stem-loop upstream (middle row). For some sequences both conformations were predicted; all predicted structures are shown. The two exceptions destroyed the stem-loop as in the case of the M and L segments.

Cap structures are known to recruit cap-binding proteins (reviewed by Lewis & Izaurralde, 1997). This and the fact that the primers are cap-snatched by L suggests that the first few bases of the primer might not actually be free to base-pair. The effect of such a phenomenon was investigated by placing constraints on the folding parameters by preventing the first few bases of each primer from base-pairing. The primers that had been predicted not to interfere with the stem-loop were then predicted to elongate it in the same fashion as the others (Fig.6.5, bottom row). The exception to this was primer S22, which has a GAU sequence in the place of the AGU or GGU sequence found in all others.

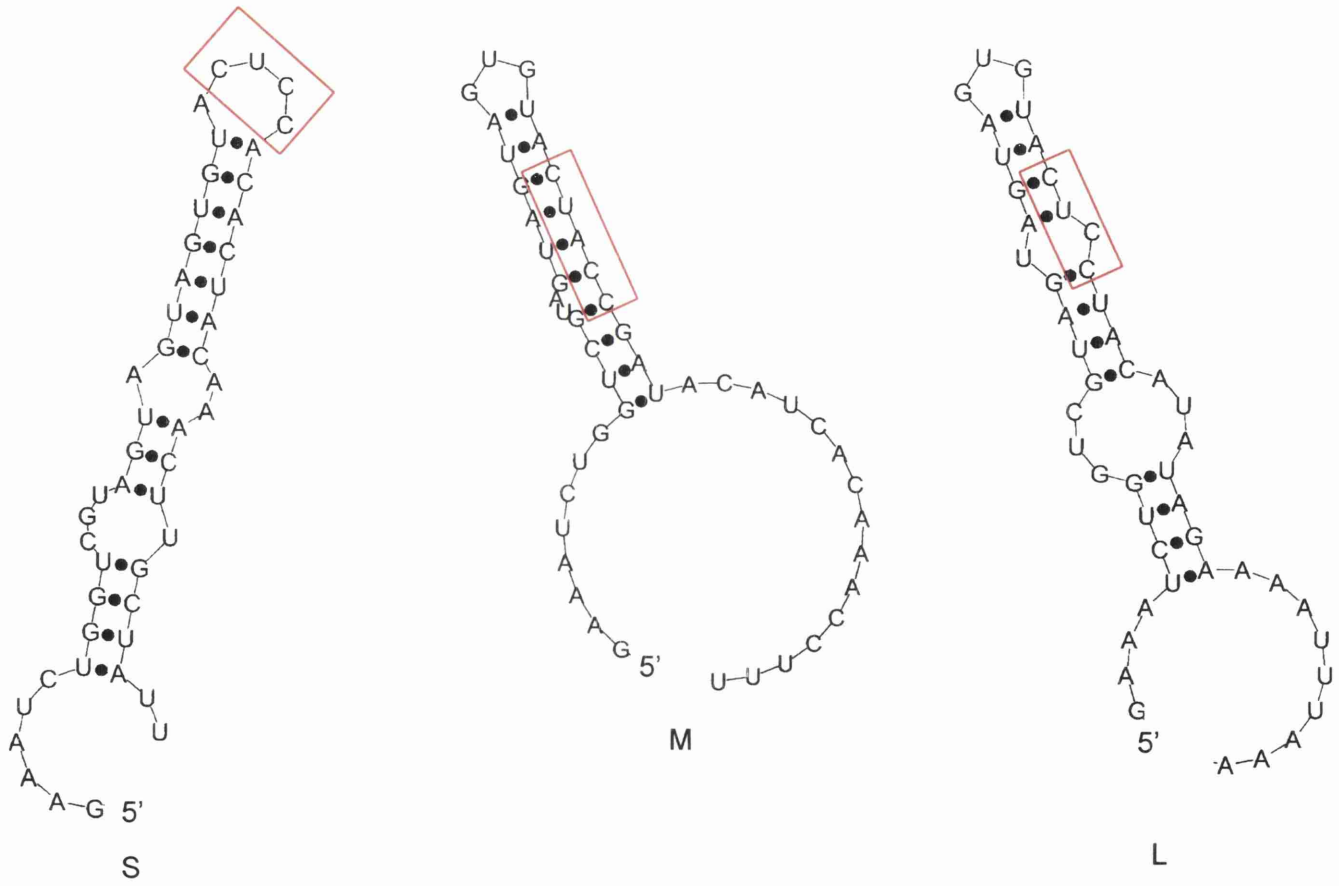

Fig.6.4. Secondary structure predicted in 5' termini with the non-templated primer. Shown are Mfold predictions for the secondary structure of the first 32b of each positive-sense segment with the sequence of the non-templated primer S1 at the 5' end; i.e., the predicted structure of the immediate 5' end of nascent BUN mRNA. The primer was predicted to have the effect of elongating the stem-loop and adding a bulge in the case of the S segment, and of destroying the stem-loop present in the M and L segments. In each case the CU(A)CC sequence previously present in the loop is depicted in a red box.

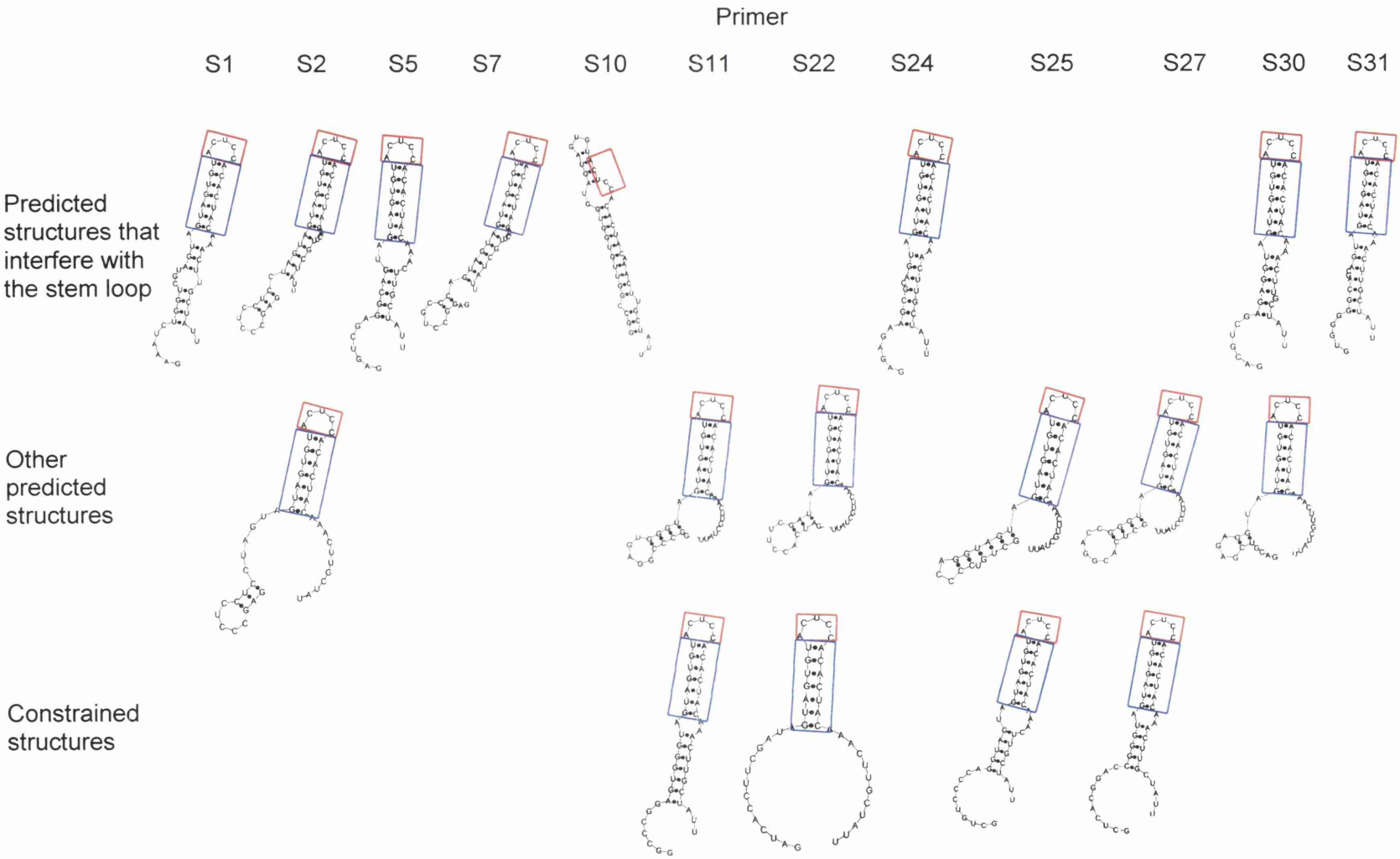
Primer
S1
S2
S5
S7
S10
S11
S22
S24
S25
S27
S30
S31
Predicted structures that interfere with the stem loop
Other predicted structures
Constrained structures

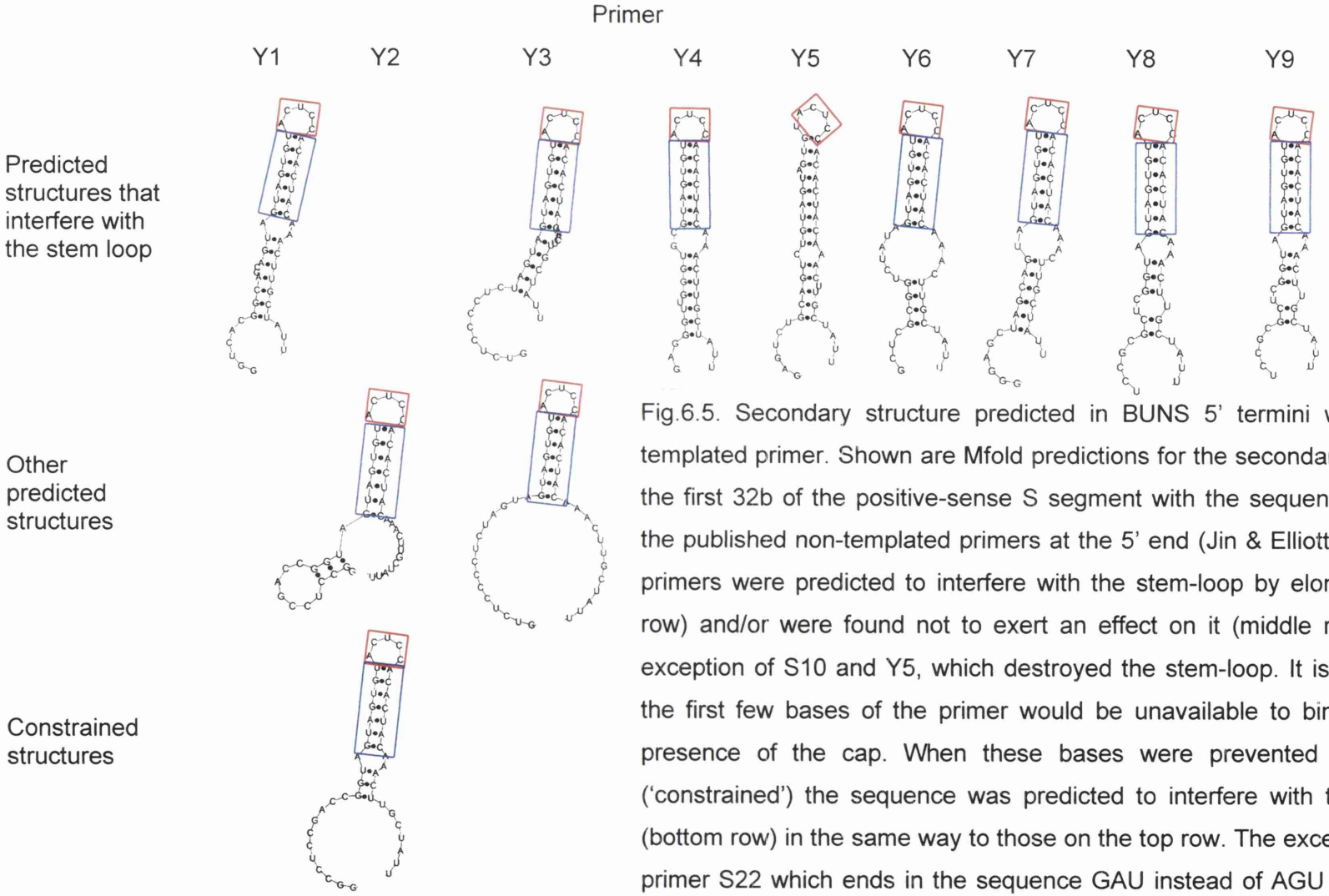

Fig.6.5. Secondary structure predicted in BUNS 5' termini with the non templated primer. Shown are Mfold predictions for the secondary structure of the first 32b of the positive-sense S segment with the sequence of each of the published non-templated primers at the 5' end (Jin & Elliott, 1993a). The primers were predicted to interfere with the stem-loop by elongating it (top row) and/or were found not to exert an effect on it (middle row), with the exception of S10 and Y5, which destroyed the stem-loop. It is possible that the first few bases of the primer would be unavailable to bind due to the presence of the cap. When these bases were prevented from binding ('constrained') the sequence was predicted to interfere with the stem-loop (bottom row) in the same way to those on the top row. The exception was the primer S22 which ends in the sequence GAU instead of AGU or GGU. The clone Y4 had been found to lack the first A of the viral sequence. The stem loop and/or sequence predicted to lie within the loop are indicated.

Determination of actual structural data on BUN sequences with primers was attempted but failed due to difficulties experienced in synthesising and 3' end-labelling the RNA.

6.3. Discussion

In all RNA species bound by N with a high degree of selectivity an identical stem-loop termed SL1 was predicted at the 5' terminus (Fig.6.1). This would place it at the extreme 5' terminus of the BUNS segment. Other similar stem-loops with similar bases anticipated in the loop were predicted for all other segments (Fig.6.3). The element responsible for selective binding was mapped to within 32nt of the 5' end of BUNS (last chapter), including the region within which SL1 was predicted. An RNA species containing the same sequence but predicted not to form SL1 was not bound selectively (Fig.6.1f); the best competitor was predicted to form a second, possibly stabilising stem-loop downstream (Fig.6.1c&d). Encapsidation signals in RNA viruses have often found to be stem-loop structures, discussed in section 1.2. This raises the possibility that SL1 is responsible for mediating the selective binding observed, effectively constituting an encapsidation signal. Subsequently, Severson *et al.* (2001) have reported that a selective binding signal resides within the first 39nt of the negative-sense hantavirus S segment, and implicated secondary structure in the selective binding event. This lends support to the hypothesis that SL1 constitutes an encapsidation signal in BUN S segment.

However, in rhabdoviruses adenine-rich motifs have been implicated in the encapsidation initiation event (Blumberg *et al.*, 1983; Yang *et al.*, 1998). The presence of only three or four consecutive adenines and no repetitive pattern of adenines in the 5' terminal sequence of some of the segments made a similar implication unlikely in BUN. In fact, the inability of both the ORF- and 5'BUNS(32/29) competitors to be bound selectively despite the presence of stretches of consecutive adenines that were predicted to be similarly unstacked would argue against adenines being the sole contributors of selective binding (Figs. 6.1 & 6.2). Indeed, if N were to bind any stretch of polyA selectively, encapsidation would not be restricted to viral RNA. As none of the adenine stretches at the 5' terminus of any competitor BUNS species was predicted to be structured it is also unlikely that selective binding involves an adenine motif within secondary structure. Hence, the data are interpreted to argue that BUN encapsidation initiation does not exclusively involve an adenine motif although their contribution cannot be excluded. This might reflect a difference to initiation in nonsegmented NSVs.

The high degree of secondary structure predicted in the RNA species ORF- and ORF+, both of which competed for binding at a low level, supports the observation made in the previous chapter that dsRNA is unlikely to be the mediator of selective binding in BUN (Fig.6.2).

The relatively heterogeneous nature of the stem-loops predicted in the different BUN segments suggests that it is not the structure alone that would be important in recognition by N (Fig.6.3). Binding of stem-loops can often be attributed to the bases in the loop region, which serves to open up the RNA grooves so that the protein can gain access to the bases (Draper, 1999). Most proteins then act by pulling unstacked bases into their binding pockets in what is essentially sequence-specific binding. Some, for instance HIV-1 NP binding to the SL3-RNA recognition element, directly bind the major groove, here opened up by the four-base loop in SL3 (de Guzman *et al.*, 1998; Fig.1.7). The latter type of binding requires binding to both the phosphodiester backbone and the bases. When this is taken into account it is interesting that the stem-loops predicted in all BUN segments contain the sequence CU(A)CC in the loop region, despite the heterogeneity of the stem regions. The coat protein from MS2 phage binds a hairpin in the viral RNA genome in a fashion insensitive to the five specific base-pairs in the bulged stem. Instead, binding occurs exclusively to three of the four bases in the loop and an adenine constituting a bulge in the stem (Valegàrd *et al.*, 1994). Taking this into account it is possible that N binds bases in the loop region of SL1. Subsequently, Severson *et al.* (2001) have suggested that the sequences within the loops of stem-loops predicted at the 5' termini of hantavirus segments are important for selective binding. Similarly to the stem-loops predicted at the 5' termini of BUN segments, the hantavirus stem-loops are predicted to be heterogeneous in nature. However, they do not appear to contain common sequences in the loop region.

The results of effects of point mutations in the region of SL1 on relative CAT levels in the BUN minireplicon system performed by Dunn (2000) are interesting when the possibility of N binding bases within the loop is considered. Bases found to be important or essential for CAT activity are shown in fig.6.6, superimposed on the predicted structure for the 5'BUNS terminal sequence. The system requires the reconstitution of intact and active synthetic nucleocapsids in mammalian cells; thus, any mutation that has an effect on the activity of the system may do so by affecting the binding of RNA by either N or L, so bases found to be important may exclusively affect the viral promoter. However, it is interesting to note that every base in the CU(A)CC sequence mentioned

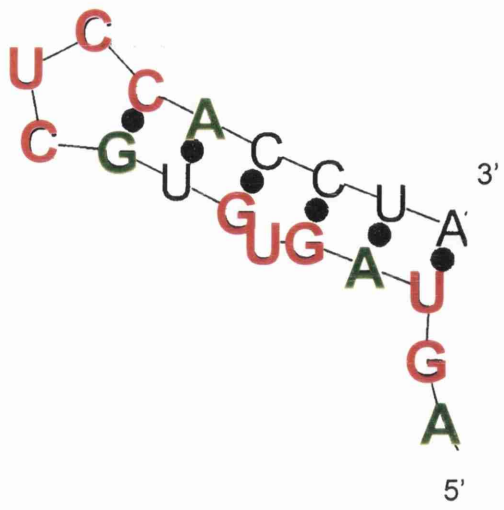

Fig.6.6. Important nucleotides in the BUNS 5' terminus. Shown are the positions of essential (red) and important (green) bases determined by the use of point mutations in the BUN reverse genetic system (Dunn, 2000), superimposed on the putative encapsidation signal predicted by Mfold in the 5' terminus. Highlighted bases might be important as promoter elements and not as part of the encapsidation signal. Essential bases are those that, when mutated, dropped the CAT activity to below 20% of the wild-type sequence, and important bases those that dropped it to between 20 and 49%. The bases in the loop and bulge regions of the predicted structure were all determined to be essential.

above was found to be essential in the system. The GUG around the bulge region was also found to be essential but the bulge was not predicted in any other segment so its potential contribution to selective binding is questionable.

The competitor BUNM+5'(65) demonstrated an intermediate level of competition, possibly suggesting that it was bound with a limited degree of selectivity, although it was predicted to form the stem-loop that might be necessary for selective binding (Figs.5.3 & 6.1). This could be attributable to structural instability, in which case the degree of selectivity might be able to be increased by using a shorter RNA, or it might be indicative of different rates of encapsidation initiation of different segments.

The homologous competitor BUNS5'(32)/3'(33) was predicted to form a strict panhandle structure and not SL1 (Fig.6.1a). This could be an explanation for its mediocre level of competitive binding, although the binding kinetics were found to be almost identical to those of the best competitor species, BUNS5'(65). Another possibility is that a small proportion of the RNA molecules exists with SL1, although this is not supported by GEMSA experiments in which the RNA was easily saturated by N (Fig.4.1). Possible explanations are that, although SL1 is not predicted by Mfold it exists in *in vitro* transcribed RNA, or that N is capable of forcing this particular RNA into the correct conformation. Structural rearrangement or conformational adaptation has been observed in all RNA-protein complexes for which structural data exist (Varani & Nagai, 1998). As an example, the RNA loop in the hairpin bound by MS2 coat protein mentioned above was found to be disordered in free RNA (Borer *et al.*, 1995).

If the predicted stem-loop does in fact constitute an encapsidation signal it is worth considering the implications on the structure of the nucleocapsid. Nucleocapsids purified from infected cells were found to possess a circular conformation, presumably due to the formation of the panhandle structure. It could be the case that SL1 is melted after binding by N and the full panhandle structure forms. Another possibility is that SL1 remains and restricted base-pairing between the termini takes place. This would result in the presence of a hook or corkscrew structure in the termini, as has been suggested in Germiston bunyavirus segments (Pardigon *et al.*, 1982) and some predictions of orthomyxovirus terminal structure (Flick *et al.*, 1996; Leahy *et al.*, 1997; Weber *et al.*, 1997; Flick & Hobom, 1999).

Further analysis of selective binding to the 5' terminus using point mutations in the RNA sequence will be of limited benefit unless the actual structure of the RNA is taken into account. This can be determined using structure-probing analysis of free and bound

RNA. It should be aimed to cleave or nick each molecule only once which is facilitated by longer RNAs; hence, there should be a compromise between the length of the RNA molecule and the stability of the predicted stem-loop. If SL1 and its homologues in the other segments do indeed prove to constitute an encapsidation signal it will be interesting to discover whether it is sufficient to mediate encapsidation of a non-viral sequence placed downstream *in vitro*, suggested by the success of the terminal sequences to drive encapsidation of a CAT gene in the minireplicon system (Dunn, 2000). This would also require structure-probing analysis to ascertain that the stem-loop is not disturbed by the non-viral sequence. Attempts to structure-probe the 5' terminus were unsuccessful due to difficulties encountered in nicking the short RNAs only once.

The apparent role of the non-templated primer in priming transcription initiation has been discussed in the Introduction. In this chapter it was suggested that the primer may be able to disrupt or destroy the putative encapsidation signal in positive-sense transcripts, thereby preventing N binding viral mRNA. Effects of primers on the positive-sense 5' terminus on the putative encapsidation signal stem-loop were predicted to fall into three categories (Fig.6.5):

- Those that elongated the stem of the stem-loop and introduced at least one bulge. The loop region was predicted to be unaltered. These primers were all predicted to bind an ACU in the viral RNA with an AGU or GGU at their extreme 3' end. These bases are believed to be important in priming transcription (Jin & Elliott, 1993a). Prevention of encapsidation would presumably act by hindering the progression of encapsidation from the otherwise intact encapsidation signal. Some of these primers were also predicted to fall into the next category.
- Those that had no effect on the stem-loop. Of these, nearly all were found to fall into the previous category when the first few bases were prevented from binding, a possible effect of binding by cap-binding proteins or L. Those that were predicted not to lacked the 'GU' sequence at the 3' end of the primer. Hence, it is difficult to imagine how they could act efficiently to prime transcription. It would be interesting to discover whether these primers can be used to generate active mRNAs in infected cells.
- Those that destroyed the stem-loop, thus destroying the encapsidation signal and preventing encapsidation of viral mRNA.

It is interesting that in many cases involving the S segment the primer was predicted to elongate the encapsidation signal. It would be conceivable that as the encapsidation signal is still intact, high concentrations of N might be able to overcome the disruption and cause the encapsidation of S mRNA observed under such conditions (Hacker *et al.*, 1989).

It is also notable that, in those cases in which the putative encapsidation signal is modified, the primer bases responsible for binding to sequences downstream of the signal are those that are thought to be added to the sequence by L in order to prime transcription (Jin & Elliott, 1993a). They are therefore likely to be conserved in that position.

Experimental evidence for interference of the primer with encapsidation cannot be gathered using selective binding assays due to the presence in most cases of an intact predicted stem-loop. Instead, it might be possible to take advantage of the pattern of bands observed on polyacrylamide GEMSA. It is possible that the initial shift into a single band observed in a polyacrylamide GEMSA at low concentrations of N is attributable to binding to the encapsidation signal (section 4.1.1; Fig.4.1). If this is correct, at the correct concentration of N a ladder would be expected on binding to 5' positive-sense BUNS RNA lacking the primer but only a single shift would be seen on binding to the same RNA including the primer sequence. It should be taken into account that the length of the 5' positive-sense BUNS RNA might have to be altered to increase the stability of the putative stem-loop, and the result might be confounded by the ability of N to bind any RNA indiscriminately at a high concentration. Attempts to investigate the effects of the primer on binding were unsuccessful due to difficulties generating the RNA species.

Chapter 7: Analysis of BUN N-N interactions

7.1. The mammalian two-hybrid system

7.1.1. Introduction

It is likely that N exists in a multimeric state within nucleocapsids. This is based on the following observations.

- The nucleoproteins of other NSVs have been shown to homo-oligomerise (discussed in section 1.2.3).
- The positive co-operativity observed in binding of N to RNA in binding assays suggests that there are interactions between N proteins (section 4.2.2).
- Multiple bands observed on Western blots of N were believed to be representative of multimers of N (section 3.2.3.1, Fig.3.8).

It should be noted that here the term 'multimerisation' is used to describe the association of at least two N proteins and therefore includes dimerisation. The assays used in this chapter cannot distinguish the association of two monomers from that of more N monomers.

The hypothesis that N is capable of multimerisation was investigated using the mammalian two-hybrid (M2H) system, a tool for analysing protein-protein interactions in mammalian cells. A two-hybrid system was originally developed by Fields & Song (1989) for analysing interactions in yeast. Variations for use in mammalian cells were subsequently introduced by Vasavada *et al.* (1991), and Takacs *et al.* (1993). The proteins of interest are expressed mammalian cells, one as the bait, the other as the target. The bait protein is expressed fused to the DNA-binding domain of the Gal4 protein (termed BD) and the target protein is expressed fused to the activation domain of the transactivating protein VP16 (termed AD). The fusion proteins are transported to the nucleus where the BD binds to Gal4 binding sites upstream of a reporter gene on a reporter plasmid. If the bait and target proteins interact the AD is brought into close proximity to the reporter gene promoter, and the gene is transactivated (Fig.7.1a). Reporter gene activity can then be detected. If there is no interaction the AD is not brought into proximity with the reporter gene and the gene remains inactive (Fig.7.1b). In practice the system relies on the ability of the bait and target proteins to enter the

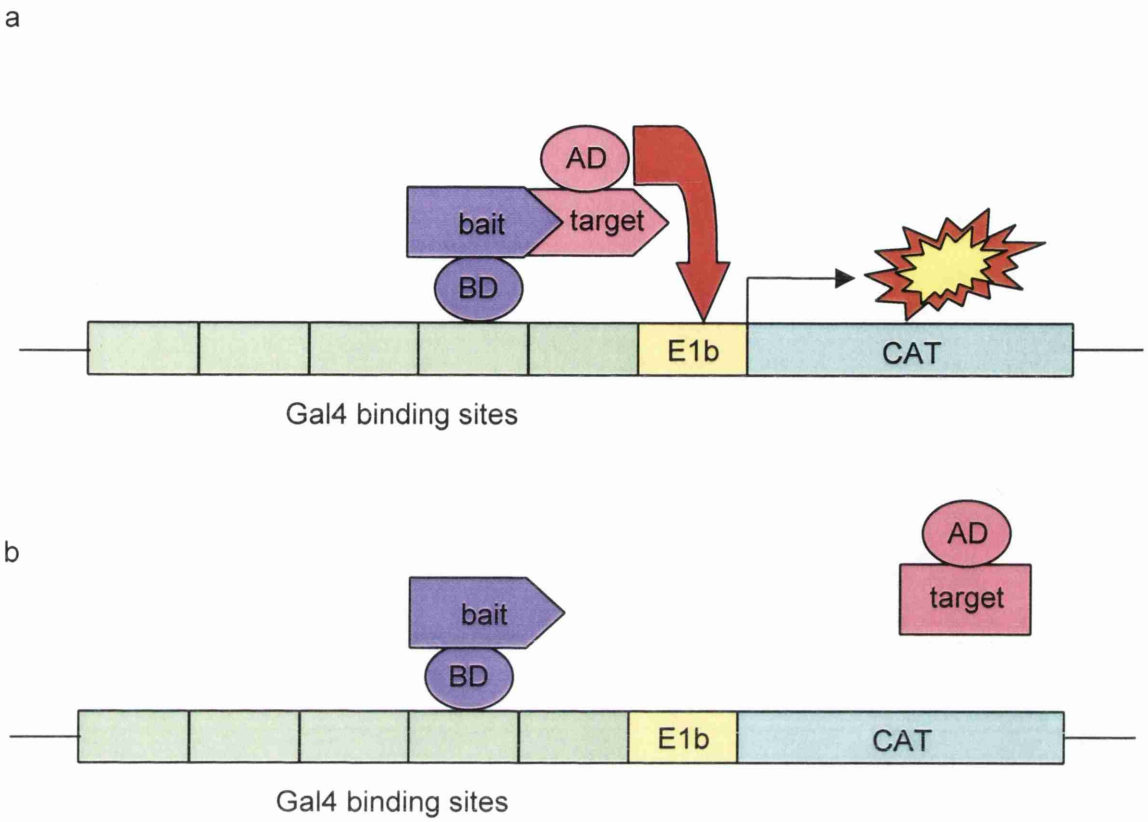

Fig.7.1. The mammalian two-hybrid system. The bait protein is expressed fused to the DNA–binding domain of Gal4 (BD) and the target protein expressed fused to the VP16 activation domain (AD). The BD binds Gal4 binding sites on the reporter plasmid pG_5BCAT. If the bait and target proteins interact, the AD is brought into proximity to the E1b promoter controlling the CAT gene and transactivation of CAT occurs (a). If the proteins do not interact the CAT gene remains inactive (b).

nucleus, and that the fusion domains do not interfere with any interaction between the proteins.

The vectors used in this project comprised the original mammalian two-hybrid vectors used by Takacs *et al.* (1993; see Materials & Methods for details) and those from the commercial Mammalian Matchmaker Two-Hybrid assay system (Clontech). The latter system was utilised to facilitate cloning into one of the vectors and to provide the positive control plasmid pM3VP16. The reporter gene used was the chloramphenicol acetyltransferase (CAT) gene which can be detected by the ability of its product to acetylate chloramphenicol in the presence of acetyl CoA. The CAT assay technique used is detailed in Methods.

7.1.2. Optimisation of conditions

A number of different cell lines and DNA transfection techniques were used to optimise the result from the M2H system. The positive controls used to test the system were the Mammalian Matchmaker Two-Hybrid Assay kit plasmid pM3VP16 (Clontech), consisting of the AD fused to the BD and thus a potent transactivator by itself, and bait and target proteins that were known to interact and give a positive signal in the M2H system. These constituted pGALP and pVPN (encoding the VSV P and N proteins; Takacs *et al.*, 1993) or pGalMxA and pVPMxA (F Weber). Initially, pM3VP16 was not available. The cell lines BHK-21, 293, COS7 and HeLa were tested for their ability to support the system (Fig.7.2). The preparation of and transfection conditions for all transfection techniques utilised is described in Methods. Detectable, but not useful, levels of CAT activity were observed in BHKs transfected with 'in-house' manufactured liposomes (a) and DEAE-dextran (b). No signal resulted from transfection using PEI (c). Liposomes had previously been used successfully to transfect many other cell lines (data not shown) and thus were chosen to attempt to obtain a strong M2H signal in other cell lines. 293 cells were tested because of their high transfection efficiency and allowed a good signal for transactivation with pM3VP16 but not for interactions between positive control proteins (d). COS7 and HeLa cells were found to give satisfactory results (e,f), particularly at a low confluency (30-50%), and were subsequently utilised.

Satisfactory CAT signals were obtained with only 1μg of each plasmid. In addition, transfection of 10μg of each plasmid had not given a proportional increase in the CAT signal in BHK-21 cells when in-house liposomes were used (Fig.7.2a). Hence, 1μg of

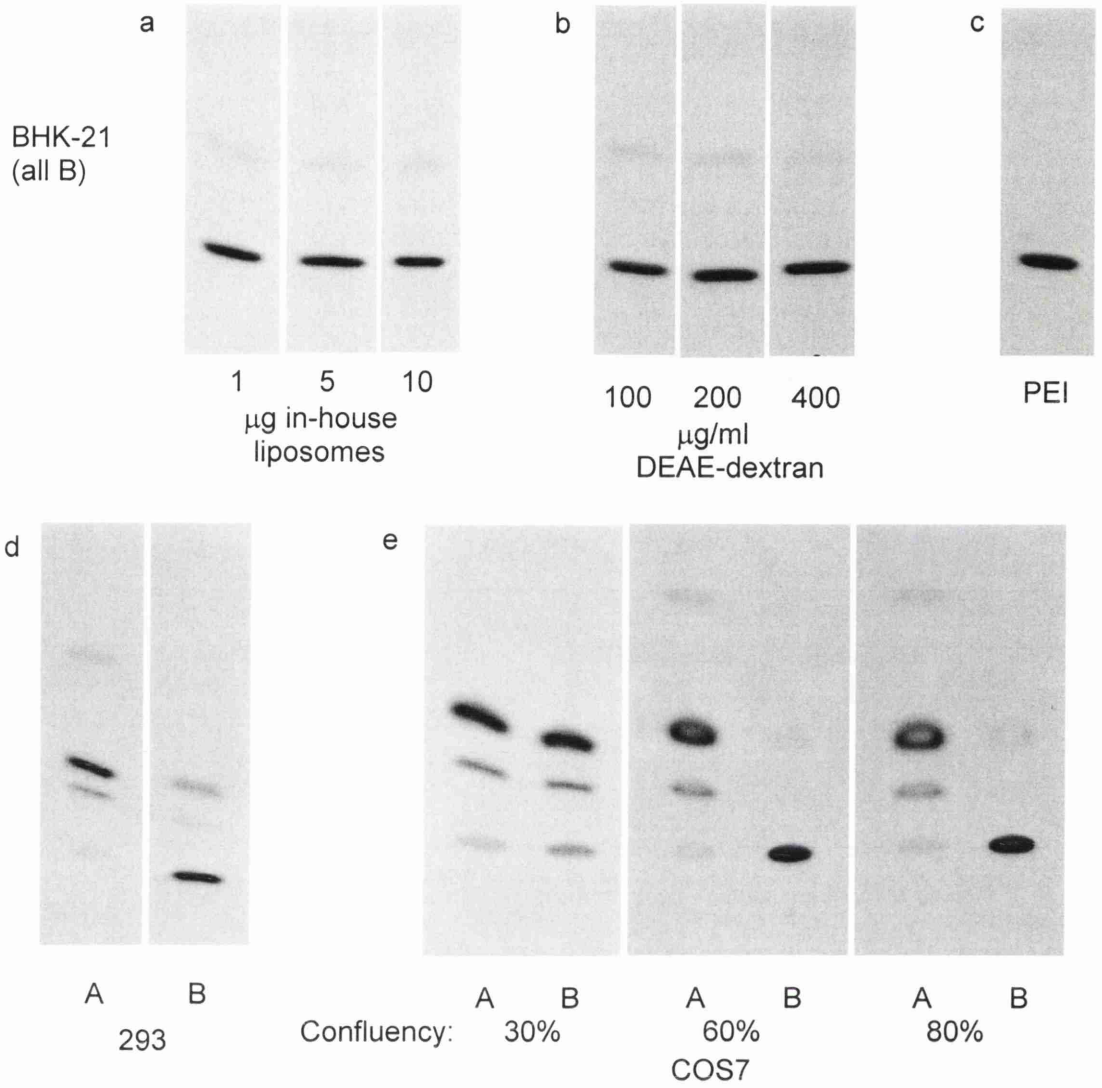

Fig. 7.2. Optimisation of the mammalian two-hybrid system. The cell lines BHK-21, 293, COS7 and HeLa were tested for their ability to support the M2H system using the positive control plasmids pM3VP16 (A) which is a transfection control and plasmids encoding proteins known to interact strongly (B). Transfection with in-house liposomes was used in each case; DEAE-dextran and PEI-mediated transfection was also attempted with BHK cells. A poor signal was obtained with BHK-21 cells using all methods tried (a-c). 293 cells gave a strong signal for transfection but a weak signal for the interaction (d). At a low confluency COS7 (e) and HeLa (f) cells provided a reasonable signal for both. 1μg each plasmid was transfected unless otherwise stated.

each plasmid was chosen as the resulting signal with the control plasmids was considered to be of a sufficiently high level.

7.1.3. Construction of M2H vectors expressing N

During initial cloning into M2H vectors the Matchmaker plasmids were not available. Cloning into the plasmid pSG424 was confounded by the presence of two *Eco*RI sites and two *Sma*I sites in the multiple cloning site. These were removed by digesting the plasmid with *Sal*I and *Sac*I, blunt-ending with the Klenow fragment of *E. coli* polymerase I and re-ligating the plasmid (Fig.7.3a). The resulting vector was designated pSG424b.

N was cloned into both pSG424b as the bait, and pVP16 as the target protein (Fig.7.3a&b). In each case the N ORF was amplified by PCR from codon 1 to stop codon 234 using pT7riboBUNN as the template (Bridgen *et al.*, 2001) and ligated into the *Eco*RI and *Bam*HI sites of pSG424b (designated pSGN) or *Eco*RI and *Hin*dIII sites of pVP16 (designated pVPBunN). The plasmid pT7riboBUNN was used as the template for PCR as the N ORF in this plasmid lacks the NSs translation start signal (Bridgen *et al.*, 2001). Hence, the possible co-expression of NSs was prevented in case it would affect the result. Both sequences were checked for PCR-induced errors but none was found. The resulting constructs encoded N with a BD (pSGN) or AD (pVPBunN) fusion tag at the N-terminus.

7.1.4. Putative N-N interactions in the M2H system

The constructs pSGN and pVPBunN were used in the M2H system to investigate any interaction between N proteins. A weak signal was obtained in COS7 cells (Fig.7.4). Attempts were made to increase the signal strength by titrating the relative amounts of each plasmid against one another and the signal strength was found to increase with the amount of pVPBunN added, but not pSGN. This suggested pVPBunN or its product was the limiting factor, which could be explained by a low level of expression or interference of the AD fusion tag with the function of the protein.

To attempt to increase the signal strength further N was expressed with a C-terminal AD fusion tag, achieved by subcloning the N ORF into pVP16AASV19N (Fig.7.5). The N ORF was amplified by PCR, again without the NSs start codon, and ligated into the blunt *Eco*RV site present in pVP16AASV19N. The *Eco*RV site is situated upstream of the AD in this vector and therefore allowed expression of N with a C-terminal AD tag. The construct was sequenced and designated pAASN to distinguish it from pVPBunN.

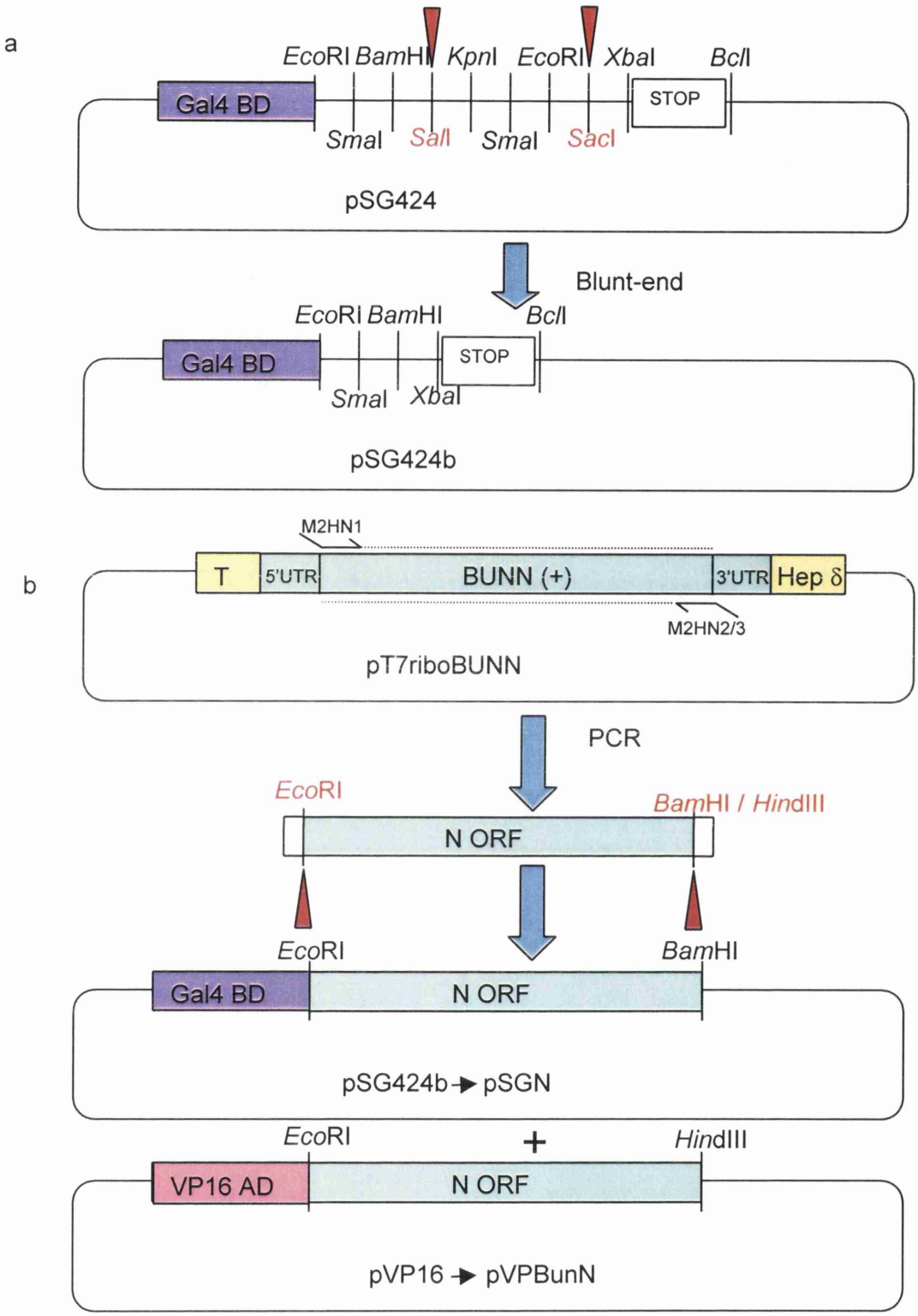

Fig.7.3. Construction of M2H vectors expressing N. The extra *Sma*I and *Eco*RI sites in the MCS of pSG424 were removed by cleavage with *Sal*I and *Sac*I, blunt-ending and religation to form pSG424b (a). Plasmids pSGN and pVPBunN were generated by ligation of PCR-amplified N ORF into the *Eco*RI/*Bam*HI sites of pSG424b or *Eco*RI/*Hin*dIII sites of pVP16, respectively (b).

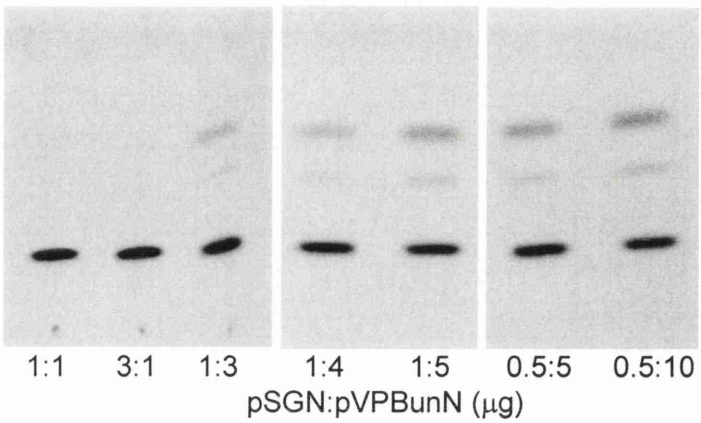

Fig.7.4. Titration of pSGN and pVPBunN in the mammalian two-hybrid system in COS7 cells. A weak CAT signal was observed only when pVPBunN was present in excess of pSGN. The strength of the signal was found to increase with an increase in the amount of pVPBunN added, but not pSGN.

C

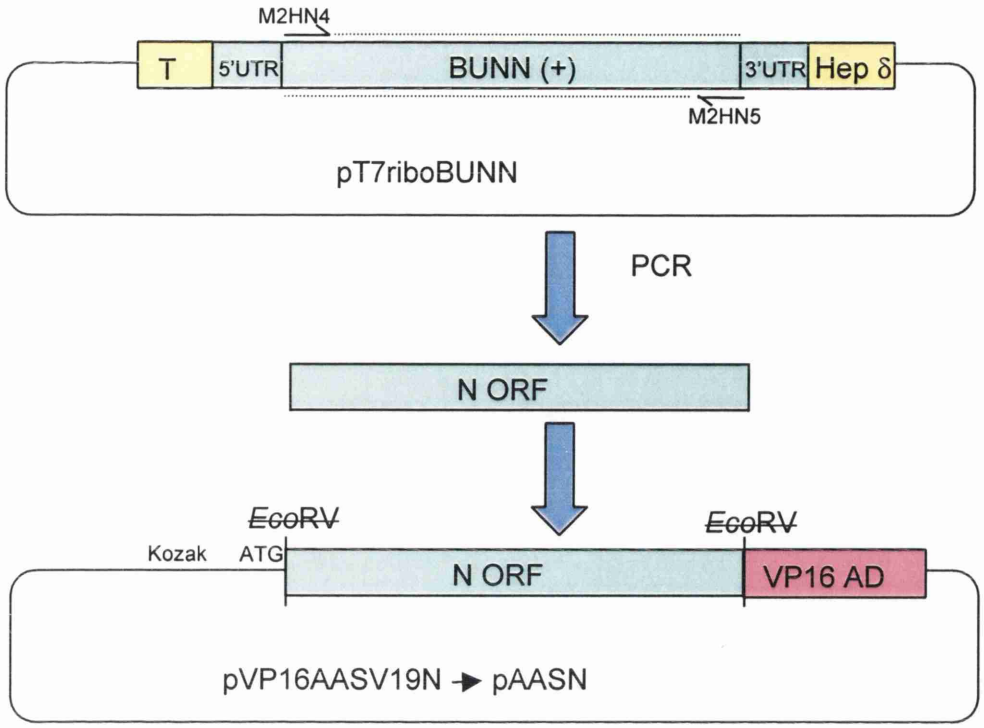

Fig.7.5. Construction of the plasmid pAASN. The N ORF was amplified by PCR and ligated into the *Eco*RV site of pVP16AASV19N, allowing N to be expressed with a C-terminal VP16 AD fusion.

The constructs pSGN and pVPBunN or pAASN were used in the M2H system in HeLa cells (Fig.7.6). When tried alongside pVPBunN, pAASN gave a significantly stronger CAT signal (compare lanes 3 & 4). Transfection of each plasmid separately with the reporter plasmid failed to yield CAT activity, proving that all three plasmids had to be present for a positive signal to result (lanes 5-7). Hence, the signal was not due to contamination of the plasmid stock or binding of AD-tagged N to DNA.

7.2. Co-immunoprecipitation assays

7.2.1. Introduction

The positive result for the N proteins obtained in the M2H assay did not necessarily indicate an interaction between N proteins due to a limitation of the system. When both the bait and target proteins have RNA binding properties, as in this case, it is possible that a positive signal is achieved by both proteins binding the same RNA intermediate and thereby bringing the AD into proximity with the reporter gene without a protein-protein interaction taking place (Fig.7.7). It was therefore necessary to identify the interaction as a protein-protein interaction by utilising an assay that would allow the removal of the RNA intermediate, or 'bridge'.

Co-immunoprecipitation (co-IP) involves the immunoprecipitation of a protein using an antibody to an epitope exclusive to that protein. Molecules bound to the protein are 'pulled down' in the precipitation and can be detected (Fig.7.8a). As this assay includes stages in which the immune complex can be modified prior to the detection stage it presents an opportunity for removal of the RNA by nuclease digestion (b). This technique has been utilised by other groups for eliminating protein-RNA-protein interactions (Elton *et al.*, 1999a).

To use co-IP to investigate N-N interactions it was necessary to generate an N protein with an exclusive epitope to act as a target for the antibody. The ideal epitope would be small enough not to interfere with the protein function but would have to be large enough to make the protein distinguishable from non-tagged N on SDS-PAGE, as well as being highly immunogenic. The epitope tag of choice was the 6xHis tag because it was known not to interfere with at least some of the protein's functions in *in vitro* assays, and its high charge means that it exerts a large effect on the electrophoretic mobility of proteins despite its small size. It is detected by a number of commercially-available antibodies including the monoclonal anti-pentaHis antibody (Qiagen).

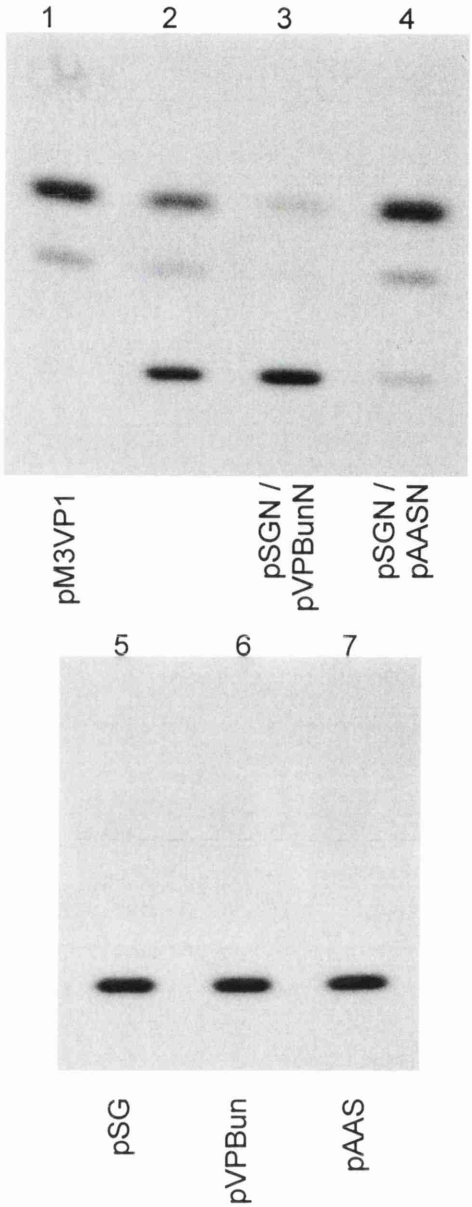

Fig.7.6. Putative interaction between N proteins in the mammalian two-hybrid system using HeLa cells. 1μg each plasmid was used in each transfection. Lane 1 constitutes the positive control CAT signal obtained from plasmid pM3VP16, which encodes both the DNA-binding and transactivation domains as one fusion protein, and lane 2 is a positive control obtained using the plasmids pVPMxA and pGalMxA. The plasmids pSGN and pVPBunN yielded a weak CAT signal as observed previously with COS7 cells (lane 3). When pVPBunN was replaced with pAASN, thereby moving the AD tag from the N to the C terminus of N, a strong signal was obtained (lane 4). No CAT signal was observed when the plasmids were individually transfected with pG_5CAT, indicating that the signal obtained when the complementary N plasmids were transfected together is the result of both products being expressed (lanes 5-7).

a

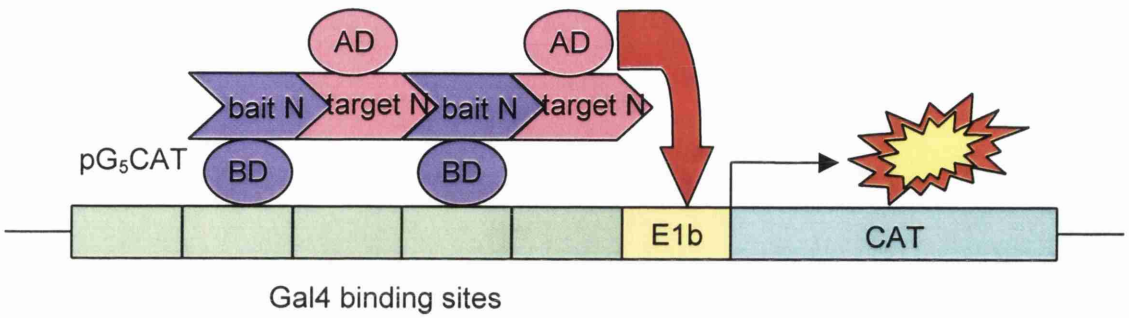

b

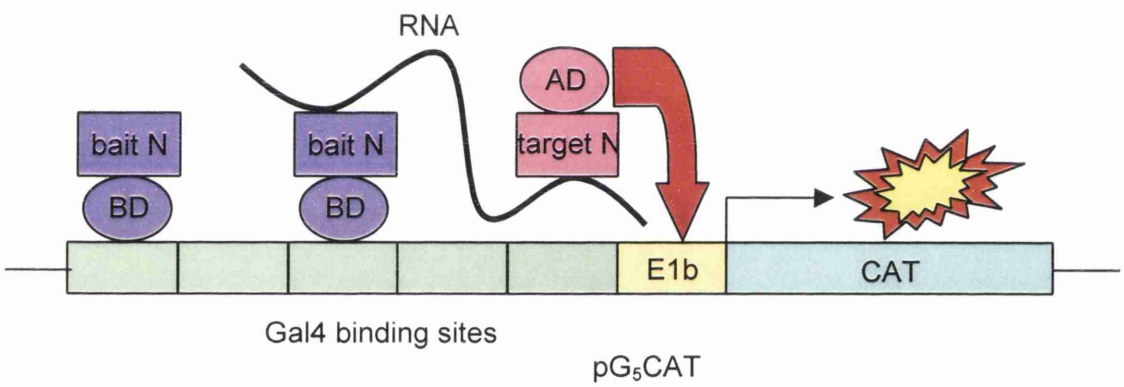

Fig.7.7. Involvement of an RNA bridge in M2H false-positives. The positive CAT signal obtained when pSGN and pAASN were tested in the M2H system might indicate that N proteins can interact with one another, which is likely to be part of a multimerisation event (a). However, the AD could be brought into proximity with the E1b promoter by the interaction of both N species with the same piece of RNA, resulting in CAT activity without any interaction taking place between the protein molecules (b).

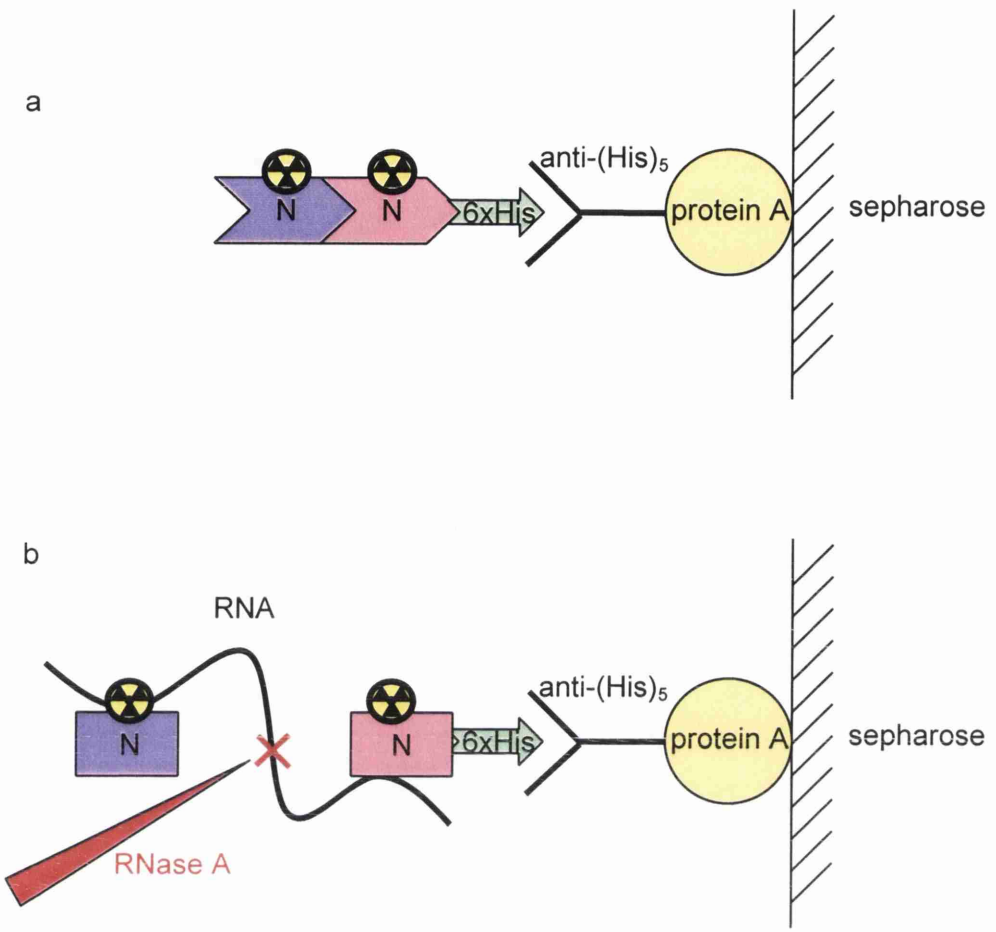

Fig.7.8. Strategy for the co-IP of N with His-tagged N. A 6xHis-tagged N protein can be bound by anti penta-His antibody, which recognises the His epitope, and immunoprecipitated using protein A-sepharose (a). If the His tagged N is bound to a non-tagged N this will also be immunoprecipitated and the difference in size and charge used to distinguish one N protein from the other. As in the M2H system false-positives can be obtained if both N proteins bind the same piece of RNA (b), resulting in the non-tagged N being pulled down without it interacting with the tagged N. This possibility can be ruled out by digestion of the RNA bridge with RNase A.

Proteins were expressed from the plasmid pTM1 which directs a high level of protein expression in mammalian cells with the use of a T7 promoter and an internal ribosome entry site (IRES).

7.2.2. Construction of plasmids for use in N-N co-IP

Non-tagged N in pTM1, termed pTM1N, had been previously constructed by F Weber. To make constructs expressing tagged N the N ORF was amplified by PCR from codons 1 to 233 and ligated into the *Nco*I/*Xba*I sites of pTM1, lacking the NSs start signal (Fig.7.9). The *Nco*I site of pTM1 also incorporates the ATG translation start signal of the IRES so to make sure that expression of the protein would start with the precise initial N-terminal amino acid, the restriction sites *Bsa*I or *BsmB*I were used to generate the 5' end of the insert. These recognition sites are remote from their cleavage sites and their use resulted in the *Nco*I site being destroyed on ligation of the insert. The 6xHis epitope tag was added on the 5' or 3' PCR primer to allow expression of proteins tagged at the N or C terminus, respectively. A unique *Sma*I site was incorporated between the tag and the N gene in each case to facilitate manipulation of the construct. The resultant constructs were sequenced and designated pTMNHisN and pTMCHisN for the expression of N and C-terminally tagged proteins ('NHisN' and 'CHisN'), respectively.

7.2.3. Detection of N-N interactions by co-IP

pTM1N was transfected into subconfluent (approximately 50%) HeLa cells with pTMNHisN or pTMCHisN with the use of in-house liposomes. T7 polymerase was provided by infection of the cells with the recombinant T7-expressing vaccinia virus vTF7-3 (Fuerst *et al.*, 1986) at 5 m.o.i., 1h prior to transfection. The cells were incubated 16h post-transfection before being labelled with ^{35}S-methionine for 3h followed by immediate lysis. A co-IP was performed on the lysate using the antibody anti-pentaHis. In this initial assay the lysates were not treated with RNase. After precipitation of the antibody with protein A-sepharose beads and washing with LiCl the precipitated proteins were dissociated by boiling in protein dissociation buffer and separated by SDS-PAGE (Fig.7.10). Both 6xHis-tagged proteins succeeded in co-precipitating the non-tagged N (lanes 1&2). NHisN ran as a double band, implying that the 6xHis tag is less stable when at the N-terminus (lanes 3 & 4). Investigation of the co-IP in the presence of RNase utilised N and CHisN proteins produced by *in vitro*

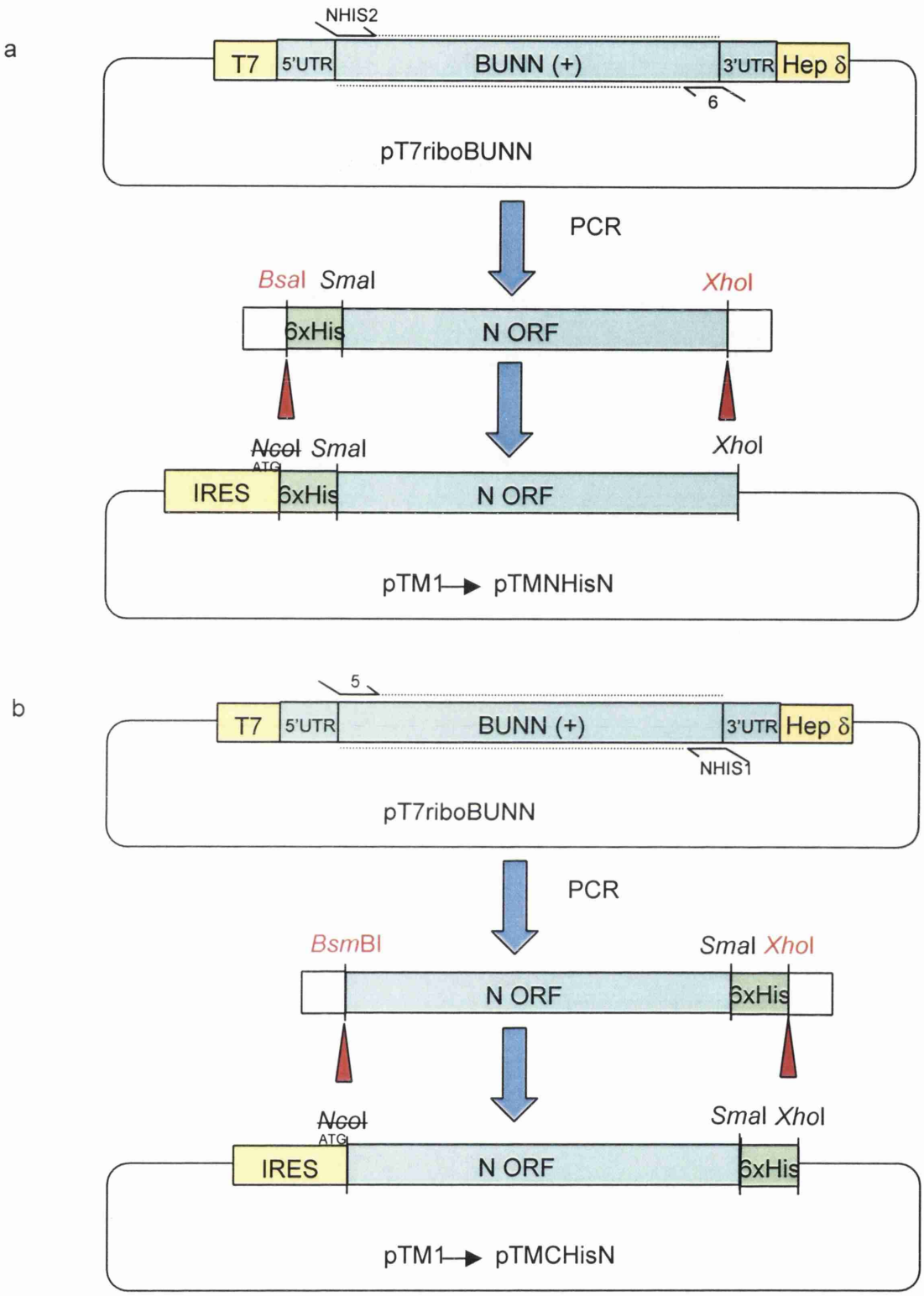

Fig.7.9. Construction of plasmids for use in N-N co-IP. The N ORF was amplified by PCR with the incorporation of a 6xHis tag at the N or C terminus. The products were ligated into the NcoI/XhoI sites of pTM1 to form pTMNHisN (a) and pTMCHisN (b). Restriction endonucleases that cut remote from the recognition site were used to generate the authentic 5' end of the ORF in each case.

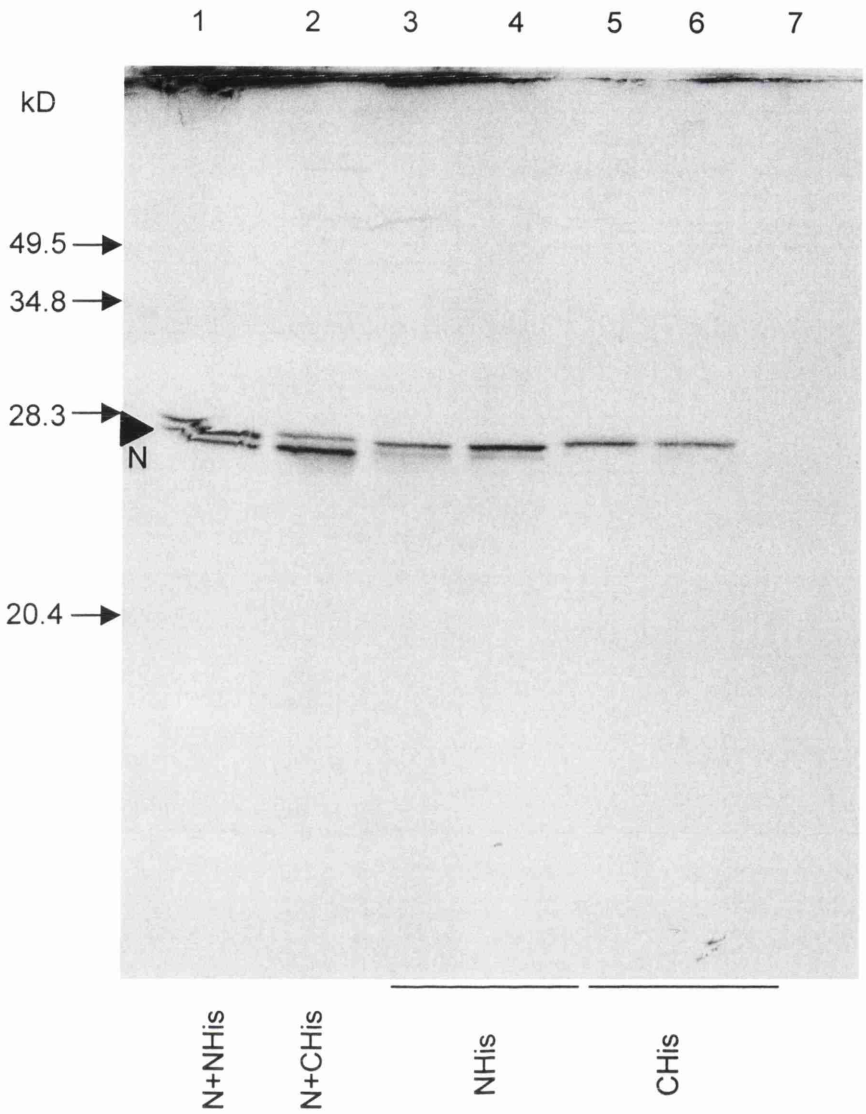

Fig. 7.10. Co-IP of N with His-tagged N. N was expressed in HeLa cells with N tagged at the N terminus (NHisN) or C terminus (CHisN). The His-tagged proteins were immunoprecipitated using the anti-pentaHis antibody and protein A-sepharose beads, and the products separated on a 15% SDS-PAGE gel. N was pulled down with both NHisN and CHisN (lanes 1 and 2) but not by the antibody on its own (lane 7). NHisN was found to run as a doublet band with the lower band having a similar electrophoretic mobility to N (lanes 3 and 4); CHisN ran as a single band (lanes 5 and 6).

transcription/translation (TnT) reactions comprising reticulocyte lysates treated with RNase and mixed with T7 polymerase (Promega). NHisN was not used due to its tendency to run as a doublet. Treatment with RNase A was performed immediately after incubation of the reaction. As TnT reactions are significantly smaller than cell lysates (25μl versus 500μl) they facilitated a much higher concentration of RNase in the reaction. RNase A was used at 5mg/ml, a 5000-fold excess over that required to digest the RNA in *in vitro* assembled N-RNA complexes, to be certain that the RNA was removed completely. The reactions were then subjected to IP as before (Fig.7.11). The ability of CHisN to pull down full-length N in a TnT reaction was verified (lane 1). Lane 4 shows that the relative quantities of tagged and untagged N in the reaction prior to IP were approximately equal. Untagged N was observed to be present in IP which shows that the interaction takes place between N proteins and is not mediated by an RNA bridge (lane 2). The band corresponding to N was less intense after RNase treatment, although it was significantly stronger than the band of N subjected to IP in the absence of His-tagged N (lane 3). This implies that some but not all of the apparent binding observed is due to the presence of an RNA bridge.

7.3. Mapping the N multimerisation sites

It is conceivable that, as N multimerises, each monomer requires at least two sites for binding to other N monomers in order to form an oligomer 'chain' as proposed for influenza virus NP (Ruigrok & Baudin, 1995). On alignment of bunyavirus N protein primary sequences, the protein appeared to consist of two domains, each representing approximately half of the protein and possessing different degrees of conservation of residues, with a region of low homology between them (Fig.1.11; discussed in section 1.2.4.3). It was considered possible that each half constitutes a separate domain and possesses at least one separate binding site, as has subsequently been observed in rabies virus N (Schoehn *et al.*, 2001). If this were the case, each half of N should be able to bind full-length N by itself. In order to test this hypothesis mutant N proteins were generated which included extensive truncations exclusively from either terminus, resulting in deletions of approximately each half of the protein around the *Kpn*I site in the ORF, which is situated in close proximity to the central region of low homology (Fig.1.11). When used in a co-IP assay these should indicate whether each half is sufficient to mediate dimerisation. Each mutant would be tested for its ability to bind full-

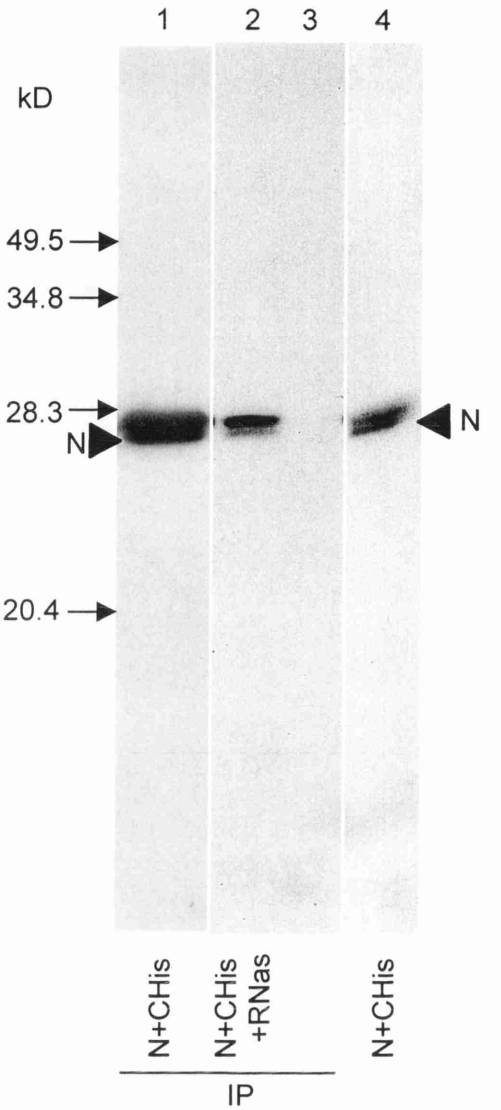

Fig.7.11. Co-IP of N in the presence of RNase. N and CHisN were expressed in a TnT reaction, co-immunoprecipitated with anti-pentaHis antibody and subjected to SDS-PAGE on a 15% gel (lane 1), resulting in the co-IP of N. When a similar reaction was incubated with 5mg/ml RNase A and an immunoprecipitation performed a small amount of N was precipitated (lane 2). No N was precipitated in the absence of CHisN (lane 3). Lane 4 shows a sample of the reaction in lane 2 but without immunoprecipitation; both proteins are present in approximately equal ratios. More protein was run in lane 1 than in the following lanes. 1μg each plasmid was used in each reaction.

length N. If a positive interaction resulted, it would then be tested against itself or the other mutant to identify the reciprocal site involved in the interaction.

7.3.1. Generation of constructs expressing truncated N proteins

Each approximate half of the N protein was expressed individually from plasmids made by amplifying the N ORF from codon 1 to 100 and 101 to 234 (stop) by PCR and ligating the fragments separately into the *Nco*I and *Xba*I sites of pTM1 (Fig.7.12a&b). Again, the restriction sites *Bsa*I or *BsmB*I were used to generate the 5' end. Codon 100 corresponds to the position of the *Kpn*I site in the N ORF, allowing the resulting plasmids to be comparable with other constructs in which the *Kpn*I site had been utilised to create deletions in N (for instance, pQENN, Fig.3.5). The constructs encoding the N and C halves of N ('NN' and 'NC') were sequenced and termed pTMNN and pTMNC, respectively.

7.3.2. Use of truncated N proteins in co-IP assays

The extensively truncated N proteins were expressed in *in vitro* transcription/translation (TnT) reactions with His-tagged N protein and immunoprecipitation performed using anti-pentaHis antibody as before (Fig.7.13). TnT reactions were chosen because they allow expression of highly labelled proteins, and as the truncated proteins were short this would be beneficial. The mutant proteins were expressed and found to be of the expected size (lanes 9 & 10). The low intensity of the band for NN (lane 9) relative to that of the band for NC (lane 10) was due to the relatively low number of methionine residues present in NN. However, the low intensity of either band compared to that for N (lane 8) suggests they were expressed at lower levels than N. An interaction between full-length N proteins expressed in TnT reactions had been observed previously (Fig.7.11, lanes 1 & 2). However, neither mutant was pulled down with a His-tagged N protein, inferring that neither half of N on its own can bind full-length N (Fig.7.13 lanes 1-4). The C-terminal half of N ('NC') appeared to be precipitated to a small extent by the antibody (lane 7) but the intensity of this band and the corresponding band for NN (lane 6) did not increase when immunoprecipitation was performed in the presence of the His-tagged proteins (lanes 1-4).

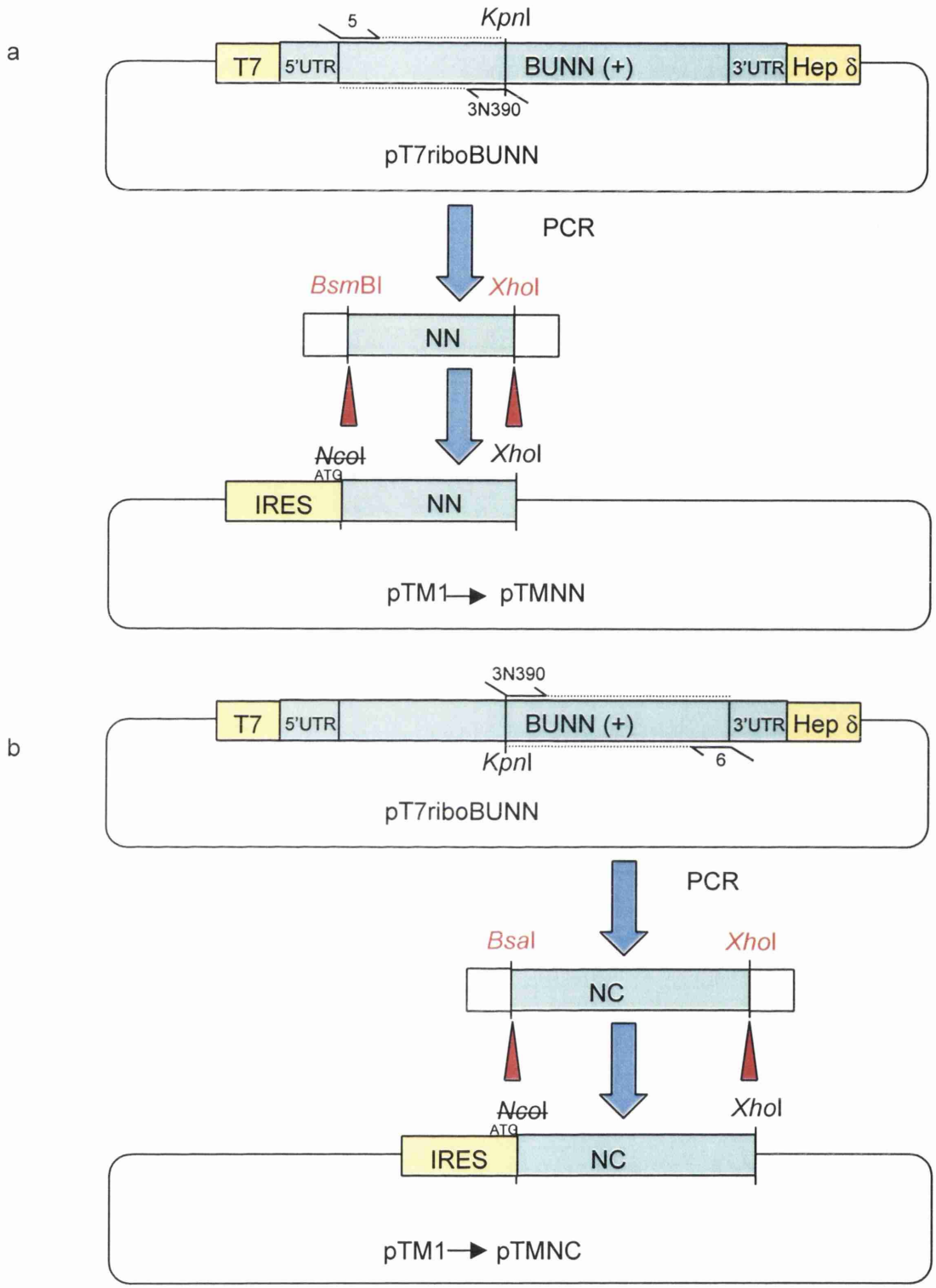

Fig. 7.12. Construction of N protein truncation mutants. The N-terminal region of the N ORF up to the *Kpn*I site and C-terminal region of the N ORF from the *Kpn*I site were amplified separately by PCR and the products ligated into the *Nco*I and *Xho*I sites of pTM1 to form pTMNN (a) and pTMNC (b), respectively. As in the construction of pTMNHisN and pTMCHisN restriction endonucleases that cleaved remote from their recognition sequences were used to generate the precise 5' ends of the ORF sections.

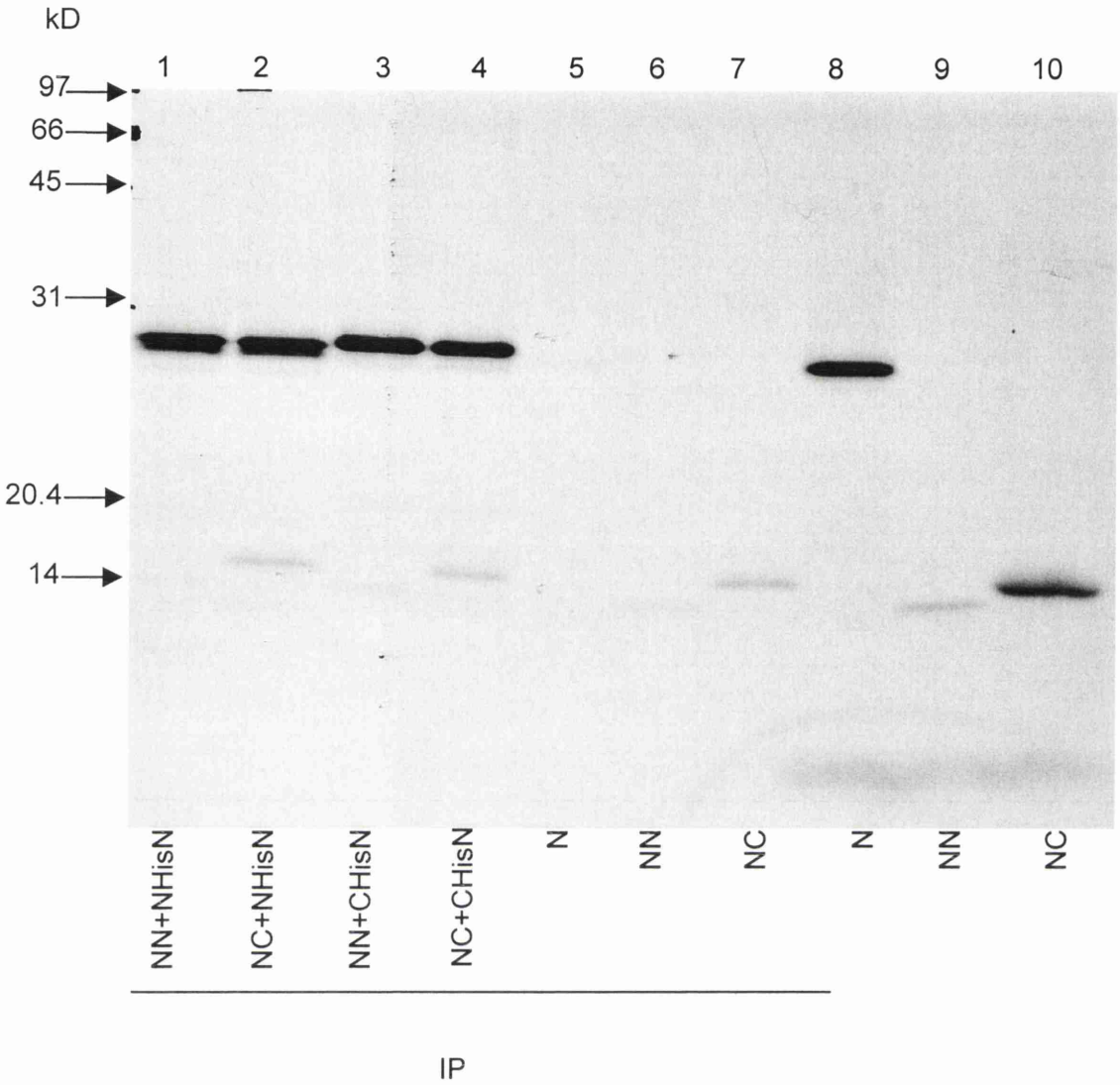

Fig.7.13. Attempted co-IP of truncated N proteins. Polypeptides consisting of the N terminus (NN) or C terminus (NC) of N were expressed in *in vitro* transcription/translation reactions with or without His-tagged N. On immunoprecipitation of the His-tagged proteins with anti-pentaHis antibody and separation on a 15% gel the truncated proteins did not appear to be pulled down, indicated by the failure of the NN and NC bands in lanes 1-4 to be stronger than those in lanes 6 & 7, which were subjected to the immunoprecipitation regime in the absence of a His-tagged protein. As a comparison, only a small amount of N was pulled down by the beads in the absence of a His-tagged protein (lane 5). Lanes 8-10 show reactions containing N, NN and NC proteins which were not subjected to immunoprecipitation and were used to check that the proteins were being expressed. The NC band is weaker than the band for NN due to the presence of fewer labelled methionine residues.

7.4. Discussion

In this chapter it was determined that BUN N is capable of dimerisation in the absence of full-length viral RNA sequences (although the N ORF transcript constitutes synthetic viral RNA, no segment terminal sequences were present). The interaction was detected both in mammalian cells and in the products of TnT reactions (Figs.7.10 & 7.11). The co-IP assay used to identify the interaction detected N-N dimers but the possibility of larger multimers, as thought to be present in Western blots of N (Fig.3.8), cannot be excluded. Further multimerisation of N could be analysed using surface plasmon resonance analysis and size exclusion chromatography, as well as by taking advantage of the multiple bands visualised on Western blotting of N (Fig.3.8). Binding was shown to take place both in the presence and absence of RNase A at a concentration 5000-fold higher than that earlier demonstrated to digest RNA in *in vitro* assembled complexes (Figs. 7.10 & 7.11; section 4.3.2) and at a similar excess to that found to digest authentic nucleocapsids isolated from infected cells (Kolakofsky & Hacker, 1991). The concentration was considered more than sufficient to effect complete digestion of any RNA bridges and was too high to allow the RNase to be inhibited significantly by rRNasin RNase inhibitor present in the TnT reaction. Hence, the co-IP of untagged N with His-tagged N is not exclusively mediated by an RNA bridge.

Mutant N proteins incorporating the approximate N or C-terminal half of the protein failed to be precipitated with full-length, His-tagged N (Fig.7.13). This argues against the presence of a separate N-binding domain in each half of the protein. Uhrig *et al.* (1999) used truncated TSWV N protein mutants in a yeast two-hybrid assay to investigate interactions between mutants ('homo-typic') and between mutant and full-length proteins. This allowed them to distinguish between mutants that could interact with both the full-length protein and with themselves, with the full-length protein only, or with neither. Thus, a mutant with both intact sites could bind either the full-length protein or itself. A mutant with only one intact site could undergo binding to the full-length protein, but not homotypic interaction. Of course, a mutant lacking both sites could bind neither. In this way they determined that a head-to-tail interaction occurred, with reciprocal sites located at the extreme ends of the protein.

If this were the case in BUN, each mutant N protein tested for its ability to bind full-length N contained one intact terminus which should have been able to bind the reciprocal terminus on the full-length molecule. It is unlikely that the His-tag interfered

with binding as this was not observed with binding between full-length N proteins, and would only be expected to interfere with binding to the C-terminus whereas neither mutant bound successfully. When the fact that neither half of the protein was able to bind was considered, no proof of a head-to-tail interaction was found.

Oligomerisation has recently also been shown to be a property of SNV hantavirus N protein (Alfadhli *et al.*, 2001). Similarly to the results obtained with BUN N, neither approximate half of SNV N was able to bind full-length N in the yeast two-hybrid system, and SNV N was found to require the presence of both termini in order to interact. Interactions could take place even if the central part was deleted. Hence, it would appear that the termini of SNV N are important in binding although a head-to-tail interaction seems unlikely.

Hantavirus N proteins were found to be non-covalently associated and oligomerisation was determined to be mediated by disulphide bonds between cysteine residues (Alfadhli *et al.*, 2001). This is interesting in the light of the fact that BUN N does not contain any cysteine residues, suggesting that the two proteins utilise fundamentally different mechanisms to mulitmerise.

RNase treatment of complexes formed between full-length BUN N proteins resulted in a decrease in the amount of N pulled down by His-tagged N (Fig.7.11), suggesting that a proportion of the N pulled down in the absence of RNase was due to the presence of an RNA bridge. The apparent inability of His-tagged N to pull down either half of N in the absence of RNase suggests that neither half of the protein is capable of binding RNA.

Oligomerisation of protein molecules results in an increase in their hydrophobicity which has been implicated in the association of some viral proteins with cell membranes (Gething *et al.*, 1986; Winkler *et al.*, 1988 & 1989; Flamand *et al.*, 1992; Doms *et al.*, 1993; Oomens *et al.*, 1995; Prokudina-Kantorovich & Semenova, 1996). In the absence of a matrix protein for bunyaviruses it is possible that the increased hydrophobicity of multimerised N is sufficient to allow the association of nucleocapsids with the cell membrane and/or viral glycoproteins on viral assembly, as has been suggested for influenza virus NP protein (Prokudina-Kantorovich & Semenova, 1996). In their analysis of NP, Prokudina-Kantorovich & Semenova (1996) used a two-phase partitioning system in which hydrophilic and hydrophobic proteins are separated into an aqueous and Triton X-114 detergent phase (Bordier, 1981). It would be interesting to investigate the hydrophobicity of monomeric and multimeric BUN N using the same system.

Chapter 8: Interactions between other viral proteins

8.1. Introduction

The formation of an intact, active nucleocapsid in infected cells is likely to require many inter-molecular interactions. These must include interactions between the RNA and both L and N. Multimerisation of N was demonstrated in the previous chapter. It is probable that an interaction also exists between L and N because:

- L must gain access to the RNA on transcription, so presumably has to melt local N-RNA bonds.
- N is thought to switch L between transcriptional and replicative modes (discussed in section 1.2).

In addition to intra-nucleocapsid binding, interactions may exist between a component of the nucleocapsid and the glycoproteins and/or NSs. As the function of NSs was at that time unknown, the identification of any interactions that it has with other proteins would be important in assigning possible functions to it. Any interactions between N, L and NSs might be detected using the M2H system. To this end, L and NSs were subcloned into the appropriate vectors.

8.2. Subcloning L and NSs into M2H vectors

8.2.1. Subcloning sections of L

The large size of L (260kD) meant that it was unlikely that the full-length protein could be expressed as a fusion protein in mammalian cells in useful quantities, and even less likely that it could be transported into the nucleus. It was therefore deemed necessary to express separate sections of the protein individually. The L gene can be conveniently dissected into five separate sections by digestion with restriction endonucleases *Eco*RI and *Bam*HI (Fig.8.1a). Of the resulting restriction fragments, three were found to be in the correct reading frame for ligating directly into the appropriate sites in pSG424 or pSG424b. The remaining two fragments would be amplified by PCR to enable the reading frame to be adjusted on ligation. All manipulations were performed on the plasmid pT7riboL.

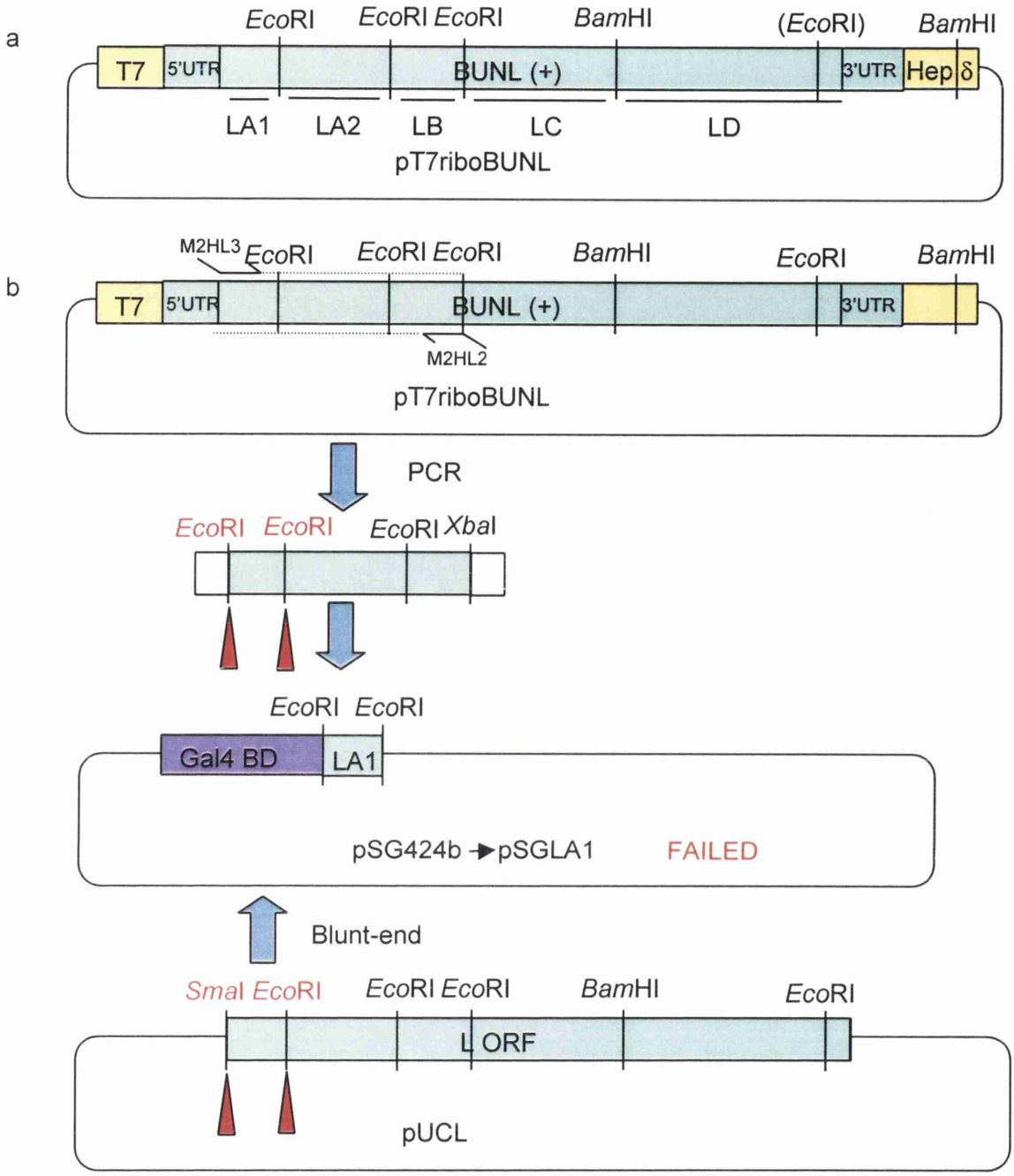

Fig.8.1a,b. Construction of M2H vectors expressing sections of L. The L ORF in pT7riboBUNL was divided up into sections based on the positions of restriction sites (a). Two strategies were employed to attempt to subclone section LA1 into pSG424b (b), utilising PCR amplification of that section of the ORF and isolation of the section from pUCL. Neither was successful.

Subcloning of the section LA1, constituting approximately 7% of the ORF, was attempted both by amplifying the fragment by PCR and then ligating the product into pSG424, and by cleaving the fragment from pUCL using the 5' *Sma*I and 3' internal *Eco*RI site prior to blunt-ending and ligation into the *Sma*I sites of pSG424 (Fig.8.1b). Neither technique worked despite repeated attempts.

Section LA2 was generated on digestion of the LA PCR fragment (generated during attempts to subclone LA1) with *Eco*RI and was isolated from an agarose gel and ligated into the *Eco*RI sites of pSG424 to create pSGLA2 (Fig.8.1c). Section LB was amplified by PCR and cloned into the *Bam*HI/*Xba*I sites of pSG424 to form pSGLB (Fig.8.1d). Sections LC and LD were isolated from restriction digestion of pT7riboL with *Eco*RI and *Bam*HI. They were ligated into the *Eco*RI/*Bam*HI, and *Bam*HI sites of pSG424b to make pSGLC and pSGLD, respectively (Fig.8.1e & f). All constructs were sequenced to check the reading frame.

8.2.2. Subcloning NSs

The NSs ORF was amplified by PCR and ligated into the *Eco*RI/*Bam*HI sites of pSG424b to form pSGNSs (Fig.8.2). The construct was sequenced, then the ORF was cleaved, isolated from an agarose gel and ligated into pVP16. The resultant construct was sequenced and termed pVPNSs. The presence of the NSs gene in both vectors would allow an investigation into whether NSs is capable of homo-oligomerisation.

8.3. Interactions between other viral proteins in the M2H system

The constructed M2H vectors were used to investigate possible interactions between:

- N and sections of L
- NSs and sections of L
- N and NSs
- NSs and NSs

The possibility to express N with the AD fusion polypeptide at either terminus (section 7.1) meant that an interaction with N would be more likely to be identified as one of the fusion tags might interfere with an interaction. All combinations of pairs of complementary M2H constructs were transfected into HeLa cells with the reporter plasmid. The transfection reagent Lipofectamine (Gibco BRL) was used in place of in-house liposomes to increase the transfection efficiency and hence the likelihood of

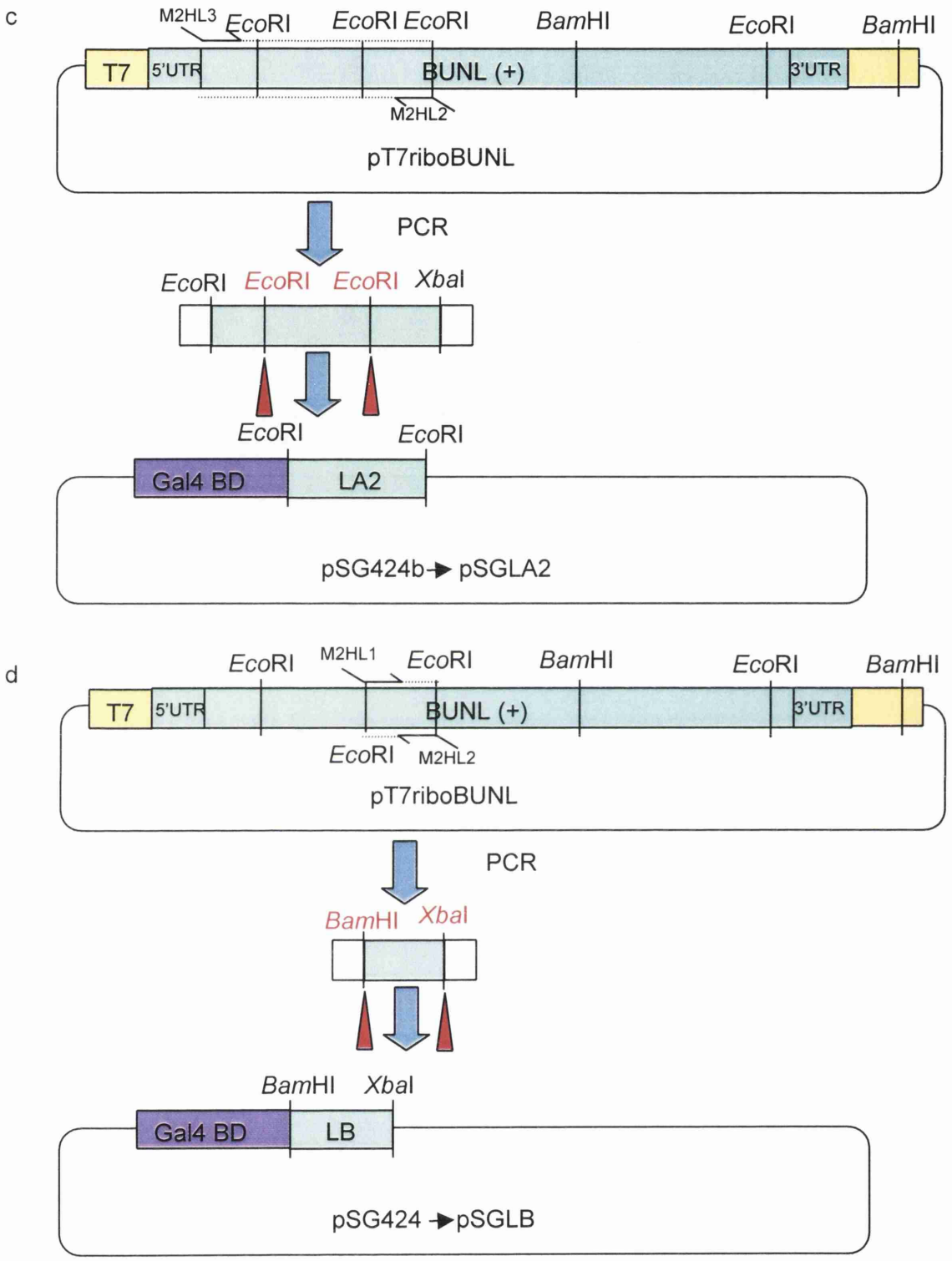

Fig.8.1c,d. Construction of M2H vectors expressing sections of L. Section LA2 was isolated from the PCR product generated whilst attempting to subclone section LA1 and was ligated into the *Eco*RI site of pSG424a (c). Section LB was generated by PCR amplification and was ligated into the *Bam*HI/*Xba*I sites of pSG424 (d).

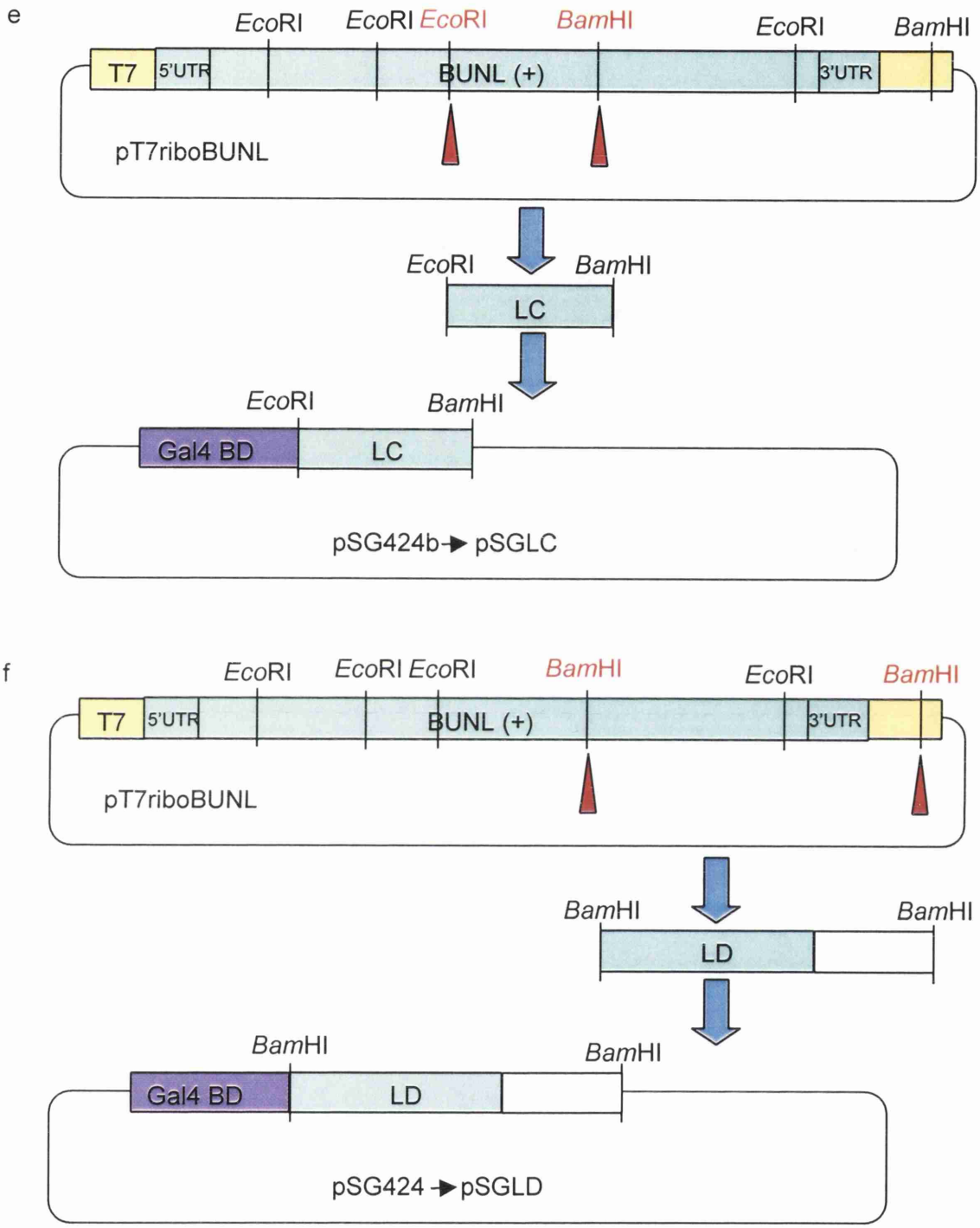

Fig.8.1e,f. Construction of M2H vectors expressing sections of L. Section LC was isolated as an *Eco*RI/*Bam*HI restriction fragment from pT7riboBUNL and ligated into the same sites in pSG424b (e). Section LD was isolated as a *Bam*HI restriction fragment from pT7riboL and ligated into the *Bam*HI site of pSG424 (f).

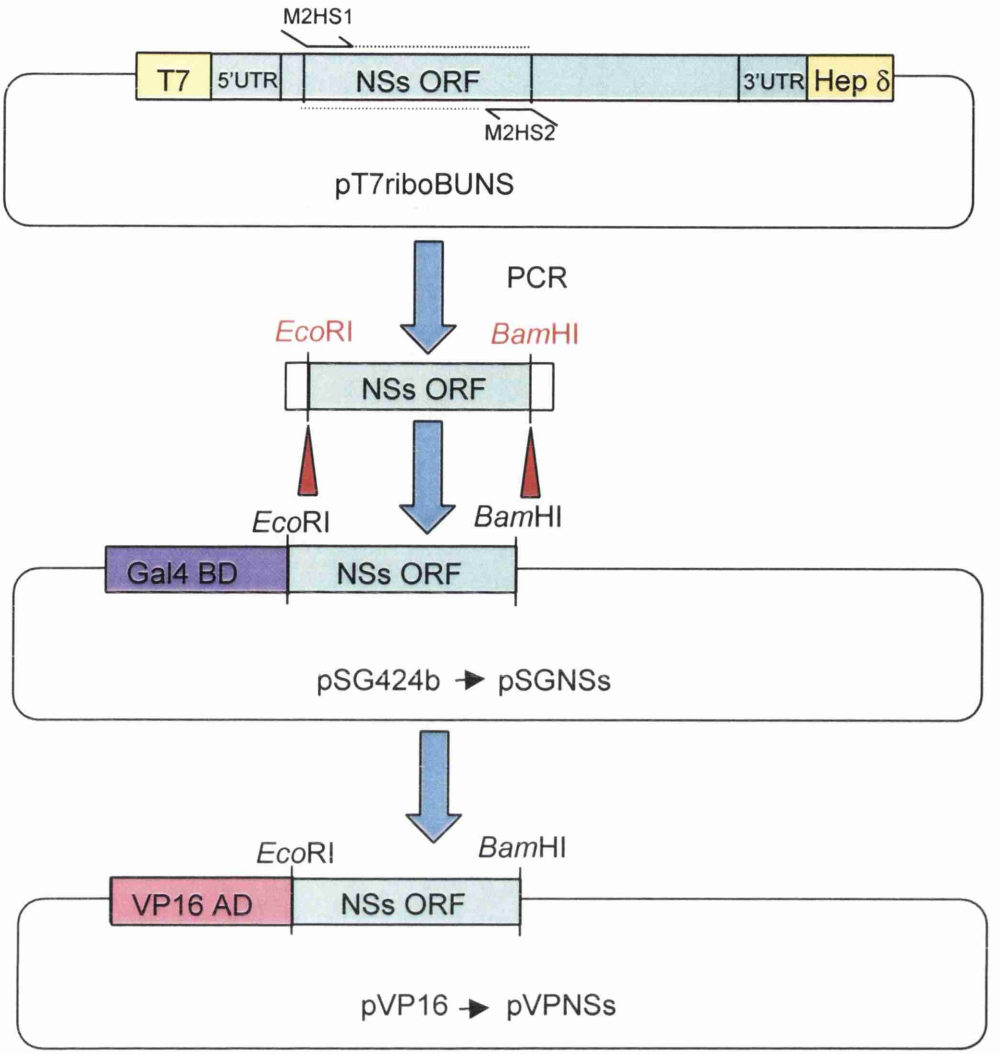

Fig.8.2. Construction of M2H vectors expressing NSs. The NSs ORF was amplified from pT7riboS by PCR and ligated into the *Eco*RI/*Bam*HI sites of pSG424b to form pSGNSs. The ORF was then cleaved using the same restriction sites, and ligated into pVP16 to form pVPNSs.

detecting a weak interaction. The cells were harvested and CAT activity assayed as previously described (Fig.8.3a&b).

No interactions were observed between the sections of the L protein used and N or NSs. NSs was not found to homo-oligomerise. However, a relatively weak signal was obtained between NSs and the N protein with a C-terminal AD fusion tag (Fig.8.3b, lane 7). The signal was not obtained when other conformations of N protein fusion were tested. The result has subsequently been found to be reproducible (C Noonan & RM Elliott, personal communication).

8.4. Discussion

In this chapter an apparent association between the BUN N and NSs proteins was discovered using the M2H system (Fig.8.3b, lane 7). However, N binds RNA and, as the exact method of action of NSs is unknown it cannot be excluded that it also binds RNA. There is therefore a possibility that the apparent association is mediated by an RNA bridge between the molecules as discussed for N-N interactions (chapter 7). Of course, it is also possible that NSs binds both N and RNA. The existence of an N-NSs interaction will require verification using co-IP experiments in which any RNA bridge is destroyed by digestion with RNase. Further work in this area is currently awaiting the production of an antibody against NSs.

Subsequent titration of the plasmids expressing N and NSs in the M2H system has indicated that the signal is increased when the amount of NSs-expressing plasmid is reduced (C. Noonan & RM Elliott, personal communication). This correlates with the observation that expression of NSs in mammalian cells is cytotoxic (Weber *et al.*, 2001). As previously mentioned, the mechanism of function of NSs is unknown although some of its functions have been determined. Firstly, NSs was found to be an inhibitor of transcription and replication by the BUN L protein in the minireplicon system (Weber *et al.*, 2001). The authors speculated that one consequence of this might be to prevent superinfection by a closely-related virus, as segment reassortment between bunyaviruses (requiring superinfection) tends to occur early on in infection, and NSs levels increase in the cytoplasm during infection (Iroegbu & Pringle, 1981; Scallan & Elliott, 1992).

Nonstructural proteins of other NSVs have been shown to exert effects of polymerase inhibition (Curran *et al.*, 1991; Cadd *et al.*, 1996; Collins *et al.*, 1996; Watanabe *et al.*, 1996; Atreya *et al.*, 1998; Tober *et al.*, 1998; Lee *et al.*, 2000). The Sendai virus

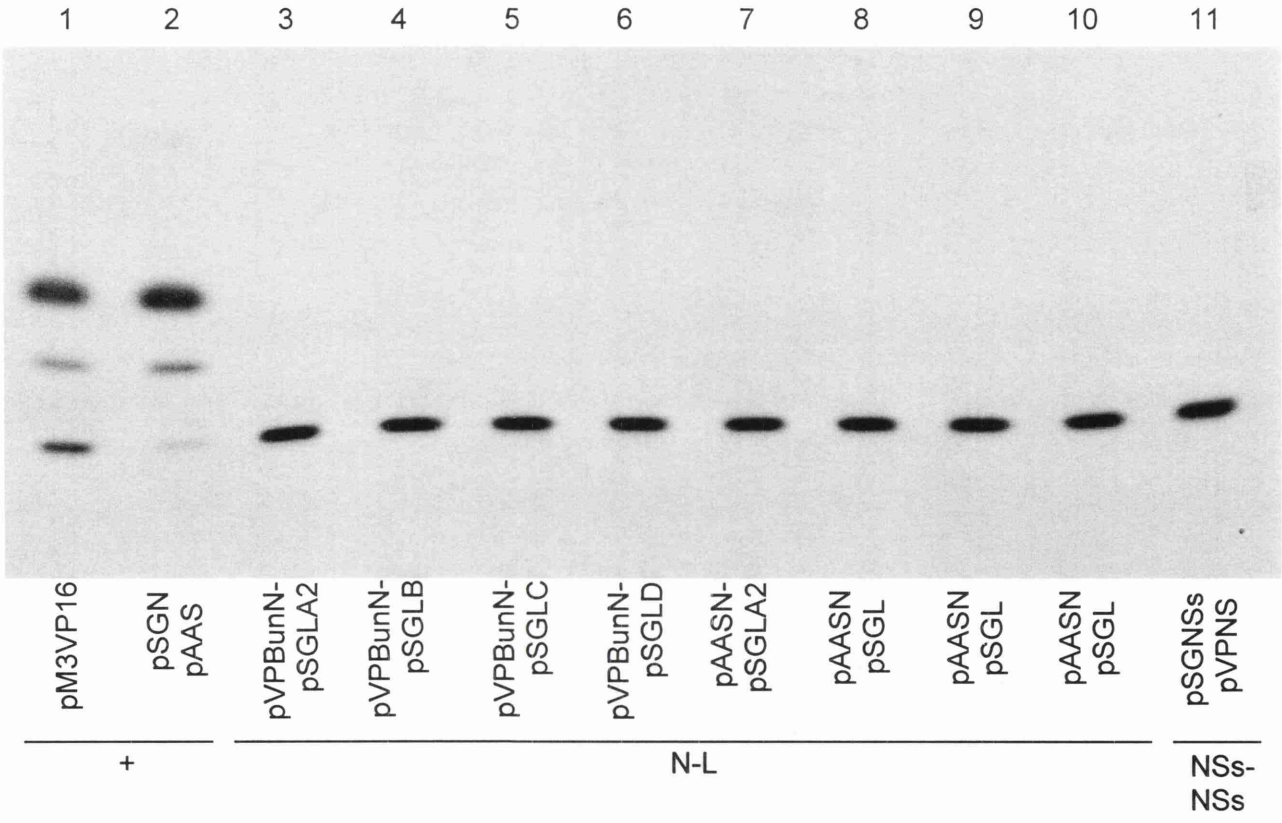

Fig.8.3a. Mammalian two-hybrid assay for protein-protein interactions in BUN using HeLa cells: screen for N-L and NSs-NSs interactions. Positive controls constituted the CAT signals obtained with plasmid pM3VP16 (lane 1), and pSGN and pAASN (lane 2). Attempts to identify an interaction between N and L involved using N with a C-terminal (lanes 3-6) or N-terminal (lanes 7-10) AD fusion tag, and sections of the L protein. No positive signal was observed. A possible interaction between NSs proteins was investigated using both NSs proteins with N-terminal fusion tags. Again, no signal was obtained (lane 11). 1μg of each plasmid was used in each transfection.

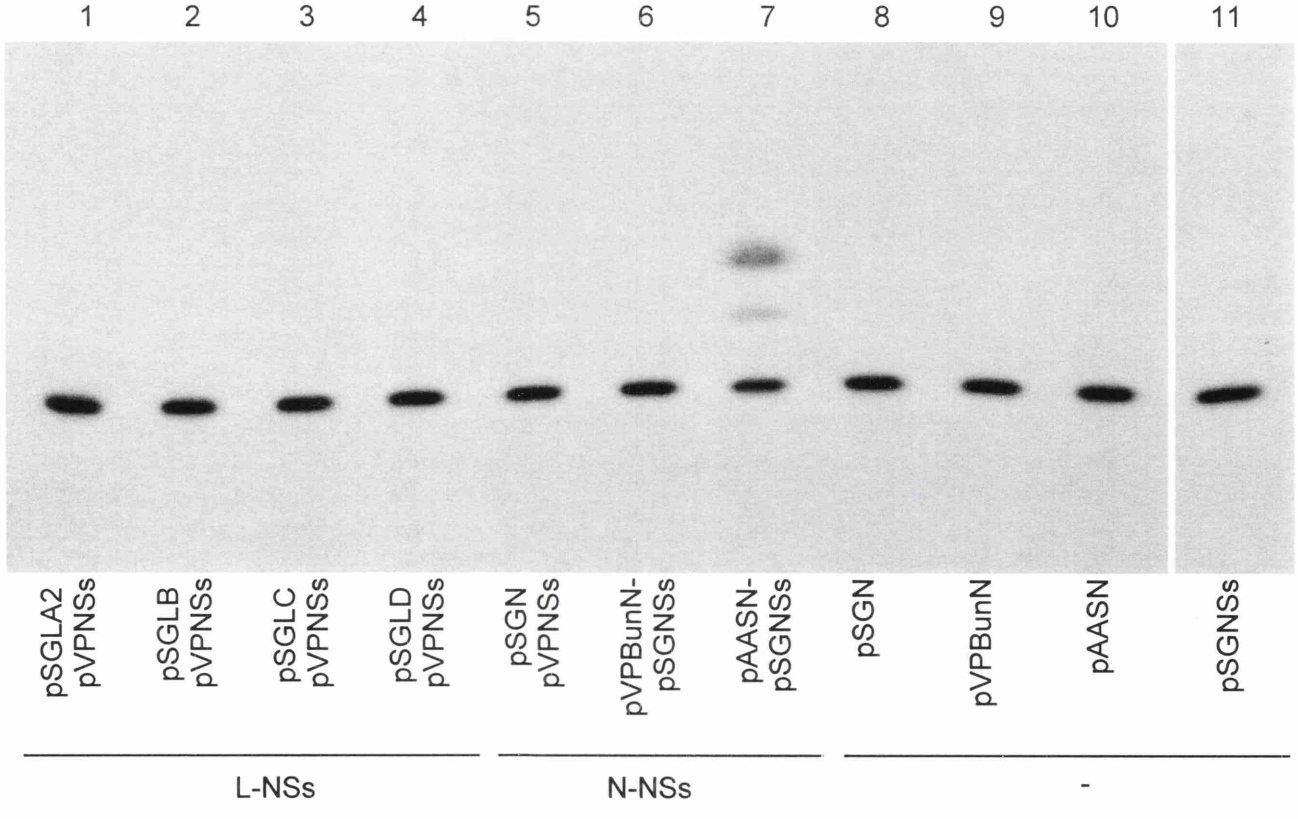

Fig.8.3b. Mammalian two-hybrid assay for protein-protein interactions in BUN using HeLa cells: screen for L-NSs and N-NSs interactions. The positive controls are shown in Fig.53a. No interaction was found between sections of L and NSs (lanes 1-4). A weak signal was obtained between N and NSs when N was expressed with the AD fusion tag at the C-terminus (lane 7), but not when the tag was placed at the other terminus (lane 6) or when NSs was used as the target protein and N as the bait (lane 5). No CAT signal was seen when the proteins were expressed individually with the reporter plasmid (lanes 8-11). 1μg of each plasmid was used in each transfection.

polymerase-inhibiting C protein was demonstrated to bind directly to the viral polymerase (Horikami *et al.*, 1997); however, no interaction between BUN NSs and sections of L was found (Fig.8.3). It is possible that BUN NSs interferes with the function of L by binding N in the nucleocapsid. For instance, inhibition could then be brought about by NSs restricting the rate at which L melts the N-RNA complex in order to gain access to the bases, or by steric hindrance.

Secondly, NSs was found to be a potent interferon-β antagonist (Bridgen *et al.*, 2001). Many other NSVs have been demonstrated to possess interferon-antagonistic properties, often attributable to nonstructural proteins (Garcia-Sastre *et al.*, 1998; Harcourt *et al.*, 1998; Tan & Katze, 1998; Fujii *et al.*, 1999; Garcin *et al.*, 1999; Gotoh *et al.*, 1999; Hariya *et al.*, 1999; Schlender *et al.*, 2000; Sekellick *et al.*, 2000; Talon *et al.*, 2000; Wang *et al.*, 2000; Young *et al.*, 2000 (and references therein)). Induction of type I interferons is mediated by dsRNA which can be viral in origin. In BUN the mode of inhibition by NSs was discovered to be via NFK-B and IRF-3 (an interferon response factor; Weber *et al.*, in preparation). One action of influenza virus NS1 protein was also the inhibition of IRF-3, which it achieved by binding dsRNA and hence sequestering it from detection (Hatada & Fukuda, 1992; Talon *et al.*, 2000). BUN NSs might function similarly, in which case the positive signal for the N-NSs interaction detected in the M2H system might indeed be due to an RNA bridge. However, NSs does not contain a known RNA-binding motif (Bridgen *et al.*, 2001).

An alternative model explaining interferon antagonism by NSs uses the observation that NSs inhibits the action of L, described above. By regulating the relative amounts of N, viral genomic and antigenomic RNA and mRNA in the infected cell NSs could prevent association between unencapsidated genomic RNA and mRNA or antigenomic RNA, thereby preventing the formation of dsRNA.

Thirdly, generation of the BUNdelNSs virus lacking NSs identified NSs as a virulence factor. Infection with the mutant virus resulted in impaired host protein shut-off, smaller plaque sizes, lower virus titres and reduced pathogenicity in mice. N protein expression was increased ten-fold (Bridgen *et al.*, 2001). It is conceivable that the low virus titres and reduction in plaque size and pathogenicity are related directly to the interferon-antagonistic properties of NSs. The increase in N expression levels is presumably attributable to altered ribosome scanning in the absence of the NSs start signal on the mutated S segment transcript. The presence of the NSs ORF within the N ORF in the

wild-type virus is interesting as it implies that it is important to keep the ratio of the two proteins stable (Bridgen *et al.*, 2001).

Host protein shut-off by LAC is thought to be due to an induction of instability of host mRNA as a result of the cleavage of the cap by L (Raju & Kolakofsky, 1988). NSs could function by exercising an inhibitory effect on cellular polymerases (which would explain its cytotoxicity). It is difficult to see how the mechanism could involve an interaction with N.

In addition to the known functions of NSs, others can be hypothesised from analysis of its properties and analogy with the nonstructural proteins of other NSVs. In cells infected with wild-type BUN, N is strictly cytoplasmic but in BUN NSs minus-infected cells N can be seen to enter the nucleus (Bridgen *et al.*, in preparation). It has therefore been proposed that NSs acts by preventing N from entering the nucleus, which might involve it interacting with N.

Another possible function for NSs would be to assist in packaging of the nucleocapsids into the virion. Its hydrophobic properties suggest that it might be capable of associating with the cell membrane. Interaction with N could help chaperone N to the membrane. It is difficult to envisage how NSs would escape being packaged itself, although definitive proof that NSs is truly not a structural protein has yet to be provided.

The fact that no interaction was found between sections of L and N or NSs is perhaps attributable to binding sites having been destroyed by expressing L as separate segments. Hence, one or both interactions might take place in the infected cell. Co-IP assays to detect binding between L and N are currently underway.

No dimerisation of NSs was observed in the M2H system. This is interesting when it is considered that influenza virus NS1 protein multimerises (Nemeroff *et al.*, 1995). However, dimerisation of NSs cannot be ruled out due to the limitations of the M2H system. A possible self-association could be investigated further using a co-IP assay.

Chapter 9: Conclusions

9.1. Fulfilment of the project aims

The main aim of the project was to identify and characterise an interaction of N with viral RNA using biochemical methods. In addition, this would be used to provide information on the process of encapsidation of viral RNA, and to address the question of why non-viral RNA and mRNA are normally not encapsidated.

N-RNA interactions were identified *in vitro* and progressive binding of N along the RNA visualised by polyacrylamide GEMSA. RNA was considered to be fully encapsidated by N in *in vitro* reactions, and the N-RNA complexes formed by *in vitro* techniques were judged to be representative of authentic nucleocapsid structures. This was based on the similar resistance of the complexes to digestion by RNase A, the binding of multiple N proteins to the RNA and the formation of complexes with a finite maximum size. The co-operativity of binding to RNA had been suggested for hantavirus and tospovirus N proteins (Gött *et al.*, 1993; Richmond *et al.*, 1998; Severson *et al.*, 1999) but this is the first time that it has been mathematically supported for a member of the *Bunyaviridae.* The dissociation constant for BUN N-RNA binding indicated a strong interaction and was similar to that obtained for hantavirus N (Severson *et al.*, 1999). However, the ability of BUN N to bind RNA over a particularly wide range of ionic conditions and to bind both double-stranded and single-stranded RNA suggested a different mode of binding to hantavirus and tospovirus N (Gött *et al.*, 1993; Richmond *et al.*, 1998; Severson *et al.*, 1999). In addition, the absence of dependency on precise ionic conditions implied that electrostatic interactions are not the sole mediators of the binding event, suggesting that binding does not occur exclusively to the phosphodiester backbone.

The 5' terminus of the BUN S segment was discovered to be bound preferentially, and the signal responsible for selective binding mapped to within the first 32nt of the 5' terminus. This is in accordance with the predictions made by Raju & Kolakofsky (1987b) implicating the 5' terminus of genomes and antigenomes in the initiation of encapsidation, and with the observation made by Dunn (2000) that the terminal 32 and 33nt of the 5' and 3' termini are sufficient to direct transcription. It is understandable that encapsidation would initiate at this point as it is the first part of the RNA to be synthesised, and therefore allows the nascent transcript to be encapsidated fully whilst synthesis is progressing. This hypothesis is supported by the observation that the

presence of the 3' terminus did not increase the degree of selective binding, arguing against the requirement of encapsidation initiation for both termini.

In rhabdoviruses, adenine-rich sequences were proposed to mediate binding by N (Blumberg *et al.*, 1983; Yang *et al.*, 1998). However, although the BUN 5' terminal sequences are relatively rich in adenine (as are all BUN sequences) there is no regular pattern of adenines. In addition, although there are stretches of consecutive adenines in the terminal sequences, some 5' terminal sequences contain just one stretch of only three consecutive adenines. Other RNAs, one possessing the 5'BUNS terminal sequences, that were predicted to contain multiple, similarly unstructured stretches of three or four consecutive As were not bound selectively. In addition, the structure of the poly-A sequences in the 5' BUN terminal sequences was not always predicted to be altered in the presence of the non-templated primer; hence, the elimination of an encapsidation signal consisting of a poly-A stretch in BUN cannot be explained by structural modification of the sequence. This appears to make their involvement as an encapsidation signal unlikely. If this is the case, it may reflect the differences between segmented and nonsegmented NSVs. Nevertheless, an involvement of adenine in BUN encapsidation cannot be excluded entirely.

A stem-loop predicted in the 5' terminus was suggested to be important for selective binding as it was not predicted in a transcript that consisted of the 5' terminus and yet was not bound selectively. In addition, the stem-loop is similar to those determined to be encapsidation signals in positive-strand RNA viruses and HIV-1, similar stem-loops were predicted in other BUN segments, and the modification of the putative encapsidation signal by a nontemplated primer can explain the inability of mRNAs to be encapsidated. The bases predicted within the loop region are common between BUN segments and were determined by Dunn (2000) to be essential for transcription using the BUN minireplicon system. Recently, Severson *et al.* (2001) have implicated stem-loops in the selective binding of hantavirus RNA, also proposing that single-stranded RNA within the loop is important. Hence, there is evidence that initiation of encapsidation of BUN segments occurs at the 5' terminus and is mediated by secondary structure comprising an encapsidation signal, explaining why non-viral RNA is not encapsidated. It is interesting that an RNase-resistant band was observed when N-RNA complexes were treated with RNase, possibly constituting the stem-loop predicted at the BUNS 5' terminus. The observation that N can also bind any RNA non-selectively, although to a lower degree, suggests that this is the mechanism for general

encapsidation of RNA once encapsidation has been initiated at the 5' terminus. The existence of two modes of binding, namely selective and non-specific, has also been documented for positive-strand RNA viruses, as well as VSV and rabies virus (see Introduction).

Predictions of the secondary structure at the 5' terminus of S mRNA suggested that the non-templated primer acts by destroying or modifying the putative encapsidation signal. In the case of signal modification, the important bases were predicted also to be responsible for annealing the primer to the template RNA. These predictions are in agreement with observations that mRNA is not encapsidated (Bouloy *et al.*, 1984). Previous attempts to explain why encapsidation does not take place included the recruitment of cap-binding factors or the signal being placed out of context (Raju & Kolakofsky, 1987b). The hypothesis presented here that the primer prevents encapsidation by altering the signal structurally represents a novel model for the inhibition of encapsidation of mRNA.

A second objective was to identify whether N is capable of self-association, and if so, to determine the domains responsible.

The co-operativity of N-RNA binding observed suggested that N was capable of interacting with itself, and that this could be an important event in the process of encapsidation. The presence of RNase-resistant but boiling-sensitive bands of higher molecular weight detected by all antibodies on Western blotting of bacterially-expressed N suggested that N could multimerise. BUN N proteins were shown to interact with one another in both the mammalian two-hybrid system and co-immunoprecipitation assays, and the association was not mediated entirely by an RNA intermediate, although the complexes formed in TnT reactions appeared to be more sensitive to RNase treatment than bacterially-expressed N. Neither half of BUN N was found to be capable of association independently. This quality has recently been observed for hantavirus N (Alfadhli *et al.*, 2001). There was no evidence that the interaction in BUN is mediated by head-to-tail binding as observed with tospovirus N (Richmond *et al.*, 1998). In addition, N is incapable of the disulphide bonding that has been demonstrated to be responsible for hantavirus N oligomerisation (Alfadhli *et al.*, 2001). Thus, the mechanism of N multimerisation in BUN would appear to be fundamentally different to that of hantaviruses and possibly also tospoviruses. This is interesting in the light of the fact

that the nature of the BUN N-RNA interaction would also appear to differ from that in hantaviruses and tospoviruses.

A third aim was to investigate any interaction between N and L, which was considered to be likely to take place.
An interaction between N and sections of L was investigated using the mammalian two-hybrid system but was not apparent. This might be attributable to the limitations of the system and to the expression of L in sections.

The final objective was to detect any interactions between NSs and itself, N or L, with the intent to provide information on the function of NSs.
An apparent interaction between N and NSs was detected using the mammalian two-hybrid system. Currently the interaction is awaiting verification by another method as there is a possibility that it was in fact mediated by an RNA intermediate. Nevertheless, this is the first time that an interaction with NSs has been demonstrated and will probably be critical in elucidating the mechanisms of the protein's functions. The interaction may be involved in regulation of transcription (Weber *et al.*, 2001), or in the interferon antagonistic property of NSs that appears to be the basis of its role as a virulence factor (Bridgen *et al.*, 2001).
Interactions between NSs and sections of L were investigated using the mammalian two-hybrid system but none was observed. In addition, no evidence of self-association of NSs was obtained with the mammalian two-hybrid system.

9.2. A model for encapsidation in BUN

The results obtained in the project can now be consolidated to attempt to build a model of encapsidation of S segment RNA in BUN. The hypothesis is that early in transcription to generate genome or antigenome RNA from the 3' terminus of the template, approximately the first twenty bases of the nascent transcript assemble into a stem-loop structure that constitutes the encapsidation signal and is immediately bound selectively by N. This could proceed in a process similar to that observed on binding stem-loops in encapsidation initiation by HIV-1 NCp7 (de Guzman *et al.*, 1998) or recognition of a stem-loop by MS2 coat protein, which specifically recognises bases in the loop (Valegård *et al.*, 1994). As more of the transcript emerges from the polymerase it is bound co-operatively but non-selectively by N, i.e. by association of N with other N

molecules and the RNA. This is similar to the model proposed for encapsidation of rhabdovirus and paramyxovirus genomes, which is thought to initiate at an encapsidation signal in the (5') leader region of the genome, and progress through nonspecific interactions between N and the RNA (see Introduction). It is possible that the initial interaction of N with the encapsidation signal is aided *in vivo* by the proximity of the 5' end of the early nascent transcript to the encapsidated template RNA; hence, N-N interactions may also be important at this point. The mechanism of N-N interactions in BUN remains unknown.

On transcription to generate mRNA the bases at the 3' end of the primer (usually AGU or GGU; Jin & Elliott, 1993a) are thought to be used to prime the transcript by annealing to the UCA triplet on the template. Once priming has concluded the (A/G)GU triplet dissociates from the template and base-pairs with a UCA triplet downstream of the encapsidation signal, elongating its stem and forming a bulge. Bases at the 5' end of the primer could be prevented from base-pairing due to binding by cap-binding proteins. When the primer triplet binds the transcript UCA the initial binding of N to the encapsidation signal may already have taken place. However, addition of more N molecules is blocked by steric hindrance resulting from elongation of the stem-loop and the presence of the bulge in the stem. Therefore, the mRNA is not encapsidated.

Late in infection of mosquito cells the concentration of N in the cell reaches a point at which N is capable of overcoming the steric hindrance (the concentration of N was found to be critical for binding RNA) and encapsidation proceeds along the transcript, preventing expression of more N from the mRNA by blocking the ribosome, as has been suggested in LAC-infected cells (Hacker *et al.*, 1989). It should be noted here that the only primer sequences that have been determined for BUN are those from S mRNAs; hence only S mRNA is discussed here as the theory might not be applicable to other segments. It is possible that in the mRNA of other segments the encapsidation signal is usually destroyed as there is no requirement for their products to be regulated by encapsidation of the transcript.

The mechanism behind the switch from transcription to replication has yet to be elucidated, and an interaction of N with L could not be demonstrated using the mammalian two-hybrid system. It is possible, however, that the ability of N to bind RNA non-selectively to a relatively low degree and its apparent concentration-dependency of binding to RNA result in N binding the non-templated primer, as has been suggested for rhabdoviruses (Yang *et al.*, 1999). This could result in the inability of the primer to

anneal with the template RNA and would thereby force L to begin replicative transcription.

9.3. A mammalian three-hybrid system for analysis of encapsidation *in vivo*

As mentioned in chapter 3, it was initially necessary to analyse encapsidation using an *in vitro* approach in order to investigate binding kinetics and observe N binding RNA directly. Now that N-RNA binding has been characterised *in vitro* it would be interesting to investigate encapsidation of RNA further *in vivo*. This could:

- Permit the analysis of the effects of other molecules such as NSs, L and cellular factors on the encapsidation event.
- Be used to determine the degree of binding of N to BUN or heterologous RNA at concentrations of viral proteins attained on infection by infecting the cells with BUN.
- Incorporate a rapid way to screen the effects of mutations in the RNA or proteins without having to transcribe or express and purify them *in vitro*.

The BUN minireplicon system has the disadvantage that it requires the transcription of an RNA template by L. This means that mutations in the BUN termini might affect the viral promoter and mutations in the N protein could affect its binding to L. Hence, it would be useful to develop a mammalian three-hybrid system to analyse N-RNA interactions. No mammalian three-hybrid system exists in which the RNA of interest can be placed at the 5' end of the hybrid RNA. A yeast three-hybrid system has been developed in which the sequence of interest is placed upstream of two enhanced bacteriophage MS2 coat protein-binding sites (SenGupta *et al.*, 1996). The MS2 sequences are bound by the MS2 coat protein fused to an activation domain. The protein of interest is provided fused to a DNA binding domain so that, if it binds the RNA sequence of interest, the activation domain is pulled into proximity with the promoter of a reporter plasmid to which the DNA binding domain is bound and reporter activity results.

In this system there is a region of RNase P RNA upstream of the RNA sequence of interest. However, in a mammalian system a hybrid RNA could be transcribed as a ribozyme sequence under the control of a modified T7 promoter as has been performed previously (Bridgen & Elliott, 1996). The MS2 coat protein could then be expressed as a fusion protein, in this case fused with the binding domain (BD) of Gal4, after subcloning it into the mammalian two-hybrid plasmid pSG424 (Fig.9.1a).

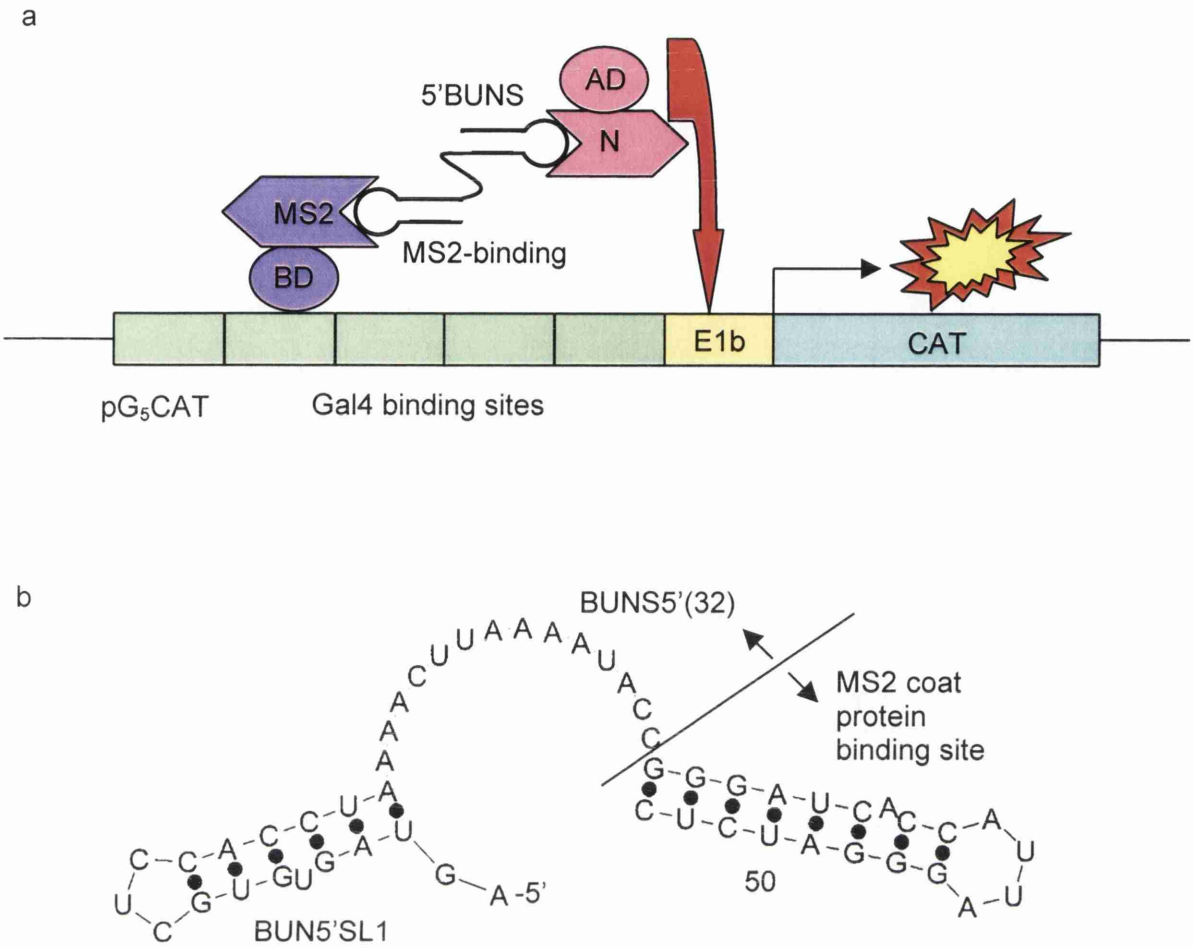

Fig.9.1. A mammalian three-hybrid system for studying BUN N-RNA interactions. (a). The system would incorporate a hybrid RNA consisting of the MS2 coat protein binding site and the 32b of the 5' terminus of BUNS at the 5' end of the RNA. The MS2 site would be bound by the MS2 coat protein fused with the DNA-binding domain of Gal4 (BD), which would bind Gal4 binding sites upstream of a reporter gene on a reporter plasmid. The 5'BUNS sequence would be bound by N fused to the activation domain of VP16 (AD), thereby bringing the AD into proximity with the reporter gene's promoter and resulting in reporter gene activity. (b). The only structure of the hybrid RNA predicted by Mfold. The structure shows that the MS2-binding stem-loop and BUN5'SL1 stem-loop are both predicted to form in the hybrid RNA and are not expected to interfere with one another.

The use of MS2 as the bait protein in this case would allow the expression of N with either an N or C-terminal fusion with the VP16 activation domain (AD), expressed from the existing mammalian two-hybrid plasmids pVPN and pAASN. The use of multiple MS2 binding sites and the MS2 coat protein fused to the AD in the yeast three-hybrid system was used to increase the sensitivity of system as MS2 binds co-operatively. However, N also binds co-operatively to BUN RNA so the sensitivity might not be reduced on expressing MS2 fused to the BD. The reporter gene pG_5CAT could also be taken from the mammalian two-hybrid system. If necessary the system could be modified to utilise a mammalian protein and RNA sequence.

The sequence of interest would in this case constitute the 5' BUNS terminus. However, in competitive binding assays it was observed that the structure of RNA in this region, which might be essential for binding by N, can be disrupted by placing an interfering sequence downstream. Nevertheless, placing an MS2 coat protein binding site downstream of BUNS5'(32) RNA is predicted not to interfere with the expected secondary structure of the 5' terminus when analysed by the Mfold RNA-folding program (Matthews *et al.*, 1999; Zuker *et al.*, 1999; Fig.9.1b).

Mutations in the RNA sequence could be quantified directly by the ability of the RNA to be bound by N. Mutations in N found to disrupt binding to the RNA might, however, be effected by the inability of N to multimerise; this could then be tested by observing the activity of the construct directly in the mammalian two-hybrid system. In this case the possible presence of an RNA bridge would not arise as N would have already been found not to bind RNA.

References

Abraham, G, & AK Pattnaik (1983). Early RNA synthesis in Bunyamwera virus-infected cells. J. Gen. Virol. 64:1277-1290

Agapov, EV, I Frolov, BD Lindenbach, BM Pragai, S Schlesinger, & CM Rice (1998). Noncytopathic Sindbis virus RNA vectors for heterologous gene expression. Proc. Natl. Acad. Sci. USA. 1998 95:12989-12994

Albo, C, A Valencia, & A Portela (1995). Identification of an RNA binding region within the N-terminal third of the influenza A virus nucleoprotein. J. Virol. 69:3799-3806

Alfadhli, A, Z Love, B Arvidson, J Seeds, J Willey, & E Barklis (2001). Hantavirus nucleocapsid protein oligomerization. J. Virol. 75:2019-2023

Allen, P, B Collins, D Brown, Z Hostomsky, & L Gold (1996). A specific RNA structural motif mediates high affinity binding by the HIV-1 nucleocapsid protein (NCp7). Virology 225:306-315

Anderson, GW, Jr, & JF Smith (1987). Immunoelectron microscopy of Rift Valley fever viral morphogenesis in primary rat hepatocytes. Virology 161:91-100

Arikawa, J, LC Connors, M Wang, & CD Schmaljohn (1990). Coding propoerties of the S and the M segments of Sapporo rat virus: Comparison to other causative agents of hemorrhagic fever with renal syndrome. Virology 176:114

Atreya, PL, ME Peeples, PL Collins. (1998). The NS1 protein of human respiratory syncytial virus is a potent inhibitor of minigenome transcription and RNA replication. J. Virol. 72:1452-1461.

Bankamp, B, SM Horikami, PD Thompson, M Huber, M Billeter, & SA Moyer (1996). Domains of the measles virus N protein required for binding to P protein and self-assembly. Virology 216:272-277

Baudin, F, C Bach, S Cusack, & RWH Ruigrok (1994). Structure of influenza RNP. I. Influenza virus melts secondary structure in panhandle RNA and exposes the bases to solvent. EMBO J. 13:3158-3165

Beaton, AR, & RM Krug (1986).Transcription antitermination during influenza viral template RNA synthesis requires the nucleocapsid proteins and the absence of a 5' capped end. Proc. Natl. Acad. Sci. USA 83:6282-6286

Becht, H, & H-P Weiss (1991). 'The influenza virus-infected host cell, a target for the immune response'. Behring Inst. Mitt., Justus-Liebig-Universität, Giessen. 89:1-11

Bellocq, C, & D Kolakofsky (1987). Translational requirement for La Crosse virus S-mRNA synthesis: a possible mechanism. J. Virol. 61:3960-3967

Bellocq, C, R Raju, J Patterson, & D Kolakofsky (1987). Translational requirement of La Crosse virus S-mRNA synthesis: in vitro studies. J Virol 61:87-95

Berat, C, O Schatz, S LeGrice, & JL Darlix (1993). Analysis of the interaction of the HIV-1 replication primer tRNA(lys3) with nucleocapsid protein and reverse transcriptase. J. Mol. Biol. 231:185-190

Berglund, JA, B Charpentier, & M Rosbash (1997). A high affinity binding site for the HIV-1 nucleocapsid protein. Nuc. Acids Res. 25:1042-1049

Berkowitz, RD, J Luban, & SP Goff (1993). Specific binding of human immunodeficiency virus type I *gag* polyprotein and nucleocapsid protein to viral RNAs detected by RNA mobility shift assays. J. Virol. 67:7190-7200

Betenbaugh, M, M Yu, K Kuehl, J White, D Pennock, K Spik, & C Schmaljohn (1995). Nucleocapsid- and virus-like particles assemble in cells infected with recombinant baculoviruses or vaccinia viruses expressing the M and the S segments of Hantaan virus. Virus Res. 38:111-124

Bishop, DHL, & DD Auperin. (1987). Arenavirus gene structure and organization. Curr. Top. Microbiol. Immunol. 133:5-17

Bishop, DH, ME Gay, & Y Matsuoko (1983). Nonviral heterogeneous sequences are present at the 5' ends of one species of snowshoe hare bunyavirus S complementary RNA. Nucleic Acids Res. 11:6409-6418

Bishop, DHL, & RE Shope (1979). *Bunyaviridae.* Compr. Virol. 14:1-156

Bishop, DHL (1996). Biology and molecular biology of bunyaviruses. In The *Bunyaviridae*, pp. 19-53. Ed: RM Elliott. Plenum Press, New York

Biswas, SK, PL Boutz, & DP Nayak (1998). Influenza virus nucleoprotein interacts with influenza virus polymerase proteins. J. Virol. 72:5493-5501

Black, DL, R Chan, H Min, J Wang, & L Bell (1998). The electrophoretic mobility shift assay for RNA binding proteins. In: RNA:protein interactions, pp. 109-136. Ed: CWJ Smith. Oxford University Press, Oxford, United Kingdom

Blumberg, BM, C Giorgi, & D Kolakofsky (1983). N protein of vesicular stomatitis virus selectively encapsidates leader RNA *in vitro.* Cell 32:559-567

Borer, PN, S Wang, MW Rogeenbuck, JM Gott, OC Uhlenbeck, & I Pelczer (1995). Proton NMR and structural features of a 24-nucleotide RNA hairpin. Biochemistry 34:6488-6503

Boussif, O, F Lezoualc'h, MA Zanta, MD Mergny, D Scherman, B Demeneix, & J-P Behr (1995). A versatile vector for gene and oligonucleotide transfer into cells in culture and *in vivo*: Polyethylenimine. Proc. Natl. Acad. Sci. USA 92:7297-7301

Bordier, C (1981). Phase separation of integral membrane proteins in Triton X-114 solution. J. Biol. Chem. 256:1604-1607

Bouloy, M, & C Hannoun (1976). Studies on Lumbo virus replication. I. RNA dependent RNA polymerase associated with virions. Virology 69:258-268

Bouloy, M, S Krams-Ozden, F Horodniceanu, & C Hannoun (1973/74). Three segment RNA genome of Lumbo virus (bunyavirus). Intervirology 2:173-180

Bouloy, M, N Pardigon, S Gerbaud, P Vialat, & M Girard (1984). Transcription of the S segment of Germiston bunyavirus. In: Segmented Negative-Strand Viruses, pp. 29-35. Eds: RW Compans & DHL Bishop. Academic Press, New York/London

Bouloy, M, N Pardigon, P Vialat, S Gerbaud, & M Girard (1990). Characterisation of the 5' and 3' ends of viral messenger RNAs isolated from BHK21 cells infected with Germiston virus (*Bunyavirus*). Virology 75:50-58

Boussif, O, F Lezoualc'h, MA Zanta, MD Mergny, D Scherman, B Demeneix, & J-P Behr (1995). A versatile vector for gene and oligonucleotide transfer into cells in culture and *in vivo*: Polyethyleneimine. Proc. Natl. Acad. Sci. USA 92:7297-7301

Boyle, JF, & KV Holmes (1986). RNA-binding proteins of bovine rotavirus. J. Virol. 58:561-568

Braam, J, I Ulmanen, & RM Krug (1983). Molecular model of a eukaryotic transcription complex: functions and movements of influenza P proteins during capped RNA-primed transcription. Cell 34:609-618

Bradford, MM (1976). A rapid and sensitive method for the quantitation of microgram quantities of protein utilizing the principle of protein-dye binding. Anal. Biochem. 72:248-254

Bridgen, A, F Weber, JK Fazakerly, & RM Elliott (2001). Bunyamwera bunyavirus nonstructural protein NSs is a nonessential gene product that contributes to viral pathogenesis. Proc. Natl. Acad. Sci. USA 98:664-669

Bridgen, A, & RM Elliott (1996). Rescue of a segmented negative-strand RNA virus entirely from cloned complementary DNAs. Proc. Natl. Acad. Sci. USA 93:15400-15404

Buchholz, CJ, C Retzler, HE Homann, & WJ Neubert (1994). The carboxyl-terminal domain of Sendai virus nucleocapsid protein is involved in complex formation between phosphoprotein and nucleocapsid-like particles. Virology 204:770-776

Buchholz, CJ, D Spehner, R Drillien, WJ Neubert, & HE Homann (1993). The conserved N-terminal region of Sendai virus nucleocapsid protein NP is required for nucleocapsid assembly. J. Virol. 67:5803-5812

Butler, PJG (1999). Self-assembly of tobacco mosaic virus: the role of an intermediate aggregate in generating both specificity and speed. Philo. Trans. R. Soc. Lond. B. Biol. Sci. 354:537-550

Cadd, T, D Garcin, C Tapparel, M Itoh, M Homma, L Roux, J Curran, & D Kolakofsky (1996).. The Sendai paramyxovirus accessory C proteins inhibit viral genome amplification in a promoter-specific fashion. J. Virol. 70:5067-5074

Calisher, C (1991). Classification and nomenclature of viruses. Fifth report of the international committee on taxonomy of viruses. Arch. Virol. Suppl. 2:273-283

Calisher, CH (1996). History, classification, and taxonomy of viruses in the family *Bunyaviridae*. In: The *Bunyaviridae*, pp.1-17. Ed: RM Elliott. Plenum Press, New York

Cann, AJ (1997). Principles of Molecular Virology, 2nd edition. Academic Press, California / London

Casals, J & L Whitman (1961). Group C, a new serological group of hitherto undescribed arthropod-borne viruses: Immunological studies. Am. J. Trop. Med. Hyg. 10:250

Cash, P, AC Vezza, JR Gentsch, & DH Bishop (1979). Genome complexities of the three mRNA species of snowshoe hare bunyavirus and in vitro translation of S mRNA to viral N polypeptide. J. Virol. 31:685-694

Chanda, PK, & AK Banerjee (1981). Identification of promoter-proximal olgonucleotides and a unique dinucleotide, pppGpC, from in vitro transcription products of vesicular stomatitis virus. J. Virol. 39:93-103

Cianci, C, L Tiley, & M Krystal (1995). Differential activation of the influenza virus polymerase by template RNA binding. J. Virol. 69:3995-3999

Clerx-van Haaster, C, & DHL Bishop (1980). Analyses of the 3'-terminal sequences of snowshoe hare and La Crosse bunyaviruses. Virology 105:564-574

Collett, MS (1986). Messenger RNA of the M segment RNA of Rift Valley fever virus. Virology 151:151-156

Collins PL, MG Hill, J Cristina, & H Grosfeld. (1996). Transcription elongation factor of respiratory syncytial virus, a nonsegmented negative-strand RNA virus. Proc. Natl. Acad. Sci. USA 93:81-85.

Cook, RF, JA Sinclair, & A Mumford (1988). Detection of influenza NP antigen in nasal secretions from horses infected with A/eq influenza (H3N8) viruses. J. Virol. Methods 20:1-12

Creighton, TE (1993). Proteins: Structures and Molecular Properties. 2nd Edition. WH Freeman, New York

Cullen, BR (1987). Use of eukaryotic expression technology in the functional analysis of cloned genes. Methods Enzymol. 152:684-704

Cunningham, C, & JF Szilàgyi (1987). Viral RNAs sythesized in cells infected with Germiston Bunyavirus. Virology 157:431-439

Curran, J, J-B Marq, & D Kolakofsky (1995). An N-terminal domain of the Sendai paramyxovirus P protein acts as a chaperone for the NP protein during the nascent chain assembly step of genome replication. J. Virol. 69:849-855

Curran, J, R Boeck, & D Kolakofsky. (1991). The Sendai virus P gene expresses both an essential protein and an inhibitor of RNA synthesis by shuffling modules via mRNA editing. EMBO J. 10:3079-3085.

Darlix, JL, M Lapadat-Tapolsky, H de Rocquigny, & BP Roques (1995). First glimpses at structure-function relationships of the nucleocapsid protein of retroviruses. J. Mol. Biol. 254:523-537

Das, T, BM Chakrabarti, D Chattopadhyay, & AK Banerjee (1999). Carboxy-terminal five amino acids of the nucleocapsid protein of vesicular stomatitis virus are required for encapsidation and replication of genome RNA. Virology 259:219-227

Das, T, M Mathur, AK Gupta, GM Janssen, & AK Banerjee (1998). RNA polymerase of vesicular stomatitis virus specifically associates with translation elongation factor-1 alphabetagamma for its activity. Proc. Natl. Acad. Sci. USA 95:1449-1454

Das, T, AK Pattnaik, AM Takacs, T Li, LN Hwang, & AK Banerjee (1997). Basic amino acid residues at the carboxy-terminal eleven amino acid region of the phosphoprotein (P) are required for transcription but not for replication of vesicular stomatitis virus genome RNA. Virology 238:103-114

De Avila, AC, C Huguenot, R de O Resende, EW Kitajima, RW Goldbach, & D Peters (1990). Serological differentiation of 20 isolates of tomato spotted wilt virus. J. Gen. Virol. 71:2801

De Guzman, RN, ZR Wu, CC Stalling, L Pappalardo, PN Borer, & MF Summers (1998). Structure of the HIV-1 nucleocapsid protein bound to the SL3 psi-RNA recognition element. Science 279:384-388

De Haan, P, L Wagemakers, D Peters, & R Goldbach (1990). The S RNA segment of tomato spotted wilt virus has an ambisense character. J. Gen. Virol. 71:1001-1007

Desselberger, U, VR Racaniello, JJ Zazra, & P Palese (1980). The 3' and 5' terminal sequences of influenza A, B and C RNA segments are highly conserved and show partial inverted complemetarity. Gene 8:315-328

Digard, P, D Elton, K Bishop, E Medcalf, A Weeds, & B Pope (1999). Modulation of nuclear localization of the influenza virus nucleoprotein through interaction with actin filaments. J. Virol. 73:2222-2231

Doms, RW, RA Lamb, JK Rose, & A Helenius (1993). Folding and assembly of viral membrane proteins. Virology 193:545-562

Draper, DE (1999). Themes in RNA-protein recognition. J. Mol. Biol. 293:255-270

Duesberg, P (1969). Distinct subunits of the ribonucleoprotein of influenza virus. J. Mol. Biol. 42:485-499

Duggal, R, & TC Hall (1993). Identification of domains in brome mosaic virus RNA-1 and coat protein necessary for specific interaction and encapsidation. J. Virol. 67:6406-6412

Dunn, EF (2000). Development of a reverse genetic system to investigate Bunyamwera virus RNA synthesis. PhD thesis

Dunn, EF, DC Pritlove, & RM Elliott (1994). The S RNA genome segments of Batai, Cache Valley, Guaroa, Kairi, Lumbo, Main Drain and Northway bunyaviruses: sequence determination and analysis. J. Gen Virol. 75:597-608

Dunn, EF, DC Pritlove, H Jin, & RM Elliott (1995). Transcription of a recombinant bunyavirus RNA template by transiently expressed bunyavirus proteins. Virology 211:133-143

El-Ghorr, AA, AC Marriott, VK Ward, TF Booth, S Higgs, EA Gould, & PA Nuttall (1990). Characterization of Dugbe virus (Nairovirus, Bunyaviridae) by biochemical and immunochemical procedures using monoclonal antibodies. Arch. Virol. [Suppl. 1]:169

Elliott, RM (1990). Molecular biology of the *Bunyaviridae*. J. Gen. Virol. 71:501-522

Elliott, RM (1995). Evolution of the *Bunyaviridae*. In: Co-evolution of viruses and their hosts, pp. 321-337. Eds: AJ Gibbs, CH Calisher, F Garcia-Arenal. Cambridge University Press, Cambridge

Elliott, RM (1996). The *Bunyaviridae*: concluding remarks and future prospects. In: The *Bunyaviridae*, pp. 295-332. Ed: RM Elliot. Plenum Press, New York

Elliott, RM (1997). Emerging viruses: the *Bunyaviridae*. Molecular Medicine 3:572-577

Elliott, RM, M Bouloy, CH Calisher, R Goldbach, JT Moyer, ST Nichol, R Pettersson, A Plyusnin, & CS Schmaljohn (2000). *Bunyaviridae*. In: Seventh Report of the International Committee on Taxonomy of Viruses. Eds: MHV van Regenmortel, CM Fauquet, DHL Bishop, EB Carstens, MK Estes, SM Lemon, J Maniloff, MA Mayo, DJ McGeoch, CR Pringle, & RB Wickner. Academic Press

Elliott, RM, CS Schmaljohn, & MS Collett (1991). *Bunyaviridae* genome structure and gene expression. Curr. Top. Microbiol. Immunol. 169:91-141

Elliott, RM, M Smith, & A McGregor (1989). Expression of the bunyavirus S RNA segment. In: Genetics and pathogenicity of negative strand viruses, pp. 67-73. Eds: BWJ Mahy, & D Kolakofsky. Elsevier Biomedical Press, Amsterdam

Elton, D, E Medcalf, K Bishop, & P Digard (1999a). Oligomerization of the influenza virus nucleoprotein: identification of positive and negative sequence elements. Virology 260:190-200

Elton, D, L Medcalf, K Bishop, D Harrison, & P Digard (1999b). Identification of amino acid residues of influenza virus nucleoprotein essential for RNA binding. J. Virol. 73:7357-7367

Emery, VC, & DHL Bishop (1987). Characterization of Punta Toro S mRNA species and identification of an inverted complementary sequence in the intergenic region of Punta Toro virus phlebovirus ambisense S RNA that is involved in mRNA transcription termination. Virology 156:1-11

Eshita, Y, & DHL Bishop (1984). The complete sequence of the M RNA of snowshoe hare bunyavirus reveals the presence of internal hydrophobic domains in the viral glycoproteins. Virology 137:227

Eshita, Y, B Ericson, V Romanowski, & DH Bishop (1985). Analyses of the mRNA transcription processes of snowshoe hare bunyavirus S and M RNA species. J. Virol. 55:681-689

Fazakerly, JK, F Gonzalez-Scarano, J Strickler, B Dietzschold, F Karush, & N Nathanson (1988). Organization of the middle RNA segment of snowshoe hare Bunyavirus. Virology 167:422-432

Fields, S, & O. Song (1989). A novel genetic system to detect protein-protein interactions. Nature 340:245-246

Flamand, M, V Deubel, & M Girard (1992). Expression and secretion of Japanese encephalitis virus nonstructural protein NS1 by insect cells using a recombinant baculovirus. Virology 191:826-838

Flick, R, & G Hobom (1999). Interaction of influenza virus polymerase with viral RNA in the 'corkscrew' conformation. J. Gen. Virol. 80:2565-2572

Flick, R, G Neumann, E Hoffmann, E Neumeier, & G Hobom (1996). Promoter elements in the influenza vRNA terminal structure. RNA 2:1046-1057

Fodor, E, DC Pritlove, & GG Brownlee (1994). The influenza virus panhandle is involved in the initiation of transcription. J. Virol. 68:4092-4096

Fooks, AR, JR Stephenson, A Warnes, AB Dowsett, BK Rima, & GWG Wilkinson (1993). Measles virus nucleocapsid protein expressed in insect cells assembles into nucleocapsid-like structures. J. Gen. Virol. 74:1439-1444

Fuerst, TF, EG Niles, FW Studier, & B Moss (1986). Eukaryotic expression system based on recombinant vaccinia virus that synthesizes bacteriophage T7 RNA polymerase. Proc. Natl. Acad. Sci. USA 83:8122-8126

Fujii, N, N Yokosawa, & S Shirakawa (1999). Suppression of interferon response gene expression in cells persistently infected with mumps virus, and restoration from its suppression by treatment with ribavirin. Virus Res. 65:175-185

Garcia-Sastre A, A Egorov, D Matassov, S Brandt, DE Levy, JE Durbin, P Palese, & T Muster. (1998). Influenza A virus lacking the NS1 gene replicates in interferon-deficient systems. Virology 252:324-30

Garcia-Sastre, A, & P Palese (1993). Genetic manipulation of negative-strand virus genomes. Annu. Rev. Microbiol. 47:765-790

Garcin D, P Latorre, & D Kolakofsky. (1999). Sendai virus C proteins counteract the interferon-mediated induction of an antiviral state. J Virol. 73:6559-65

Garcin, D, M Lezzi, M Dobbs, RM Elliott, C Schmaljohn, CY Kang, & D Kolakofsky (1995). The 5' ends of Hantaan virus (*Bunyaviridae*) RNAs suggest a prime-and-realign mechanism for the initiation of RNA synthesis. J. Virol. 69:5754-5762

Gavrilovskaya, IN, M Shepley, R Shaw, MH Ginsberg, & RE Mackow (1998). Beta 3 integrins mediate the cellular entry of hantaviruses that cause respiratory failure. Proc. Natl. Acad. Sci. USA 95:7074-7079

Gentsch, J, DHL Bishop, & JF Obijeski (1977). The virus particle nucleic acids and proteins of four bunyaviruses. J. Gen. Virol. 34:257

Gerbaud, S, P Vialat, N Pardigon, C Wychowski, M Girard, & M Bouloy (1987). The S segment of the Germiston virus RNA genome can code for three proteins. Virus Res. 8:1-13

Gething, MJ, K McCammon, & J Sambrook (1986). Expression of wild type and mutant forms of influenza HA: The role of folding in intracellular transport. Cell 46:939-950

Giorgi, C (1996). Molecular biology of phleboviruses. In: The *Bunyaviridae*, pp.105-128. Ed: RM Elliott. Plenum Press, New York

Giorgi, C, L Accardi, L Nicoletti, MC Gro, K Takehara, C Hilditch, S Morikawa, & DHL Bishop (1991). Sequences and coding strategies of the S RNAs of Toscana and Rift Valley fever viruses compared to those of Punta Toro, Sicilian sandfly fever and Uukuniemi viruses. Virology 180:733

Giorgi, C, B Blumberg, & D Kolakofsky (1983). Sequence determination of the (+) leader RNA regions of the vesicular stomatitis virus chandipura, cocal, and piry subtype genomes. J. Virol. 46:125-130

Gött, P, R Stohwasser, P Schnitzler, G Dorai, & EKF Bautz (1993). RNA binding of recombinant nucleocapsid proteins of hantaviruses. Virology 194:332-337

Goldbach, R, & D Peters (1996). Molecular and biological aspects of tospoviruses. In: The *Bunyaviridae*, pp129-157. Ed: RM Elliott. Plenum Press, New York

Goldbach, R, & D Peters (1994). Possible causes of the emergence of tospovirus diseases. Semin. Virol. 5:113

Goldsmith, C, L Elliott, C Peters, & S Zaki (1995). Ultrastructural characteristics of Sin Nombre virus, causative agent of hantavirus pulmonary syndrome. Arch. Virol. 140:2107-2122

Gonzalez-Scarano, F (1985). La Crosse virus G1 glycoprotein undergoes a conformational change at the pH of fusion. Virology 140:209

Gonzalez-Scarano, F, K Bupp, & N Nathanson (1996). Pathogenesis of diseases caused by viruses of the *Bunyavirus* genus. In: The *Bunyaviridae*, pp. 227-244. Ed: RM Elliott. Plenum Press, New York

Gonzalez-Scarano, F, MJ Endres, & N Nathanson (1991). *Bunyaviridae*: pathogenesis. Curr. Top. Microbiol. Immunol. 169:217-249

Gonzalez-Scarano, F, RS Jansen, JA Najjar, N Pobjecky, & N Nathanson (1985). An avirulent G1 glycoprotein variant of La Crosse bunyavirus with defective fusion function. J. Virol. 54:757

Gonzalez-Scarano, F, N Pobjecky, & N Nathanson (1984). La Crosse bunyavirus can mediate pH-dependent fusion from without. Viology 132:222

Gorman, CM, LF Moffat, & BH Howard (1982). Recombinant genomes which express chloramphenicol acetyltransferase in mammalian cells. Mol. Cell. Biol. 2:1044-1051

Gotoh B, K Takeuchi, T Komatsu, J Yokoo, Y Kimura, A Kurotani, A Kato, & Y Nagai. (1999). Knockout of the Sendai virus C gene eliminates the viral ability to prevent the interferon-alpha/beta-mediated responses. FEBS Lett. 459:205-10

Grady, LJ, ML Sanders, & WP Campbell (1983). Evidence for three separate antigenic sites on the G1 protein of La Crosse virus. Virology 194:395-397

Grady, LJ, ML Sanders, & WP Campbell (1987). The sequence of the M RNA of an isolate of La Crosse virus. J. Gen Virol. 68:3057

Hacker, DL (1995). Identification of a coat protein binding site on southern bean mosaic virus RNA. Virology 207:562-565

Hacker, D, R Raju, & D. Kolakofsky (1989). La Crosse virus nucleocapsid protein controls its own synthesis in mosquito cells by encapsidating its mRNA. J. Virol. 63:5166-5174

Hacker, D, S Rochat, & D Kolakofsky (1990). Anti-mRNAs in La Crosse bunyavirus-infected cells. J. Virol. 64:5051-5057

Hagen, M, TDY Chung, JA Butcher, & M Krystal (1994). Recombinant influenza virus polymerase: requirement of both 5' and 3' viral ends for endonuclease activity. J. Virol. 68:1509-1515

Harcourt, BH, A Sanchez, & MK Offermann (1998). Ebola virus inhibits induction of genes by double-stranded RNA in endothelial cells. Virology 252:179-188

Hariya Y, S Shirakawa, N Yonekura, N Yokosawa, GI Kohama, & N Fujii. (1999). Augmentation of verotoxin-induced cytotoxicity/apoptosis by interferon is repressed in cells persistently infected with mumps virus. J. Interferon Cytokine Res. 19 :479-85

Hatada, E, & R Fukuda (1992). Binding of influenza A virus NS1 protein to dsRNA in vitro. J Gen Virol. 73:3325-9

Hayashi, T, T Shioda, Y Iwakura, & H Shibuta (1992). RNA packaging signal of human immunodeficiency virus type 1. Virology 188:590-599

Henderson, LE, RC Sowder, TD Copeland, S Oroszlan, & RE Benveniste (1990). Gag precursors of HIV and SIV are cleaved into six proteins found in the mature virions. J. Med. Primat. 19:411-419

Hercyk, N, SM Horikami, & SA Moyer (1988). The vesicular stomtaitis virus L protein possesses the mRNA methyltransferase activities. Virology 163:222-225

Herz, C, E Stavnezer, RM Krug, & T Gurney (1981). Influenza virus, an RNA virus, synthesizes its messenger RNA in the nucleus of infected cells. Cell 26:391-400

Hewlett, MJ, RF Pettersson, & D Baltimore (1977). Circular forms of Uukuniemi virion RNA: an electron microscopic study. J. Virol. 21:1085-1093

Honda, A, K Ueda, K Nagata, & A Ishihama (1988). RNA polymerase of influenza virus: role of NP on RNA chain elongation. J. Biochem. 104:1021-1026

Horikami, SM, J Curran, D Kolakofsky, & SA Moyer (1992). Complexes of Sendai virus NP-P and P-L proteins are required for interfering particle genome replication *in vitro*. J. Virol. 66:4901-4908

Horikami, SM, F De Ferra, & SA Moyer (1984). Characterization of the infection of permissive and nonpermissive cells by host range mutants of vesicular stomatitis virus defective in RNA methylation. Virology 138:1-15

Horikami, SM, RE Hector, S Smallwood, & SA Moyer. (1997). The Sendai virus C protein binds the L polymerase protein to inhibit viral RNA synthesis. Virology 235:261-270

Horikami, SM, & SA Moyer (1982). Host range mutants of vesicular stomatitis virus defective in *in vitro* RNA methylation. Proc. Natl. Acad. Sci. USA 79:7694-7698

Howard, M, & GW Wertz (1989). Vesicular stomatitis virus RNA replication: A role for the NS protein. J. Gen. Virol. 70:2683-2694

Hsu, M-T, JD Parvin, S Gupta, M Krystal, & P Palese (1987). Genomic RNAs of influenza viruses are held in a circular conformation in virions and infected cells by a terminal panhandle. Proc. Natl. Acad. Sci. USA 84:8140-8144

Hudson, LD, C Condra, & RA Lazzarini (1986). Cloning and expression of a viral phosphoprotein: structure suggests vesicular stomatitis virus NS may function by mimicking an RNA template. J. Gen. Virol. 67:1571-1579

Hung, T, SM Xia, TX Zhao, JY Zhou, G Song, GX Liao, WW Ye, YL Chu, & CS Hang (1983). Morphological evidence for identifying the viruses of hemorrhagic fever with renal syndrome as candidate members of the Bunyaviridae family. Arch. Virol. 78:137-144

Hutchinson, KL, CJ Peters, & ST Nichol (1996). Sin Nombre virus mRNA synthesis. Virology 224:139-149

Ihara, T, H Akashi, & DH Bishop (1984). Novel coding strategy (ambisense genomic RNA) revealed by sequence analyses of Punta Toro Phlebovirus S RNA. Virology 136:293-306

Ihara, T, Y Matsuura, & DH Bishop (1985). Analyses of the mRNA transcription processes of Punta Toro phlebovirus (*Bunyaviridae*). Virology 147:317-325

Inoue-Nagata, A, R Kormelink, J-Y Sgro, T Nagata, E. Kitajima, R Goldbach, & D Peters (1998). Molecular characterization of tomato spotted wilt virus defective interfering RNAs and detection of truncated L proteins. Virology 248:342-356

Iroegbu, CU, and CR Pringle (1981). Genetic interactions among viruses of the Bunyamwera complex. J. Virol. 37:383-394.

Ishihama, A, & P Barbier (1994). Molecular anatomy of viral RNA-directed RNA polymerases. Arch. Virol. 134:235-258

Jackson, DA, AJ Caton, SJ McCready, & PR Cook (1982). Influenza virus RNA is synthesized at fixed sites in the nucleus. Nature 296:366-368

Jin, H, & RM Elliott (1991). Expression of functional Bunyamwera virus L protein by recombinant vaccinia viruses. J. Gen. Virol. 65:4182-4189

Jin, H, & RM Elliott (1992). Mutagenesis of the L protein encoded by Bunyamwera virus and production of monospecific antibodies. J. Gen. Virol. 73:2235-2244

Jin, H, & RM Elliott (1993a). Characterization of Bunyamwera virus S RNA that is transcribed and replicated by the L protein expressed from recombinant vaccinia virus. J. Virol. 67:1396-1404

Jin, H, & RM Elliott (1993b). Non-viral sequences at the 5' ends of Dugbe nairovirus mRNAs. J. Gen. Virol. 74:2293-2297

Karabatsos, N (1985). International catalogue of arboviruses including other viruses of invertebrates. 3rd edition. Am. Soc. Trop. Med. Hyg., San Antonio

Kascask, RJ, & MJ Lyons (1978). Bunyamwera virus. II. The generation and nature of defective interfering particles. Virology 89:539-546

Khromykh, AA, & EG Westaway (1996). RNA binding properties of core protein of the flavivirus Kunjin. Arch. Virol. 141:685-699

Kingsbury, DW, IM Jones, & KG Murti (1987). Assembly of influenza ribonucleoprotein in vitro using recombinant nucleoprotein. Virology 156:396-403

Kingsford, L, & DW Hill (1983). The effect of proteolytic cleavage of La Crosse virus G1 glycoprotein on antibody neutralization. J. Gen. Virol. 64:2147-2156

Klumpp, K, RWH Ruigrok, & F Baudin (1997). Roles of the influenza virus polymerase and nucleoprotein in forming a functional RNP structure. EMBO J. 16:1248-1257

Kobayashi, M, T Toyoda, DM Adyshev, Y Azuma, & A Ishihama (1994). Molecular dissection of influenza virus nucleoprotein: deletion mapping of the RNA binding domain. J. Virol. 68:8433-8436

Kolakofsky, D, & D Hacker (1991). Bunyavirus RNA synthesis: genome transcription and replication. Curr. Top. Microbiol. Immunol. 169:143-159

Kormelink, R, P de Haan, C Meurs, D Peters, & R Goldbach (1992c). The nucleotide sequence of the M RNA segment of tomato spotted wilt virus, a bunyavirus with two ambisense RNA segments. J. Gen. Virol. 73:2795

Kormelink, R, P de Haan, D Peters, & R Goldbach (1992a). Viral RNA synthesis in tomtato spotted wilt virus-infected Nicotiana rustica plants. J. Gen. Virol. 73:687-693

Kormelink, R, M Storms, J van Lent, D Peters, & R Goldbach (1994). Expression and subcellular location of the NSm protein of tomato spotted wilt virus (TSWV), a putative viral movement protein. Virology 200:56-65

Kormelink, R, F van Poelwijk, D Peters, & R Goldbach (1992b). Non-viral heterogeneous sequences at the 5' ends of tomato spotted wilt virus mRNAs. J. Gen. Virol. 73:2125-2128

Kromykh, AA, & EG Westaway (1996). RNA binding properties of the core protein of the flavivirus Kunjin. Arch. Virol. 141:685-699

Krug, RM (1981). Priming of influenza virus RNA transcription by capped heterologous RNAs. Curr. Top. Microbiol. Immunol. 93:125-149

Kuismanen, E, P Bang, M Hurme, & RF Pettersson (1984). Uukuniemi virus maturation: Immunofluorescence microscopy with monoclonal glycoprotein-specific antibodies. J. Virol. 51:137

La Ferla, FM, & RW Peluso (1989). The 1:1 N-NS protein complex of vesicular stomatitis virus is essential for efficient genome replication. J Virol. 63:3852-3857.

Lamb, RA, & D Kolakofsky (1996). Paramyxoviridae: the viruses and their replication. In: *Fields Virology,* pp. 1177-1204. Eds: BN Fields, DM Knipe, & PM Howley. Lippincott-Raven, Philadelphia

Lamb, RA, C-J Lai, & PW Choppin (1981). Sequences of mRNAs derived from genome RNA segment 7 of influenza virus: colinear and interrupted mRNAs code for overlapping proteins. Proc. Natl. Acad. Sci. USA 78:4170-4174

Law, MD, J Speck, & JW Moyer (1992). The M RNA of impatiens necrotic spot Tospovirus (*Bunyaviridae*) has an ambisense genomic organization. Virology 188:732-741

Leahy, MB, JT Dessens, & PA Nuttall (1997). Striking conformational similarities between the transcription promoters of Thogoto and influenza A viruses: evidence for intrastrand base pairing in the 5' promoter arm. J. Virol. 71:8352-8356

Leahy, MB, JT Dessens, DC Pritlove, & PA Nuttall (1998). The Thogoto orthomyxovirus cRNA promoter functions as a panhandle but does not stimulate cap snatching *in vitro*. J. Gen. Virol. 79:457-460

Lee, HW (1996). Epidemiology and pathogenesis of hemorrhgic fever with renal syndrome. In: The *Bunyaviridae*, pp. 253-267. Ed: RM Elliott. Plenum Press, New York

Lee, KJ, IS Novella, MN Teng, MB Oldstone, & JC de La Torre. (2000). NP and L proteins of lymphocytic choriomeningitis virus (LCMV) are sufficient for efficient transcription and replication of LCMV genomic RNA analogs. J. Virol. 74:3470-3477

Lees, JF, CR Pringle, & RM Elliott (1986). Nucleotide sequence of the Bunyamwera virus M RNA segment: conservation of structural features in the bunyavirus glycoprotein gene product. Virology 148:1-14

Leslie, M, et al. (1999). Update: hantavirus pulmonary syndrome – United States, 1999. Morb. Mortal. Wkly Rep. 48:521-525

Lewis, JD, & E Izaurralde (1997). The role of the cap structure in RNA processing and nuclear export. Eur. J. Biochem. 247:461-469

Ludwig, GV, BM Christensen, TM Yuill, & KT Schultz. (1989). Enzyme processing of La Crosse virus glycoprotein G1: a bunyavirus-vector infection model. Virology 171:108-113

Madoff, DH, & J Lenard (1982). A membrane glycoprotein that accumulates intracellularly: cellular processing of the large glycoprotein of La Crosse virus. Cell 28:821-829

Marriott, AC, & PA Nuttall (1992). Comparison of the S RNA segments and nucleoprotein sequences of Crimean-Congo hemorrhagic fever, Hazara and Dugbe viruses. Virology 189:795

Martin, ML, H Lindsey Regnery, DR Sasso, JB McCormick, & E Palmer (1985). Distinction between *Bunyaviridae* genera by surface structure and comparison with Hantaan virus using negative stain electron microscopy. Arch. Virol. 86:17-28

Masters, PS, & AK Banerjee (1988). Complex formation with vesicular stomatitis virus phosphoprotein NS prevents binding of nucleocapsid protein N to nonspecific RNA. J. Virol. 62:2658-2664

McKee, KT, JW Le Duc, & CJ Peters (1991). Hantaviruses. In: Textbook of human virology, p. 615. Ed: RB Belshe. Mosby-Year Book, St. Louis

Medcalf, L, E Poole, D Elton, & P Digard (1999). Temperature-sensitive lesions in two influenza A viruses defective for replicative transcription disrupt RNA binding by the nucleoprotein. J. Virol. 73:7349-7356

Mena, I, E Jambrina, C Albo, B Perales, J Ortin, M Arrese, D Vallejo, & A Portela (1999). Mutational analysis of influenza A virus nucleoprotein: identification of mutations that affect RNA replication. J. Virol. 73:1186-1194

Meyer, BJ, & C Schmaljohn (2000). Accumulation of terminally deleted RNAs may play a role in Seoul virus persistence. J. Virol. 74:1321-1331

Morrill, JC, & DJ McClain (1996). Epidemiology and pathogenesis of Rift Valley fever and other phleboviruses. In: The Bunyaviridae, pp. 281-293. Ed: RM Elliott. Plenum Press, New York

Moss, B, O Elroy-Stein, T Mizukami, WA Alexander, & TR Fuerst (1990). New mammalian expression vectors. Nature 348: 91-92

Moyer, SA, & AK Banerjee (1976). In vivo methylation of vesicular stomatitis virus and its host cell messenger RNA species. Virology 70:339-351

Moyer, SA, S Smallwood-Kentro, A Haddad, & L Prevec (1991). Assembly and transcription of synthetic vesicular stomatitis virus nucleocapsids. J. Virol. 65:2170-2178

Muller, R, O Poch, M Delarue, DH Bishop, & M Bouloy (1994). Rift Valley fever virus L segment: correction of the sequence and possible functional role of newly identified regions conserved in RNA-dependent polymerases. J. Gen. Virol. 75:1345-1352

Murphy, FA, AK Harrison, & SG Whitfield (1973). Bunyaviridae: morphologic and morphogenetic similarities of Bunyamwera serologic serogroup viruses and several other arthropod-borne viruses. Intervirology 1:297-316

Myers, TM, & SA Moyer (1997). An amino-terminal domain of the Sendai virus nucleocapsid protein is required for template function in viral RNA synthesis. J. Virol. 71:918-924

Nakai, T, & AF Howatson (1968). The fine structure of vesicular stomatitis virus. Virology 32:268-281

Nakitare, GW, & RM Elliott (1993). Expression of the Bunyamwera virus M genome segment and intracellular localisation of NSm. Virology 195:511-520

Nemeroff, ME, XY Qian, & RM Krug (1995). The influenza virus NS1 protein forms multimers in vitro and in vivo. Virology 212:422-428

Newcombe, WW, & JC Brown (1981). Role of the vesicular stomatitis virus matrix protein in maintaining the viral nucleocapsid in the condensed form found in native virions. J. Virol. 39:295-299

Newcombe, WW, GJ Tobin, JJ McGowan, & JC Brown (1982). In vitro reassembly of vesicular stomatitis virus skeletons. J. Virol. 41:1055-1062

Nichol, ST, & JJ Holland (1987). Genome RNA terminus conservation and diversity among vesiculoviruses. J. Virol. 61:200-205

Nichol, ST, TG Ksiazek, PE Rollin, & CJ Peters (1996). Hantavirus pulmonary syndrome and newly described hantaviruses in the United States. In: The *Bunyaviridae*, pp. 269-279. Ed: RM Elliott. Plenum Press, New York

Obijeski, JF, & FA Murphy (1977). *Bunyaviridae*: recent biochemical developments. J. Gen. Virol. 37:1-14

Obijeski, JF, DHL Bishop, FA Murphy, & EL Palmer (1976a). Structural proteins of La Crosse virus. J. Virol. 19:985-997

Obijeski, JF, DHL Bishop, E Palmer, & FA Murphy (1976b). Segmented genome and nucleocapsid of La Crosse virus. J. Virol. 20:664-675

Ortega, J, J Martin-Benito, T Zürcher, JM Valpuesta, JL Carracascosa, & J Ortin (2000). Ultrastructual and functional analyses of recombinant influenza virus ribonucleoproteins suggest dimerization of nucleoprotein during virus amplification. J. Virol. 74:156-163

Oomens, AGP, SA Monsma, & GW Blissard (1995). The baculovirus GP64 envelope fusion protein: Synthesis, oligomerization, and processing. Virology 209:592-603

Pardigon, N, P Vialat, S Gerbaud, M Girard, & M Bouloy (1988). Nucleotide sequence of the M segment of Germiston virus: Comparison of the M gene product of several bunyaviruses. Virus Res. 11:73

Pardigon, N, P Vialat, M Girard, & M Bouloy (1982). Panhandles and hairpin structures at the termini of Germiston virus RNAs (Bunyavirus). Virology 122:191-197

Patel, AH, & RM Elliott (1992). Characterisation of Bunyamwera virus defective interfering particles. J. Gen. Virol. 73:389-396

Pattnaik, AK, & G Abraham (1983). Identification of four complementary RNA species in Akabane virus-infected cells. J. Virol. 47:452-462

Patterson, JL, B Holloway, & D Kolakofsky (1984). La Crosse virus virions contain a primer-stimulated RNA polymerase and a methylated cap-dependent endonuclease. J. Virol. 52:215-222

Patterson, JL, & D Kolakofsky (1984). Characterization of La Crosse virus small-genome transcripts. J. Virol. 49:680-685

Patterson, JL, D Kolakofsky, BP Holloway, & JF Obijeski (1983). Isolation of the ends of La Crosse virus small RNA as a double-stranded structure. J. Virol. 45:882-884

Pennington, TH, CR Pringle, & MA McCrae (1977). Bunyamwera virus-induced polypeptide synthesis. J. Virol. 24:397-400

Perrault, J (1981). Origin and replication of defective interfering particles. Curr. Top. Microbiol. Immunol. 93:151-207

Pettersson, RF, E Kuismanen, R Rönnholm, & I Ulmanen (1985). In: Viral Messenger RNA: Transcription, Processing, Splicing and Molecular Structure, pp. 283-300. Ed: Y Becker. Nijhoff, The Hague

Pettersson, RF, & L Melin (1996). Synthesis, assembly, and intracellular transport of *Bunyaviridae* membrane proteins. In: The Bunyaviridae, pp. 159-188. Ed: RM Elliott. Plenum Press, New York

Pettersson, R, L Kääriäinen, CH von Bonsdorf, & N Okerblom (1971). Structural components of Uukuniemi virus, a non-cubical tick-borne arbovirus. Virology 46:721-729

Pettersson, RF, & CH von Bonsdorff (1975). Ribonucleoproteins of Uukuniemi virus are circular. J. Virol. 15:386-392

Pettersson, RF, & CH von Bonsdorff (1987). Bunyaviridae. In: Animal Virus Structure, pp. 147-157. Eds: MV Nermut & AC Steven. Elsevier, Amsterdam

Plotch, SJ, M Bouloy, I Ulmanen, & RM Krug (1981). A unique cap (m7GpppXm)-dependent influenza virion endonuclease cleaves capped RNAs to generate the primers that initiate viral RNA transcription. Cell 23:847-858

Poch, O, I Sauvaget, M Delarue, & N Tordo (1989). Identification of four conserved motifs among the RNA-dependent polymerase encoding elements. EMBO J. 8:3867-3874

Pons, MW, IT Schulze, GK Hirst, & R Hauser (1969). Isolation and characterization of the ribonucleoprotein of influenza virus. Virology 39:250-259

Poon, LLM, DC Pritlove, J Sharps, & GG Brownlee (1998). The RNA polymerase of influenza virus, bound to the 5' end of virion RNA, acts in *cis* to polyadenylate mRNA. J. Virol. 72:8214-8219

Pringle, CR (1996). Genetics and genome segment reassortment. In: The *Bunyaviridae*, pp. 189-226. Ed: RM Elliott. Plenum Press, New York

Prins, M & R Goldbach (1998). The emerging problem of tospovirus infection and nonconventional methods of control. Trends Microbiol. 6:31-34

Pritlove, DC, LLM Poon, E Fodor, J Sharps, & GG Brownlee (1998). Polyadenylation of influenza virus mRNA transcribed in vitro from model virion RNA templates: requirement for 5' conserved sequences. J. Virol. 72:1280-1286

Prokudina-Kantorovich, EN, & NP Semenova (1996). Intracellular oligomerization of influenza virus nucleoprotein. Virology 223:51-56

Prokudina, EN, & NP Semenova (1991). Localization of the influenza virus nucleoprotein: Cell-associated and extracellular nonvirion forms. J. Gen. Virol. 72:1699-1702

Qiagen (1997). The *QIA*expressionist. A handbook for high-level expression and purification of 6xHis-tagged proteins. 3rd edition. Qiagen, Hilden, Germany

Raju, R, & D Kolakofsky (1986). Inhibitors of protein synthesis inhibit both La Crosse virus S-mRNA and S genome syntheses in vivo. Virus Res. 5:1-9

Raju, R, & D Kolakofsky (1987a). Translational requirement of La Crosse virus S-mRNA synthesis: in vivo studies. J. Virol. 61:96-103

Raju, R, & D Kolakofsky (1987b). Unusual transcripts in La Crosse virus-infected cells and the site for nucleocapsid assembly. J. Virol. 61:667-672

Raju, R, & D Kolakofsky (1988). La Crosse virus infection of mammalian cells induces mRNA instability. J. Virol. 62:27-32

Raju, R, & D Kolakofsky (1989). The ends of La Crosse virus genome and antigenome RNAs within nucleocapsids are base paired. J. Virol. 63:122-128

Ravkov, E, S Nichol, & R Compans (1997). Polarized entry and release in epithelial cells of Black Creek Canal virus, a new world hantavirus. J. Virol. 71:1147-1154

Ravkov, E, S Nichol, C Peters, & R Compans (1998). Role of actin mircofilaments in Black Creek Canal virus morphogenesis. J. Virol. 72:2865-2870

Resende, R de O, P de Haan, AC de Avila, EW Kitajima, R Kormelink, R Goldbach, & D Peters (1991). Generation of envelope and defective interfering RNA mutants of tomato spotted wilt virus by mechanical passage. J. Gen. Virol. 72:2375-2383

Resende, R de O, P de Haan, E van de Vossen, AC Avila, R Goldbach, & D Peters (1992). Defective interfering L RNA segments of tomato spotted wilt virus retain both virus genome termini and have extensive internal deletions. J. Gen. Virol. 73:2509-2516

Reusken, CBEM, L Neelman, & JF Bol (1994). The 3'-untranslated region of alfalfa mosaic virus RNA 3 contains at least two idependent binding sites for viral coat protein. Nu. Acids Res. 22:1346-1353

Richmond, KE, K Chenault, JL Sherwood, & TL German (1998). Characterization of the nucleic acid binding properties of tomato spotted wilt virus nucleocapsid protein. Virology 248:6-11

Rose, JK (1975). Heterogeneous 5'-terminal structures occur on vesicular stomatitis virus mRNAs. J. Biol. Chem. 250:8098-8104

Rose, JK, L Buonocore, & MA Whitt (1991). A new cationic liposome reagent mediating nearly quantitative transfection of animal cells. Biotechniques 10:520-525

Rossier, C, R Raju, & D Kolakofsky (1988). LaCrosse virus gene expression in mammalian and mosquito cells. Virology 165:539-548

Rozhon, EJ, P Gensemer, RE Shope, & DHL Bishop (1981). Virology 111:125-138

Ruigrok, RWH, & F Baudin (1995). Structure of influenza virus ribonucleoprotein particles II. Purified RNA-free influenza virus ribonucleoprotein forms structures that are indistinguishable from the intact influenza virus ribonucleoprotein particles. J. Gen. Virol. 76:1009-1014

Ruusala, A, R Persson, CS Schmaljohn, & RF Pettersson (1992). Coexpression of the membrane glycoproteins G1 and G2 of Hantaan virus is required for targeting to the Golgi complex. Virology 186:53

Samso, A, M bouloy, & C Hannoun (1975). Présence de ribonucléoproteins circulaires dans le virus Lumbo (Bunyavirus). Compze rendue de l'Academie des sciences D280:779-782

Scallan, MF, & RM Elliott (1992). Defective RNAs in mosquito cells persistently infected with Bunyamwera virus. J. Gen. Virol. 73:53-60

Schlender J, B Bossert, U Buchholz, & KK Conzelmann. (2000). Bovine respiratory syncytial virus nonstructural proteins NS1 and NS2 cooperatively antagonize alpha/beta interferon-induced antiviral response. J Virol. 74:8234-42

Schmaljohn, CS (1996a). Bunyaviridae: The viruses and their replication. In: Fields Virology, 3rd Edition, pp. 1447-1471. Eds: BN Fields, DM Knipe, PM Howley. Lippincott-Raven, Philadelphia

Schmaljohn, CS (1996b). Molecular biology of hantaviruses. In: The Bunyaviridae, pp. 63-86. Ed: RM Elliott. Plenum Press, New York

Schmaljohn, CS, AL Schmaljohn, & JM Dalrymple (1987). Hantaan virus M RNA: Coding strategy, nucleotide sequence, and gene order. Virology 157:31

Schoehn, G, F Iseni, M Mavrakis, D Blondel, & RWH Ruigrok (2001). Structure of recombinant rabies virus nucleoprotein-RNA complex and identifictaion of the phosphoprotein binding site. J. Virol. 75:490-498

Scholtissek, C, & H Becht (1971). Binding of ribonucleic acids to the RNP-antigen of influenza viruses. J. Gen. Virol. 10:11-16

Sekellick, MJ, SA Carra, A Bowman, DA Hopkins, & PI Marcus (2000). Transient resistance of influenza virus to interferon action attributed to random multiple packaging and activity of NS genes. J. Interferon Cytokine Res. 20:963-970

Seong, BL, & GG Brownlee (1992). Nucleotides 9 to 11 of the influenza A virion RNA promoter are crucial for activity in vitro. J. Gen. Virol. 73:3115-3124

Severson, W, L Partin, CS Schmaljohn, & CB Jonsson (1999). Characterization of the Hantaan nucleocapsid protein-ribonucleic acid interaction. J. Biol. Chem. 274:33732-33739

Severson, WE, X Xu, & CB Jonsson (2001). *Cis*-acting signals in encapsidation of Hantaan virus S-segment viral genomic RNA by its N protein. J. Virol. 75:2646-2652

Shapiro, GI, & RM Krug (1988). Influenza virus RNA replication in vitro: synthesis of viral template RNAs and virion RNAs in the absence of an added primer. J. Virol. 62:2285-2290

Shaw, MW, & RA Lamb (1994). A specific sub-set of host cell mRNAs prime influenza virus mRNAs synthesis. Virus Res. 1:455-467

Shope, RE, & OR Causey (1962). Further studies on the serological relationships of Group C arthropod-borne viruses and the application of those relationships to rapid identification of types. Am. J. Trop. Med. Hyg. 11:283

Shuman, S (1997). A proposed mechanism of mRNA synthesis and capping by vesicular stomatitis virus. Virology 227:1-6

Sibold, C, H Meisel, DH Kruger, M Labuda, J Lysy, O Kozuch, M Pejcoch, A Vaheri, & A Plyusnin (1999). Recombination in Tula hantavirus evolution: analysis of genetic lineages from Slovakia. J. Virol. 73:667-675

Simons, JF, U Hellman, & RF Pettersson (1990). Unukuniemi virus S RNA segment: ambisense coding strategy, packaging of complementary strands into virions, and homology to members of the genus Phlebovirus. J. Virol. 64:247-255

Simons, JF, & RF Pettersson (1991). Host-derived 5' ends and overlapping complementary 3' ends of the two mRNAs transcribed from the antisense S segment of Uukuniemi virus. J. Virol. 65:4741-4748

Smallwood, S, & SA Moyer (1993). Promoter analysis of the vesicular stomatits virus RNA polymerase. Virology 192:254-263

Smith, JF, & DY Pifat (1982). Morphogenesis of sandfly viruses (Bunyaviridae family). Virology 121:61-81

Smithburn, KC, AJ Haddow, & AF Mahaffy (1946). Neurotropic virus isolated from *Aedes* mosquitoes caught in Semliki forest. Am. J. Trop. Med. Hyg. 26:189

Soellick, T-R, JF Uhrig, GL Bucher, J-W Kellmann, & PH Schreier (2000). The movment protein NSm of tomato spotted wilt tospovirus (TSWV): RNA binding, interaction with the TSWV N protein, and identification of interacting plant proteins. Proc. Natl. Acad. Sci. USA 97:2373-2378

Spehner, D, A Kirn, & R Drillien (1991). Assembly of nucleocapsid-like structures in animal cells infected with a vaccinia virus recombinant encoding the measles virus nucleoprotein. J. Virol. 65:6296-6300

Sprague, J, JH Condra, H Arnheiter, & RA Lazzarini (1983). Expression of a recombinant DNA gene coding for the vesicular stomatitis virus nucleocapsid protein. J. Virol. 45:773-781

Stillman, EA, & MA Whitt (1999). Transcript initiation and 5'-end modification are separable events during vesicular stomatitis virus transcription. J. Virol. 73:7199-7209

Stitz, L, C Schmitz, D Binder, R Zinkernagel, E Paoletti, & H Becht (1990). Characterization and immunological properties of influenza A virus nucleoprotein (NP): Cell-associated NP expressed by vaccinia recombinant virus do not confer protection. J. Gen. Virol. 71:1169-1171

Stohlman, SA, RS Baric, GN Nelson, LH Soc, LM Welter, & RJ Deans (1988). Specific interactions between coronavirus leader RNA and nucleocapsid protein. J. Virol. 62:4288-4295

Storms, MM, R Kormelink, D Peters, JW van Lent, & RW Goldbach (1995). The nonstructural NSm protein of tomato spotted wilt virus induces tubular structures in plant and insect cells. Virology 214:485-493

Suzich, JA, LT Kakach, & MS Collett (1990). Expression strategy of a phlebovirus: Biogenesis of proteins from the Rift Valley fever virus M segment. J. Virol. 64:1549

Takacs, AM, T Das, & AK Banerjee (1993). Mapping of interacting domains between the nucleocapsid protein and the phosphoprotein of vesicular stomatitis virus by using a two-hybrid system. Proc. Natl. Acad. Sci. USA 90:10375-10379

Talmon, Y, BV Prasad, JP Clerx, GJ Wang, W Chiu, & MJ Hewlett (1987). Electron microscopy of vitrified-hydrated La Crosse virus. J. Virol. 61:2319-2321

Talon, J, CM Horvath, R Polley, CF Basler, T Muster, P Palese, & A Garcia-Sastre (2000). Activation of interferon regulatory factor 3 is inhibited by the influenza A virus NS1 protein. J. Virol. 74:7989-7996

Tan SL, & MG Katze. (1998). Biochemical and genetic evidence for complex formation between the influenza A virus NS1 protein and the interferon-induced PKR protein kinase. J Interferon Cytokine Res. 18:757-66

Tiley, L, M Hagen, JT Matthews, & M Krystal (1994). Sequence-specific binding of the influenza virus RNA polymerase to sequences located at the 5' ends of the viral RNAs. J. Virol. 68:5108-5116

Tober, C., M Seufert, H Schneider, MA Billeter, IC Johnston, S Niewiesk, V ter Meulen, & S Schneider-Schaulies. (1998). Expression of measles virus V protein is associated with pathogenicity and control of viral RNA synthesis. J. Virol. 72:8124-8132

Uhrig, JF, T-R Soellick, CJ Mincke, C Philipp, J-W Kellmann, & PH Schreier (1999). Homotypic interaction and multimerization of nucleocapsid protein of tomato spotted wilt tospovirus: Identification and characterization of two interacting domains. Proc. Natl. Acad. Sci. USA 96:55-60

Ulmanen, I, P Seppäla, & RF Pettersson (1981). In vitro translation of Uukuniemi virus-specific RNAs: Identification of a nonstructural protein and a precursor to the membrane glycoproteins. J. Virol. 37:72

Urquidi, V, & DHL Bishop (1992). J. Gen. Virol. 73:2255-2265

Valegård, K, JB Murray, PG Stockley, NJ Stonehouse, & L Liljas (1994). Crystal structure of an RNA bacteriophage coat protein-operator complex. Nature 371:623-626

Varani, G, & K Nagai (1998). RNA recognition by RNP proteins during RNA processing. Annu. Rev. Biophys. Biomol. Struct. 27: 407-445

Vasavada, HA, S Ganguly, FJ Germino, ZX Wang, & SM Weissman (1991). A contingent replication assay for the detection of protein-protein interactions in animal cells. Proc. Natl. Acad. Sci. USA 88:10686-10690

Vezza, AC, PM Repik, P Cash, & DH Bishop (1979). In vivo transcription and protein synthesis capabilities of bunyaviruses: wild-type snowshoe hare virus and its temperature-sensitive group I, group II, and group I/II mutants. J. Virol. 31:426-436

Vialat, P, & M Bouloy (1992). Germiston virus transcriptase requires active 40S ribosomal subunits and utilizes capped cellular RNAs. J. Virol. 66:685-693

Wang, J, & AE Simon (2000). 3'-end stem-loops of the subviral RNAs associated with turnip crinkle virus are involved in symptom modulation and coat protein binding. J. Virol. 74:6528-6537

Wang, X, M Li, H Zheng, T Muster, P Palese, AA Beg, & A Garcia-Sastre (2000). Influenza A virus NS1 protein prevents activation of NF-kappaB and induction of Alpha/Beta interferon. J. Virol. 74:11566-11573

Watanabe, K., Handa, H., Mizumoto, K., and Nagata, K. (1996). Mechanism for inhibition of influenza virus RNA polymerase activity by matrix protein. J. Virol. 70:241-247.

Watret, GE, CR Pringle, & RM Elliott (1985). Synthesis of bunyavirus-specific proteins in a continuous cell line (XTC-2) derived from Xenopus laevis. J. Gen. Virol. 66:473-482

Weber, F, EF Dunn, A Bridgen & RM Elliott (2001). The Bunyamwera virus nonstructural protein NSs inhibits viral RNA synthesis in a minireplicon system. Virology 281:67-74

Weber, F, O Haller, & G Kochs (1997). Conserved vRNA end sequences of Thogoto-orthomyxovirus suggest a new panhandle structure. Arch. Virol. 142:1029-1033

Wei, N, & TJ Morris (1991). Interactions between viral coat protein and a specific binding region on turnip crinkle virus RNA. J. Mol. Biol. 222:437-443

Wei, N, DL Hacker, & TJ Morris (1992). Characterization of an internal element in turnip crinkle virus RNA involved in both coat protein binding and replication. Virology 190:346-355

Wertz, GW, MB Howard, N Davis, & J Patton (1987). The switch from transcription to replication of a negative-strand RNA virus. Cold Spring Harbor Symp. Quant. Biol. 38:17-26

Winkler, G, VB Randolph, GR Cleaves, TE Ryan, & V Stoller (1988). Evidence that the mature from of flavivirus nonstructural protein NS1 is a dimer. Virology 162:187-196

Winkler, G, SE Maxwell, C Ruemmler, & V Stoller (1989). Newly synthesized dengue-2 virus nonstructural protein NS1 is a soluble protein but becomes partially hydrophobic and mambrane-associated after dimerization. Virology 171:302-305

Witherell, GW, JM Gott, & OC Uhlenbeck (1991). Specific interaction between RNA phage coat proteins and RNA. Prog. Nucleic Acid Res. Mol. Biol. 40:185-220

Worobey, M, & EC Holmes (1999). Evolutionary aspects of recombination in RNA viruses. J. Gen. Virol. 80:2535-2543

Wright, RE, RW Anslow, WH Thompson, GR DeFoliart, G Seawright, & RP Hanson (1970). Isolations of La Crosse virus of the California group from Tabanide in Wisconsin. Mosq. News 30:600

Wunner, WH (1991). The chemical composition and molecular structure of rabies viruses. In: Natural History of Rabies, 2nd Edition, pp. 31-67. Ed: GM Baer. CRC Press, Boca Raton, Florida

Yamanaka, K, A Ishihama, & K Nagata (1990). Reconstitution of influenza virus RNA-nucleoprotein complexes structurally resembling native viral ribonucleoprotein cores. J. Biol. Chem. 265:11151-11155

Yang, J, DC Hooper, WH Wunner, H Koprowski, B Dietzschold, & ZF Fu (1998). The specificity of rabies virus RNA encapsidation by nucleoprotein. Virology 242:107-117

Yang, J, H Koprowski, B Dietzschold, & ZF Fu (1999). Phosphorylation of rabies virus nucleoprotein regulates viral RNA transcription and replication by modulating leader RNA encapsidation. J. Virol. 73:1661-1664

Yewdell, JW, E Frank, & W Gerhard (1981). Expression of influenza A virus internal antigens on the surface of infected P815 cells. J. Immunol. 126:1814-1819

Young, DF, L Didcock, S Goodbourn, & RE Randall (2000). Paramyxoviridae use distinct virus-specific mechanisms to circumvent the interferon response. Virology 269:383-390

Zhirnov, OP, & AG Bukrinskaya (1984). Nucleoprotein of animal influenza viruses, in contrast to those of human strains, are not cleaved in infected cells. J. Gen. Virol. 65:1127-1134

Zhou, M, AK Williams, S-I Chung, L Wang, & EW Collisson (1996). The infectious bronchitis virus nucleocapsid protein binds RNA sequences in the 3' terminus of the genome. Virology 217:191-199